Manipulating cell death and RNA interference processes for mosquito control

By

Paul Morgan Airs

A dissertation submitted in partial fulfillment of

the requirements for the degree of

Doctor of Philosophy

(Comparative Biomedical Sciences)

at the

UNIVERSITY OF WISCONSIN-MADISON

2018

Date of final oral examination: 22 May 2018

The dissertation is approved by the following members of the Final Oral Committee:

Lyric Bartholomay, Associate Professor, Pathobiological Sciences

Adel Talaat, Professor, Pathobiological Sciences

Michael Kimber, Associate Professor, Biomedical Sciences (Iowa State University)

Mostafa Zamanian, Assistant Professor, Pathobiological Sciences

Mehdi Kabbage, Assistant Professor, Plant Pathology

Abstract

This work unfolded as a pursuit for deeper understanding of mosquito physiology and mosquito-pathogen interactions, which inspired a research quest for novel vector control strategies. The mosquito, *Aedes triseriatus* is a primary vector for La Crosse virus, which causes a deadly pediatric encephalitis in Midwestern and Mid-Atlantic states in the U.S. The virus is transmitted both horizontally and vertically from female mosquito to progeny. To understand how this virus thwarts cell death events in developing follicles and embryos, we undertook a characterization of oogenesis to include the requisite cell death events that occur as a function of nutritional limitations (follicular atresia), oocyte development and maturation (nurse cell death and death of the follicular epithelium). The results of this work are presented in Chapter 2. These studies inspired an exploration of the role of cell death genes on cell and organismal survival, and spurred an effort to generate species-specific insecticides that capitalize on powerful gene suppression capacity of the RNA interference machinery. In particular, targeting the Inhibitor of Apoptosis 1 gene relieves the suppression of apoptosis and produces a rapidly lethal phenotype (Chapter 4). We attempted to develop this technique in multiple mosquito vector species, but found that even if an RNAi trigger was designed to comparable regions of the target gene, the resulting phenotype differed dramatically depending on RNAi design, species, and delivery method (Chapter 4). This variation became a curiosity worth pursuing. Rather than ignoring negative results, cell death inducing RNAi experiments became a tool, used alongside others, to study the mosquito RNAi response. We used a two-pronged approach to investigate further: 1) an exhaustive meta-analysis of experimental parameters used in RNAi studies represented in the published literature (Chapter 5), and 2) *in vitro* and *in vivo* analysis of distribution of RNAi triggers intracellularly, across tissue

types, and across species to understand whether tissues or environments in the mosquito are inherently recalcitrant to RNAi (Chapter 3). To translate this work into a field applicable and inexpensive field-applicable tool, we tested the possibility of using the Attractive Toxic Sugar Bait (ATSB) approach for *per os* delivery of an RNAi trigger and, in the process, found that sugar composition alone can enhance the toxicity of an ATSB (Chapter 6). All totaled, this dissertation work produced informative RNAi design studies and tools that address the limitations and strengths of RNAi as a basic molecular biology tool as well as an applied vector control approach.

Dedications

To Hannah, Kieran, Megan, Joy, and Peter; for whom I strive.

Acknowledgements

First and foremost, I want to thank Dr. Lyric Bartholomay for noticing my input in the classroom, hiring me as a technician, re-hiring me as a scholar, mentoring me through three years of graduate school at Iowa State University, then mentoring me through another four years at the University of Wisconsin Madison. The tremendous privileges that have been bestowed upon me: the freedom to learn and to grow, the opportunities to teach and to make connections, are all thanks to her continued faith and support. I can never fully repay these years; but hope to acknowledge them with affection repeatedly in some form or other throughout my career.

I of course would not have completed this task if it were not for the help of many individuals all of whom I am grateful for. I would like to especially thank Dr. Yashdeep Phanse for his mentorship, friendship, and sage advice on literally everything. Additionally, Dr. Michael Kimber, Dr. Mostafa Zamanian, Dr. Adel Talaat, and Dr. Mehdi Kabbage have been a fantastically helpful and inspiration dissertation committee who have prompted me to think a little deeper about every aspect of my work. In the lab, I would be lost if it were not for the thousands of hours dedicated to raising mosquitoes spent by undergraduates and technicians, in particular Brendan Dunphy, Skye Harnesberger, and Ryan Swanson. I am thankful to have known the late, great Robin Mittenthal, whose existence was the epitome of living by example. His being continues to lead me towards living more effectively through compassion. I am also in a tremendous debt to my students Bailey Lubinski and Katherina Kudrna who have put up with my incoherent experimental planning and remained consistent over the years, excelling as students and young scientists despite impossibly high expectations.

Table of Contents

Chapter 1 - Molecular and nano-scale alternatives to traditional insecticides for in situ control of mosquito vectors

Abstract

Mosquito control, integrated vector management, and insecticide resistance management approaches are constrained by the number of safe and effective insecticides that are registered for use and manufacture. Capitalizing on the RNA interference (RNAi) machinery to suppress genes of interest in mosquitoes could help to clear these roadblocks in the future. The RNAi pathway can be activated via RNA molecules with a double-stranded appearance (RNAi triggers), resulting in silencing of target genes with exceptional target specificity. This approach thereby provides a new paradigm for vector control that can be mediated entirely by natural, non-toxic chemistries that can provide control for nuisance and vector species while minimizing impacts on non-target organisms and the environment. Importantly, an RNAi-based system would provide a platform for rapid development and delivery of new RNAi triggers to control larval and adult mosquitoes, with the potential to tap into different physiologies and modes of action to thwart or respond to development of insecticide resistance. Here we highlight the armamentarium for mosquito control chemistries and propose that RNAi could be a valuable addition to existing and developing control strategies with some additional translational efforts to move the technology to the point of being field-applicable. We review the importance of RNAi trigger design, tissue distribution, and fate in mosquitoes to maximize gene suppression and thereby phenotypic impact. Finally, we discuss existing and burgeoning technologies that can be tailored for production and delivery of RNAi triggers in the field.

1. Overview of mosquito control products

1.1. Adulticides

There are four classes of insecticide currently available to control adult mosquitoes, all of which function as neurotoxins. Pyrethroids and DDT (an organochlorine) modulate votage-gated sodium channels and prevent normal termination of action potential in neurons. Organophosphates and carbamates similarly target the nervous system and act by inhibiting acetylcholinesterase and also thereby prevent normal degradation of neurotransmitters. These products have been in use for decades. In the U.S. for example, synthetic pyrethroids (beginning with Resmethrin) have been in use for mosquito control since 1967 and registration for use of this particular product expired in 2015 *(1, 2)*. The organophospates Malathion and Naled were registered for use by the EPA in 1956 and 1959, respectively *(1)*.

In the U.S., pyrethroids are typically dispersed by ultra-low volume truck-mounted sprayers, and the OPs are delivered both by ULV and aerial sprays. Outside of the U.S., recommendations from the WHO Pesticide Evaluation Scheme (WHOPES) specify that only pyrethroid derivatives can be used for insecticide-treated (ITN) and long-lasting insecticidal nets (LLIN) *(3)*. Similarly WHOPES dictates that pyrethroid derivatives and malathion are recommended for space spraying. Per WHOPES guidelines, organophasphate and carbamate insecticide classes are only recommended for use with indoor residual spraying alongside pyrethroids *(3)*.

1.2. Larvicides

The repertoire of products available for larval mosquito control ranges from organophosphates (Temephos) to biological control in the form of microbial endotoxins that disrupt midgut membranes *(4)*, and oils and films that impede respiration. Temephos, an organophoshpate (OP)

was registered for use by the EPA in 1965, but is no longer registered and cannot be manufactured in the US. *Bacillus thuringiensis* (Bt) var. *israelensis* – the first variant of Bt with toxicity to flies – was isolated from soil samples taken from mosquito breeding sites in 1977 *(5)* and was registered for use in the U.S. in 1983 *(1)*. *B. sphaericus* was first registered for use by the EPA in the U.S. in 1991. Both bacteria produce toxic crystal (Cry proteins) that disrupt midgut integrity (see Table 1) *(4)*, and both are in widespread use in vector control programs across the U.S. Likewise, insect growth regulators, including juvenile hormone mimics and pyriproxyfen which prevent proper molting and growth of the insect, are in widespread use for larval control. Methoprene was first registered in U.S in 1982 *(1, 6)*.

The most recent addition to the repertoire of larvicides, spinosad, modulates the activity of nicotinic acetylcholine receptors. Molecules with distinct mosquitocidal activity were discovered from a fermentation product from a soil bacterium, *Saccharopolyspora spinosa (7)*. Spinosad was formulated in a plaster matrix for slow release in water for use in larval mosquito control by Clarke.

Outside of the U.S., WHOPES recommends products that contain *B. thuringiensis* var. *israelensis* and *B. sphaericus* and spinosad for larval control, along with pyriproxyfen, diflubenzuron and novaluron for insect growth regulators, and also include Temephos and other organophospates *(3)*.

1.3 Summary

This brief review of the chemistries available for mosquito control in the U.S. and globally for both aquatic and adult life stages underscores the limitations in products available for use, and the limited number of targets/modes of action – midgut integrity, molting and neurobiology. This

is a perilously limited armamentarium, particularly because insecticide resistance is widespread in vector populations, and because vector control strategies should both take an integrated approach and account for insecticide resistance management. This is juxtaposed with the profound value of vector control in disease control programs; for example, between 2000 and 2015, *Plasmodium falciparum* infections decreased by half in sub-Saharan African countries. A major contributor to this success was widespread use of ITNs *(8)*. In response, the Innovative Vector Control Consortium (IVCC) has put forth herculean efforts to rescue or co-opt agrochemicals for public health and vector control (see, for example *(9)*). The IVCC essential attributes for a new insecticide include activity against adult mosquitoes, lethality within 72 hours post-exposure, activity equal to permethrin against even insecticide resistant strains of mosquito, activity against multiple vector species, amenability to insecticide treated nets and formulation for surface sprays, with acceptable toxicology profiles *(10)*. Herein, we propose that RNAi triggers could fit the ideal IVCC Target Product Profile, and provide insight into optimizing RNAi triggers to affect a phenotype of interest for control.

2. RNAi as an elegant approach to control of mosquitoes

RNA interference (RNAi) is an indispensable laboratory tool for functional genomics studies of arthropods. We and many others have used RNAi to silence genes in mosquitoes and other arthropods to elucidate gene function, and interfere with virus replication *(11-15)*. RNAi in mosquitoes can silence target gene expression across a number of mosquito species, strains, life stages, and tissue types *(16, 17)*. The robust nature of RNAi in mosquitoes and the flexibility of using such a system has resulted in significant interest in development of RNAi-based vector

control approaches *(18, 19)*. Herein we highlight some key characteristics of RNAi that are advantageous in the context of manipulating vector biology to achieve mosquito control.

A major advantage of any RNAi based vector control strategy is species-specificity. Almost all other insecticides that are currently under development or are EPA-registered have broad spectrum activity for control of agricultural, structural and public health pests and as such there is room for development of mosquito-specific approaches. Double-stranded RNA molecules that induce an RNAi response (hereafter referred to as "RNAi triggers") can be selected or engineered to control one mosquito species, a group of related species, or potentially all mosquitoes (see Figure 1). Furthermore, an RNAi trigger can be designed to targeting any given gene with any function, provided that the RNAi trigger induces sufficient knockdown and that functional redundancy does not exist elsewhere in the transcriptome. Therefore genes required for mosquito survival, reproduction, vector competence, feeding behavior, and many other physiologies are ripe for the picking when exploring production of RNAi triggers *(17)*. Using the wealth of genome and transcriptome sequence available for mosquito species, one can readily identify conserved and unique sequences of a target gene for development of an RNAi trigger with exquisite species specificity. For example, Whyard *et al*. *(20)* engineered dsRNAs targeting vATPase genes of fruit flies, pea aphids, flour beetles, and tobacco hornworm, then compared dsRNA toxicity across taxa. No untoward effect was detected when the insects were challenged with non-homologous dsRNA but homologous vATPase RNAi trigger exposure resulted in lethality *(20)*. The same investigators further demonstrated the power of RNAi to differentiate between related species. Using a variable 3' untranslated region of the highly conserved Beta-tubulin gene, the investigators generated 40 nucleotide siRNA sequences from *D. melanogaster,*

D. sechellia, D. yakuba, and D. psuedoobscura that selectively killed the homospecific but spared the heterospecific flies *(20)*.

The challenge to implementing RNAi as an elegant approach to mosquito control lies in delivering an RNAi trigger to the mosquito in sufficient quantity in field settings. To this end, RNAi triggers could be provided as a naked dsRNA, or associated with a polymer-based particle to ensure protection and delivery of RNAi triggers to target tissues in insects (see section 3.1 and 3.2). Alternatively, a paratransgenic approach could be taken, wherein an organism that associates with a mosquito as a pathogen or a food source drives the expression of an RNAi trigger (e.g., entomopathogenic fungi, insecticidal *Bacillus* species, or insect-specific viruses *(21, 22)*) (see section 3.3).

2.1 RNAi form and function in mosquitoes

Understanding the uptake and processing of RNAi triggers is critical to development of an RNAi-based insect control approach. In mosquitoes, RNAi is post-transcriptional gene suppression mechanism that plays an essential role in antiviral immunity, by limiting arbovirus replication so that it is non-lethal, and thereby facilitating establishment of a persistent infection *(23-30)*. The RNAi pathway is triggered detection and subsequent cleavage of long double-stranded RNAs (dsRNAs) by Dicer 2, which produces ~21 nucleotide short-interfering RNAs (siRNAs). Endogenous Dicer-2 produced siRNAs, and exogenously produced siRNAs, act as triggers for Argonaute 2, which melts the duplex into guide and passenger strands and forms the RNA Induced Silencing Complex (RISC) (along with other proteins) *(31-33)*. The guide strand then acts as template for the RISC to detect and cleave matching nascent mRNAs by base complementarity. The high specificity of RNAi base complementarity is itself a balance which

can be utilized when developing broad or narrow spectrum RNAi insecticides (see Figure 1).

Consider that essential genes are typically more highly conserved and (*in lieu* of functional

redundancy) cannot accumulate non-synonymous mutations without inducing lethality. These

regions of high similarity across taxa could be utilized to produce broad spectrum RNAi triggers.

At the same time RNAi triggers could be generated against variable regions of essential genes

that are species- or even strain-specific and have little to no off-target effects.

2.2. Systemic RNAi in Diptera

RNAi knockdown success is dependent upon uptake, amplification, and spread of RNAi triggers

across cells and tissues to produce a systemic RNAi response. In some insect species, RNAi

triggers are amplified by RNA-dependent RNA polymerases (RDRP) and transported

systemically by SID-1 dsRNA-gated channels *(18, 34-36)*. Because flies (Diptera) lack SID-1

and RDRPs, it was thought that they were recalcitrant to systemic RNAi *(18)*. However,

systemic RNAi is in fact essential for antiviral immunity in *Drosophila (27, 37)*. During virus

infection, viral dsRNA is reverse-transcribed to complementary DNA (cDNA) by endogenous

retrotransposons *(25, 37)*. The cDNA produces secondary RNAi triggers which are exported by

exosomes to prime other cells against superinfection *(37)*. Intriguingly, this mechanism is

conserved in the mosquito, *Aedes albopictus (25)*. Although the current paradigm for RNAi

approaches discussed impact target individuals *in situ*, evidence of genomic integration of viral

dsRNAs in *Drosophila* may provide avenues to consider heritable RNAi approaches for

mosquito and/or mosquito-borne pathogen control *(25, 29)*.

2.3 RNAi trigger destination, design and knockdown success

RNAi-based insecticide design for mosquitoes should be informed by the nuances of uptake and processing of RNAi triggers in particular cells and tissues and according to mosquito species, life stage and nutritional status *(16)*. Previous work in *An. gambiae* and *Ae. aegypti* revealed differential uptake of RNAi triggers, such that injected siRNAs localize to pericardial and other phagocytic cells, while delivery to the salivary glands requires higher doses of the trigger *(38, 39)*. We observed limited uptake of siRNAs in the whole body of *Ae. aegypti*, but significant uptake in hemocytes such that intrathoracic exposure to an siRNA for the Inhibitor of Apoptosis 1 gene led to hemocyte depletion and immunocompromisation following challenge with a non-lethal bacterium *(16)*. Furthermore, siRNAs often require transfection reagents in order to reach the cytosol of endocytic cells in adults, but not in embryonic or larval stage mosquitoes *(21, 40-45)*. Uptake of long dsRNAs occurs in many tissues, but these triggers are also primarily located in phagocytic cells and cells capable of pinocytosis *(16)*. For the betterment of RNAi study in mosquito species as well as the development of RNAi tools as vector control agents, there needs to be thorough delineation of RNAi trigger spread or distribution, longevity of the trigger, and resulting phenotype.

In addition to the tissue-specific dissemination and cellular uptake of the RNAi trigger, RNAi knockdown success is no doubt impacted by RNAi trigger design. An archetypical siRNA is a 19 bp double helix with 2 nucleotide 3′-overhanging ends *(46)*. This structure (+/- 1 nucleotide) is the product of Dicer-based dsRNA cleavage in both *D. melanogaster* and mammalian cells *(47, 48)*. That said, structural variations of siRNAs can also be made without impeding knockdown. For instance, siRNAs with mismatching 3' overhangs induced 74% knockdown of the CLIPA3 serine protease gene in adult *Ae. aegypti* salivary glands. Even in the absence of 3' overhangs, siRNAs for enolase phosphatase e-1, Chaperonin 60KD, and Spermatogenesis-

associated factor genes produced 95% knockdown in *Ae. albopictus* C6/36 cells *(46, 49, 50)*. Conversely, overhang extensions (4 nucleotides or greater) impede Dicer processing on short (< 100 bp) dsRNA but not for longer products *(48)*. Other chemical modifications to RNAi trigger structures can also be made without interrupting RNAi knockdown and have been reviewed by previously *(17)*.

2.4 RNAi trigger position vs success

There is a general belief that the 5' end of a transcript gene is a desirable target for RNAi trigger design; the authors of a study in *Ae. aegypti* noted, "targeting a ~ 500 bp region near the N-terminus is often optimal for reproducible knockdown of > 90% in > 90% of injected mosquitoes"*(51)*. We tested the impact of RNAi trigger position on knockdown success using RNAi triggers designed to pan the length of the Inhibitor of Apoptosis 1 (IAP1) transcript *(16)*. In *Ae. aegypti*, RNAi trigger location dramatically alters both transcript knockdown and phenotypic outcome; higher knockdown results in rapid mortality and lower knockdown having no noticeable impact on longevity compared to controls. This design effect did not translate to *Ae. albopictus, An. gambiae,* and *Cx. pipiens*, in which we did not see a difference in lethality based on location along the transcript. For *Ae. albopictus* and *An. gambiae,* IAP RNAi triggers were all effective and induced death in at least 50% of exposed individuals, but no death was observed in *Cx. pipiens*. Ultimately this study shows that RNAi trigger position can dramatically alter outcome but this is dependent upon both the sequence and the species tested and is not a function of position at the 5' or 3' end of the gene.

The RNAi trigger design also appears to control knockdown success for siRNAs, with more effective siRNAs inducing higher knockdown at lower doses (compare Lv *et al* 2015 & Zhang *et*

al 2015 to Liu *et al* 2010 and Lee *et al* 2015) *(40, 49, 52, 53)*. It may also be that using multiple

siRNAs or dsRNAs will increase likelihood and success of knockdown. For instance in *Ae.*

aegypti embryos, multiplexing two siRNAs resulted in a 9-13% increased suppression compared

to either siRNA alone *(44)*. Similarly, in the emerald ash borer, *Agrilus planipennis*, greater

mortality was achieved when insects were exposed to RNAi triggers targeting multiple genes as

compared to single genes at the same dose *(54)*.

2.5 RNAi trigger length vs success

The length of any dsRNA is generally thought to be linked directly to the efficacy of RNAi

mediated suppression, on the basis that longer dsRNAs cover a greater proportion of the target

gene and as such are more likely to contain an effective siRNA. However 21 nucleotide siRNAs

can yield >95% knockdown in mosquito cells *(49)*. Yet some 'short dsRNAs' (i.e. between 25-

100 bp) are significantly less effective *(48, 55)*. For instance, in *D. melanogaster* lysate, RNAi

trigger products <38 bp did not suppress the reporter and were processed less efficiently than

longer dsRNAs *(48)*. In *Drosophila* S2 cells, shorter dsRNAs and siRNAs are limited by lack of

uptake and may explain for poorer results when using short dsRNAs without transfection *(56)*.

Still, short dsRNAs (96 and 100 bp in length) produced more than 85% knockdown of aldehyde

dehydrogenase 3 transcripts when injected to *Ae. aegypti*, and exemplify the idea that smaller

dsRNAs can be highly functional *in vivo (57)*. By contrast, short ~200 bp RNAi triggers for

IAP1 in *An. gambiae* were significantly less effective at inducing apoptosis compared to longer

~400-650 bp products *(16)*. All of this evidence strongly suggests that extraneous factors such as

sequence structure or transcript abundance may have a greater impact on overall knockdown

than the RNAi trigger length (see Figure 1).

3. Deploying RNAi in the field

3.1 RNAi trigger delivery systems for naked dsRNA

There is potential for delivery of RNAi triggers for insect pest control utilizing a variety of RNAi trigger forms (Figure 2A). Naked, unmodified, RNAi triggers are the simplest delivery approach, exposing insects directly to purified RNAi triggers, but can suffer from environmental degradation as well as degradation in the midgut or hemolymph of the target insect *(58-60)*. Despite these boundaries, numerous examples of successful use of this approach; for instance, naked RNAi triggers can be fed directly, or mixed with food for *per os* delivery *(20).* Feeding RNAi triggers for *Actin* induces RNAi knockdown, stunting and mortality in the Colorado potato beetle, *Leptinotarsa decemlineata (61)*. Knockdown following feeding of dsRNAs targeting *B-tubulin* and *vATPase* produces similar results in other beetle species *(62)*. In flies, prolonged gene knockdown in tsetse fly midguts was observed after *per os* administration of an RNAi trigger for a midgut gene, *tsetseEP (63)*. The cotton bollworm P450 monooxygenase gene was suppressed by plant-mediated expression of an RNAi trigger *(64). Per os* delivery of dsRNAs targeting a cellulose enzyme and a case-regulatory hexamerin storage protein reduced fitness and induced mortality in termites, demonstrating great potential as a novel termiticide *(65)*. In adult mosquitoes, there is a limited number of studies that reveal successful knockdown following *per os* exposure. In *Ae. aegypti*, *vATPase C* was suppressed following exposure to an RNAi trigger in a sucrose meal *(66)*. Alternatively, exposure of dsRNA via blood meals suppressed the early trypsin gene in 30% of exposed *Ae. aegypti (67)*. Un-modified RNAi triggers also are functional when produced as long hairpin RNAs from plasmid expression vectors. RNAi triggers expressed from a plasmid vector, and purified hairpin RNAs have been reported to produce knockdown following injection *(68, 69)*.

Although exposure of naked RNAi triggers is effective in laboratory settings, environmental stability could limit the efficacy of this approach; for example, UV exposure will degrade dsRNA in the field *(61)*. To prevent against degradation, environmental stability can also be enhanced through chemical modification of RNAi triggers (see Figure 2). One option to overcome degradation is to use chemical modifications of nucleotides which can be used to produce a modified base triggers (e.g., morpholinos) or end-stabilized triggers with modifications at the termini. End-stabilized siRNAs with 2'-methoxyl-nucletides or 5' polyethylene glycol can induce target gene knockdown when introduced to *Plutella xylostella*, the diamondback moth *(70, 71)*. In *An. gambiae*, base-modified morpholinos targeting *Mitogen activated protein kinase* induced transcript suppression following *per os* exposure in a synthetic bloodmeal *(72)*.

Although blood-feeding approaches are useful means of delivery in laboratory settings, they are not feasible in a field context. Alternatively, delivery via sugar meals is possible, as demonstrated by Coy *et al (66)* and could have potential to be included in Attractive Toxic Sugar Bait (ATSB) strategies. Sugar meals are deposited in the crop and are released into the midgut when it is potentially free of a peritrophic matrix, and thereby presents the sugar meal content directly to polarized midgut cells. Our studies have shown that naked dsRNA provided in a wide variety of different sugar chemistries rapidly precipitates and does not interact with midgut cells, so an additional carrier or expression system would likely be required to facilitate cellular RNAi trigger uptake.

3.2 Biological expression systems

Beyond production of RNAi triggers by enzymatic or chemical synthesis, long hairpin or short hairpin double-stranded RNAs can be produced by a live bacterium or yeast expression system in a bioreactor context (for mass production of the product), or for both production and delivery of the RNAi trigger (see Figure 2B). The bioreactor production strategy for dsRNA is highly scalable as compared to currently available chemical synthesis approaches. *E. coli* HT115 is dsRNA RNAse-deficient so produces dsRNA without worry of RNA degradation *(73, 74)*. Transformed *E. coli* can be grown in large volume with resulting dsRNA purified in bulk by phenol:chloroform extraction. In one study, a Pet17B plasmid containing an ampicillin resistance cassette, origin of replication, and cloned inverted repeats targeting 3 genes of interest, was mass produced in HT115 *E. coli (75)*. Purified dsRNA inverted repeats were then provided to 2-day-old *Ae. aegypti* larvae resulting in 81- 97% gene suppression of 3 target genes in larval midguts.

Others take this one step further and expose mosquitoes directly to the organism producing the dsRNA. There are several lines of thought for taking on such an approach. For one, biologically produced dsRNA does not need to be expressed in the mosquito and as such does not require transfection or a mosquito-specific promoter. Because RNA is UV-labile and can be quickly degraded in the environment *(58, 59)*, production of dsRNA within an organism such as a bacterium, fungi, or virus may protect the RNA until ingestion by a mosquito larvae or adult. This concept was originally explored by feeding dsRNA-producing *E. coli* to *C. elegans (76)*. The method was translated to mosquito larvae with remarkable efficiency. In one study, live *E. coli* expressing *Ae. aegypti* sexual dependency genes (embedded in agar pellets) were fed to larvae, resulting in sterility in up to 90% of adults *(77)*. Direct injection of the same dsRNAs to pupae resulted in ~ 70-95% gene suppression and similar levels of sterility, underscoring the efficacy of the approach. Although *E. coli* serves as a model for RNAi trigger production,

transformation of entomopathogenic bacteria is possible (Table 1). For instance, *E. coli* expressing chymotrypsin RNAi triggers were fed to *Spodoptera exigua* and produced knockdown and reduced pupation rate, despite rapid degradation of dsRNA in the insect midgut *(78)*. Interestingly, exposure to *E. coli* expressing RNAi triggers led to over-expression of target genes in the oriental fruit fly *Bactrocera dorsalis (74)*.

Knockdown of target genes can also be mediated through expressing RNAi triggers via insect microbial symbionts. In the kissing bug, *Rhodnius prolixus,* the midgut symbiont, *Rhodococcus rhodnii*, was transformed to express and RNAi trigger for a heme-binding protein and catalase gene; when this bacterium was fed to nymphs and adults, target gene suppression was observed and phenotypically resulted in disrupted oviposition *(79)*. Symbionts are essential for development and fitness including: immunity, nutrient uptake, and reproductive success in mosquito species *(80)*. A wide variety of symbionts exist in mosquito midguts but vary by local environment and as such it is not likely that any specific combination of symbionts is essential *(81)*. For instance, in *Ae. aegypti,* axenic larvae lack the capacity to molt and develop, and provision of *Escherichia coli* rescues development *(82).* In *An. gambiae*, transformed *Pantoea agglomerans* and *Serratia* AS1 bacterial symbionts can establish and proliferate in adult midguts *(83, 84).* Considering this, it is feasible to utilize laboratory, symbiotic, or even entomopathogenic bacteria as delivery systems for RNAi triggers in mosquito species. Bacterial bio-control species as *Wolbachia* are well known to colonize mosquitoes and act as living 'gene drive' systems through altering reproductive success *(85, 86)*. Taking this a step further, molecular gene drive systems such as CRISPR/Cas9 have been successfully used for gene editing in *Bacillus subtilis* and perhaps could be used to drive expression of an RNAi trigger in *Bacillus thuringiensis* and *Bacillus sphaericus,* and possibly even *Wolbachia (87)*. Combined

microbial and RNAi strategies have yet to be explored for control of mosquitoes or mosquito-borne pathogens, and would likely be subject to regulatory constraints or considerations for use in the field.

Yeast expression likewise offer a viable means of producing RNAi triggers. In one study, *Pichia pastoris* were transformed with the pPicZB plasmid containing a long hairpin RNAi trigger for the *Ae. aegypti* juveline hormone acid methyl transferase gene *(88)*. Yeasts were fermented and fed to larvae. At 144 hours post-feeding, methyl transferase transcripts were measured, finding greater than 90% knockdown in larvae which had died as a result of exposure, as well as greater than 50% knockdown in living larvae. *P. pastoris* have also been successfully transformed using CRISPR/Cas9 *(89, 90)*. With high-throughput, heritable transformation systems in place, numerous RNAi triggers could be tested and subsequently produced *en masse,* overcoming the issue of scaling findings from lab to field settings.

In addition to easy to cultivate bioreactor expression systems, entomopathogenic fungi have also been transformed with insecticidal toxins resulting in rapid mortality (Table 1, Figure 2). Entomopathogenic fungi are currently showing promise when applied to cloth and may be translatable to deliver RNAi triggers to mosquitoes via bed nets in the future *(91)*. *B. bassiana* is also amenable to CRISPR/Cas9 transformation and therefore can also be utilized to deliver RNAi triggers that enhance mortality and species-specificity *(92)*. Alternatively, delivery of *Beuvaria bassiana* via the proboscis reduces longevity of *An. gambiae* and therefore may be utilized in *per os* approaches such as ATSBs *(93)*.

Finally, viral expression systems offer a sophisticated means of delivering RNAi triggers and are well-studied in the context of controlling a variety of insect pests *(94)*. A virus expression vector

has the advantage of delivering an RNAi trigger directly to the cytosol and therefore the RNAi cellular machinery. A short hairpin or long hairpin dsRNA sequence can be inserted into an infectious clone of a viral genome to enable expression of the RNAi trigger directly. As a case in point, a modified densovirus containing a hairpin dsRNA for ATPase reduced the lifespan of *Ae. albopictus* larvae beyond densovirus infection alone *(95)*. One can imagine the possibilities of utilizing vertically transmitted, insect-specific flaviviruses *(96)* to express an RNAi trigger and thereby reduce target gene expression.

3.3 Nanoparticle RNAi delivery systems

The vast majority of nanoparticle systems used for delivery of RNAi triggers in insects are polymer-based. RNAi triggers can be combined with nanoparticles by degradable or non-degradable linker chemistries (Figure 2 C). Here, we separate approaches into three sub-classes of polymer type nanoparticles, including: *enmeshment* of RNAi triggers into a defined matrix or layer-by-layer particle (e.g. PEG particles), *encapsulation* of RNAi triggers during formation of self-aggregating structures (e.g. chitosan particles), or *chemical linkage* of RNAi triggers to the exterior of biological macromolecules or polymers (e.g. cell penetrating peptides) (see Figure 2).

Encapsulated nanoparticles can take a variety of chemistries and forms, but in general these particles self-aggregate and are not covalently linked to RNAi triggers, but rather capture them in solution during formation. Encapsulation can facilitate both uptake and protect RNAi triggers from degradation. For instance topical application of RNAi triggers was successfully applied to the tick *Rhipicephalus haemaphysaloides* when RNAi triggers are encapsulated in liposomes *(97)*. In our work, we have found that topical application results in no uptake nor phenotypic change when mosquitoes are exposed to RNAi triggers targeting *IAP1 (16)*.

Chitosan nanoparticles are the most well studied example of this in insects. Chitosan

encapsulation of dsRNAs resulted in knockdown following *per os* delivery in *An. gambiae* and

Ae. aegypti larvae *(53, 98-100)*. Delivery of dsRNA cognate to an *An. gambiae* chitinase gene

(*AgCHS1*) to larval midgut cells dramatically reduced chitin synthesis in epidermal cells,

demonstrating not only efficient *per os* environmental delivery of an RNAi effector molecule but

also a systemic response in the target organism *(98)*. Furthermore, chitosan-based nanoparticles

generate complexes with siRNA large enough for cell uptake so may promote the efficacy of

these small RNA species *(98)*. Similarly, *Ae. aegypti* larvae treated with chitosan nanoparticles

targeting the wing development gene *vestigial* died prior to adulthood *(99)*. In a comparative

analysis of nanoparticle delivery systems targeting *Ae. aegypti* larvae, chitosan was less toxic

and increased target gene knockdown when compared to polyethylene glycol (PEG) based

quantum dots and amine-functionalized silica nanoparticles *(100)*.

Other than chitosan, synthetic polymer encapsulation approaches for insect delivery include

RNAi triggers incorporated into PEG particles, silica particles, perfluorocarbon and phospholipid

nanodroplet emulsions, or complexed with amine / methacrylate co-polymers *(100-105)*. RNAi

triggers encapsulated in PEG particles formed using PRINT (Particle Replication in Non-wetting

Templates) technology have been are internalized in *An. gambiae* cells and have been exposed to

larval and adult stage mosquitoes *(101, 102)*. As mentioned above, PEG based quantum dots are

also functional as delivery systems for RNAi knockdown in *Ae. aegypti* larvae, but are mildly

toxic alone (~20% larval mortality when complexed with GFP dsRNA) *(100)*. Indeed, graphene

quantum dots were also found to be inherently toxic to both *Anopheles stephensi* larvae and

Plasmodium and as such these particular quantum dots may need additional scrutiny for safety

(106). For use in *Spodoptera exigua,* co-polymer particles were designed to withstand alkaline

gut pH and deliver RNAi triggers capable of inducing larval mortality *(103)*. Emulsions of perfluorocarbon and phosopholipids have also been utilized to successfully deliver RNAi triggers to both bees and aphids through the spiracles via an aerosol spray approach *(104, 105, 107)*. Overall, polymer based particles are particularly attractive for development because polymer production is scalable as well as moldable and can be modified to alter particle charge, shape, or other surface chemistries required for tissue distribution and RNAi trigger fate in larval and adult mosquitoes.

Finally, enmeshed nanoparticle approaches to RNAi trigger delivery are limited in insects, however in *Acyrthosiphon pisum* pea aphids *per os* delivery of dsRNAs enmeshed in bi-layer branched amphiphilic peptide capsules resulted in knockdown and death *(108)*. More sophisticated enmeshed type PEG nanoparticles have also been developed and tested in mammalian systems whereby pH cleavable linkers between the particle and RNAi trigger facilitate direct cytosol release *(109)*. Development of enmeshed RNAi nanoparticles in mosquitoes is lacking despite a wealth of knowledge regarding polymeric and non-biotic nanoparticles as insecticides *(110)*.

A less-developed system for delivery of chemically-linked RNAi triggers in insects is cell penetrating peptides (CPPs) and double stranded RNA binding proteins, which bind via covalent modification linkages or via ionic binding and deliver siRNAs to the cytosol through cell-penetration or endocytosis *(111-113)*. While many designs exist and progress has been made to deliver RNAi triggers in mammalian cells, there is limited exploration of CPPs in insects. However one study successfully demonstrated CPP uptake of plasmid DNA to *Spodoptera frugiperda (114)*. A number of CPPs are also toxic to insects and protozoan parasites and have

impact on mosquitoes and *Plasmodium (115, 116)*; this could be further developed to include an RNAi trigger as a synergist to the observed activity.

4. Conclusions

RNAi technology for arthropod pest control is already providing a next generation of insecticidal interventions for a number of agricultural pests. The technology affords potential to rapidly adapt new lethal RNAi targets to pest species with ever-evolving specific and metabolic insecticide resistance mechanisms. Using an informed, biorational approach to develop an RNAi trigger to a gene with the desired adverse phenotype, one could generate triggers that provide maximum levels of gene suppression and deliver that RNA species to the target tissue of interest using the method of delivery most likely to put the RNAi trigger in its place. For public health pest control purposes, this is truly a life-saving proposition because vector control has repeatedly proven to reduce human cases of a number of mosquito-borne diseases.

Literature cited

1. EPA-USA. *Mosquito Control | US EPA*. December 19 2016 [cited 2018 May 18]; Available from: https://www.epa.gov/mosquitocontrol.

2. EPA-USA. *Permethrin, Resmethrin, d-Phenothrin (Sumithrin®): Synthetic Pyrethroids For Mosquito Control | US EPA*. March 28 2017; Available from: https://www.epa.gov/mosquitocontrol/permethrin-resmethrin-d-phenothrin-sumithrinr-synthetic-pyrethroids-mosquito-control.

3. WHO. *WHO specifications for pesticides used in public health*. [cited 2018 May 18]; Available from: http://www.who.int/whopes/quality/newspecif/en/.

4.   Lacey, L.A., *Bacillus thuringiensis serovariety israelensis and Bacillus sphaericus for mosquito control.* J Am Mosq Control Assoc, 2007. **23**(2 Suppl): p. 133-63.

5.   Goldberg, L.J. and J. Margalit, *Bacterial Spore Demonstrating Rapid Larvicidal Activity against Anopheles-Sergentii, Uranotaenia-Unguiculata, Culex-Univitattus, Aedes-Aegypti and Culex-Pipiens.* Mosquito News, 1977. **37**(3): p. 355-361.

6.   EPA-USA. *Insect Growth Regulators: S-Hydroprene (128966), S-Kinoprene (107502), Methoprene (105401), S-Methoprene (105402) Fact Sheet* [cited 2018 May 18]; Available from: https://www3.epa.gov/pesticides/chem_search/reg_actions/registration/fs_G-107_06-Dec-01.pdf.

7.   Kirst, H.A., *The spinosyn family of insecticides: realizing the potential of natural products research.* J Antibiot (Tokyo), 2010. **63**(3): p. 101-11.

8.   Bhatt, S., et al., *The effect of malaria control on Plasmodium falciparum in Africa between 2000 and 2015.* Nature, 2015. **526**(7572): p. 207-211.

9.   Hoppe, M., et al., *Evaluation of Commercial Agrochemicals as New Tools for Malaria Vector Control.* Chimia (Aarau), 2016. **70**(10): p. 721-729.

10.   Turner, J.A., C.N. Ruscoe, and T.R. Perrior, *Discovery to Development: Insecticides for Malaria Vector Control.* Chimia (Aarau), 2016. **70**(10): p. 684-693.

11.   Vijayendran, D., et al., *Arthropod viruses and small RNAs.* J Invertebr Pathol, 2013. **114**(2): p. 186-95.

12.   Sanchez-Vargas, I., et al., *RNA interference, arthropod-borne viruses, and mosquitoes.* Virus Res, 2004. **102**(1): p. 65-74.

13.   Blair, C.D., *Mosquito RNAi is the major innate immune pathway controlling arbovirus infection and transmission.* Future Microbiol, 2011. **6**(3): p. 265-77.

14.   Loy, J.D., et al., *Sequence-optimized and targeted double-stranded RNA as a therapeutic antiviral treatment against infectious myonecrosis virus in Litopenaeus vannamei.* Dis Aquat Organ, 2013. **105**(1): p. 57-64.

15.   Bartholomay, L.C., et al., *Nucleic-acid based antivirals: augmenting RNA interference to 'vaccinate' Litopenaeus vannamei.* J Invertebr Pathol, 2012. **110**(2): p. 261-6.

16.   Airs, P.M., *Manipulating cell death and RNA interference processes for mosquito control*, in *Pathobiological Sciences*. 2018, University of Wisconsin Madison.

17.   Airs, P.M. and L.C. Bartholomay, *RNA Interference for Mosquito and Mosquito-Borne Disease Control.* Insects, 2017. **8**(1).

18.   Scott, J.G., et al., *Towards the elements of successful insect RNAi.* J Insect Physiol, 2013. **59**(12): p. 1212-21.

19.   Yu, N., et al., *Delivery of dsRNA for RNAi in insects: an overview and future directions.* Insect Sci, 2013. **20**(1): p. 4-14.

20.   Whyard, S., A.D. Singh, and S. Wong, *Ingested double-stranded RNAs can act as species-specific insecticides.* Insect Biochem Mol Biol, 2009. **39**(11): p. 824-32.

21.   Hapairai, L.K., et al., *Lure-and-Kill Yeast Interfering RNA Larvicides Targeting Neural Genes in the Human Disease Vector Mosquito Aedes aegypti.* Scientific Reports, 2017. **7**(1): p. 13223.

22.   Makkonen, K.E., K. Airenne, and S. Yla-Herttulala, *Baculovirus-mediated gene delivery and RNAi applications.* Viruses, 2015. **7**(4): p. 2099-125.

23.   Sánchez-Vargas, I., et al., *Dengue Virus Type 2 Infections of Aedes aegypti Are Modulated by the Mosquito's RNA Interference Pathway.* PLOS Pathogens, 2009. **5**(2): p. e1000299.

24.   Blair, C.D., *Mosquito RNAi is the major innate immune pathway controlling arbovirus infection and transmission.* Future microbiology, 2011. **6**(3): p. 265-277.

25.   Goic, B., et al., *Virus-derived DNA drives mosquito vector tolerance to arboviral infection.* Nat Commun, 2016. **7**: p. 12410.

26.   Kemp, C., et al., *Broad RNA interference-mediated antiviral immunity and virus-specific inducible responses in Drosophila.* J Immunol, 2013. **190**(2): p. 650-8.

27.   Saleh, M.C., et al., *Antiviral immunity in Drosophila requires systemic RNA interference spread.* Nature, 2009. **458**(7236): p. 346-50.

28.   Nayak, A., et al., *RNA interference-mediated intrinsic antiviral immunity in invertebrates.* Curr Top Microbiol Immunol, 2013. **371**: p. 183-200.

29.   Mongelli, V. and M.C. Saleh, *Bugs Are Not to Be Silenced: Small RNA Pathways and Antiviral Responses in Insects.* Annu Rev Virol, 2016. **3**(1): p. 573-589.

30.   Olson, K.E. and C.D. Blair, *Arbovirus-mosquito interactions: RNAi pathway.* Curr Opin Virol, 2015. **15**: p. 119-26.

31.   Hoa, N.T., et al., *Characterization of RNA interference in an Anopheles gambiae cell line.* Insect biochemistry and molecular biology, 2003. **33**: p. 949-957.

32.   Sontheimer, E.J., *Assembly and function of RNA silencing complexes.* Nat Rev Mol Cell Biol, 2005. **6**(2): p. 127-38.

33.   van Rij, R.P., et al., *The RNA silencing endonuclease Argonaute 2 mediates specific antiviral immunity in Drosophila melanogaster.* Genes Dev, 2006. **20**(21): p. 2985-95.

34.   Sijen, T., et al., *On the role of RNA amplification in dsRNA-triggered gene silencing.* Cell, 2001. **107**(4): p. 465-76.

35.   Winston, W.M., C. Molodowitch, and C.P. Hunter, *Systemic RNAi in C. elegans requires the putative transmembrane protein SID-1.* Science, 2002. **295**(5564): p. 2456-9.

36.   Gordon, K.H. and P.M. Waterhouse, *RNAi for insect-proof plants.* Nat Biotechnol, 2007. **25**(11): p. 1231-2.

37.   Tassetto, M., M. Kunitomi, and R. Andino, *Circulating Immune Cells Mediate a Systemic RNAi-Based Adaptive Antiviral Response in Drosophila.* Cell, 2017. **169**(2): p. 314-325.e13.

38.   Boisson, B., et al., *Gene silencing in mosquito salivary glands by RNAi.* FEBS Lett, 2006. **580**(8): p. 1988-92.

39.   Mysore, K., et al., *siRNA-Mediated Silencing of doublesex during Female Development of the Dengue Vector Mosquito Aedes aegypti.* PLoS neglected tropical diseases, 2015. **9**: p. e0004213.

40.   Liu, C., et al., *Distinct olfactory signaling mechanisms in the malaria vector mosquito Anopheles gambiae.* PLoS biology, 2010. **8**.

41.   Nguyen, C., et al., *Functional genetic characterization of salivary gland development in Aedes aegypti.* EvoDevo, 2013. **4**: p. 9.

42.   Sarro, J., et al., *Requirement for commissureless2 function during dipteran insect nerve cord development.* Developmental dynamics : an official publication of the American Association of Anatomists, 2013. **242**: p. 1466-77.

43.   Clemons, A., et al., *siRNA-mediated gene targeting in Aedes aegypti embryos reveals that frazzled regulates vector mosquito CNS development.* PloS one, 2011. **6**: p. e16730.

44.   Haugen, M., et al., *Semaphorin-1a is required for Aedes aegypti embryonic nerve cord development.* PloS one, 2011. **6**: p. e21694.

45.   Mysore, K., et al., *Yeast interfering RNA larvicides targeting neural genes induce high rates of Anopheles larval mortality.* Malaria Journal, 2017. **16**(1): p. 461.

46.   Elbashir, S.M., et al., *Functional anatomy of siRNAs for mediating efficient RNAi in Drosophila melanogaster embryo lysate.* EMBO J, 2001. **20**(23): p. 6877-88.

47.   Elbashir, S.M., et al., *Duplexes of 21-nucleotide RNAs mediate RNA interference in cultured mammalian cells.* Nature, 2001. **411**(6836): p. 494-8.

48.   Elbashir, S.M., W. Lendeckel, and T. Tuschl, *RNA interference is mediated by 21- and 22-nucleotide RNAs.* Genes Dev, 2001. **15**(2): p. 188-200.

49.   Lee, R.C.H. and J.J.H. Chu, *Proteomics profiling of chikungunya-infected Aedes albopictus C6/36 cells reveal important mosquito cell factors in virus replication.* PLoS neglected tropical diseases, 2015. **9**: p. e0003544.

50.   Conway, M.J., et al., *Mosquito saliva serine protease enhances dissemination of dengue virus into the mammalian host.* Journal of virology, 2014. **88**: p. 164-175.

51.   Isoe, J., et al., *Molecular genetic analysis of midgut serine proteases in Aedes aegypti mosquitoes.* Insect biochemistry and molecular biology, 2009. **39**: p. 903-912.

52.   Lv, Y., et al., *Venom allergen 5 is Associated With Deltamethrin Resistance in Culex pipiens pallens (Diptera: Culicidae).* Journal of medical entomology, 2015. **52**: p. 672-682.

53.   Zhang, Q., G. Hua, and M.J. Adang, *Chitosan/DsiRNA nanoparticle targeting identifies AgCad1 cadherin in Anopheles gambiae larvae as an in vivo receptor of Cry11Ba toxin of Bacillus thuringiensis subsp. jegathesan.* Insect biochemistry and molecular biology, 2015. **60**: p. 33-38.

54.   Rodrigues, T.B., et al., *Development of RNAi method for screening candidate genes to control emerald ash borer, Agrilus planipennis.* Scientific Reports, 2017. **7**(1): p. 7379.

55.   Hammond, S.M., et al., *An RNA-directed nuclease mediates post-transcriptional gene silencing in Drosophila cells.* Nature, 2000. **404**(6775): p. 293-6.

56.   Saleh, M.C., et al., *The endocytic pathway mediates cell entry of dsRNA to induce RNAi silencing.* Nat Cell Biol, 2006. **8**(8): p. 793-802.

57.   Rivera-Perez, C., et al., *Aldehyde dehydrogenase 3 converts farnesal into farnesoic acid in the corpora allata of mosquitoes.* Insect biochemistry and molecular biology, 2013. **43**: p. 675-682.

58.   Dubelman, S., et al., *Environmental fate of double-stranded RNA in agricultural soils.* PLoS One, 2014. **9**(3): p. e93155.

59.   Fischer, J.R., et al., *Aquatic fate of a double-stranded RNA in a sediment-water system following an over-water application.* Environ Toxicol Chem, 2016.

60.   Wynant, N., et al., *Identification, functional characterization and phylogenetic analysis of double stranded RNA degrading enzymes present in the gut of the desert locust, Schistocerca gregaria.* Insect Biochem Mol Biol, 2014. **46**: p. 1-8.

61.   San Miguel, K. and J.G. Scott, *The next generation of insecticides: dsRNA is stable as a foliar-applied insecticide.* Pest Manag Sci, 2016. **72**(4): p. 801-9.

62.   Baum, J.A., et al., *Control of coleopteran insect pests through RNA interference.* Nat Biotechnol, 2007. **25**.

63.   Walshe, D.P., et al., *Prolonged gene knockdown in the tsetse fly Glossina by feeding double stranded RNA.* Insect Mol Biol, 2009. **18**(1): p. 11-9.

64.   Mao, Y.B., et al., *Silencing a cotton bollworm P450 monooxygenase gene by plant-mediated RNAi impairs larval tolerance of gossypol.* Nat Biotechnol, 2007. **25**(11): p. 1307-13.

65. Zhou, X., et al., *RNA interference in the termite Reticulitermes flavipes through ingestion of double-stranded RNA.* Insect Biochem Mol Biol, 2008. **38**(8): p. 805-15.

66. Coy, M.R., et al., *Gene silencing in adult Aedes aegypti mosquitoes through oral delivery of double-stranded RNA.* Journal of Applied Entomology, 2012. **136**: p. 741-748.

67. Brackney, D.E., B.D. Foy, and K.E. Olson, *The effects of midgut serine proteases on dengue virus type 2 infectivity of Aedes aegypti.* Am J Trop Med Hyg, 2008. **79**(2): p. 267-74.

68. Peng, R., et al., *In vivo functional genomic studies of sterol carrier protein-2 gene in the yellow fever mosquito.* PLoS One, 2011. **6**(3): p. e18030.

69. Abraham, E.G., et al., *An immune-responsive serpin, SRPN6, mediates mosquito defense against malaria parasites.* Proc Natl Acad Sci U S A, 2005. **102**(45): p. 16327-32.

70. Gong, L., et al., *Testing insecticidal activity of novel chemically synthesized siRNA against Plutella xylostella under laboratory and field conditions.* PLoS One, 2013. **8**(5): p. e62990.

71. Gong, L., et al., *Silencing of Rieske iron-sulfur protein using chemically synthesised siRNA as a potential biopesticide against Plutella xylostella.* Pest Manag Sci, 2011. **67**(5): p. 514-20.

72. Pietri, J.E., K.W. Cheung, and S. Luckhart, *Knockdown of mitogen-activated protein kinase (MAPK) signalling in the midgut of Anopheles stephensi mosquitoes using antisense morpholinos.* Insect molecular biology, 2014. **23**: p. 558-565.

73. Takiff, H.E., S.M. Chen, and D.L. Court, *Genetic analysis of the rnc operon of Escherichia coli.* J Bacteriol, 1989. **171**(5): p. 2581-90.

74. Li, X., M. Zhang, and H. Zhang, *RNA interference of four genes in adult Bactrocera dorsalis by feeding their dsRNAs.* PLoS One, 2011. **6**(3): p. e17788.

75.   Saengwiman, S., et al., *In vivo identification of Bacillus thuringiensis Cry4Ba toxin receptors by RNA interference knockdown of glycosylphosphatidylinositol-linked aminopeptidase N transcripts in Aedes aegypti larvae.* Biochemical and biophysical research communications, 2011. **407**: p. 708-713.

76.   Timmons, L., D.L. Court, and A. Fire, *Ingestion of bacterially expressed dsRNAs can produce specific and potent genetic interference in Caenorhabditis elegans.* Gene, 2001. **263**(1-2): p. 103-12.

77.   Whyard, S., et al., *Silencing the buzz: a new approach to population suppression of mosquitoes by feeding larvae double-stranded RNAs.* Parasites & vectors, 2015. **8**: p. 96.

78.   Vatanparast, M. and Y. Kim, *Optimization of recombinant bacteria expressing dsRNA to enhance insecticidal activity against a lepidopteran insect, Spodoptera exigua.* PLOS ONE, 2017. **12**(8): p. e0183054.

79.   Taracena, M.L., et al., *Genetically modifying the insect gut microbiota to control Chagas disease vectors through systemic RNAi.* PLoS Negl Trop Dis, 2015. **9**(2): p. e0003358.

80.   Strand, M.R., *Chapter 11 - The Gut Microbiota of Mosquitoes: Diversity and Function A2 - Wikel, Stephen K*, in *Arthropod Vector: Controller of Disease Transmission, Volume 1*, S. Aksoy and G. Dimopoulos, Editors. 2017, Academic Press. p. 185-199.

81.   Dickson, L.B., et al., *Diverse laboratory colonies of Aedes aegypti harbor the same adult midgut bacterial microbiome.* Parasit Vectors, 2018. **11**(1): p. 207.

82.   Coon, K.L., et al., *Bacteria-mediated hypoxia functions as a signal for mosquito development.* Proc Natl Acad Sci U S A, 2017. **114**(27): p. E5362-e5369.

83.   Wang, S., et al., *Driving mosquito refractoriness to Plasmodium falciparum with engineered symbiotic bacteria.* Science, 2017. **357**(6358): p. 1399-1402.

84.   Wang, S., et al., *Fighting malaria with engineered symbiotic bacteria from vector mosquitoes.* Proceedings of the National Academy of Sciences of the United States of America, 2012. **109**(31): p. 12734-12739.

85.   Bourtzis, K., et al., *Harnessing mosquito–Wolbachia symbiosis for vector and disease control.* Acta Tropica, 2014. **132**: p. S150-S163.

86.   Werren, J.H., *Biology of Wolbachia.* Annual Review of Entomology, 1997. **42**(1): p. 587-609.

87.   Altenbuchner, J., *Editing of the Bacillus subtilis Genome by the CRISPR-Cas9 System.* Appl Environ Microbiol, 2016. **82**(17): p. 5421-7.

88.   Van Ekert, E., et al., *Control of larval and egg development in Aedes aegypti with RNA interference against juvenile hormone acid methyl transferase.* Journal of insect physiology, 2014. **70**: p. 143-150.

89.   Weninger, A., et al., *Expanding the CRISPR/Cas9 toolkit for Pichia pastoris with efficient donor integration and alternative resistance markers.* J Cell Biochem, 2018. **119**(4): p. 3183-3198.

90.   Weninger, A., et al., *Combinatorial optimization of CRISPR/Cas9 expression enables precision genome engineering in the methylotrophic yeast Pichia pastoris.* Journal of Biotechnology, 2016. **235**: p. 139-149.

91.   Silva L. E. I., et al., *A new method of deploying entomopathogenic fungi to control adult Aedes aegypti mosquitoes.* Journal of Applied Entomology, 2018. **142**(1-2): p. 59-66.

92.   Chen, J., et al., *CRISPR/Cas9-mediated efficient genome editing via blastospore-based transformation in entomopathogenic fungus Beauveria bassiana.* Sci Rep, 2017. **8**: p. 45763.

93.   Ishii, M., et al., *Proboscis infection route of Beauveria bassiana triggers early death of Anopheles mosquito.* Scientific Reports, 2017. **7**(1): p. 3476.

94.   Kolliopoulou, A., et al., *Viral Delivery of dsRNA for Control of Insect Agricultural Pests and Vectors of Human Disease: Prospects and Challenges.* Frontiers in Physiology, 2017. **8**(399).

95.   Gu, J., et al., *Development of an efficient recombinant mosquito densovirus-mediated RNA interference system and its preliminary application in mosquito control.* PloS one, 2011. **6**: p. e21329.

96.   Blitvich, B.J. and A.E. Firth, *Insect-Specific Flaviviruses: A Systematic Review of Their Discovery, Host Range, Mode of Transmission, Superinfection Exclusion Potential and Genomic Organization.* Viruses, 2015. **7**(4): p. 1927-1959.

97.   Zhang, Y., et al., *Liposome mediated double-stranded RNA delivery to silence ribosomal protein P0 in the tick Rhipicephalus haemaphysaloides.* Ticks and Tick-borne Diseases, 2018. **9**(3): p. 638-644.

98.   Zhang, X., J. Zhang, and K.Y. Zhu, *Chitosan/double-stranded RNA nanoparticle-mediated RNA interference to silence chitin synthase genes through larval feeding in the African malaria mosquito (Anopheles gambiae).* Insect molecular biology, 2010. **19**: p. 683-693.

99.   Ramesh Kumar, D., et al., *Delivery of chitosan/dsRNA nanoparticles for silencing of wing development vestigial (vg) gene in Aedes aegypti mosquitoes.* Int J Biol Macromol, 2016. **86**: p. 89-95.

100.   Das, S., et al., *Chitosan, Carbon Quantum Dot, and Silica Nanoparticle Mediated dsRNA Delivery for Gene Silencing in Aedes aegypti: A Comparative Analysis.* ACS Appl Mater Interfaces, 2015. **7**(35): p. 19530-5.

101. Paquette, C.C., et al., *Biodistribution and trafficking of hydrogel nanoparticles in adult mosquitoes.* PLoS Negl Trop Dis, 2015. **9**(5): p. e0003745.

102. Phanse, Y., et al., *Biodistribution and Toxicity Studies of PRINT Hydrogel Nanoparticles in Mosquito Larvae and Cells.* PLoS Negl Trop Dis, 2015. **9**(5): p. e0003735.

103. Christiaens, O., et al., *Increased RNAi Efficacy in Spodoptera exigua via the Formulation of dsRNA With Guanylated Polymers.* Frontiers in Physiology, 2018. **9**(316).

104. Thairu M. W., et al., *Efficacy of RNA interference knockdown using aerosolized short interfering RNAs bound to nanoparticles in three diverse aphid species.* Insect Molecular Biology, 2017. **26**(3): p. 356-368.

105. Li-Byarlay, H., et al., *RNA interference knockdown of DNA methyl-transferase 3 affects gene alternative splicing in the honey bee.* Proc Natl Acad Sci U S A, 2013. **110**(31): p. 12750-5.

106. Murugan, K., et al., *Nanofabrication of Graphene Quantum Dots with High Toxicity Against Malaria Mosquitoes, Plasmodium falciparum and MCF-7 Cancer Cells: Impact on Predation of Non-target Tadpoles, Odonate Nymphs and Mosquito Fishes.* Journal of Cluster Science, 2017. **28**(1): p. 393-411.

107. Kaneda, M.M., et al., *Mechanisms of nucleotide trafficking during siRNA delivery to endothelial cells using perfluorocarbon nanoemulsions.* Biomaterials, 2010. **31**(11): p. 3079-3086.

108. Avila, L.A., et al., *Delivery of lethal dsRNAs in insect diets by branched amphiphilic peptide capsules.* J Control Release, 2018. **273**: p. 139-146.

109. Dunn, S.S., et al., *Reductively responsive siRNA-conjugated hydrogel nanoparticles for gene silencing.* J Am Chem Soc, 2012. **134**(17): p. 7423-30.

110.   Benelli, G., *Mode of action of nanoparticles against insects.* Environ Sci Pollut Res Int, 2018.

111.   Eguchi, A., et al., *Efficient siRNA delivery into primary cells by a peptide transduction domain-dsRNA binding domain fusion protein.* Nat Biotechnol, 2009. **27**(6): p. 567-71.

112.   Meade, B.R. and S.F. Dowdy, *Exogenous siRNA delivery using peptide transduction domains/cell penetrating peptides.* Adv Drug Deliv Rev, 2007. **59**(2-3): p. 134-40.

113.   Meade, B.R., et al., *Efficient delivery of RNAi prodrugs containing reversible charge-neutralizing phosphotriester backbone modifications.* Nat Biotechnol, 2014. **32**(12): p. 1256-61.

114.   Chen, Y.J., et al., *A gene delivery system for insect cells mediated by arginine-rich cell-penetrating peptides.* Gene, 2012. **493**(2): p. 201-10.

115.   Arrighi, R.B., et al., *Cell-penetrating peptide TP10 shows broad-spectrum activity against both Plasmodium falciparum and Trypanosoma brucei brucei.* Antimicrob Agents Chemother, 2008. **52**(9): p. 3414-7.

116.   Hughes, S.R., P.F. Dowd, and E.T. Johnson, *Cell-penetrating recombinant peptides for potential use in agricultural pest control applications.* Pharmaceuticals (Basel), 2012. **5**(10): p. 1054-63.

117.   Frankenhuyzen, K.v., *Insecticidal activity of Bacillus thuringiensis crystal proteins.* Journal of Invertebrate Pathology, 2009. **101**(1): p. 1-16.

118.   Berry, C., et al., *Genetic determinants of host ranges of Bacillus sphaericus mosquito larvicidal toxins.* Journal of Bacteriology, 1993. **175**(2): p. 510-518.

119.   Rungrod, A., et al., *Bacillus sphaericus Mtx1 and Mtx2 toxins co-expressed in Escherichia coli are synergistic against Aedes aegypti larvae.* Biotechnology Letters, 2009. **31**(4): p. 551-555.

120.   Wirth, M.C., et al., *Mtx Toxins Synergize Bacillus sphaericus and Cry11Aa against Susceptible and Insecticide-Resistant Culex quinquefasciatus Larvae.* Applied and Environmental Microbiology, 2007. **73**(19): p. 6066-6071.

121.   Jones, G.W., et al., *The Cry48Aa-Cry49Aa binary toxin from Bacillus sphaericus exhibits highly restricted target specificity.* Environmental Microbiology, 2008. **10**(9): p. 2418-2424.

122.   Zlotkin, E., Y. Fishman, and M. Elazar, *AaIT: From neurotoxin to insecticide.* Biochimie, 2000. **82**(9): p. 869-881.

123.   Ji, S.J., et al., *Recombinant scorpion insectotoxin AaIT kills specifically insect cells but not human cells.* Cell Research, 2002. **12**: p. 143.

124.   Deng, S.-Q., et al., *Scorpion neurotoxin AaIT-expressing Beauveria bassiana enhances the virulence against Aedes albopictus mosquitoes.* AMB Express, 2017. **7**(1): p. 121.

125.   Higgs, S., et al., *Mosquito sensitivity to a scorpion neurotoxin expressed using an infectious Sindbis virus vector.* Insect Molecular Biology, 1995. **4**(2): p. 97-103.

126.   Fiorenzano, J.M., P.G. Koehler, and R.D. Xue, *Attractive Toxic Sugar Bait (ATSB) For Control of Mosquitoes and Its Impact on Non-Target Organisms: A Review.* Int J Environ Res Public Health, 2017. **14**(4).

Tables & Figures

Table 1. Mosquito control strategies with capacity for RNAi integration

Approach	Active component	RNAi integration potential	Spectrum of activity	Note	Ref
Bacterial toxins					
Bacillus thuringiensis israeliensis	*Cry* toxins	expression of hairpin RNA	Diptera	Many *Cry* toxins, varied host specificity.	*(117)*
Bacillus sphaericus	*Mtx* & *Cry* toxins	expression of hairpin RNA	Mosquito	Toxins differentially synergistic against mosquito genera.	*(118-120)*
Bacillus sphaericus	Cry48Aa/Cry49Aa	expression of hairpin RNA	*Culex*	Not active against *Aedes, Anopheles,* Dipterans, Lepidoptera tested.	*(121)*
Spider & Scorpion toxins					
Metarhizium pingshaense	AaIT* toxin & Hybrid toxin†	expression of hairpin RNA	Insect	Toxins and fungus have broad spectrum insect activity	*(122, 123)*
Beauveria bassiana	AaIT* toxin	expression of hairpin RNA	Insect	Toxins and fungus have broad spectrum insect activity	*(124)*
Arboviruses	AaIT* toxin	expression of hairpin RNA	Mosquito	Virus limits host specificity, requires artificial blood-meal for uptake.	*(95, 125)*
Chemical insecticides					
ATSB	Chemical insecticides[Δ]	Naked RNA	Varied	May result in limited uptake due to condensation or degradation of RNAi trigger	*(66, 126)*

ATSB	Chemical insecticides$^\Delta$	Modified nucleic acid / Morpholino	Varied	Only tested example uses artificial blood-meal with sufficient uptake.	*(72)*
ATSB	Chemical insecticides$^\Delta$	Nanoparticle complexed RNA	Varied	Only tested using PEG nanoparticles.	*(101)*
ATSB	Chemical insecticides$^\Delta$	Bacterial expression	Varied	Used targeting larval stage but has potential to target adults.	*(21, 77)*
ATSB	Chemical insecticides$^\Delta$	Yeast expression	Varied	Mostly tested against larval stage, but yeast commonly used in ATSBs	*(21, 88)*
LLIN/ ITN/ IRS	Pyrethroids	Naked RNA, nanoparticle complexed RNA	Arthropod		

* from *Androctonus australis* † = from *Hadronyche versuta* Δ = Boric acid, Spinosad,

Tolfenpyrad, Chlorfenapyr, & Ivermectin

Figure 1 – RNAi trigger design considerations. Illustration of hypothetical target gene with 5' and 3' untranslated regions (UTR) and coding sequence. Below are examples of target genes, RNAi trigger placement, RNAi trigger length, and steric factors that can impact RNAi knockdown.
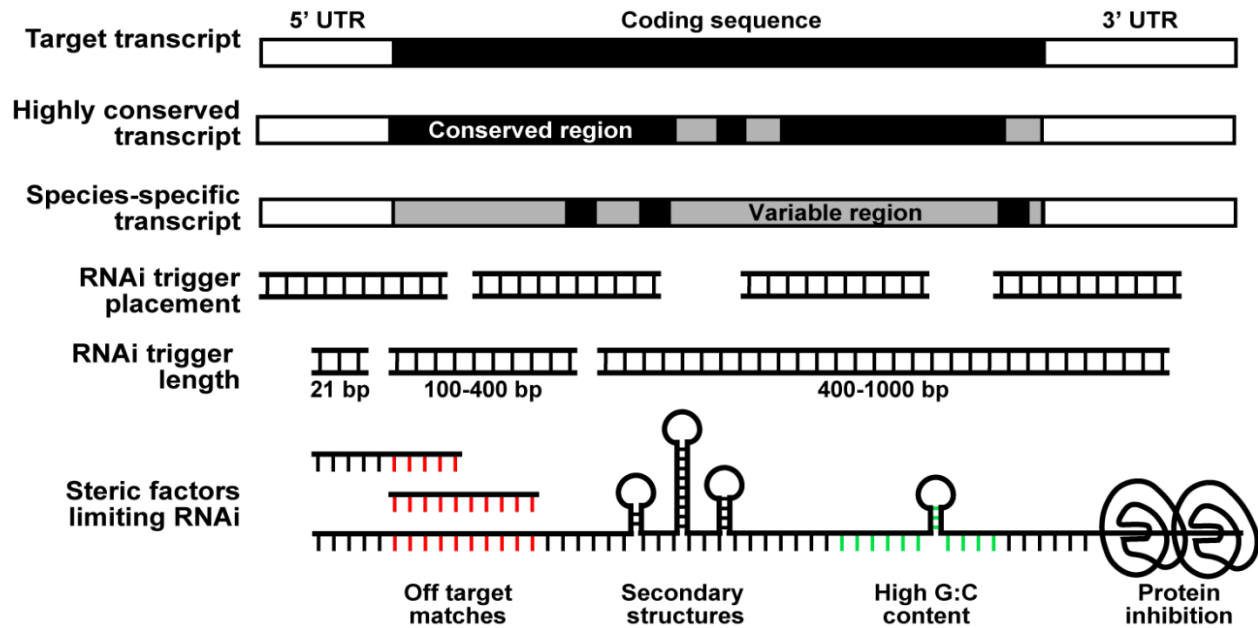
Figure 2 – RNAi trigger production and delivery. (A) Illustrations of RNAi trigger forms including naked (unmodified double stranded RNA), chemically modified RNAs (end-stabilized, link-modified, and base-modified), and hairpin double stranded RNA. (B) Illustrations of transformation approaches and biological expression systems for delivery of RNAi triggers. (C) Illustrations of nanoparticle approaches for delivery of RNAi triggers. Modified and naked RNAi triggers can be delivered alone (see section 3.1), incorporated into biological delivery systems (see section 3.2), or incorporated into nanoparticle delivery systems (see section 3.3).
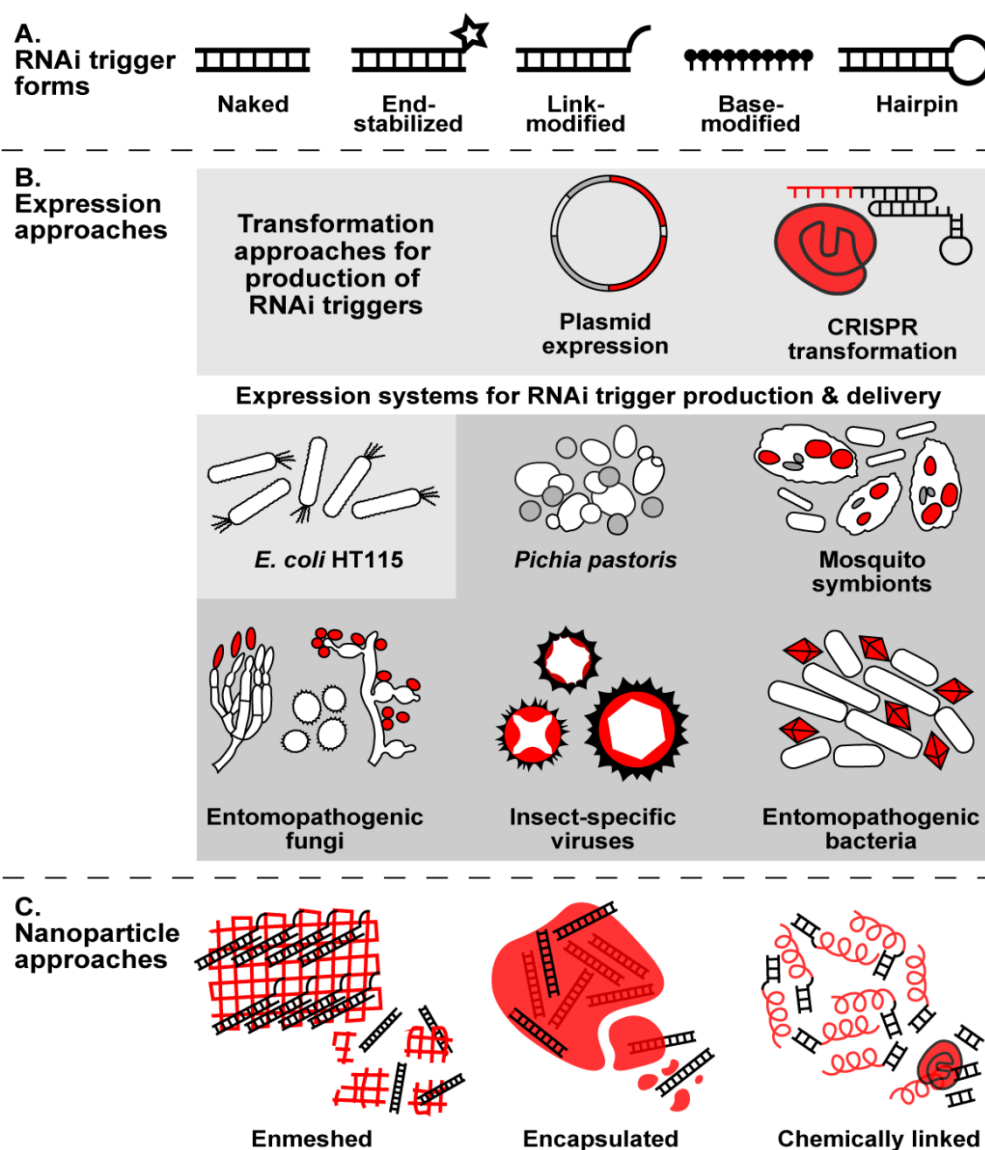
Chapter 2 - Characterizing oogenesis progress and processes in the eastern tree-hole mosquito *Aedes* (*Ochlerotatus*) *triseriatus*

Abstract

Oogenesis in flies manifests as a carefully orchestrated cascade of developmental and growth events, punctuated by cell death and absorption/autophagy. In anautogenous mosquitoes, blood feeding stimulates a synchronous release of the proximate follicle in each ovariole from a developmental gate. The oocyte begins to grow and develop through initiation and trophic phases with increasing deposition of yolk; as the oocyte reaches a point where it is greater than 90% of the length of the follicle, the nurse cells degrade. Eventually, the follicular epithelial cells secrete the chorion and also undergo cell death. We have thoroughly characterized the timing and appearance if these processes in the Eastern tree hole mosquito, *Aedes triseriatus* (Diptera: Culicidae), and noted significant differences from previous studies of other mosquito species in terms of staging and developmental gates. This mosquito transmits La Crosse virus (LACV, Bunyaviridae), a major cause of pediatric encephalitis, both horizontally and vertically via transovarial transmission. These studies reveal PCD events through which LACV must persist in order to achieve filial infection.

Introduction

The Eastern Tree Hole mosquito, *Aedes triseriatus*, is found throughout the deciduous forests of the Midwest and Eastern half of North America spanning northward into southern Canada (Darsie and Ward, 2013). *Ae. triseriatus* is the principle vector species of LaCrosse Virus (LACV) [1-3], which causes a potentially deadly pediatric encephalitis [4, 5]. The virus perpetuates during the summer through horizontal transmission to squirrel (*Sciurus carolinensis*) and chipmunk (*Tamias striatus*) amplifying vertebrate hosts [6-9]. LACV persists transseasonally even in extremely cold winters in temperate climates by transovarial and transtadial transmission [8, 10, 11]. In order to understand the mechanism by which LACV persists in ovarian follicles, and to study the impact of LAVC infections on oogenesis, we reasoned that we must first profile the timing and appearance of oogenesis in *Ae. triseriatus*.

The most complete descriptions of mosquito oogenesis are available for *Aedes aegypti, Anopheles gambiae* and *Culex quinquefasciatus* [12]. These descriptions divide the process into distinct phases (Previtellogenic, Initiation, Trophic and Post-trophic) and stages (G, I -V) based on follicle morphology and hallmark resorption events as defined by Christophers for *Anopheles* species (1911). Using these descriptions as a framework, we provide an outline of the timing and traits observed in *Ae. triseriatus* for the first gonotrophic cycle. Beyond the timing and appearance of the stages and phases of oogenesis, we characterize cell death events in the ovary between blood-feeding and chorion formation.

There is an extensive body of literature that exists to describe the morphologic and molecular changes that occur during egg development in the so-called "higher" flies including *Drosophila melanogaster*, *Drosophila virilis*, *Bactrocera oleae* (the olive fruit fly) and *Ceratitis capita* (the medfly). In each of these organisms, 14 stages of oogenesis are evident. Cell death events in

higher flies are particularly critical and evident in mid- and late-oogenesis. Mid-oogenesis is described as stages 7-8. This likely equates to stage IIIa-IIIb in the mosquito, based on the need for 20-hydroxyecdysone (20E) to trigger the transition to the next stage. The next stage involves incorporation of vitellogenin into the follicle. At mid-oogenesis, follicles of fruit flies, and medflies either proceed through oogenesis or undergo follicular atresia; degenerating egg chambers contain fragmented DNA and actin and show caspase activity. In late-oogenesis, cell death machinery is directed toward the degradation of nurse cells and follicular epithelial cells as the oocyte matures. In the mosquito, the equivalent to mid and late-stage oogenesis cell death events in fruit flies manifest as follicular atresia (FA), nurse cell death (NCD), and sloughing of the follicular epithelia (FE).

Follicular atresia occurs as a function of nutritional limitation. Increased FA during nutritional deficit has been observed in a variety of Diptera including *D. melanogaster*, *Ae. aegypti*, and *Cx pipiens pallens* [13-16]. In *Drosophila*, FA increases with inadequate nutrition [14, 16, 17]. In *Ae. aegypti*, follicles that are not developing at the same rate as surrounding follicles begin to show signs of FA manifesting as condensed the nurse cell nuclei and bright crimson staining with neutral red [12]. Nurse cell death occurs in those follicles that successfully progress with development after others have undergone FA. In *D. melanogaster* the nurse cells and oocyte form a syncytium connected by number of ring canal cytoplasmic bridges [18]. These bridges facilitate transport of bulk cytoplasmic from the nurse cells to support growth and development of the oocyte. This culminates in nurse cell 'dumping' of cellular contents to the oocyte and apoptotic death, i.e., NCD [19-21].

In this study, we provide an outline of characteristics for each phase of oogenesis in *Ae. triseriatus* according to defined descriptors with an emphasis on programmed cell death. By quantifying the prevalence and consistency of morphological events, we show that oogenesis in *Ae. triseriatus* is a highly synchronized process both within and between individuals.

Materials & Methods

Mosquito strains and rearing procedures.

Ae. triseriatus larvae were reared in enamel pans and fed daily with a slurry of ground TetraMin™ (Blacksburg, VA). Groups of 50 female pupae were collected ~24 hours prior to emergence and maintained on a 10% sucrose diet provided on a soaked cotton pad placed on top of a mesh-covered pint-size paper carton. Mosquitoes that received a blood meal were sucrose-starved for 18-24 hours prior to blood feeding, and then provided with sucrose again after blood feeding. All life stages were maintained at 28 °C at 70% relative humidity with a 16:8 hour (light:dark) photoperiod.

Blood feeding.

Three to five day old adult female *Ae. triseriatus* were provided defibrinated sheep blood (HemoStat Laboratories, CA) through a Parafilm M® (Bemis, Neenah, WI) membrane, using a blown glass membrane feeder (L.C. Rutledge, R.A. Ward, 1964). Following blood-feeding, unfed or partially fed individuals were removed from the study by aspiration from the cartons in which they were held.

Dissections.

Mosquitoes were cold-anesthetized at 4°C and immobilized on ice prior to dissection. Individuals were dissected by inserting a probe through the lateral thorax, ventral side facing upwards. Using forceps individuals were decapitated and then ovaries were removed from the 6th and 7th abdominal segments. Individual primary follicles were further dissected using probes for staining and imaging.

Neutral red and morphological measurements of healthy and atretic follicles.

Dissected follicles were submerged in filtered 0.5 % w/v neutral red (NR) in PBS for 10-30 seconds and rinsed in PBS 3 times immediately prior to bright field visualization. NR staining was used for a number of analyses including identification of: oocytes after stage IIIa, follicular atresia, nurse cell death, as well as measurements of: oocyte content, follicle length and width, and overall follicle area. In each analysis, follicles were counted and measured according to visual cues noted [12]. For each analysis, follicles were observed from at least 5 individuals from 3 or more biological replicates.

Acridine orange live cell staining.

Dissected follicles in PBS were stained in a 1:1 volume of Acridine Orange (AO) (10 µg/ml) and n-heptane for 3 minutes rotating in the dark based on a protocol adapted from Abrams *et al.* [22]. Follicles then were washed 3 times in PBS and mounted in Fluoro-gel (EMS, Hatfield PA). Fluorescence was visualized immediately using a g a Nikon Eclipse 50i fluorescence microscope and NIS Elements D (Nikon, Melville, NY) with a Nikon B-2A long pass filter. As a control, one ovary of every pair was stained with NR. *Ae. triseriatus* follicles stained with AO were measured from 3 or more biological replicates.

Fixing and fluorescent labeling with TUNEL, DAPI & Phalloidin Alexafluor 488.

Follicles were fixed in 4% paraformaldehyde (in 0.1 M sodium phosphate buffer pH 7.4) for 30 minutes, washed twice in PBS, permeablized (0.3% Triton X-100, 1% BSA, and 1% Sodium citrate in PBS), and washed twice more in PBS before staining. TUNEL staining (TMR Red *In Situ* Cell Death Detection Kit, Roche, Indianapolis, IN) was used to visualize late stage apoptosis. Ovaries were transferred to the TUNEL reaction mixture for 2 hours at 37 ℃ then rinsed 3 times in PBS. Positive controls were incubated in DNase I solution (0.1% BSA and 6u/ml DNase I in 50 mM Tris-HCl buffer) for 20 minutes at room temperature prior to staining. Negative controls were incubated in the absence of the enzyme terminal transferase. Follicles were co-stained with DAPI (25 μg/ml, Anaspec, CA) and Alexa Fluor 488 Phalloidin (0.835 μM, Life, NY) in PBS for 1 hour at room temperature. Processed ovaries were mounted in Vectashield (Vector Laboratories, CA) and visualized using a Nikon Eclipse 50i fluorescence microscope and NIS Elements D (Nikon, Melville, NY) with Nikon TRITC HYQ (TUNEL), B-2A (phalloidin) and UV-2E/C (DAPI) filters.

Imaging & Data analyses.

Photoshop CC (Adobe, San Jose, CA) photomerge tool was used to generate image composites to represent all follicles from each time-point within a single field of view. Image J (NIH, Bethesda, MD) was used to measure: follicle length, follicle width, area of oocyte, nurse cell, and follicular epithelia, quantification of FA, and quantification of NCD. For measurements regarding size and shape, the polygon tool was used. Specifically the follicle perimeter was measured to calculate total area, the interior edge of the follicular epithelium was measured to calculate the interior follicle area (i.e. the oocyte & nurse cells), and the oocyte portion was measured. Nurse cell area

was calculated as interior follicle area – oocyte area. Follicular epithelia area was calculated as total area – interior follicle area. Length and width measurements were made using the line tool measured at the longest and widest points of the follicle respectively. Follicle counts for quantifications were made using the multi-point tool. Measurements were plotted with Prism 6 (GraphPad Software, San Diego California USA).

Results & Discussion

An overview of development using neutral red (NR).

Development during the first gonotrophic cycle in *Ae. triseriatus* was measured from 0 to 120 hours post bloodmeal (HPBM) using neutral red (NR) (Fig. 1). Shortly following a bloodmeal, follicles appear ovoid with a length-width ratio of ~1 (Fig. 2B). NR staining is evident initially within lipid vesicles of the oocyte, a trait that marks the beginning of the initiation phase or stage IIIa (Fig. 1A) [23]. The follicle then doubles in size from 0-12 HPBM (compare Fig. S1A & Fig. 1B). After 24 HPBM, the follicle enlarges by 12-14x (compare Fig. 1 A-C to Fig. 1D-F & Fig. 2A). This shape is maintained with no significant change in the length to width ratio until >48 HPBM, whereupon the follicle narrows and lengthens while continuing to gain mass (compare Fig. 1D-F & Fig. 2B). The oocyte is relatively indistinguishable early (from 0-8 HPBM), but thereafter the proportion of the follicle that is oocyte increases steadily until 60 HPBM when it occupies almost the entirety of the follicle interior (Fig. 1A-F, Fig. 2C). At this point, the nurse cells stain vivid pink with NR, indicating NCD, which is a key indicator of trophic phase IVb (Fig. 1E). When the nurse cells are no longer distinguishable, remnants of can be seen as speckles on the surface of the FE (Fig 1F-H). By 96 HPBM, the ovarian cycle is completed with formation of

a characteristic chorionic structure (Fig. 1H). During this time, secondary follicles also grow, reaching the size of initiation phase II by 96 HPBM (compare Fig. 1H & Fig. S1A).

These attributes of oogenesis are distinct according to species. In this study, three-day-old lab-reared *Ae. triseriatus* were exposed to defibrinated sheep blood and fed until repletion; the follicles in this scenario reach maturity (stage V) by 96 HPBM. Under the same conditions, *Ae. aegypti* fed on sheep blood using the method described in this paper resulted in developmental staging comparable to previous descriptions using human or guinea pig blood (data not shown) [12]. It should also be noted that in *Ae. triseriatus* the type of blood given, the age, and the sexual naivety of the female impact on the timing of oogenesis and egg batch [24, 25]. By comparison, *Ae. aegypti* and *Ae. caspius* take 60-68 HPBM and 56 HPBM to reach stage V, respectively [23, 26].

Defining stages of oogenesis in Ae. triseriatus by morphological changes and programmed cell death. To define oogenesis in *Ae. triseriatus* in more detail, the framework and criteria for stages and phases of oogenesis were considered alongside morphological characteristics and cell death events of developing follicles (Table 1, Table S1) [12, 27].

The previtellogenic phase: stages G, Ib, IIa, IIb.

Oogenesis in an anautogenous mosquito precedes the bloodmeal with the previtellogenic phase. This process starts at stage G where follicular progenitor cells replicate in the germarium then are separated in ovarioles [23]. Primary follicles are the distalmost follicles of each germarium, develop an FE layer, and the oocyte becomes distinguishable from the nurse cells (Stage Ia-Ib). Next, the oocyte becomes more recognizable with the formation of lipid droplets, while the oocyte nucleus and nucleolus remain visible by reflected light (stage IIa-IIb). Throughout the

previtellogenic phase, follicles are resistant to NR staining. We find that immediately following a bloodmeal, *Ae. triseriatus* follicles are in previtellogenic stages Ib-IIb. Herein, follicles appear clear and spheroid with oocyte nuclei visible clearly at 150x magnification and no positive staining with NR in the oocyte (Fig. S1A). By 4 HPBM, most follicles remain at previtellogenic stages Ib-IIb and appear largely unchanged in size and shape (Fig. S1B, Fig. 2A).

The initiation phase: stage IIIa

In anautogenous mosquitoes the bloodmeal acts a cue to initiate release of ovary ecdysteroidogenic hormone (OEH) and insulin-like peptides (ILPs) from neurosecretory cells in the brain that stimulate ecdysteroid hormone (ECD) production in the ovaries [28-32]. The release of OEH and ILPs, and interaction with other pathways such as the Target of Rapamycin (TOR,) alter gene expression in the midgut to digest the bloodmeal, and initiate yolk protein production in the fat body and uptake of yolk proteins in the oocyte in lipid vesicles [32-36]. OEH, ILPs and ECD therefore act as the gate between the previtellogenic phase and the initiation phase (Table. S1), which is marked by NR staining of lipid vesicles in oocytes (Fig. 1 A). In 3 day old adults no follicles stain positive with NR 0 HPBM indicating that no follicles pass the initiation gate before or immediately following a bloodmeal and require time for production of yolk protein and uptake (Fig. S1E). This is supported by the presence of clearly visible oocyte nuclei, even at 4 HPBM (Fig. S1A-B). Occlusion of the oocyte nucleus, another mark of stage IIIa, occurs between 4 - 12 HPBM as yolk protein uptake continues and 100% of follicles stain positive with NR (Fig. 1 A-B, Fig. S1E). Interestingly, we observed that older individuals (5 day post-eclosion) contained larger follicles which stained positive with NR at 0 and 4 HPBM, indicating that some vitellogenesis and receptivity to yolk protein uptake occurs prior to or immediately following a bloodmeal (Fig. S1C-

D). To test whether age alone could facilitate a bypass of the initiation gate, ovaries from 6-, 9- and 11-day-old adults were analyzed, but were indistinguishable from 5 day old adults (data not shown). The oocyte nuclei of 5-day-old adults were still visible in many follicles, despite positive NR staining (Fig. S1 C & D arrowheads). Therefore, it may be that NR staining is not strictly indicative of stage IIIa in *Ae. triseriatus* if oocyte nuclei are still visible (Table S1).

The trophic phase: stages IIIb, IVa & IVb

Oocyte content was tracked as a percentage of overall follicular area as a key indicator of trophic phases (Fig. 1C). This metric is particularly helpful as the growth of the oocyte is not relative to the growth of the follicle and there is no change in shape until 60 HPBM (Fig. 2B). At 12 HPBM, visible oocyte content reaches 43% of the follicle, increasing to 60% by 18 HPBM (Fig. 2C). Because the cutoff for stage IIIa is 50% oocyte content, stage IIIb must begin between 12 and 18 HPBM. Stage IIIb marks the start of the trophic phase, which is not defined by a change in shape, but an increase in oocyte content from 50-75% alongside an increase in follicle size. At this point *Ae. triseriatus* deviates from the criteria set forth previously for other mosquitoes because the criteria for oocyte content alone are met at 18-24 HPBM, but size continues to increase without a shape change until 48-60 HPBM (Fig. 1A-B). By definition, trophic stage IVa, begins with a change in the shape of the follicle; these two events are uncoupled in *Ae. triseriatus* as compared to other species. Another marker of stage IIIb in *Ae. aegypti* is peak follicular atresia, which may in this case act as a secondary stage marker [12]. Here we quantified atretic follicles and discovered a distinct peak from 24-36 HPBM (Fig. 4B). Based on size increase, lack of shape change, and peak atresia, stage IIIb occurs in *Ae. triseriatus* at 18-36 HPBM.

Stage IVa is characterized by continued growth, thinning of the follicular epithelium, up to 90% oocyte content, and intact nurse cells. In *Ae. triseriatus*, IVa occurs in the window of follicular growth between two major cell death events: atresia (during stage IIIb) and NCD (during stage IVb). Because peak atresia ends at 36 HPBM (Fig. 3B) and NCD does not occur in the majority of follicles until 60 HPBM (Fig. 4B), stage IVa takes place between 36 and 60 HPBM. The morphological criteria also fit using this timeframe as follicle growth continues up beyond 60 HPBM (Fig. 2A) and FE thinning starts between 48-60 HPBM (Fig. 2B).

The end of the trophic phase marks the transition to stage IVb. At this point, the oocyte encompasses almost 100% of the follicular interior and the follicle assumes the shape of the mature egg. These criteria set stage IVb between 48-72 HPBM (compare Fig. 1E-G & Fig. 2A-B). Similar to late oogenesis in *Drosophila,* nurse cells undergo NCD when the oocyte nears maturity [37, 38]. NCD is a a hallmark of stage IVb and is evidenced by bright crimson staining of nurse cells using NR (Fig. 1E-F, Fig. 4A). This event is first observed at 48 HPBM, but does not peak until 60 HPBM (Fig. 4B). Finally Clements & Boocock note that the "follicle assumes the shape of the mature oocyte, or almost so, but has not reached full length" [12]. As follicles reach maximum length at 72 HPBM and NCD first appears at 48 HPBM, stage IVb occurs within this timeframe.

The post-trophic phase: stage V

The post-trophic stage marks the final events of oogenesis that occur in rapid succession. Here follicles reach maximum length, shed the FE, and chorionic structures become visible. At 72 HPBM, 100% of nurse cells have degraded indicating the end of the trophic phase (Fig. 4B). Follicles at this time also reach a size maximum and thinning halts (Fig. 2A-B). By 96 HPBM,

chorionic structures are also visible and the FE detaches revealing the fully developed oocyte (Fig. 1F-G).

Ageing and timing of oogenesis

As mentioned previously, the age of the mosquito has an impact the timing of phases in *Ae. triseriatus* in that older mosquitoes enter the initiation phase of oogenesis prior to a bloodmeal (see section 3.2.3, Fig. S1). To test whether older mosquitoes undergo an expedited oogenesis, the timing of NCD was compared between 3 day and 5-day-old mosquitoes. In 3-day-old mosquitoes NCD occurs in 50% of follicles at 60 HPBM, while in 5 day old mosquitoes this is seen at 50 HPBM (Fig. S3A-B). Five-day-old mosquitoes do consequently indeed display an expedited oogenesis. Therefore the result suggests that although oogenesis is initiated rapidly in older mosquitoes, it is either delayed or halted in the absence of a bloodmeal.

Secondary follicle development initiates prior to a second bloodmeal in Ae. triseriatus

During the first gonotrophic cycle, secondary follicles grow and mature from stage G to initiation phase II by 96 HPBM (compare Fig. 1H & Fig. S1A). Prior to oviposition, secondary follicles do not pass into the initiation phase but stain with NR throughout (Fig. S1A). Following oviposition, the primary follicle FE remains in the ovary and is resorbed over ~24 hours (Fig. S1B & C). Resorption of the FE appears to be essential to clear the distalmost region the ovariole to allow secondary follicles to assume this position (Fig. S1B). Immediately following oviposition, the FE remains intact and secondary follicles do not pass into stage IIIa but show characteristics of stage IIb (Fig. S1B, Table S1). Resorption of the FE is associated with the secondary follicles entering

stage IIIa and as such the FE may provide nutrition sufficient for development of some secondary follicles without need for a second bloodmeal (Fig. S1C).

Programmed cell death during oogenesis

Atresia in the ovary

In insects, FA (also known as oosorption, follicular resorption, and atresia) occurs during early-mid stages of oogenesis [13]. The process necessitates termination of yolk deposition in the oocyte and complete degradation of the follicle. In other fly species (e.g., *D. oleae* and *D. melanogaster*) FA occurs as a function of PCD in the form of apoptosis and/or autophagy [13, 39-41]. In this study, atretic follicles were identified using several concurrent visual cues including bright red NR-stained vesicles on the FE, asynchronous and smaller and/or rounder follicles, and a loss of clear follicular cell types (Fig. 3A). FA peaks with ~17% of follicles indicating resorption between 24-36 HPBM. This peak falls sharply to only 5% of follicles by 48 HPBM (Fig. 3B). All of the atretic follicles observed were equivalent or smaller in length to the average 12 HPBM follicle (Fig. 3C), which may indicate that a nutritional deficiency/sufficiency gate occurs at this time point or follicle size.

In *Ae. aegypti* FA is noted during stage IIIa and peaks during stage IIIb between 25-30 HPBM [12]. Our results show atretic follicles as early as 12 HPBM, which aligns with stage IIIa morphological data (Fig. 3B). Although this metric is not employed to define this stage in *Ae. aegypti*, it can serve as an indicator in *Ae. triseriatus*. This may be especially useful for defining stage IIIb in *Ae. triseriatus* because the transition from IIIa to IIIb in this mosquito does not fit the criteria for other species (table S1, section 3.2.3).

To assess the nature of PCD that occurs during FA, we employed TUNEL staining to reveal evidence of DNA fragmentation (Fig. 5A-C, Fig. S4A-F). Interestingly, oocyte and nurse cell nuclei did not stain with TUNEL, but the FE did. This result emulates that of NR stained atretic follicles (compare Fig. 3A & Fig. 5B). FA may be localized or controlled by the FE in *Ae. triseriatus*; this is congruent with FA in *Culex pipiens pallens* wherein active caspases are restricted to the epithelial cells of atretic follicles [42]. Similar results were seen in *Plasmodium*-infected *Anopheles stephensi,* wherein atretic follicles exhibited apoptosis mainly in the FE [43]. By contrast, in the higher flies, *D. oleae, D. melanogaster,* and *Ceratitis capitate*, apoptosis was evident in the nurse cell compartment of atretic follicles [40, 41, 44, 45].

Nurse cell death (NCD)

Nurse cells are fundamental to oogenesis in many multicellular organisms and function in much the same way in flies as in *Caenorhabditis elegans* and *Hydra* [37]. In *Drosophila*, NCD starts with permeabilization of the nuclear membrane, followed by transportation or 'dumping' of cytoplasmic contents (including large amounts of RNA and protein) to the oocyte through the ring canals, and finally degeneration and apoptosis of the remaining cell [37, 46]. To decipher the similarities of NCD between *Drosophila* and *Ae. triseriatus,* numerous staining techniques were employed. In *D. melanogaster*, AO staining produces green/red nuclei during NCD, particularly in nuclei that are permeabilized as a function of an apoptotic event [22, 43]. Microscopy of NCD using NR and AO staining reveals the sudden permeabilization of individual nurse cell nuclear envelopes at 48-72 HPBM (Fig. 4B, Fig. S3A). Interestingly, NCD is asynchronous both between and within follicles, with follicles displaying anywhere from 1-7 apoptotic nurse cells at any time (Fig. 4A). Over time, progressively more nurse cells are evident, and become increasingly more

compact as contents are lost to the oocyte or phagocytosed by the FE (Fig. 1E-G, Fig. 4D-E). The compaction of nurse cells is coupled with a shift of green to red staining and nuclear fragmentation when visualized by AO (Fig. 4D-E). The decrease in nurse cell size is probably due to cytoplasmic dumping, while the shift in color is either due to acidification of the cell during apoptosis, or increase in RNA production based on the staining characteristics of AO [47]. Additionally, red-stained vesicles were often seen dispersing from the nurse cell compartment, suggesting that AO may mark RNA or acidic vesicle movement from the nurse cell compartment to the oocyte (data not shown). Further studies are required to confirm this. Finally, the nurse cells undergoing NCD were positive for TUNEL staining (Fig. 5D-F, Fig. S4D-F).

Follciular epithelial (FE) death

The FE is a dynamic and multifunctional cell throughout oogenesis (from 0-72 HPBM) and constitutes significant area (between 15 and 30%) of the overall follicle size (Fig. S2). Ultimately, the FE deposits a protective vitelline chorion layer [23], and at the post trophic phase (stage V), the FE is sloughed to release the mature oocyte (Fig. 1H). In *D. melanogaster,* the FE appears to undergo apoptosis prior to removal [38]. To investigate whether these cells undergo apoptosis while still associated with the follicle, TUNEL staining was performed (Fig. 5 D-I, Fig. S4 A-F). The results show that only a small number FE cells stain positive with the remaining displaying large, fully formed nuclei typical of healthy cells, suggesting that there is more research to be done to reveal the mechanism behind FE death and cell sloughing. TUNEL positive FE cells could reflect phagocytosed remnants of degraded nurse cells, as is seen in *D. melanogaster* [44].

Conclusions and model of oogenesis in Ae. triseriatus

Herein we provide a comprehensive morphological description of *Ae. triseriatus* oocyte development (Table 1). Although *Ae. triseriatus* oogenesis can be described using criteria established for *Ae. aegypti* and other mosquito species [12]., the criteria do not fully capture the nature of some key stages and phases in *Ae. triseriatus*. Our analysis of PCD during oogenesis reveals some striking similarities between *Ae. triseriatus* and other Diptera, but also highlights some mosquito-specific phenomena occurring during key cell death events.

Acknowledgements

Literature cited

1.   Pantuwatana, S., et al., *Isolation of La Crosse virus from field collected Aedes triseriatus larvae.* Am J Trop Med Hyg, 1974. **23**(2): p. 246-50.

2.   Watts, D.M., et al., *Overwintering of La Crosse virus in Aedes triseriatus.* Am J Trop Med Hyg, 1974. **23**(4): p. 694-700.

3.   Darsie Jr, R.F. and R.A. Ward, *Identification and geographical distribution of the mosquitoes of North America, north of Mexico*. 2005, Gainesville, Florida, USA: University Press of Florida.

4.   Gaensbauer, J.T., et al., *Neuroinvasive arboviral disease in the United States: 2003 to 2012.* Pediatrics, 2014. **134**(3): p. e642-50.

5. Lindsey, N.P., et al., *West Nile Virus and Other Nationally Notifiable Arboviral Diseases - United States, 2014.* MMWR Morb Mortal Wkly Rep, 2015. **64**(34): p. 929-34.

6. Ksiazek, T.G. and T.M. Yuill, *Viremia and antibody response to La Crosse virus in sentinel gray squirrels (Sciuris carolinensis) and chipmunks Tamias striatus).* Am J Trop Med Hyg, 1977. **26**(4): p. 815-21.

7. Pantuwatana, S., et al., *Experimental infection of chipmunks and squirrels with La Crosse and Trivittatus viruses and biological transmission of La Crosse virus by Aedes triseriatus.* Am J Trop Med Hyg, 1972. **21**(4): p. 476-81.

8. Thompson, W.H. and B.J. Beaty, *Venereal transmission of La Crosse (California encephalitis) arbovirus in Aedes triseriatus mosquitoes.* Science, 1977. **196**(4289): p. 530-1.

9. Borucki, M.K., et al., *La Crosse virus: replication in vertebrate and invertebrate hosts.* Microbes Infect, 2002. **4**(3): p. 341-50.

10. Watts, D.M., et al., *Transovarial transmission of LaCrosse virus (California encephalitis group) in the mosquito, Aedes triseriatus.* Science, 1973. **182**(4117): p. 1140-1.

11. Balfour, H.H., Jr., et al., *Isolates of California encephalitis (La Crosse) virus from field-collected eggs and larvae of Aedes triseriatus: identification of the overwintering site of California encephalitis.* J Infect Dis, 1975. **131**(6): p. 712-6.

12. Clements, A.N. and M.R. Boocock, *Ovarian Development in Mosquitos - Stages of Growth and Arrest, and Follicular Resorption.* Physiological Entomology, 1984. **9**(1): p. 1-8.

13. Bell, W.J. and M.K. Bohm, *Oosorption in insects.* Biol Rev Camb Philos Soc, 1975. **50**(4): p. 373-96.

14.   Lea, A.O., H. Briegel, and H.M. Lea, *Arrest, resorption, or maturation of oocytes in Aedes aegypti: dependence on the quantity of blood and the interval between blood meals.* Physiological Entomology, 1978. **3**(4): p. 309-316.

15.   Klowden, M.J., *Endocrine aspects of mosquito reproduction.* Archives of Insect Biochemistry and Physiology, 1997. **35**(4): p. 491-512.

16.   McCall, K., *Eggs over easy: cell death in the Drosophila ovary.* Dev Biol, 2004. **274**(1): p. 3-14.

17.   Uchida, K., et al., *Induction of oogenesis in mosquitoes (Diptera: Culicidae) by infusion of the hemocoel with amino acids.* J Med Entomol, 2001. **38**(4): p. 572-5.

18.   Robinson, D.N. and L. Cooley, *Genetic analysis of the actin cytoskeleton in the Drosophila ovary.* Annual Review of Cell and Developmental Biology, 1997. **13**: p. 147-170.

19.   Cavaliere, V., C. Taddei, and G. Gargiulo, *Apoptosis of nurse cells at the late stages of oogenesis of Drosophila melanogaster.* Dev Genes Evol, 1998. **208**(2): p. 106-12.

20.   King, R.C., *Ovarian development in Drosophila melanogaster*. 1970, New York: Academic Press. x, 227 pages.

21.   Spradling, A.C., *Developmental genetics of oogenesis*, in *The Development of Drosophila melanogaster*, M. Bate and A. Martinez Arias, Editors. 1993, Cold Spring Harbor Laboratory Press: Plainview, N.Y. p. 1-70.

22.   Abrams, J.M., et al., *Programmed cell death during Drosophila embryogenesis.* Development, 1993. **117**(1): p. 29-43.

23.   Clements, A.N., *The biology of mosquitoes*. First edition. ed. 1992, London ; New York: Chapman & Hall. volumes.

24.   Jalil, M., *Observations on the fecundity of Aedes triseriatus (Diptera: Culicidae).* Entomologia Experimentalis et Applicata, 1974. **17**(2): p. 223-233.

25.   Mather, T.N. and G.R. DeFoliart, *Effect of host blood source on the gonotrophic cycle of Aedes triseriatus.* Am J Trop Med Hyg, 1983. **32**(1): p. 189-93.

26.   Carron, A., et al., *Christophers' stage durations and effect of interrupted blood meal in the mosquito Aedes caspius (Diptera: Culicidae).* Parasite, 2007. **14**(3): p. 225-9.

27.   Christophers, S.R., *The development of the egg follicle in Anophelines.* Paludism, 1911. **2**: p. 73-88.

28.   Dhara, A., et al., *Ovary ecdysteroidogenic hormone functions independently of the insulin receptor in the yellow fever mosquito, Aedes aegypti.* Insect Biochem Mol Biol, 2013. **43**(12): p. 1100-8.

29.   Brown, M.R., et al., *Identification of a steroidogenic neurohormone in female mosquitoes.* J Biol Chem, 1998. **273**(7): p. 3967-71.

30.   Riehle, M.A. and M.R. Brown, *Insulin stimulates ecdysteroid production through a conserved signaling cascade in the mosquito Aedes aegypti.* Insect Biochem Mol Biol, 1999. **29**(10): p. 855-60.

31.   Wen, Z., et al., *Two insulin-like peptide family members from the mosquito Aedes aegypti exhibit differential biological and receptor binding activities.* Molecular and cellular endocrinology, 2010. **328**: p. 47-55.

32.   Attardo, G.M., I.A. Hansen, and A.S. Raikhel, *Nutritional regulation of vitellogenesis in mosquitoes: implications for anautogeny.* Insect Biochem Mol Biol, 2005. **35**(7): p. 661-75.

33.   Roy, S.G., I.A. Hansen, and A.S. Raikhel, *Effect of insulin and 20-hydroxyecdysone in the fat body of the yellow fever mosquito, Aedes aegypti.* Insect biochemistry and molecular biology, 2007. **37**: p. 1317-1326.

34.   Gulia-Nuss, M., et al., *Insulin-like peptides and the target of rapamycin pathway coordinately regulate blood digestion and egg maturation in the mosquito Aedes aegypti.* PloS one, 2011. **6**: p. e20401.

35.   Gulia-Nuss, M., et al., *Ovary ecdysteroidogenic hormone activates egg maturation in the mosquito Georgecraigius atropalpus after adult eclosion or a blood meal.* The Journal of experimental biology, 2012. **215**: p. 3758-3767.

36.   Gulia-Nuss, M., et al., *Multiple factors contribute to anautogenous reproduction by the mosquito Aedes aegypti.* J Insect Physiol, 2015. **82**: p. 8-16.

37.   Baum, J.S., J.P. St George, and K. McCall, *Programmed cell death in the germline.* Semin Cell Dev Biol, 2005. **16**(2): p. 245-59.

38.   Nezis, I.P., et al., *Dynamics of apoptosis in the ovarian follicle cells during the late stages of Drosophila oogenesis.* Cell Tissue Res, 2002. **307**(3): p. 401-9.

39.   Malagoli, D., et al., *Autophagy and its physiological relevance in arthropods: current knowledge and perspectives.* Autophagy, 2010. **6**(5): p. 575-88.

40.   Nezis, I.P., et al., *Cell death during Drosophila melanogaster early oogenesis is mediated through autophagy.* Autophagy, 2009. **5**(3): p. 298-302.

41.   Nezis, I.P., et al., *Follicular atresia during Dacus oleae oogenesis.* J Insect Physiol, 2006. **52**(3): p. 282-90.

42.   Uchida, K., et al., *Follicular epithelial cell apoptosis of atretic follicles within developing ovaries of the mosquito Culex pipiens pallens.* Journal of Insect Physiology, 2004. **50**(10): p. 903-912.

43.   Hopwood, J.A., et al., *Malaria-induced apoptosis in mosquito ovaries: a mechanism to control vector egg production.* J Exp Biol, 2001. **204**(Pt 16): p. 2773-80.

44.   Nezis, I.P., et al., *Stage-specific apoptotic patterns during Drosophila oogenesis.* Eur J Cell Biol, 2000. **79**(9): p. 610-20.

45.   Nezis, I.P., et al., *Modes of programmed cell death during Ceratitis capitata oogenesis.* Tissue Cell, 2003. **35**(2): p. 113-9.

46.   Bashirullah, A., R.L. Cooperstock, and H.D. Lipshitz, *RNA localization in development.* Annu Rev Biochem, 1998. **67**: p. 335-94.

47.   Robbins, E. and P.I. Marcus, *Dynamics of Acridine Orange-Cell Interaction. I. Interrelationships of Acridine Orange Particles and Cytoplasmic Reddening.* J Cell Biol, 1963. **18**: p. 237-50.

Tables & Figures

Table 1 – Ovarian developmental stages in *Ae. triseriatus*

Phase	Stage	Oocyte (%)	Key event	Ref Figure	HBPM
Previttelogenic	G-Ia		Oocyte not visible	Fig S1 A	PreBM
	Ib – IIb	0-10%			0-8
Initiation	IIIa	≤ 50%	NR in oocyte	Fig S1 E	8-24
Trophic	IIIb	50-75%	Peak atresia	Fig 3	18-36
	IVa	~ 90%	Size and oocyte content increase	Fig 2 A & C	36-60
	IVb	90-100%	Nurse cell death Narrowing follicle	Fig 4, Fig 2 B	48-72
Post-Trophic	V	100%	Max length FE removal	Fig 2 B Fig 1 H	72-96

Supplementary Table 1 – Criteria for developmental staging of follicles during the ovarian cycle

Clements & Boocock (*Aedes aegpyti, Culex pipiens, Anopheles gambiae**) [12, 23, 28]				Christophers (Anophelines) [27]
Phase	**Stage**	**Description**	**Developmental gate (stimulus)**	**Stage**
Pre-vitellogenic	G	Follicles partially separated from germarium. Oocyte not entirely surrounded by follicular epithelium.	Germinal (20-Hydroxyecdysone)	N/A
	Ia	Follicle separate from germarium, Oocyte entirely surrounded by follicular epithelium but not distinct from nurse cells.	Stage I (Juvenile hormone) Pre-vitellogenic (unknown)	Stage 1: oocyte free from lipid granules
	Ib	Oocyte distinguishable from nurse cells. No visibility of lipid at 200X magnification.		
	IIa	Lipid visible at 200X magnification.		Stage 2: yolk granules present, but not obscuring nucleus
	IIb	Lipid visible at 20-50X magnification. No inclusions stained by neutral red. Oocyte nuclear membrane & nucleolus visible. Ooplasm clouded with inclusions visible at 10X magnification.		
Initiation	IIIa	Large yolk spheres visible. Several follicles lag and are resorbed. Oocyte clouded by yolk and progressively occupies up to 50% of the follicle length. Follicle increases in size but no change in shape.	Stage III (ovary ecdysteroidogenic hormone (OEH) and insulin-like peptides (ILPs) stimulate ecdysteroid hormone (ECD))	Stage 3: oocyte nucleus obscured, follicle still oval shape.
	IIIb	Oocyte occupies up to 75% of follicle length. Many follicles degenerate at this stage. Follicle grown further and shape change begins as follicles narrow. Nurse cells remain intact.		
Trophic	IVa	Oocyte occupies up to 90% of follicle length. From this stage on most follicles reach maturity. Follicle assumes shape of mature oocyte but not full length.		Stage 4: follicle elongate and shape of mature egg
	IVb	Nurse cells degenerate & stain bright crimson. Chorionic structures appear.		
Post-trophic	V	Oocyte at full length, Follicular epithelium degenerates and, Chorionic structures become fully formed.	Maturation (Syngamy)	Stage 5: chorionic structure visible

* Anopheles have no clear stage Ib and oocyte growth is 50% of the follicle length by IIa.

Figure 1 – Follicle morphology post bloodmeal. Live NR stained primary follicles during (A) early initiation phase IIIa at 8 HPBM, (B) late initiation phase IIIa at 12 HPBM, (C) trophic phase IIIb at 24 HPBM, (D) trophic phase IVa at 46 HPBM, (E) trophic phase IVb at 55 HPBM and (F) 60 HPBM, (G) post trophic phase V at 72 HPBM and (H) 96 HPBM. Scale bar = 100 µM and 500 µM. Secondary and tertiary follicles within the ovariole visible in all parts except E.
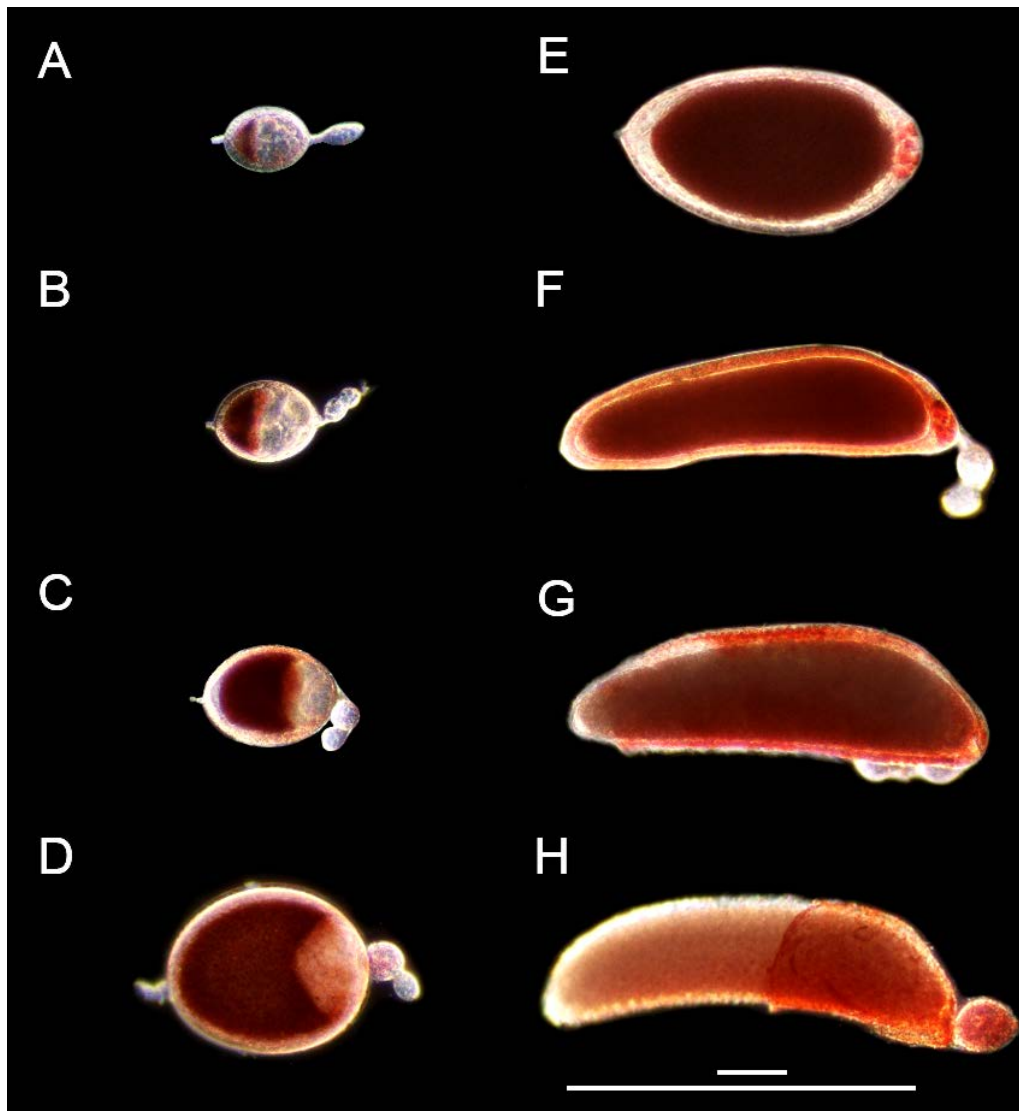
Figure 2 – Quantifying changes in follicle morphology. Size and shape of the follicle, oocyte, and nurse cell compartment was measured over time following a bloodmeal. (A) Follicular area over time (n = 30), (B) follicular length, width and ratio (L:W) over time (n = 50), (C) comparison of oocyte and nurse cell area as a percentage of inner follicle area over time (n = 15). All data are the average of 3 or more biological replicates (± SEM), n = number of follicles measured (from 10-15 mosquitoes) per time point.
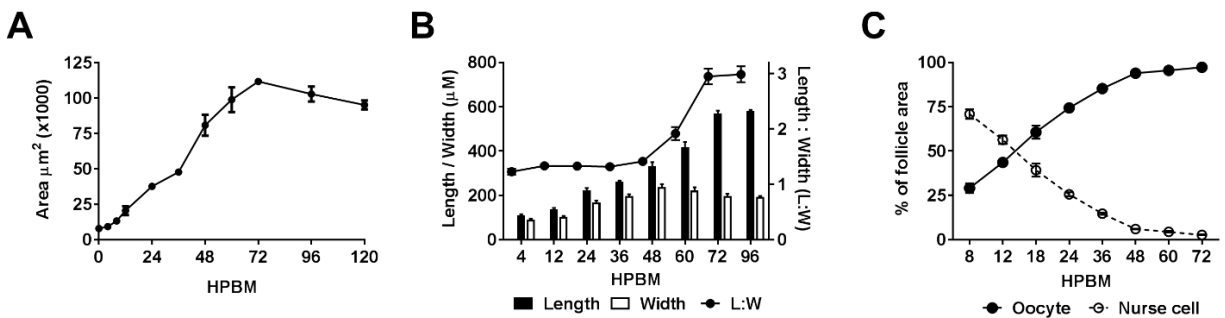
Figure 3 – Characterizing Follicular Atresia (FA). (A) Representative NR stained healthy follicles, atretic follicles (asterisks), and unstained secondary follicles (arrowheads) at 24 HPBM. Scale bar = 100 µM. (B) Atretic follicles were quantified by measuring proportion of atretic follicles per ovary over time (n = 60-537). (C) Length of healthy vs atretic follicles over time (n = 60-537). All data are the average of 3 or more biological replicates (± SEM), n = number of follicles measured (from 10-15 mosquitoes) per time point.
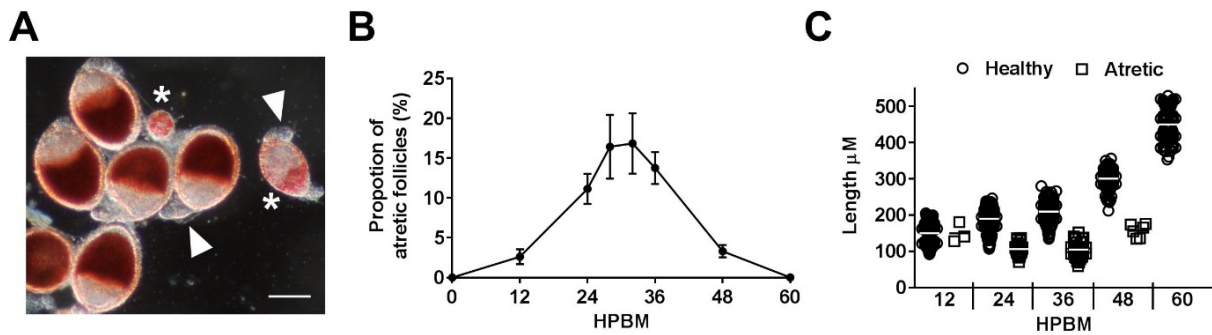
Figure 4 – Characterizing Nurse Cell Death (NCD). (A) NR stained NCD positive follicles at 60 HPBM with 1 or more dying nurse cells (arrowheads). (B) Proportion of NCD positive follicles per ovary over time (n = 76-261). (C-E) AO stained nurse cells at 58 HPBM displaying (C) impermeable nurse cells pre-NCD, (D) NCD positive nurse cells with intact nuclei, and (E) NCD positive nurse cells with bi-nucleated and degraded nuclei. Scale bars = 100 µM. All data are the average of 3 or more biological replicates (± SEM), n = number of follicles measured (from 10-15 mosquitoes) per time point.
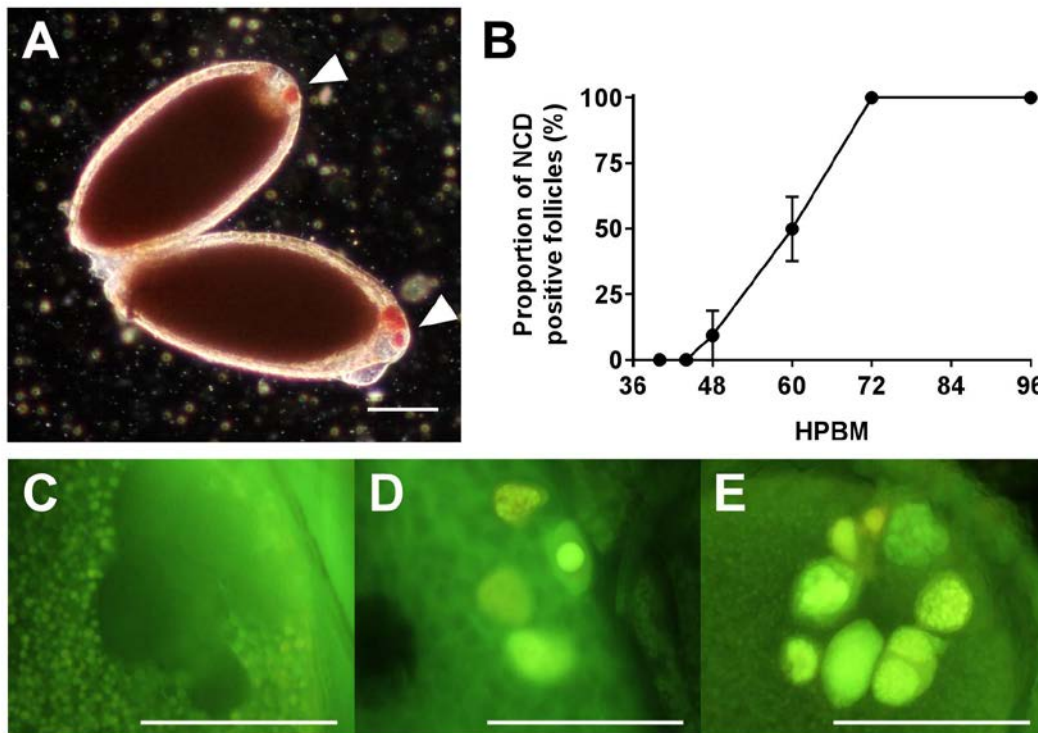
Figure 5 – FA is apoptotic in *Ae. triseriatus*. Follicles at 24 HPBM showing nuclei (DAPI), actin (Phalloidin), and TUNEL staining. (A) Early stage FA with intact nurse cell nuclei and compartments but apoptotic FE. Scale bar = 100 µM. (B) Late stage FA with no definition between FE, oocyte, and nurse cells compared to cross section of healthy primary follicle FE. 200 µM in third row. (C) Healthy primary follicle positive staining control. Scale bar = 100 µM.
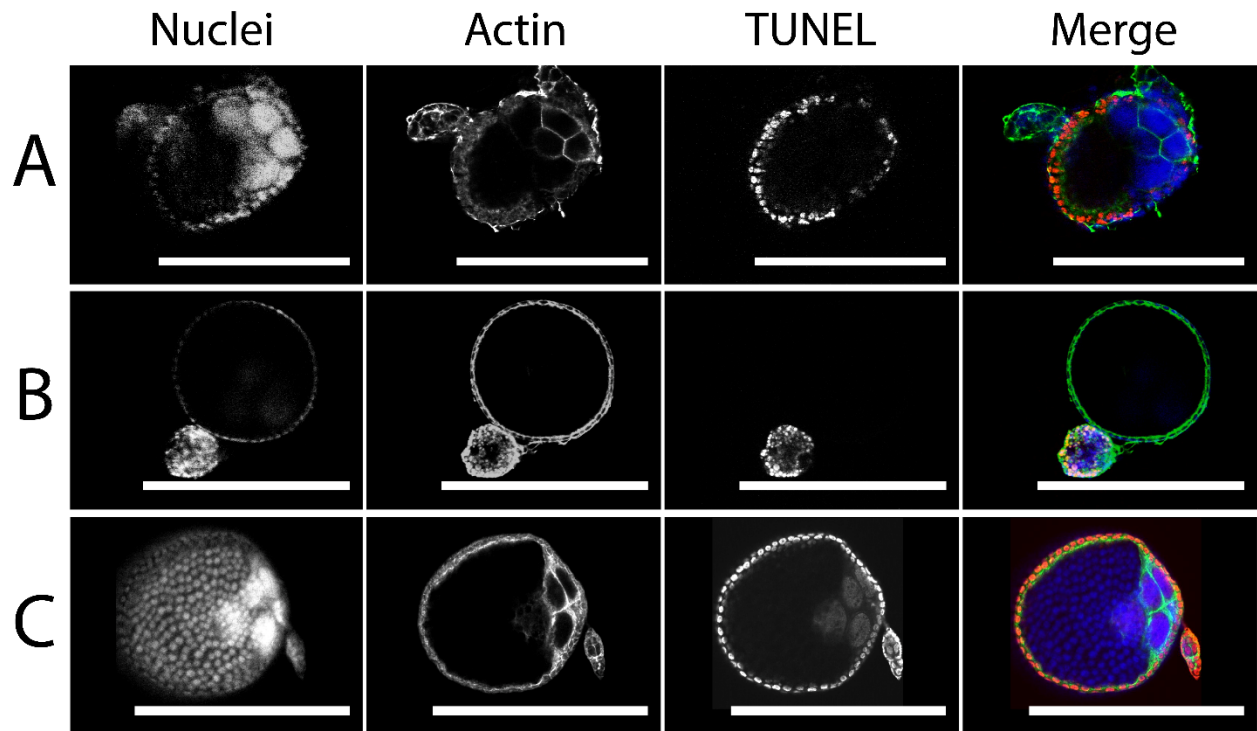
Figure 6 – Nurse cells undergo apoptosis but majority of FE does not. Follicles at (A) 60 HPBM and 96 HPBM (B & C) with showing nuclei (DAPI), actin (Phalloidin), and TUNEL staining. (A) Early stage FA with intact nurse cell nuclei and compartments but apoptotic FE. (B) Late stage FA with no definition between FE, oocyte, and nurse cells compared to cross section of healthy primary follicle FE. (C) Healthy primary follicle positive staining control. Scale bar = 100 µM.
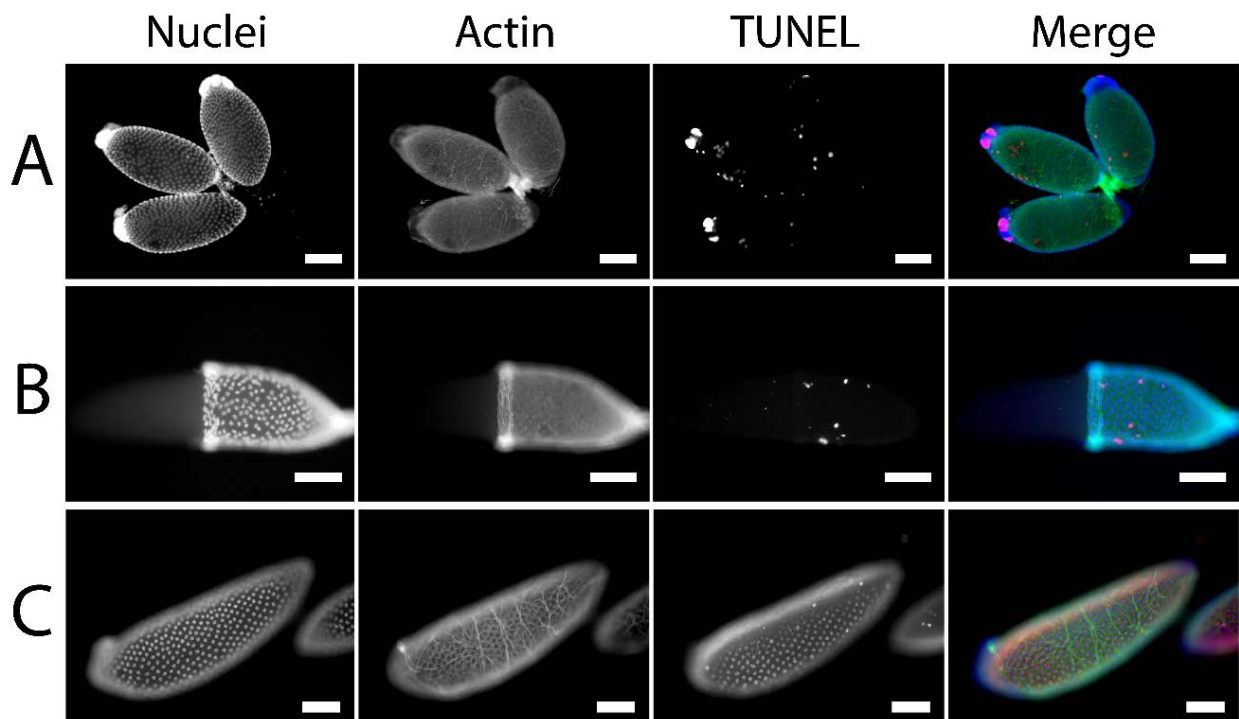
Supplementary Figure 1 - Follicles switch from previtellogenic to initiation phase based on mosquito age. Follicles from 3 day old adult mosquitoes at (A) 0 HPBM and (B) 4 HPBM. Follicles from 5 day old adult mosquitoes at (C) 0 HPBM and (D) 4 HPBM. (E)- Proportion of follicles from 3 day old adult mosquitoes with NR staining in the oocyte over time as an indicator of stage IIIa (n = 79-467). Arrowheads indicate oocyte nuclei. Scale bar = 100 µM. All data are the average of 3 or more biological replicates (± SEM), n = number of follicles measured (from 10-15 mosquitoes) per time point.
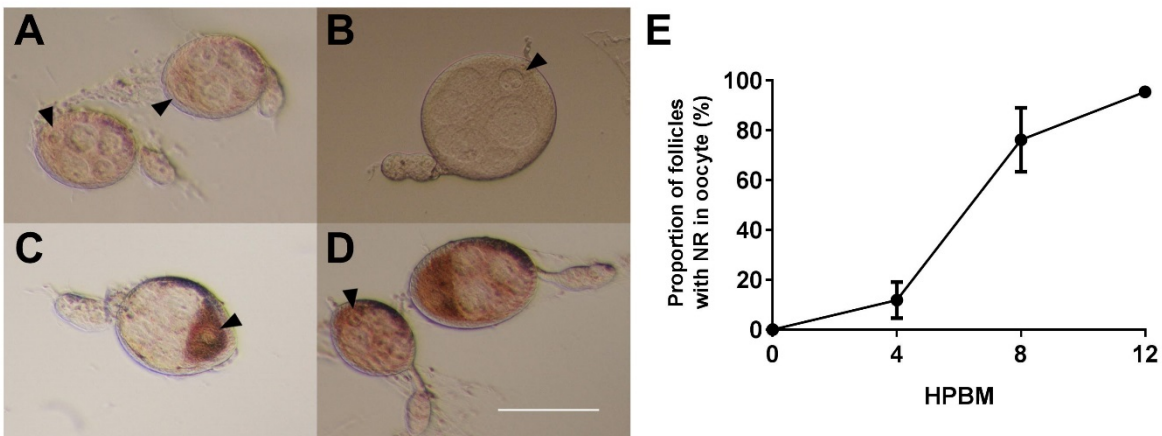
Supplementary Figure 2 – FE grows proportionally with the follicle during oogenesis.

Proportion of follicle area encompassed by the FE, oocyte, and nurse cell compartment following a bloodmeal (n = 15). The average of 3 or more biological replicates (± SEM) shown, n = number of follicles measured (from 10-15 mosquitoes) per time point.
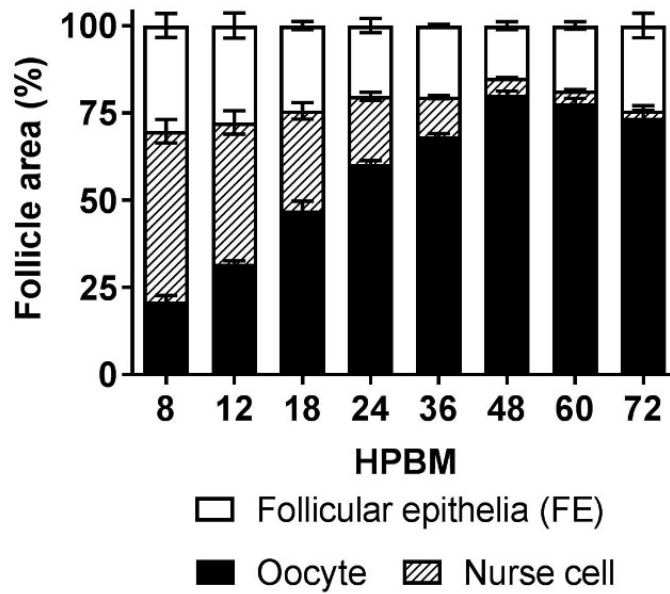
Supplementary Figure 3 – Additional studies of NCD. (A) Quantification of NCD compared between AO and NR staining methods over time (n = 76-261). (B) Proportion of NCD positive follicles per ovary in 5 day old adult mosquitoes using AO (n = 45-144). All data are the average of 3 or more biological replicates (± SEM in part B), n = number of follicles measured (from 10-15 mosquitoes) per time point.
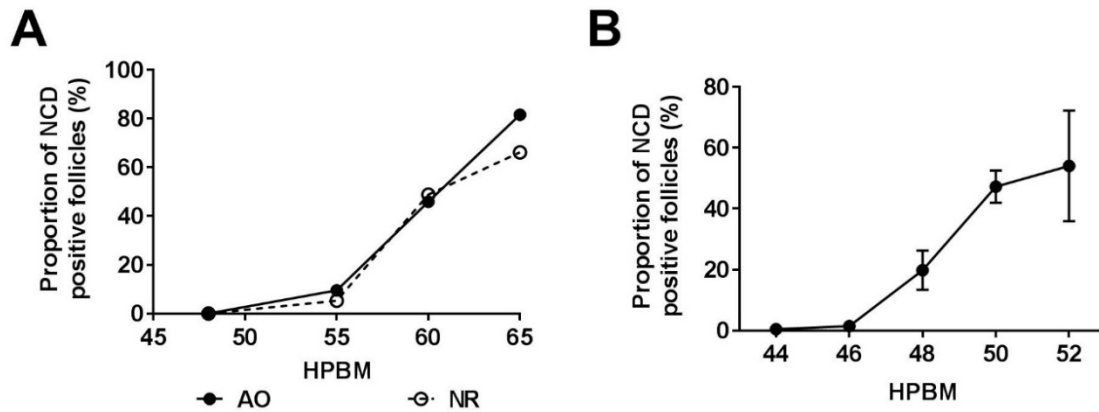
Supplementary Figure 4 – Initiation phase IIIa reached by secondary follicles following oviposition without a second bloodmeal. Follicles at 120-144 HPBM pre- and post-oviposition. (A) pre-oviposition with primary follicle with attached FE at stage V, secondary follicle at stage Ia-IIa with unusual staining, and tertiary follicle at stage G. (B) post-oviposition, with intact primary follicle FE, secondary follicles with visible FE, and oocyte nuclear envelope at stage IIb, and tertiary follicles at stage G. (C) post-oviposition, with mostly resorbed primary follicle FE and secondary follicles at stage IIIa. Scale bar = 100 µM. All data are the average of 3 or more biological replicates.
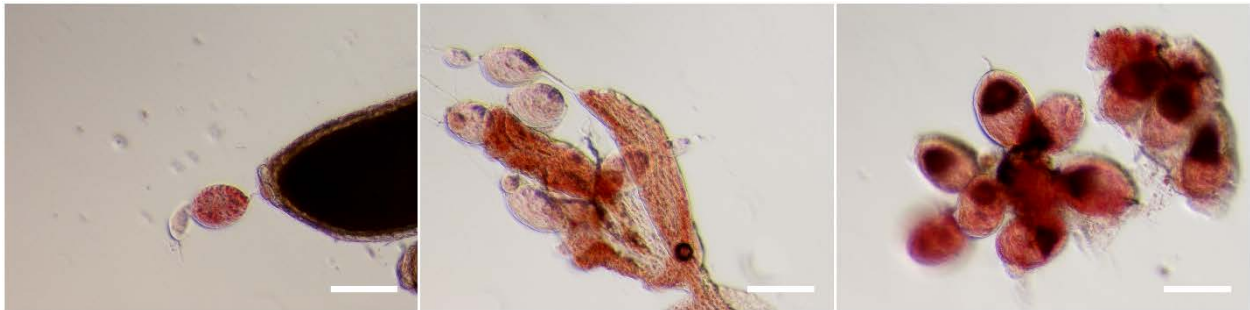
Supplementary Figure 5 – Apoptosis does not occur in late stage oogenesis prior to oviposition. Ovaries imaged at 120 HPBM including nuclei (DAPI), actin (Phalloidin), and TUNEL staining. (A-C) Primary follicles, secondary follicles, and ovarian sheath. (D-F) DNase I positive control primary follicles, secondary follicles and ovarian sheath.
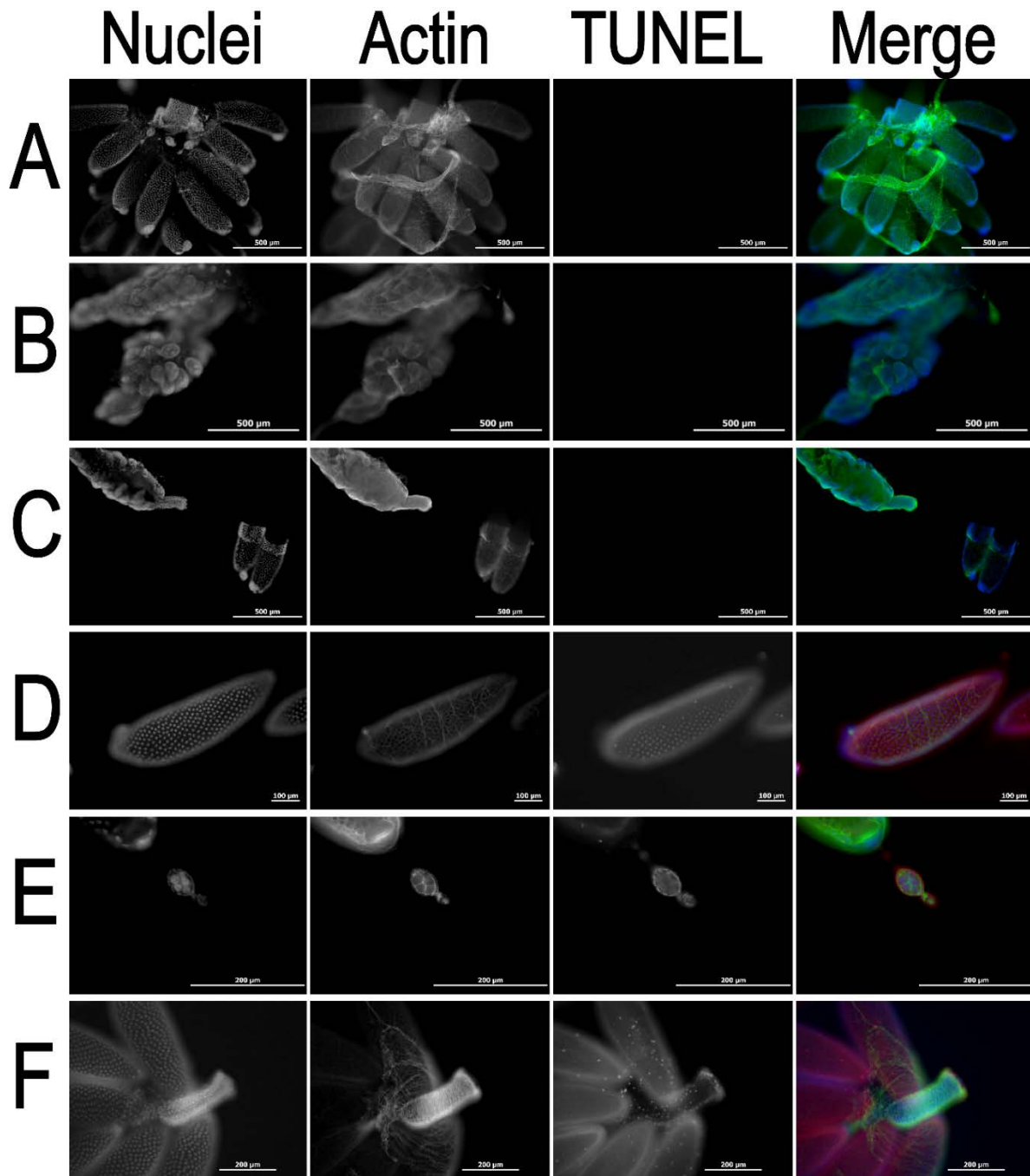
Supplementary Figure 6 – Ovarian phases timeline illustrated as described in the text.
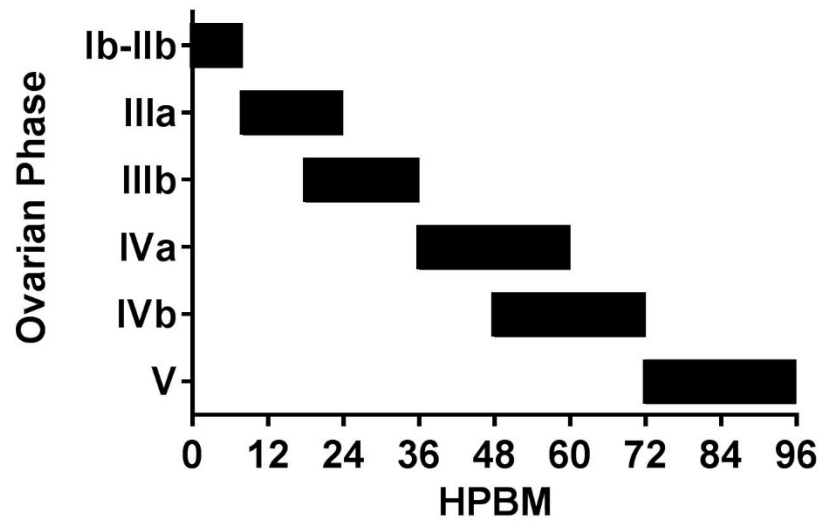
Chapter 3 – A comparative analysis of RNAi trigger uptake and distribution in mosquito vectors of disease

Abstract

RNAi, an antiviral immune pathway, has been co-opted as a widely utilized reverse genetics tool in mosquitoes. However, the barriers and limitations of RNAi across mosquitoes species has yet to be delineated. In this study, heterologous LacZ double-stranded RNA (iLacZ) was used as a proxy to measure uptake and clearance of exogenously produced RNAi triggers in *Aedes aegypti, Anopheles gambiae,* and *Culex pipiens*. Peritoneal exposure resulted in uptake and spread of iLacZ throughout the body, but was iLacZ was limited mostly to the gut lumen when exposed *per os* or to the cuticle when topically applied. Tracking fluorescently labelled iLacZ revealed uptake in a subset of cells including: hemocytes, pericardial cells of the dorsal vessel, ovarian follicles, and ganglia of the ventral nerve cord. These cell types are all known to undergo phagocytosis, pinocytosis, or both, and as such may sequester RNAi triggers by bulk uptake. In *Ae. aegypti*, iLacZ tracked by Northern blot was detected at one week post exposure in whole body extracts, but uptake and clearance differed across tissues. These results reveal that uptake of RNAi triggers is distinct and specific to particular cell types *in vivo* and dependent upon invasive exposure.

Introduction

RNAi is a highly conserved, post-transcriptional gene suppression pathway that plays an essential role in mosquito antiviral immunity (Blair, 2011; Kemp et al., 2013; Mongelli and Saleh, 2016; Nayak et al., 2013; Olson and Blair, 2015; Saleh et al., 2009). The core RNAi pathway is robust in mosquitoes and plays a role in clearance of arboviral infections, but can also function to maintain persistent viral infections (Blair, 2011; Goic et al., 2016; Sánchez-Vargas et al., 2009). Delineating the nuances of RNAi in mosquitoes is therefore key to understanding the nature of mosquito vector competence. In the cell, the core RNAi pathway is activated when Dicer 2 binds and cleaves long double-stranded RNA (dsRNA) into short interfering RNA (siRNA). Argonaute 2 binds to siRNAs and melts the duplex into guide and passenger strands as well as recruiting a number of other proteins forming the RNA Induced Silencing Complex (RISC) (Hoa et al., 2003; Sontheimer, 2005; van Rij et al., 2006). The guide strand then acts as template for the RISC to detect and cleave matching mRNAs by base complementarity, preventing translation.

The core pathway is well characterized, but little has been elucidated regarding systemic RNAi responses in mosquitoes. In many insect species, RNAi trigger amplification by RNA-dependent RNA polymerases (RDRP) and spread by SID-1 dsRNA-gated channels facilitate a systemic RNAi response (Scott et al., 2013; Sijen et al., 2001; Tassetto et al., 2017; Winston et al., 2002). Diptera lack SID-1 and RDRPs, but require systemic RNAi to prevent viral superinfection (Karlikow et al., 2014; Saleh et al., 2009; Scott et al., 2013). RNAi triggers can spread via release from ruptured apoptotic cells into the hemolymph or packaged into exosomes of circulating hemocytes (Goic et al., 2016; Saleh et al., 2006; Tassetto et al., 2017). Passage of RNAi triggers via exosomes also occurs in filarial nematodes and therefore may be a conserved means of spreading RNAi triggers within and between species (Buck et al., 2014; Zamanian et al., 2015). Understanding systemic

RNAi responses to viral infection is critical to navigating insect immunity, but does not assess the fate of exogenously produced non-viral RNAi triggers used in RNAi knockdown studies, especially when spread of RNAi triggers cannot rely on apoptosis and rupturing of the cell.

Despite frequent implementation of RNAi triggers in gene knockdown assays, the uptake and spread exogenously produced RNAi triggers in mosquitoes is not well defined. Some studies have shed light on the limited uptake of dsRNA in specific tissues such as the salivary glands in *Anopheles gambiae (Boisson et al., 2006)*. Knockdown of mosquito genes following exposure to RNAi triggers has been reported in a variety of species, strains, life-stages, and tissues; suggesting that RNAi is a robust system in mosquitoes (Airs, 2018). However, it is not known whether knockdown is mediated by direct uptake of the RNAi trigger by endocytosis, as suggested by Saleh *et al* 2006, or by systemic RNAi requiring amplification and spread from hemocytes, as witnessed by Tassetto *et al* 2018 (Saleh et al., 2006; Tassetto et al., 2017).

We reasoned that delineating and describing RNAi uptake and efficacy in a comparative manner would support more informed RNAi experimental design as well as outline the basis for systemic RNAi in a non-viral setting. In this study, the distribution of heterologous LacZ RNAi triggers (iLacZ) was characterized in *Aedes aegypti, Anopheles gambiae*, and *Culex pipiens* when provided to the insect by intrathoracic injection, *per os*, or by topical application. Using a combination of Northern blot and fluorescence microscopy analyses we track iLacZ in tissues and cells following exposure and reveal uptake of iLacZ in a subset of cells, namely: hemocytes, pericardial cells of the dorsal vessel, ovarian follicles, and ganglia of the ventral nerve cord.

Materials and Methods

Mosquito rearing and maintenance

Aedes aegypti (Liverpool), *Anopheles gambiae* (G3), and *Culex pipiens pipiens* (Iowa) larvae were reared in enamel pans and fed daily with a slurry of ground TetraMin™ (Blacksburg, VA). Unless otherwise stated, groups of 50 female pupae were collected ~24 hours prior to emergence and maintained in cartons on a 10% sucrose diet. For blood feeding, individuals were starved for ~24 hours then exposed to defibrinated sheep blood (HemoStat Laboratories, CA) maintained at 37 °C through a Parafilm M® (Bemis, WI) membrane, using a blown glass membrane feeder and circulating water bath. All life stages were maintained at 28 °C at 70% relative humidity with a 16:8 hour (light:dark) photoperiod.

RNAi trigger synthesis & labelling

LacZ RNAi triggers were produced using T7-tagged primers (Table S1) targeting the LacZ region of the pGEM®-T Easy vector (Promega). LacZ PCR products were amplified using GoTaq® Flexi polymerase (Promega), purified by Wizard® SV PCR Clean-Up kit (Promega), then subjected to the MEGAscript™ RNAi kit (Ambion) with phenol:chloforom cleanup. For siRNA generation, ShortCut® RNase III (NEB) cleavage of dsRNAs was performed followed by ethanol precipitation. Fluorescent labels were added using the Cy3 Label IT® kit (Mirus) with ethanol precipitation. All PCR products and RNAi triggers were re-suspended in nuclease free water and subjected to gel electrophoresis and quantification using a NanoDrop (Thermo Scientific) for quantification and quality control.

RNAi trigger exposure

Adult females (3 - 5 days post eclosion, and 24 hours post blood feeding if applicable) were cold anesthetized and held in a petri dish on wet ice prior to injection. Mosquitoes were intrathoracically

injected via the cervical membrane with 800-1600 ng RNAi trigger (0.5 µl for *Ae. aegypti* and *Cx. pipiens*, 0.2 µl for *An. gambiae*) using pulled borosilicate glass capillary needles (Kwik-Fill™, World Precision Instruments) and a micromanipulator. For *per os* exposures, groups of 20 adult females were starved for 1 day post-eclosion and then provided with 25-50 µl of RNAi trigger (0.8 mg/ml) in 0.5 M sucrose in a micro-centrifuge tube cap or via borosilicate glass capillary tubes. For topical exposure, groups of 50 adult females (3 day post eclosion) were cold anesthetized on ice and 0.5 µl of acetone:RNAi trigger mixtures (3:1 with 1 mg/ml RNAi trigger) were placed directly on the dorsal thorax and abdomen. Following exposure, mosquitoes were maintained in cartons with 10% sucrose and monitored daily for survival until tissues were processed.

Mosquito dissections

Cold anesthetized mosquitoes were held by probe inserted through the thorax and dissected under a Zeiss Stemi 508 microscope. The head, legs, wings were removed by No. 5 forceps followed by slicing and pulling from the 7th abdominal segment to extract internal organs (alimentary tract, ovaries, fat body) directly into room temperature nuclease free PBS. For RNA extraction studies, tissues were further separated and frozen immediately on dry ice. For imaging experiments, the abdomen and thorax were sliced to reveal internal structures.

Imaging of live and fixed mosquito tissues

Live dissected tissues were washed once in PBS, transferred to slides and immediately imaged on a Zeiss Axio Scope.A1 with QIClick™ CCD Camera (Q-imaging) and Nikon Elements D software. Image processing and representative panels were prepared using ImageJ (https://imagej.nih.gov/ij/). Fixed tissues were preserved (4% paraformaldehyde in PBS for 20

minutes), washed (3x in PBS), permeabilized (0.3% Triton X-100, 1% BSA, 1% Sodium citrate in PBS for 30 minutes and washed 3x in PBS), then mounted on slides in ProLong™ Gold Antifade with DAPI (Invitrogen) prior to imaging. Staining with Alexa Fluor 488/594 Phalloidin (Life Technologies) in micro-centrifuge tubes containing ~1ml PBS was also performed in *Ae. aegypti* adult tissues following injection and *per os* exposure.

Northern Blot analyses

RNA (1-10 µg standardized per gel) was prepared in sample running buffer at 80 °C, chilled on ice, then run on 1.2% TBE agarose gel at 90 v with ethidium bromide for 30 - 60 minutes on ice. Gels were imaged (AlphaImager HP) to determine RNA integrity and ribosomal band intensity, then transferred to BrightStar™ membrane (Ambion) using the NorthernMax™ kit (ThermoFisher). Membranes were immediately UV crosslinked and hybridized in ULTRAhyb™ buffer (Invitrogen) at 68 °C overnight. T7 LacZ PCR products served as template for synthesis of ssRNA probes containing 40% biotin-14-CTP (MAXIscript™ T7 transcription kit (Ambion)). Probes were added after 30 minutes of hybridization and washed according to NorthernMax instructions. Membranes were developed using the Biotin Chromogenic Detection kit (ThermoFisher), imaged (AlphaImager HP), and aligned with the corresponding gel/EtBR image using ImageJ and Adobe Photoshop CC.

Results

A subset of cells sequester the majority of exogenously introduced RNAi triggers in Ae. aegypti, An. gambiae, and Cx. pipiens.

To comparatively assess uptake of RNAi triggers across different mosquito species, larvae and adult females of *Ae. aegypti, An. gambiae*, and *Cx. pipiens* were exposed to a 417 base-pair (bp) fluorescently labelled iLacZ (Table 1, Table S1). Only several cell types were witnessed containing iLacZ in all species, including the pericardial cells, hemocytes, and ovarian follicles (Table 1, Figure S1-S15). Hemocytes containing iLacZ were detected throughout the body cavity including in the: head, legs, thorax, as well as amongst the fat body and trachea associated with the ovaries, and Malpighian tubules. In *Ae. aegypti*, specific fluorescence was also detected in ganglia of the ventral nerve cord (Figure S1).

Following peritoneal exposure, clearance of iLacZ from the hemolymph was noted between 24 and 120 hours post-exposure (HPE) and appeared in the alimentary tract lumen suggesting that RNAi triggers or their degradation products are actively excreted from the hemolymph (Table 1, Figures S1-S3). Providing a blood-meal did not dramatically alter the destination of injected iLacZ, but blood-feeding appears to eliminate excretion of iLacZ from the hemolymph (Table 1, Figures S4-S6). Excreted iLacZ signal may diminish in the presence of digested blood in the alimentary tract, but is more likely directed to the ovaries, which presented bright iLacZ signal in developing oocytes as soon as 1 HPE (Table 1, Figures S4-S6). Blood-feeding also stimulates increase in hemocyte proliferation from the fat body in *An. gambiae* (Bryant and Michel, 2014). Unsurprisingly, hemocytes following a blood-meal also were found containing iLacZ signal, especially in *An. gambiae*, but in *Cx. pipiens* iLacZ was also occasionally detected in larger, high lipid content fat body cells (Table 1, Figures S7-S9). Similar to adults, peritoneal exposure of fourth instar *Ae. aegypti, An. gambiae*, and *Cx. pipiens* larvae with fluorescent iLacZ resulted in uptake in pericardial cells, hemocytes, and the lumen of the alimentary tract (Table 1, Figures S7-

S9). Overall these results highlight that a small subset of cell types internalize dsRNA following peritoneal exposure and that uptake is not dependent upon species or life-stage.

Persistence of iLacZ is dependent upon tissue and nutritional status

Tracking iLacZ by fluorescence microscopy discerns location but not integrity of the RNAi trigger. To elucidate persistence of RNAi triggers, Northern blots were performed following injection or topical exposure of *Ae. aegypti* to iLacZ (Figure 1). In whole body RNA extracts, iLacZ of different lengths diminished rapidly between 24 and 72 HPE, but were detectable at one week post exposure (Figure 1 A). A finer assessment of a 417 bp iLacZ over time revealed a near full length band (~300 bp), which accumulated in whole body extracts over time (Figure 1 B). Both full length and the near-full length bands were present following DNase treatment of extracted RNA (Figure 1 C). Therefore iLacZ is either partially degraded or may be subject to reverse transcription and re-expression; a phenomenon known to occur with viral dsRNA (Tassetto et al., 2017). Interestingly, near-full length iLacZ was present in in all tissues tested at 4 HPE, but was only visible in the abdomen, midgut, and ovary extracts by 24 HPE (Figure 1 D). Following a blood-meal full-length iLacZ was detected in the head and thorax, but not in the ovaries of bloodfed *Ae. aegypti* and may be degraded during oogenesis (Figure 1 E). The detection of iLacZ in all tissues extracts does not indicate cellular uptake into target tissues, since free iLacZ in the hemolymph, hemocytes containing iLacZ, or iLacZ bound to the outer membrane of the tissue may all contribute to signal detection. To determine degradation by non-Dicer-2 dsRNA nucleases, iLacZ was tracked following exposure to Dicer-2 deficient *Aedes albopictus* C6/36 cells (Brackney et al., 2010). Here, all signal was rapidly lost following exposure to C6/36 cells (Figure 1 F). Full length

or near-full length iLacZ signal may be maintained by the presence of Dicer-2, as is known to occur with long viral genomic dsRNA (Poirier et al., 2018).

Exposure route limits uptake and spread of RNAi triggers in Ae. aegypti, An. gambiae, and Cx. pipiens.

Uptake was dependent upon exposure route, with invasive peritoneal exposure required for passage of iLacZ beyond the alimentary or cuticular barriers in the majority of cases in both larvae and adults (Table 1). Topical exposures administered in acetone to the dorsal thorax resulted in to deposition of iLacZ on the cuticle of *Ae. aegypti, An. gambiae,* and *Cx. pipiens*, but no penetration of the cuticle to internal structures was found by fluorescence microscopy and Northern blot (Table 1, Figures S10-S12, Figure 1 G). Surprisingly, topically applied iLacZ remains intact on the *Ae. aegypti* cuticle for at least one week of exposure in insectary conditions, but was not found in internal tissues (Figure 1 G). Increase in band intensity is an artefact of residual acetone contamination, which had not dried completely in earlier time-points.

Per os exposure in sucrose meals resulted in iLacZ uptake and concentration in the ventral diverticulum and alimentary tract lumen of *Ae. aegypti* and *Cx. pipiens* (Table 1, Figure 2, Figure S13-S14). Performing *per os* assays required a period of starvation and exposure to a limited volume of iLacZ-sucrose medium, which hindered attempts to study uptake in *An. gambiae* due to high mortality. Uptake beyond the gut lumen was detected in pericardial cells of *Ae. aegypti* and *Cx. pipiens* on occasion (Table 1, Figure S13-14). In *Cx. pipiens*, hemocytes in the thorax, legs, and ovaries contained iLacZ, indicating that *per os* may be a feasible exposure route in this species (Table 1, Figure S14). Exposure of iLacZ-sucrose medium to *Ae. aegypti* in insectary conditions

did not alter iLacZ integrity as assessed by gel electrophoresis, indicating that dsRNA is stable until ingestion using this assay (Figure S16).

Exposure of larvae to RNAi triggers can also be mediated *per os* by soaking of first instar or neonate larvae in small volumes of water. First instar *Ae. aegypti* larvae were continuously exposed to nuclease free water containing fluorescently labelled iLacZ for 72 hours (Table 1, Figure S15). Here, iLacZ signal was detected in the head and alimentary tract lumen, but no tissues beyond the lumen contained any detectable signal.

Ovaries are a sink for RNAi triggers with and without a blood meal.

Ovaries appear to be a primary destination of iLacZ with and without a blood-meal in *Ae. aegypti, An. gambiae,* and *Cx. pipiens* (Table 1). Within the ovary, iLacZ was found in hemocytes associated with tracheoles, as well as pre-vitellogenic and post-vitellogenic oocytes of healthy and atretic follicles (see Figures S1-S6). In *Cx. pipiens*, a facultatively-autogenous species, stronger iLacZ signal was noted in oocytes of post-vitellogenic follicles in non-bloodfed individuals (see Figure S3). Other small cells appeared to contain iLacZ signal but could not be discerned using compound fluorescence microscopy.

To determine sub-follicle localization of iLacZ, confocal microscopy was performed 24 hours post injection in non-bloodfed *Ae. aegypti* ovaries (Figure 2, Figure S17). Here, iLacZ was detectable in the follicular epithelium and oocytes of primary and secondary follicles. Strong signal was witnessed in atretic follicles (compare Figure 2 and Sigure S4). Conversely little to no signal was detected in nurse cells or cells of the ovarian sheath. These results indicate that dsRNA in the hemolymph is transported to oocytes via the follicular epithelium and may not pass through the nurse cells.

Discussion

RNAi is a frequently utilized reverse genetics tool targeting knockdown of genes across a wide range of target tissues in insects, but is hampered by variation in knockdown success and experimental outcome (Scott et al., 2013; Terenius et al., 2011). Determining factors relating to knockdown success in mosquitoes is muddled by the myriad of factors that could impact any measured outcome. As a result, no guidelines for successful RNAi experimentation exist in mosquitoes. Despite this, evidence of tissue variation in RNAi efficacy has been documented. For example, *An. gambiae* salivary glands are recalcitrant to siRNA uptake and subsequent knockdown as compared to the ovaries (Boisson et al., 2006). In *Ae. aegypti*, knockdown of oxysterol binding protein and apolipoprotein was more effective in the abdomen than the head, midgut, and ovary (Telang et al., 2013). These studies demonstrate the differences in RNAi efficacy at the tissue level, but have limited scope and may also be impacted by tissue specific target gene expression. How tissue differences relate to distribution and integrity of RNAi triggers, and whether these differences are species-specific have not been extensively explored.

In this study, we utilize iLacZ to determine distribution (using fluorescence microscopy) and persistence (by Northern blot) in *Ae. aegypti, An. gambiae*, and *Cx. pipiens*. We find distribution of iLacZ is limited to hemocytes, pericardial cells, ganglia of the dorsal vessel, as well as oocytes and follicular epithelia of ovarian follicles following peritoneal exposure. Hemocytes containing iLacZ were found throughout the body and were commonly detected in association with trachea of the Malpighian tubules and ovaries. In larvae and adult *An. gambiae*, thin trachea are a site for hemocyte binding as these sites are key for entry of pathogens into the hemocoel (League and Hillyer, 2016). Mosquito ovaries, similar to *Drosophila*, contain meroistic polytrophic ovaries. These ovaries are composed of strings of follicles where the terminal-most follicle (the primary

follicle) develops first, typically following a blood-meal (Clements, 1992). Each follicle contains an oocyte, follicular epithelia, and nurse cells. The follicular epithelial layer dictates shape of the oocyte, provides the vitelline envelope, and mediates uptake of nutrients from the hemolymph (Anderson and Spielman, 1971; Raikhel and Lea, 1991; Went, 1978). The nurse cells provide mRNA and other cytoplasmic contents to the oocyte through cytoplasmic bridges (Cheung et al., 1992; Cooley et al., 1992). Here, we find the follicular epithelium and not nurse cells transport dsRNA from the hemolymph to the oocyte and the nurse cells remain relatively devoid of introduced dsRNA (see Figure 2).

Uptake of iLacZ may be driven by phagocytosis or pinocytosis since pericardial cells (Das et al., 2008), hemocytes (Hillyer et al., 2003), nerve glia (Cantera and Technau, 1996; Kurant et al., 2008), and ovarian follicles (Anderson and Spielman, 1971; Giorgi, 1979) have been shown to uptake cargo by these pathways. In *Drosophila* cells, scavenger receptor-mediated endocytosis (Ulvila et al., 2006) and RNAi trigger length-dependant endocytosis (Saleh et al., 2006) have been demonstrated, along with phagocytosis (Rocha et al., 2011) as routes for dsRNA uptake. Uptake into the midgut and fat body was generally not witnessed and may not occur with fluorescently labelled iLacZ. However, RNAi knockdown in these tissues is well documented in a number of mosquito species. For instance, > 90% knockdown of Target of Rapamycin has been achieved in both the fat body and midgut of *Ae. aegypti* (Brandon et al., 2008; Roy et al., 2007). Indeed, a full length iLacZ band was found in the midgut and abdomen (which mostly consists of fat body cells) by Northern blot (see figure 1). As such, fluorescent detection of iLacZ signal may lack sensitivity. Alternatively, knockdown in midgut and other cell types may be mediated by a secondary signal. In *Drosophila* and *Aedes albopictus* dsRNA derived from virus is reverse transcribed, re-expressed, and exported via exosomes (Goic et al., 2016; Poirier et al., 2018). Hemocytes are

known to drive spread of re-expressed RNAi triggers in *Drosophila* (Tassetto et al., 2017) and the same may be occuring with exogenously produced dsRNA in mosquitoes. Our findings corroborate the current theory as iLacZ was sequestered by hemocytes, and potentially re-expressed iLacZ bands were detected by Northern blots in tissues that lacked fluorescent signal. It is also possible that free iLacZ in the hemolymph, or hemocytes containing iLacZ contaminated tissue samples when performing Northern blots, although all tissues were washed in PBS prior to RNA extraction.

Overall, these results highlight that RNAi triggers are sequestered by a few distinct cell types, a phenotype that is conserved across mosquito species and life-stages, but this sequestration must not eliminate knockdown in other tissues, given the wealth of evidence provided in the literature. It is possible that hemocytes play a role in amplification and spread of exogenously produced RNAi triggers, although more work is needed to confirm whether systemic RNAi knockdown occurs when mosquitoes are challenged with non-viral dsRNAs or other RNAi triggers.

Literature cited

Airs PM (2018) *Manipulating cell death and RNA interference processes for mosquito control. Ph.D. Dissertation*. Doctor of Philosophy. University of Wisconsin Madison.

Anderson WA and Spielman A (1971) Permeability of the ovarian follicle of Aedes aegypti mosquitoes. *The Journal of cell biology* 50(1): 201–221. Available at: https://www.ncbi.nlm.nih.gov/pubmed/4104968.

Blair CD (2011) Mosquito RNAi is the major innate immune pathway controlling arbovirus infection and transmission. *Future microbiology* 6(3): 265–277. DOI: 10.2217/fmb.11.11.

Boisson B, Jacques JC, Choumet V, et al. (2006) Gene silencing in mosquito salivary glands by RNAi. *FEBS letters* 580(8): 1988–1992. DOI: 10.1016/j.febslet.2006.02.069.

Brackney DE, Scott JC, Sagawa F, et al. (2010) C6/36 Aedes albopictus cells have a dysfunctional antiviral RNA interference response. *PLoS neglected tropical diseases* 4(10): e856. DOI: 10.1371/journal.pntd.0000856.

Brandon MC, Pennington JE, Isoe J, et al. (2008) TOR signaling is required for amino acid stimulation of early trypsin protein synthesis in the midgut of Aedes aegypti mosquitoes. *Insect biochemistry and molecular biology* 38(10): 916–922. DOI: 10.1016/j.ibmb.2008.07.003.

Bryant WB and Michel K (2014) Blood feeding induces hemocyte proliferation and activation in the African malaria mosquito, Anopheles gambiae Giles. *The Journal of experimental biology* 217(Pt 8): 1238–1245. DOI: 10.1242/jeb.094573.

Buck AH, Coakley G, Simbari F, et al. (2014) Exosomes secreted by nematode parasites transfer small RNAs to mammalian cells and modulate innate immunity. *Nature communications* 5: 5488. DOI: 10.1038/ncomms6488.

Cantera R and Technau GM (1996) Glial cells phagocytose neuronal debris during the metamorphosis of the central nervous system in Drosophila melanogaster. *Development genes and evolution* 206(4): 277–280. DOI: 10.1007/s004270050052.

Cheung HK, Serano TL and Cohen RS (1992) Evidence for a highly selective RNA transport system and its role in establishing the dorsoventral axis of the Drosophila egg. *Development* 114(3): 653–661. Available at: https://www.ncbi.nlm.nih.gov/pubmed/1377623.

Clements AN (1992) *The biology of mosquitoes. Volume 1. Development, nutrition and reproduction*. University Press, Cambridge, Massachusetts: Chapman and Hall.

Cooley L, Verheyen E and Ayers K (1992) chickadee encodes a profilin required for intercellular cytoplasm transport during Drosophila oogenesis. *Cell* 69(1): 173–184. Available at: https://www.ncbi.nlm.nih.gov/pubmed/1339308.

Das D, Aradhya R, Ashoka D, et al. (2008) Macromolecular uptake in Drosophila pericardial cells requires rudhira function. *Experimental cell research* 314(8): 1804–1810. DOI: 10.1016/j.yexcr.2008.02.009.

Giorgi F (1979) In vitro induced pinocytotic activity by a juvenile hormone analogue in oocytes of Drosophila melanogaster. *Cell and tissue research* 203(2): 241–247. Available at: https://www.ncbi.nlm.nih.gov/pubmed/117896.

Goic B, Stapleford KA, Frangeul L, et al. (2016) Virus-derived DNA drives mosquito vector tolerance to arboviral infection. *Nature communications* 7: 12410. DOI: 10.1038/ncomms12410.

Hillyer JF, Schmidt SL and Christensen BM (2003) Hemocyte-mediated phagocytosis and melanization in the mosquito Armigeres subalbatus following immune challenge by bacteria. *Cell and tissue research* 313(1): 117–127. DOI: 10.1007/s00441-003-0744-y.

Hoa NT, Keene KM, Olson KE, et al. (2003) Characterization of RNA interference in an Anopheles gambiae cell line. *Insect biochemistry and molecular biology* 33(9): 949–957. DOI: 10.1016/S0965-1748(03)00101-2.

Karlikow M, Goic B and Saleh M-C (2014) RNAi and antiviral defense in Drosophila: setting up

a systemic immune response. *Developmental and comparative immunology* 42(1): 85–92. DOI: 10.1016/j.dci.2013.05.004.

Kemp C, Mueller S, Goto A, et al. (2013) Broad RNA interference-mediated antiviral immunity and virus-specific inducible responses in Drosophila. *Journal of immunology* 190(2): 650–658. DOI: 10.4049/jimmunol.1102486.

Kurant E, Axelrod S, Leaman D, et al. (2008) Six-microns-under acts upstream of Draper in the glial phagocytosis of apoptotic neurons. *Cell* 133(3): 498–509. DOI: 10.1016/j.cell.2008.02.052.

League GP and Hillyer JF (2016) Functional integration of the circulatory, immune, and respiratory systems in mosquito larvae: pathogen killing in the hemocyte-rich tracheal tufts. *BMC biology* 14: 78. DOI: 10.1186/s12915-016-0305-y.

Mongelli V and Saleh M-C (2016) Bugs Are Not to Be Silenced: Small RNA Pathways and Antiviral Responses in Insects. *Annual review of virology* 3(1): 573–589. DOI: 10.1146/annurev-virology-110615-042447.

Nayak A, Tassetto M, Kunitomi M, et al. (2013) RNA interference-mediated intrinsic antiviral immunity in invertebrates. *Current topics in microbiology and immunology* 371: 183–200. DOI: 10.1007/978-3-642-37765-5_7.

Olson KE and Blair CD (2015) Arbovirus-mosquito interactions: RNAi pathway. *Current opinion in virology* 15: 119–126. DOI: 10.1016/j.coviro.2015.10.001.

Poirier EZ, Goic B, Tomé-Poderti L, et al. (2018) Dicer-2-Dependent Generation of Viral DNA from Defective Genomes of RNA Viruses Modulates Antiviral Immunity in Insects. *Cell host &*

microbe 23(3): 353–365.e8. DOI: 10.1016/j.chom.2018.02.001.

Raikhel AS and Lea AO (1991) Control of follicular epithelium development and vitelline envelope formation in the mosquito; role of juvenile hormone and 20-hydroxyecdysone. *Tissue & cell* 23(4): 577–591. Available at: https://www.ncbi.nlm.nih.gov/pubmed/1926140.

Rocha JJE, Korolchuk VI, Robinson IM, et al. (2011) A phagocytic route for uptake of double-stranded RNA in RNAi. *PloS one* 6(4): e19087. DOI: 10.1371/journal.pone.0019087.

Roy SG, Hansen IA and Raikhel AS (2007) Effect of insulin and 20-hydroxyecdysone in the fat body of the yellow fever mosquito, Aedes aegypti. *Insect biochemistry and molecular biology* 37(12): 1317–1326. DOI: 10.1016/j.ibmb.2007.08.004.

Saleh M-C, van Rij RP, Hekele A, et al. (2006) The endocytic pathway mediates cell entry of dsRNA to induce RNAi silencing. *Nature cell biology* 8(8): 793–802. DOI: 10.1038/ncb1439.

Saleh M-C, Tassetto M, van Rij RP, et al. (2009) Antiviral immunity in Drosophila requires systemic RNA interference spread. *Nature* 458(7236): 346–350. DOI: 10.1038/nature07712.

Sánchez-Vargas I, Scott JC, Poole-Smith BK, et al. (2009) Dengue virus type 2 infections of Aedes aegypti are modulated by the mosquito's RNA interference pathway. *PLoS pathogens* 5(2). Public Library of Science: e1000299. DOI: 10.1371/journal.ppat.1000299.

Scott JG, Michel K, Bartholomay LC, et al. (2013) Towards the elements of successful insect RNAi. *Journal of insect physiology* 59(12). Elsevier Ltd: 1212–1221. DOI: 10.1016/j.jinsphys.2013.08.014.

Sijen T, Fleenor J, Simmer F, et al. (2001) On the role of RNA amplification in dsRNA-triggered

gene silencing. *Cell* 107(4): 465–476. Available at:

https://www.ncbi.nlm.nih.gov/pubmed/11719187.

Sontheimer EJ (2005) Assembly and function of RNA silencing complexes. *Nature reviews. Molecular cell biology* 6(2): 127–138. DOI: 10.1038/nrm1568.

Tassetto M, Kunitomi M and Andino R (2017) Circulating Immune Cells Mediate a Systemic RNAi-Based Adaptive Antiviral Response in Drosophila. *Cell* 169(2): 314–325.e13. DOI: 10.1016/j.cell.2017.03.033.

Telang A, Rechel JA, Brandt JR, et al. (2013) Analysis of ovary-specific genes in relation to egg maturation and female nutritional condition in the mosquitoes Georgecraigius atropalpus and Aedes aegypti (Diptera: Culicidae). *Journal of insect physiology* 59(3): 283–294. DOI: 10.1016/j.jinsphys.2012.11.006.

Terenius O, Papanicolaou A, Garbutt JS, et al. (2011) RNA interference in Lepidoptera: an overview of successful and unsuccessful studies and implications for experimental design. *Journal of insect physiology* 57(2): 231–245. DOI: 10.1016/j.jinsphys.2010.11.006.

Ulvila J, Parikka M, Kleino A, et al. (2006) Double-stranded RNA is internalized by scavenger receptor-mediated endocytosis in Drosophila S2 cells. *The Journal of biological chemistry* 281(20): 14370–14375. DOI: 10.1074/jbc.M513868200.

van Rij RP, Saleh M-C, Berry B, et al. (2006) The RNA silencing endonuclease Argonaute 2 mediates specific antiviral immunity in Drosophila melanogaster. *Genes & development* 20(21): 2985–2995. DOI: 10.1101/gad.1482006.

Went DF (1978) Oocyte maturation without follicular epithelium alters egg shape in a dipteran insect. *The Journal of experimental zoology* 205(1): 149–155. DOI: 10.1002/jez.1402050118.

Winston WM, Molodowitch C and Hunter CP (2002) Systemic RNAi in C. elegans requires the putative transmembrane protein SID-1. *Science* 295(5564): 2456–2459. DOI: 10.1126/science.1068836.

Zamanian M, Fraser LM, Agbedanu PN, et al. (2015) Release of Small RNA-containing Exosome-like Vesicles from the Human Filarial Parasite Brugia malayi. *PLoS neglected tropical diseases* 9(9): e0004069. DOI: 10.1371/journal.pntd.0004069.

Tables & Figures

Table 1. Tissue distribution of iLacZ signal in live *Ae. aegypti*, *An. gambiae*, and *Cx. pipiens*. Symbols indicate: (-) no

fluorescence found in any tissues above background levels, (+) signal witnessed in single replicate only, (++) signal witnessed on

multiple occasions, (+++) signal witnessed in every replicate, and (++++) signal witnessed in every individual in every replicate.

Tissue labels include: (HD) head, (LE) leg, (TH) thorax, (HC-FB) Hemocoel and fat body, (TA-MT) tracheole associated with

Malpighian tubules, (TA-OV) tracheole associated with ovary, (PC) pericardial cells of the dorsal vessel, (VC) ventral nerve cord,

(FO) primary & secondary follicles of ovary, (DV-CA) ventral or dorsal diverticula in adults - caecum in larvae, (FG) foregut lumen,

(MG) midgut lumen, (HG) hindgut lumen, (RC) rectum lumen, (CT) cuticle, (IS) injection site. HPE = Hours Post-Exposure, NA =

Non-applicable.

Experiment		Related Figures (Fig.)	Hemocyte locations						Other cell types					DV-CA	Extracellular signal					
Species	HPE		HD	LE	TH	HC-FB	TA-MT	TA-OV	PC	FB	VC	FO	AT		FG	MG	HG	RC	CT	IS
Peritoneal exposure by intrathoracic injection – adult female																				
Ae. aegypti	24-120	S1	+++	+++	++	+++	+++	++	++++	-	++	+++	-	-	-	-	++	++	-	++
An. gambiae	24-120	S2	++	-	+	++	+++	+++	++++	-	-	+++	-	-	-	+	+	+	-	++
Cx. pipiens	24-120	S3	-	-	-	++	++	+++	++++	-	-	+++	-	-	+	+	++	+	-	+++
Peritoneal exposure by intrathoracic injection 24 hours post blood-meal – adult female																				
Ae. aegypti	1-24	S4	-	-	+	+	-	+	++++	-	-	+++	-	-	-	-	-	-	-	-
An. gambiae	1-24	S5	+++	++	-	+++	+	++	++++	-	-	+++	-	-	-	-	-	-	-	+
Cx. pipiens	1-24	S6	+	+	+	+++	+	+	++++	+	-	+++	-	-	-	-	-	-	-	++
Peritoneal exposure by intrathoracic injection – 4th instar larvae																				
Ae. aegypti	24	S7	-	NA	-	-	-	NA	++	-	-	NA	-	-	-	+	-	-	-	NA
An. gambiae	24	S8	+	NA	-	+	-	NA	++	-	-	NA	-	-	-	+	-	-	-	NA
Cx. pipiens	24	S9	-	NA	-	+	-	NA	++	-	-	NA	-	-	-	+	-	-	-	NA
Topical exposure – adult female																				
Ae. aegypti	72	S10	-	-	-	-	-	-	-	-	-	-	-	-	-	-	-	-	++++	NA
An. gambiae	72	S11	-	-	-	-	-	-	-	-	-	-	-	-	-	-	-	-	++++	NA
Cx. pipiens	72	S12	-	-	-	-	-	-	-	-	-	-	-	-	-	-	-	-	++++	NA
Per os exposure – adult female																				
Ae. aegypti	24-120	S13	-	-	-	-	-	-	+	-	-	-	-	+++	++++	++++	+++	+++	-	NA
Cx. pipiens	24-120	S14	++	++	++	+	+	++	++	-	-	+	++	+++	+++	+++	+++	+++	-	NA
Soaking exposure – 1st instar larvae																				
Ae. aegypti	2-72	S15	NA	NA	-	-	-	NA	-	-	-	-	-	NA	NA	-	+++	+++	-	NA

Supplementary Table 1 - Primers used in study. Various LacZ PCR products were produced as template for production of dsRNA and siRNA. For RNAi trigger synthesis and northern blot probe synthesis the T7 sequence (TAATACGACTCACTATAGGG) was added to the 5' of both the forward and reverse primers.

Product	Primer Name	Direction	Sequence	Product Size
LacZ 377†‡	LacZ 377 F	Forward	CTTTTGCTGGCCTTTTGCTC	377
	LacZ 377 R	Reverse	CGTAATCATGGTCATAGCTGTTTCC	
	LacZ 200 - 1000 F *	Forward	CTTTTGCTGGCCTTTTGCTC	
LacZ 200	LacZ 200 R	Reverse	GCATTAATGAATCGGCCAAC	199
LacZ 400	LacZ 400 R	Reverse	GTCACCTAAATAGCTTGGCGTAA	395
LacZ 600	LacZ 600 R	Reverse	GTTTTCCCAGTCACGACGTT	602

† = PCR products used for northern blot probe generation
‡ = PCR product used for fluorescent labeling experiments.
* The same F primer was used for LacZ 200, 400, 500, 600, 800, and 1000 products

Figure 1 - Tracking iLacZ by Northern blot in *Ae. aegypti* adult females.

(A) Whole body RNA extracts at 24, 72, and 168 HPE to 200, 400, or 600 bp iLacZ RNAi

triggers.
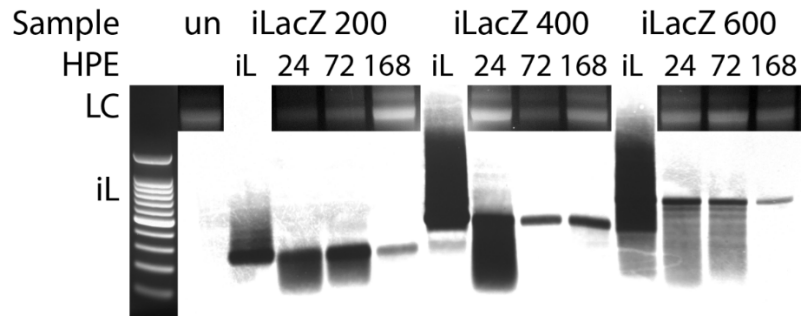
(B) Persistence of a 417 bp iLacZ (iL) following injection. Whole body RNA from untreated

(un) or injected individuals extracted over time from 0.25 to 168 HPE.
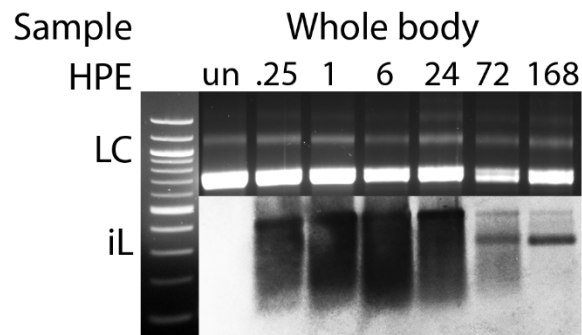
(C) Whole body extracts at 168 HPE with (+) and without (-) DNase treatment as compared

to iLacZ and untreated controls.
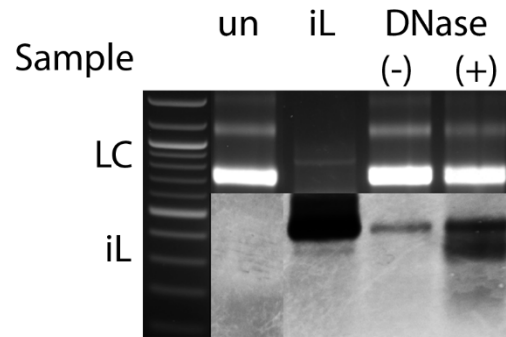
(D) Head (HE), thorax (TH), abdomen (AB), midgut (MG), and ovary (OV) tissues at 4 and

24 HPE.
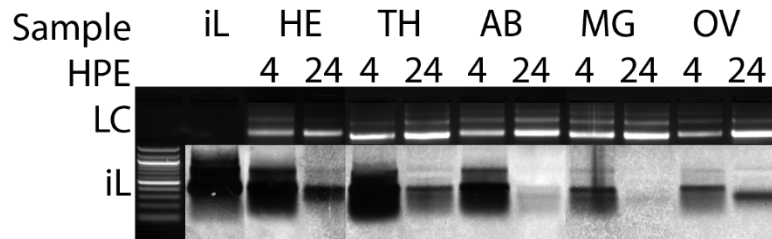
(E) Persistence of dsRNA in tissues post injection and post blood-feeding. Gel and northern

blot alignment showing (1) 100 bp Ladder, (2) 400 bp dsRNA, (3) untreated *Ae. aegypti*

RNA, (4-8) 24 hpi / 48 hpbm abdomen, alimentary tract, head, ovary, thorax, (9-13) 72

hpi / 96 hpbm abdomen, alimentary tract, head, ovary, thorax. Loading control rRNA

shown at the top of each lane.
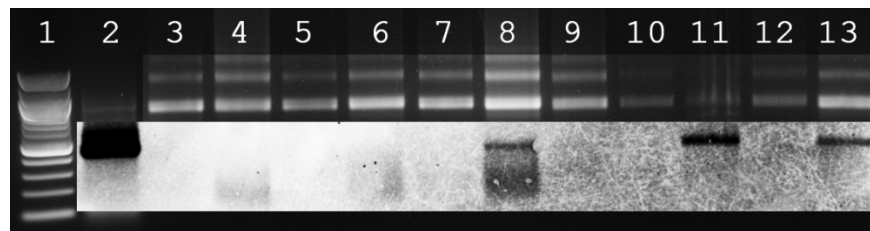
(F) C6/36 cells following iLacZ exposure. Persistence of a 417 base-pair iLacZ (iL) tracked

by Northern blot following exposure to *Ae. albopictus* C6/36 cells. Cell extracts (1 µg)

were tested at 0.25, 1, 24, and 72 HPE. Ribosomal RNA loading controls (LC) are shown

from *Ae. albopictus* RNA extracts imaged immediately prior to Northern membrane

transfer.
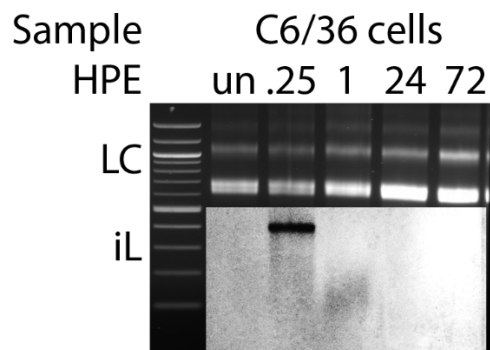
(G) Persistence of dsRNA in tissues post topical application in acetone. Gel and northern blot

alignment showing (1) 100 bp Ladder, (2) 400 bp dsRNA, (3) untreated *Ae. aegypti*

RNA, (4-6) whole body tissues at 4, 72, 168 hpe, (7-8) carcass and internal tissues 4 hpe,

(9-10) carcass and internal tissues 72 hpe. Ribosomal RNA loading controls (LC) are

shown from *Ae. aegypti* RNA extracts imaged immediately prior to Northern membrane

transfer.
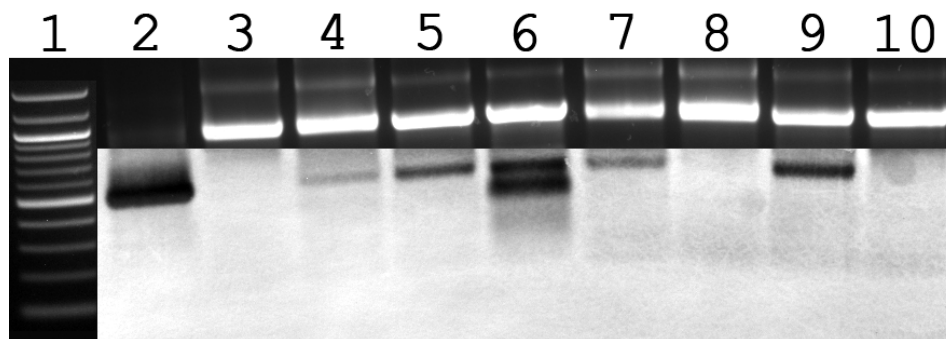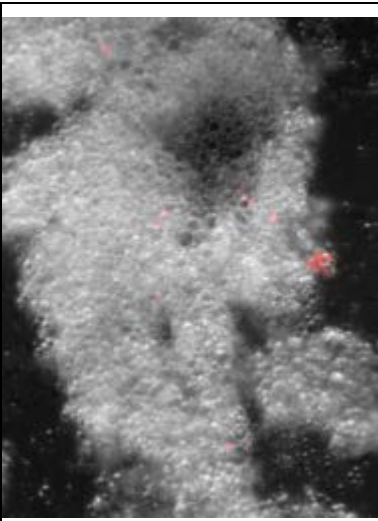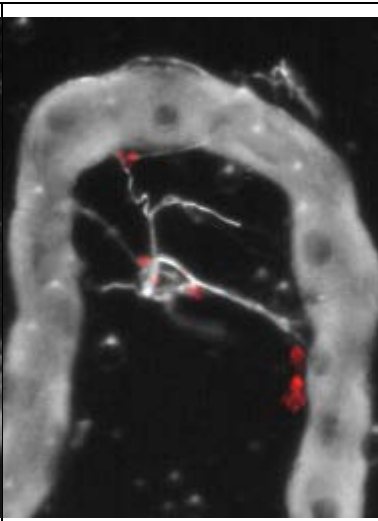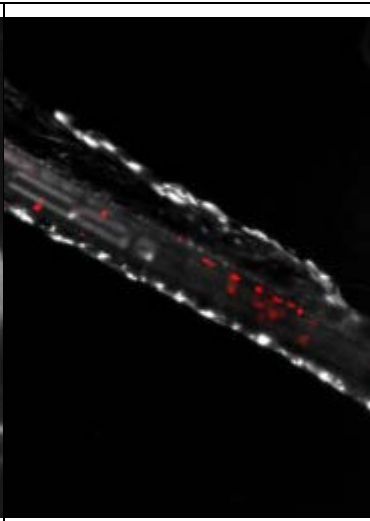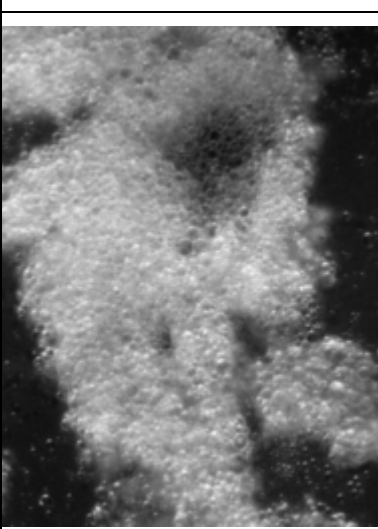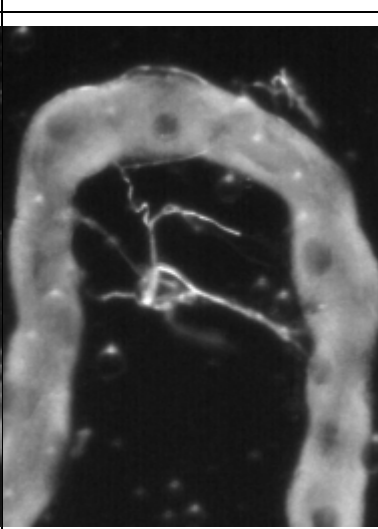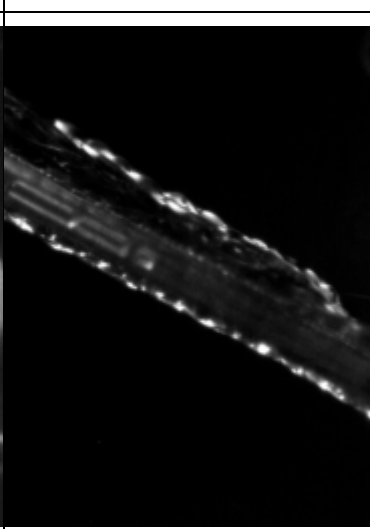
Figure 2 - Multiple cell types uptake iLacZ in *Ae. aegypti* ovaries. Confocal microscopy of ovaries dissected 24 hours post intra-thoracic injection of iLacZ or no treatment control. Cell types shown include primary follicles composed of: follicular epithelia (FE), nurse cells (NC), and oocytes (OO) as well as secondary follicles (SF) and epithelial cells of the ovarian sheath (SH). Scale bar = 100 µm.
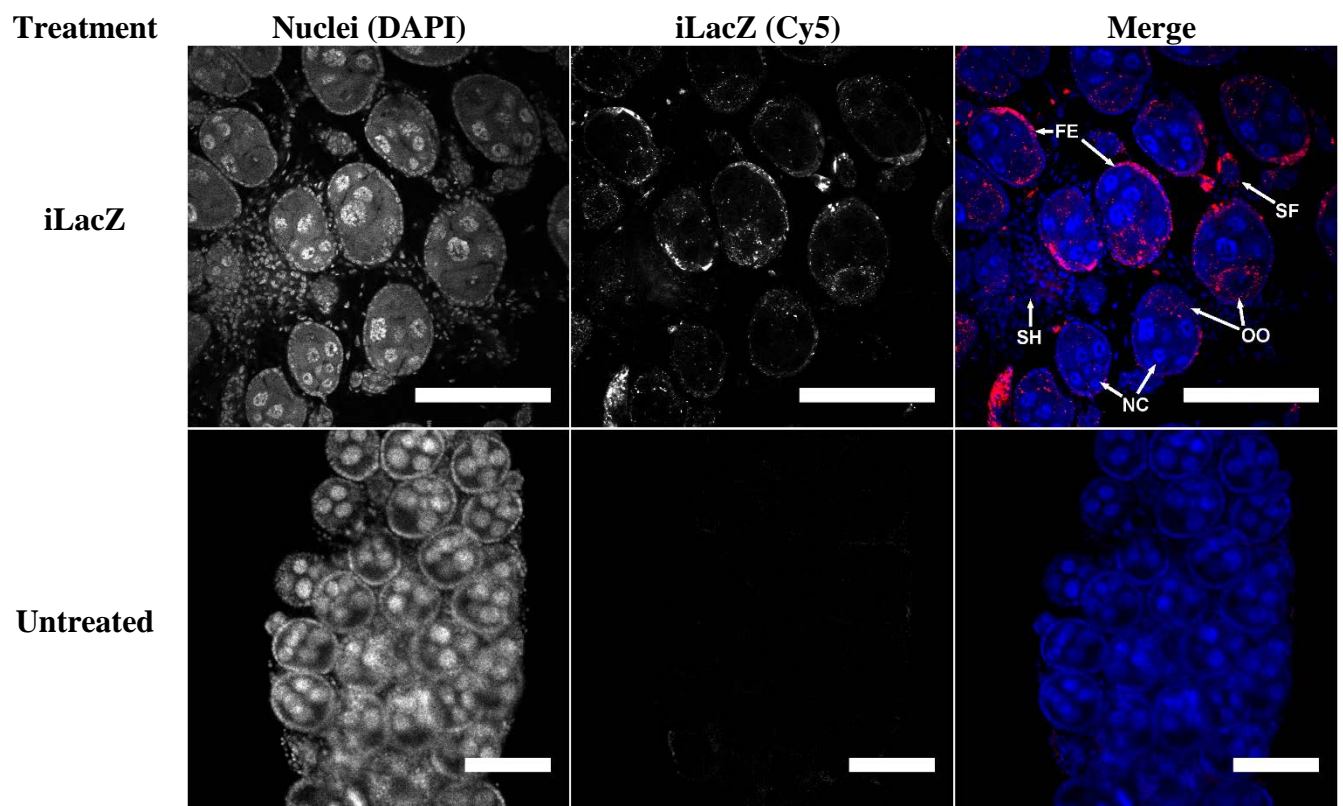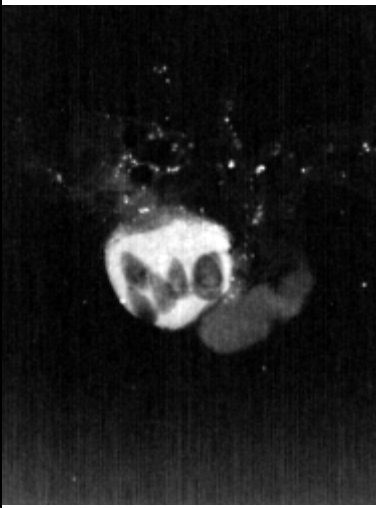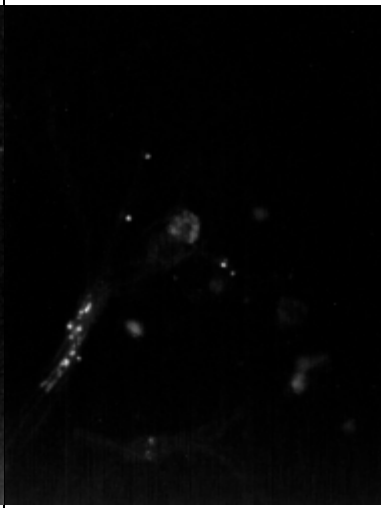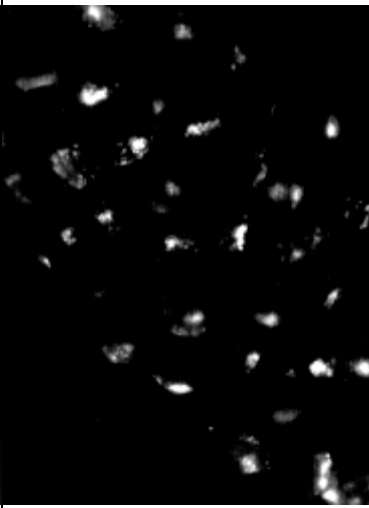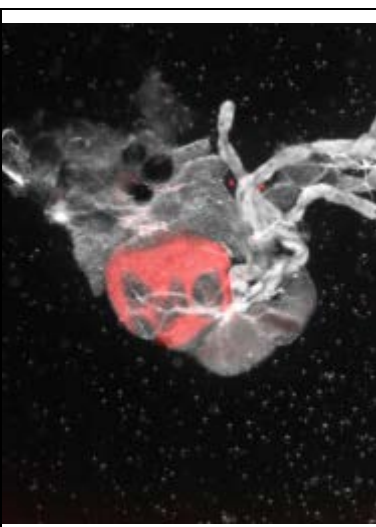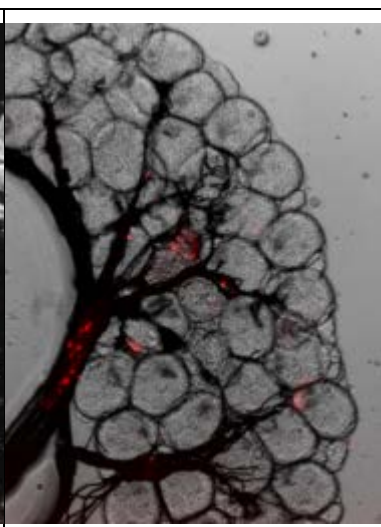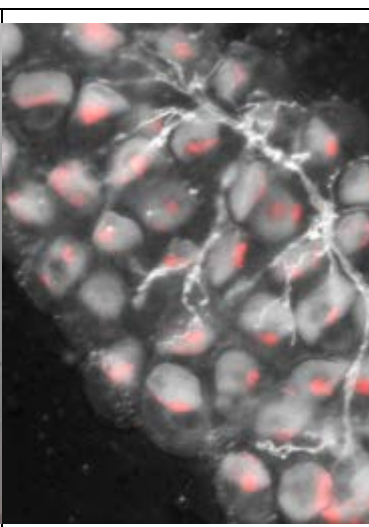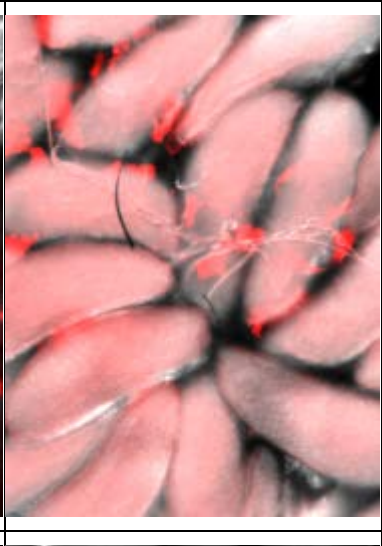
Supplementary Figure 1 – Peritoneal exposure of adult female *Ae. aegypti* with fluorescent-iLacZ

Tissue	Bright Field	RNAi trigger	Merge
Head – signal at injection site (at 24 HPE)			
Thorax – hemocytes (at 24 HPE)			

Thorax - pericardial cells and auto-fluorescence (at 72 HPE)	Abdomen - pericardial cells (at 72 HPE)	Abdomen – pericardial cells and ganglia (at 24 HPE)
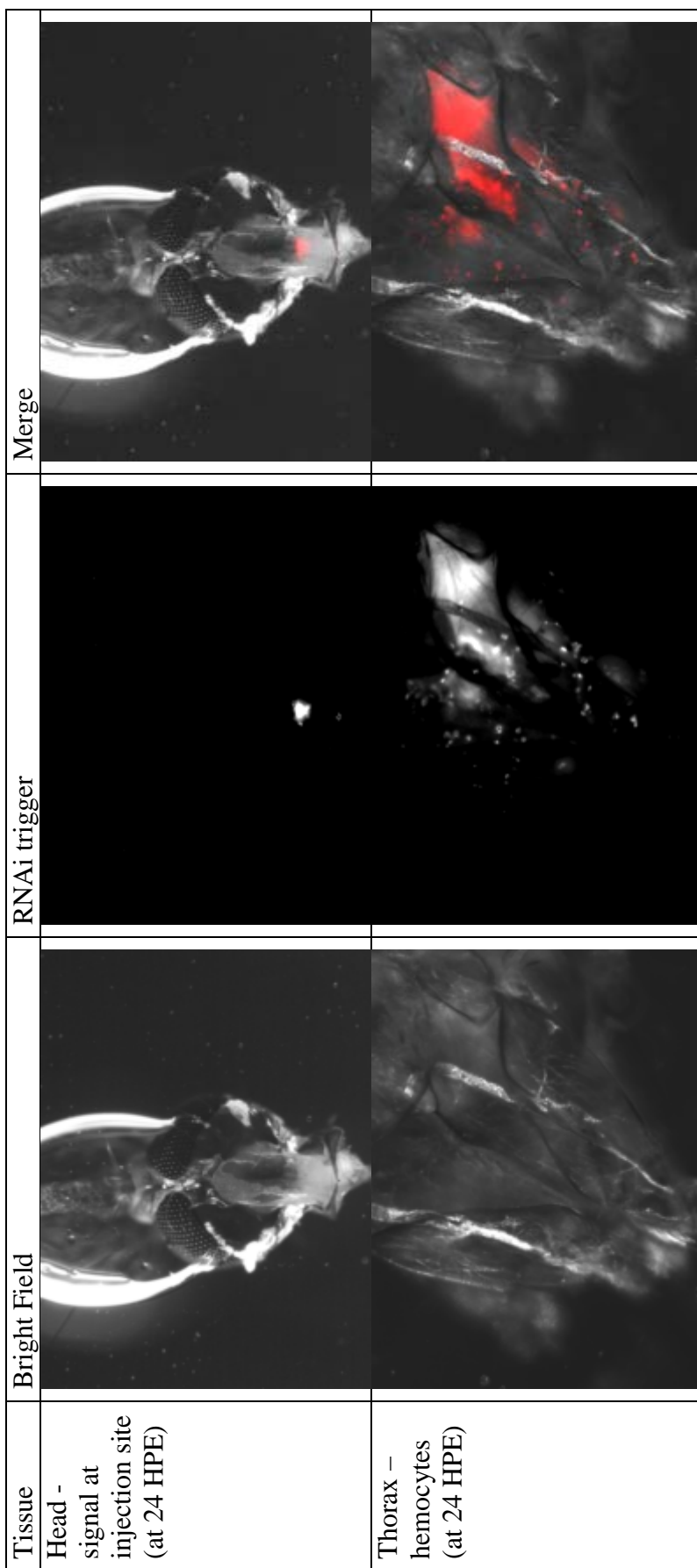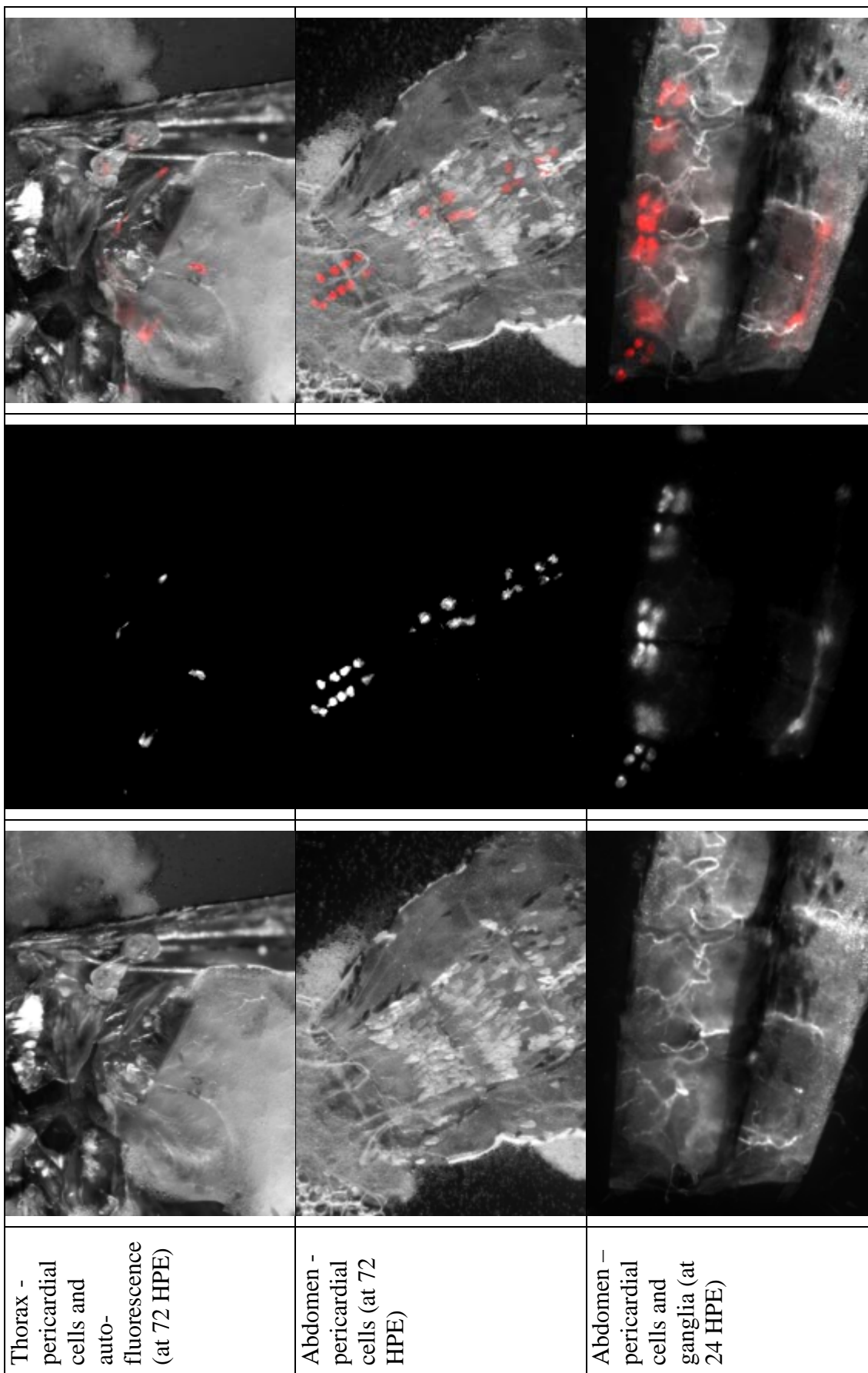
Fat body – hemocytes (at 120 HPE)	Malpighian tubules - hemocytes bound to tracheoles (at 72 HPE)	Leg - hemocytes (at 72 HPE)

Diverticula with no signal (at 72 HPE)		
Alimentary tract with no signal (at 120 HPE)		
Extracellular signal - hindgut lumen and tracheolar associated hemocytes (at 72 HPE)		
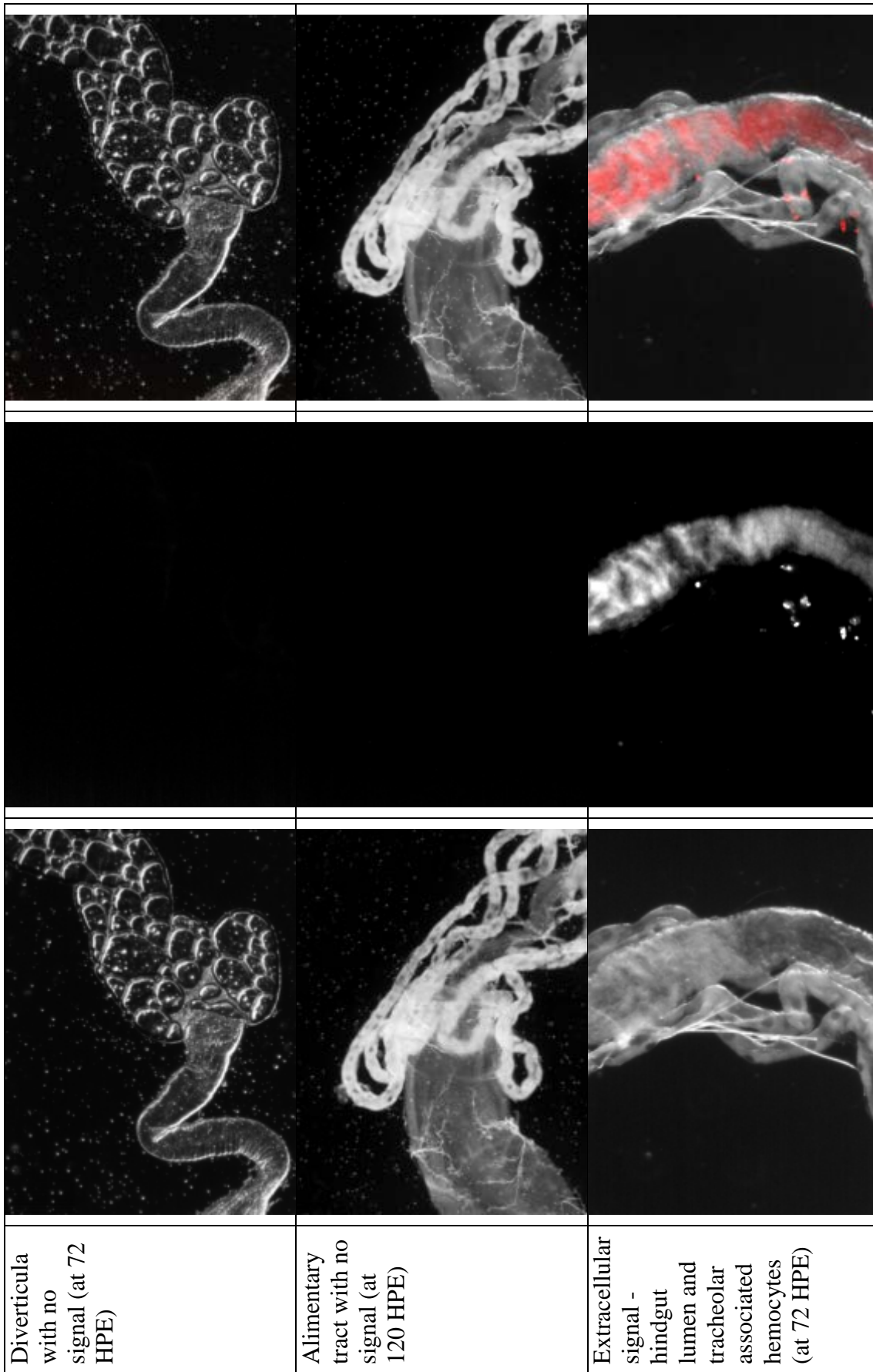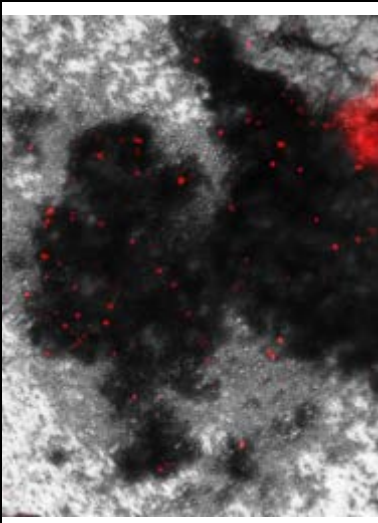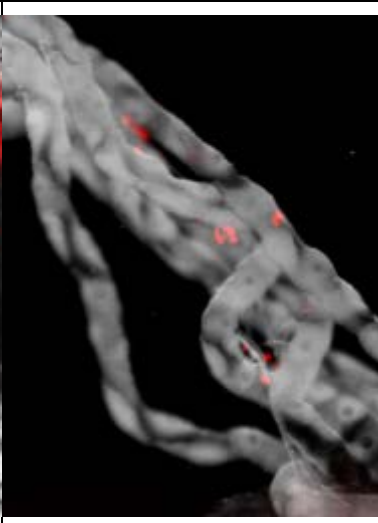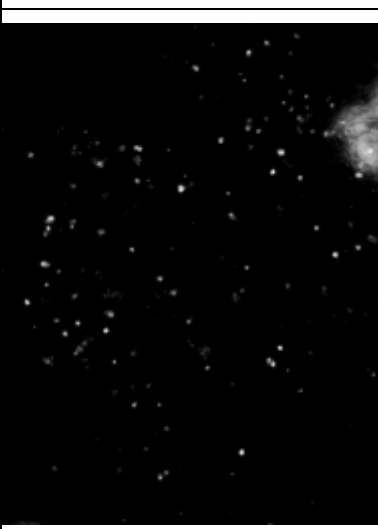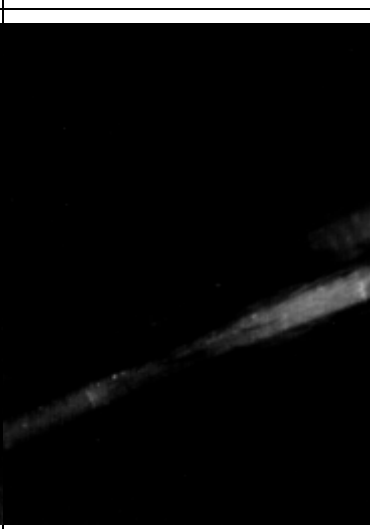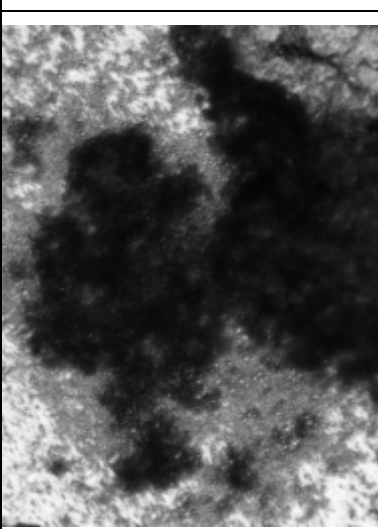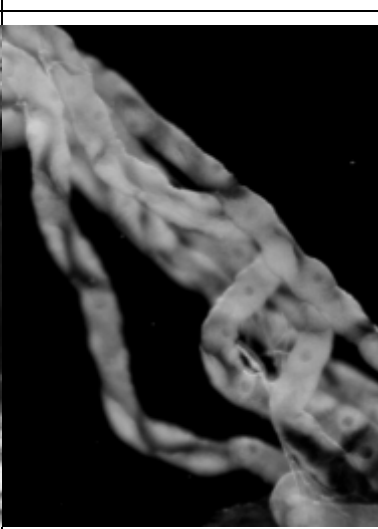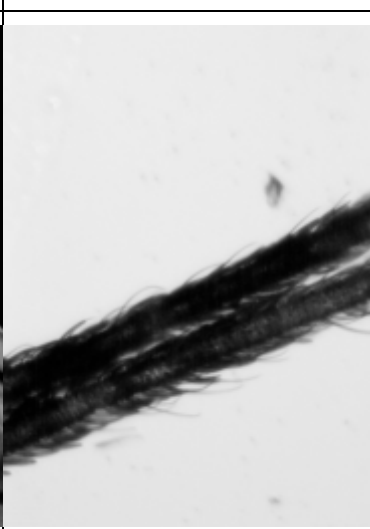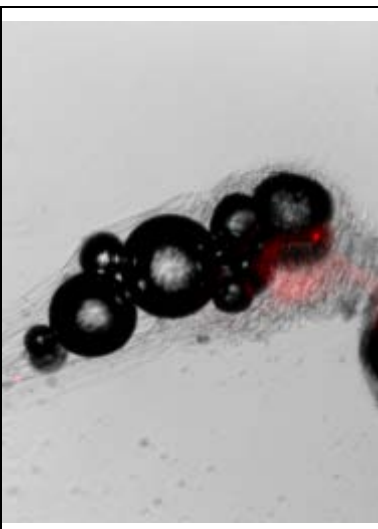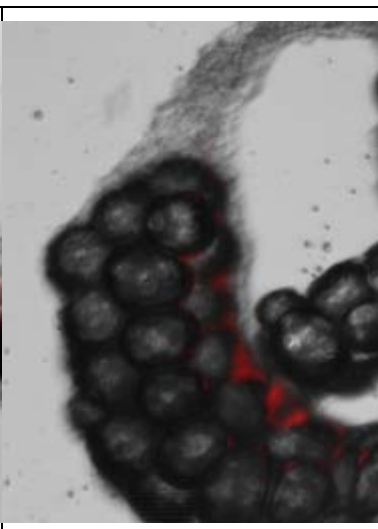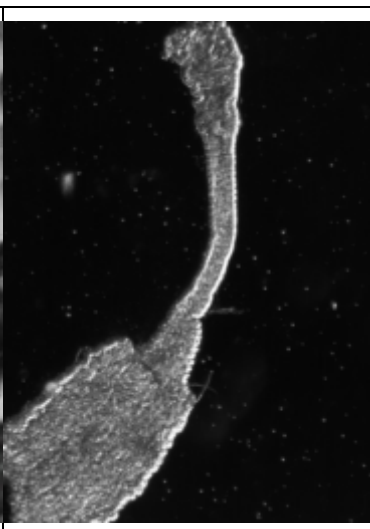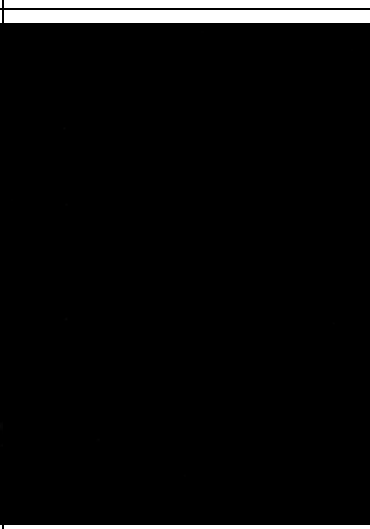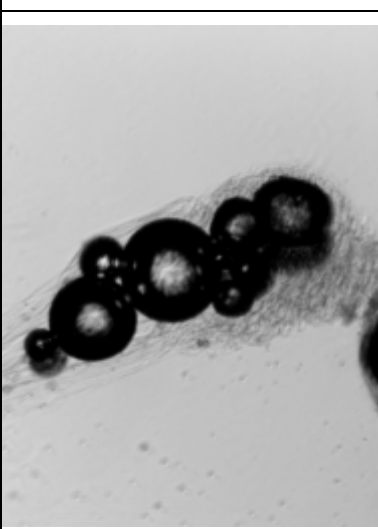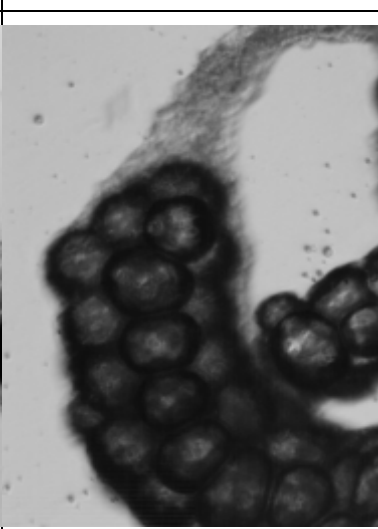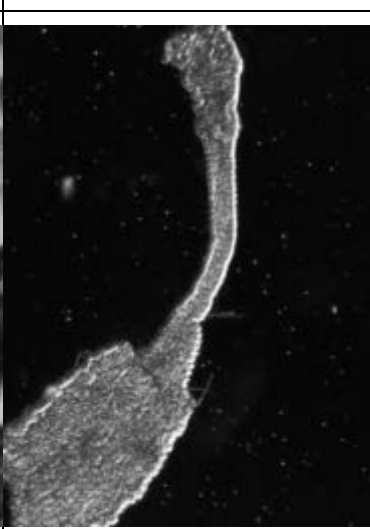
Extracellular signal - rectum lumen and signal in hemocytes (at 72 HPE)	Ovary – hemocytes (at 24 HPE)	Ovary - fluorescence in oocytes (at 120 HPE)
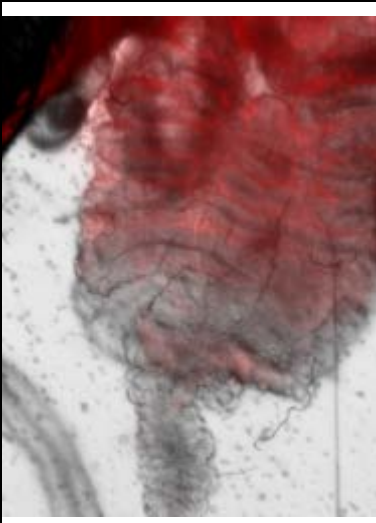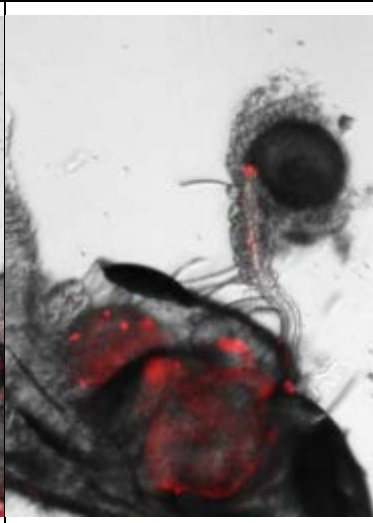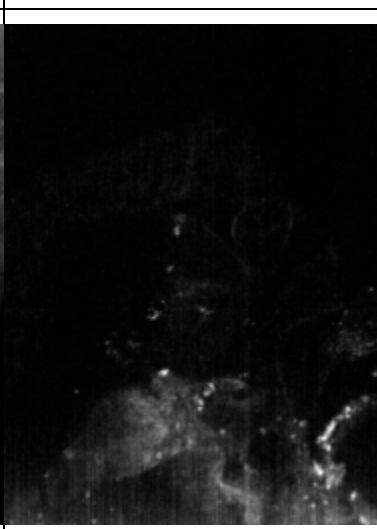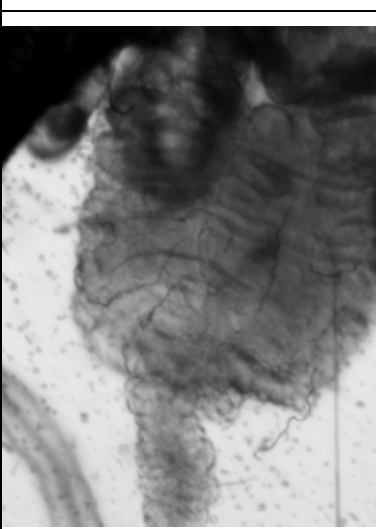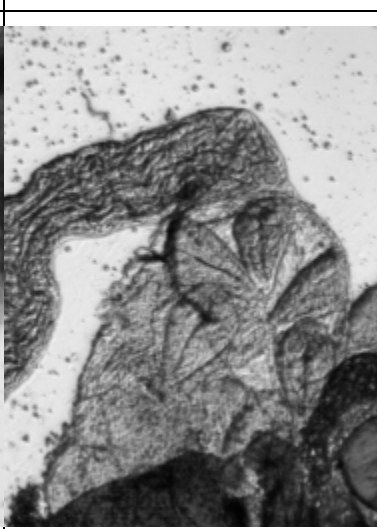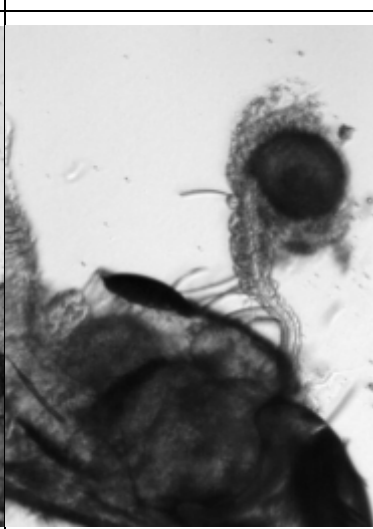
Supplementary Figure 2 – Peritoneal exposure of adult female *An. gambiae* with fluorescent-iLacZ

Tissue	Bright Field	RNAi trigger	Merge
Head - signal at injection site (at 24 HPE)			
Thorax – hemocytes, pericardial cell, and auto-fluorescence (at 24 HPE)			

Thorax – fat body and cuticle. Auto-fluorescence in cuticle (at 24 HPE)		
Abdomen - pericardial cells (at 72 HPE)		
Abdomen – pericardial cells but no ganglia (at 72 HPE)		
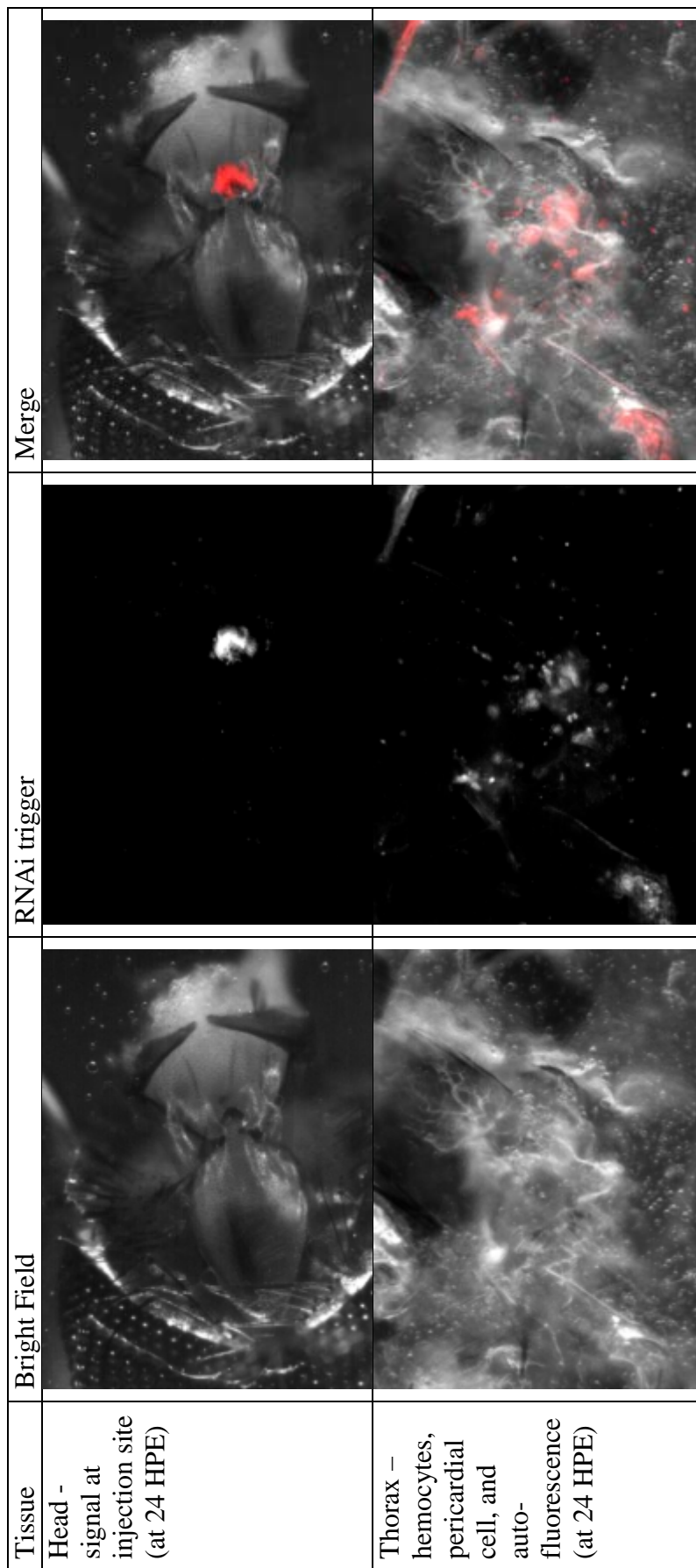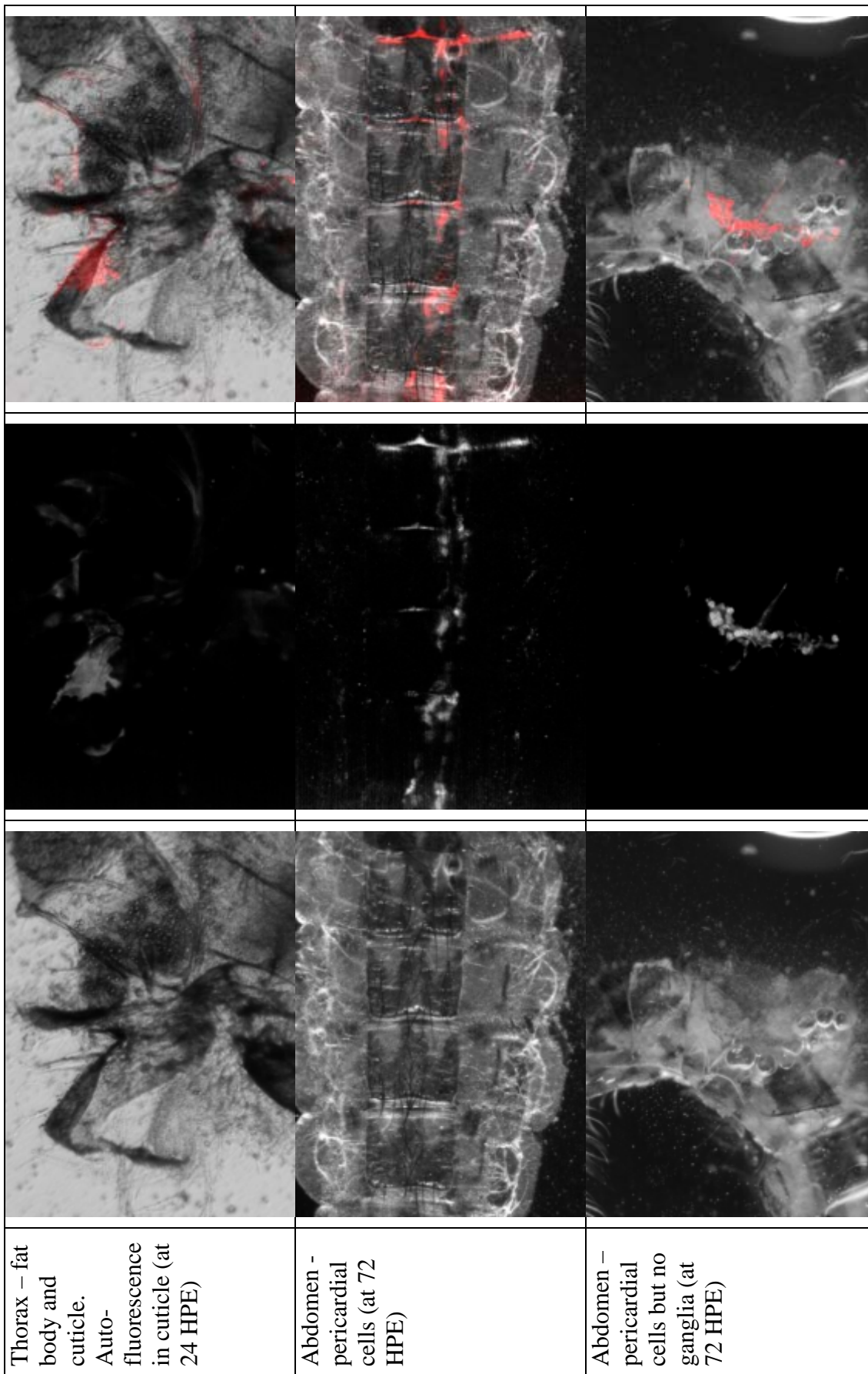
Fat body – hemocytes and pericardial cell (bottom right) (at 24 HPE)	
Malpighian tubules - hemocytes bound to tracheoles (at 72 HPE)	
Leg - hemocytes and extracellular signal (at 72 HPE)	
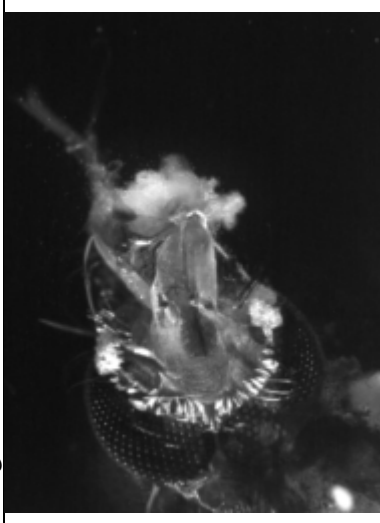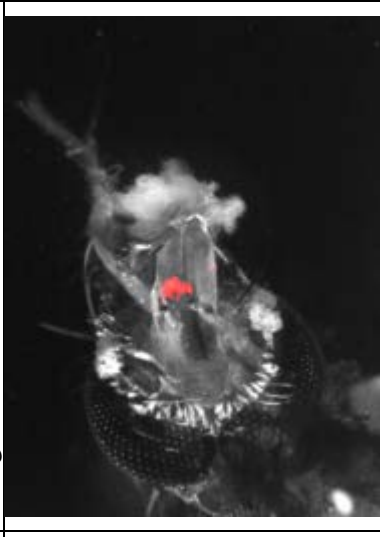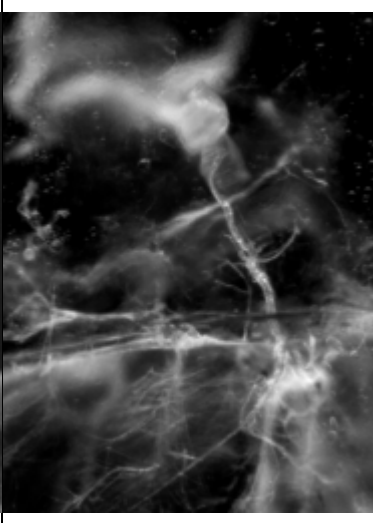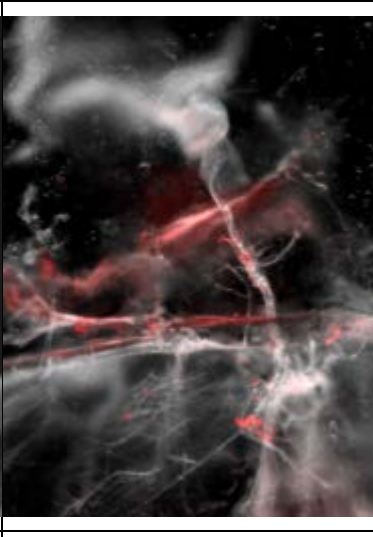
Diverticula with auto-fluorescent signal (at 72 HPE)	Diverticula with auto-fluorescent signal (at 72 HPE)	Alimentary tract with no signal (at 24 HPE)
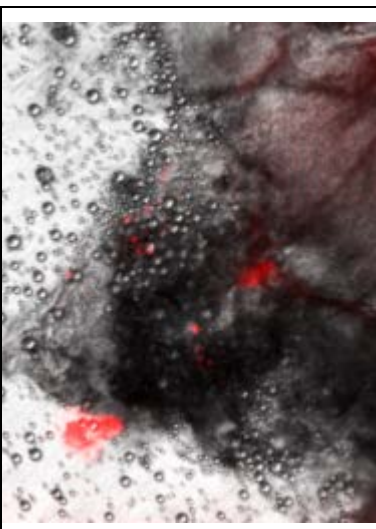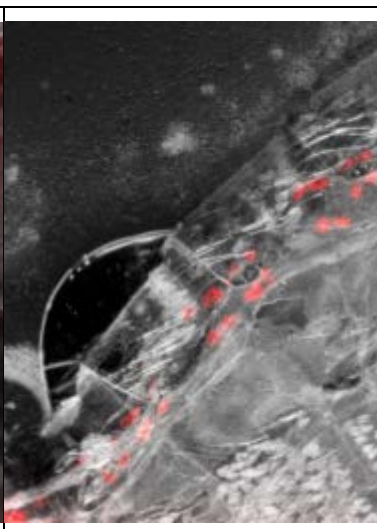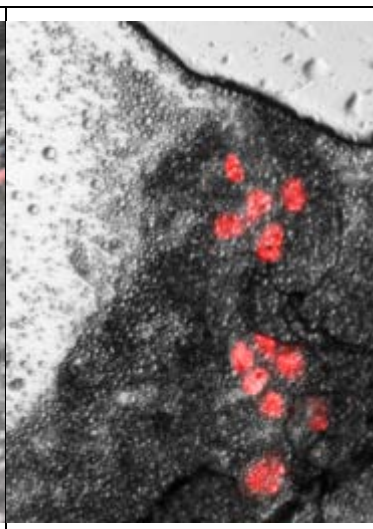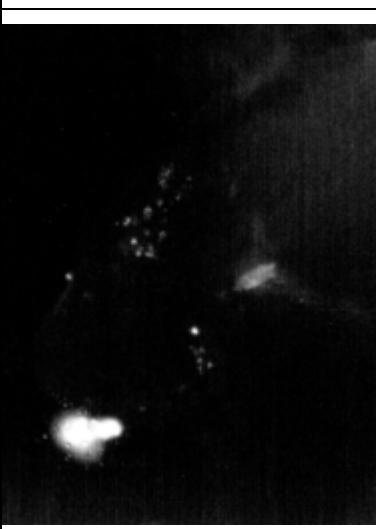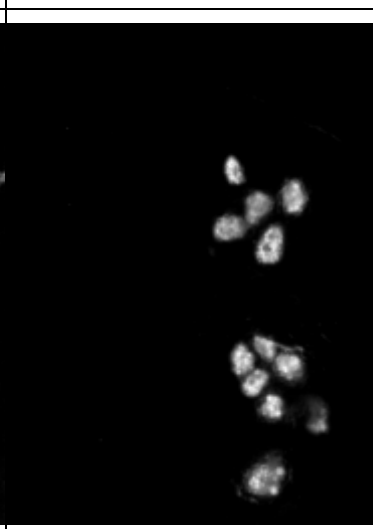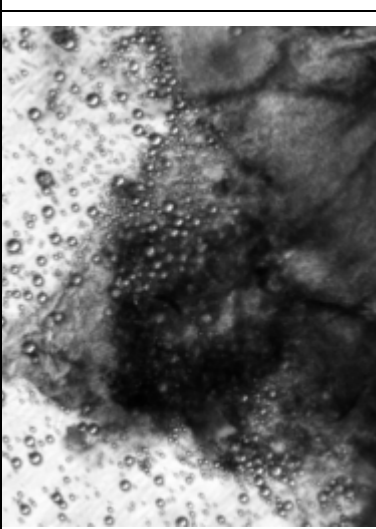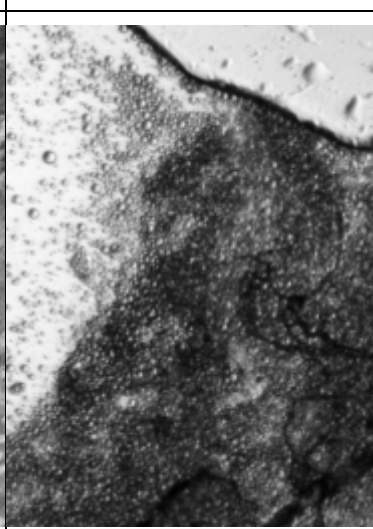
| Extracellular signal - midgut lumen (at 24 HPE) | Extracellular signal - hindgut lumen and hemocytes (at 72 HPE) | Extracellular signal - rectum lumen and signal in hemocytes (at 72 HPE) |
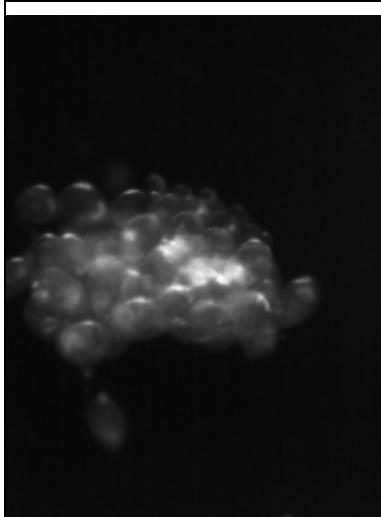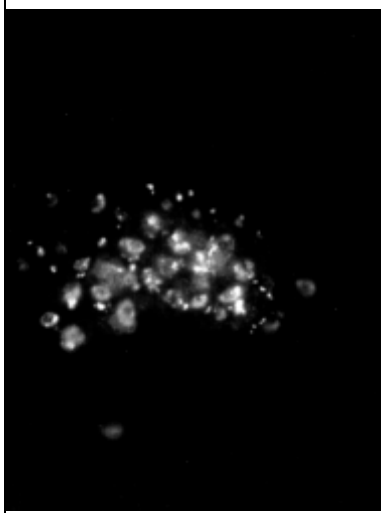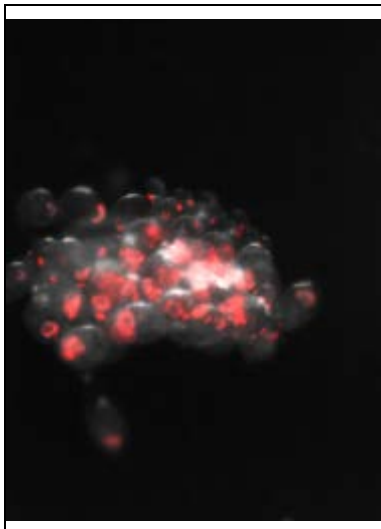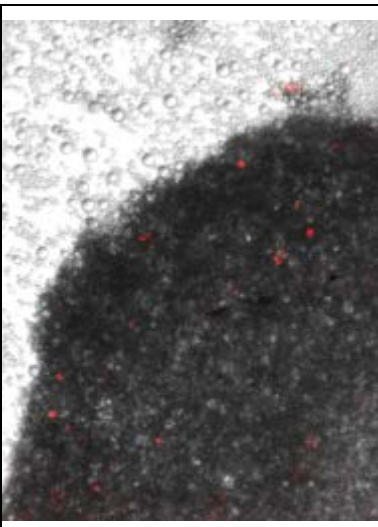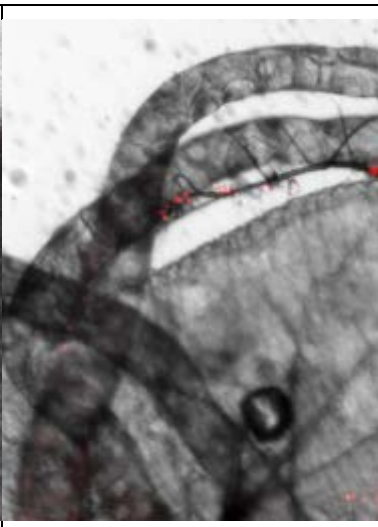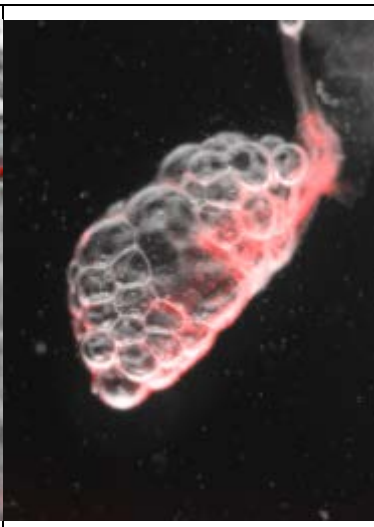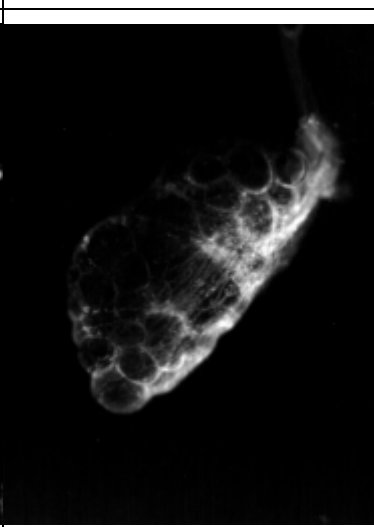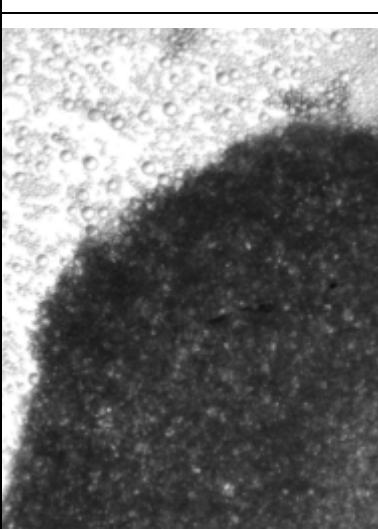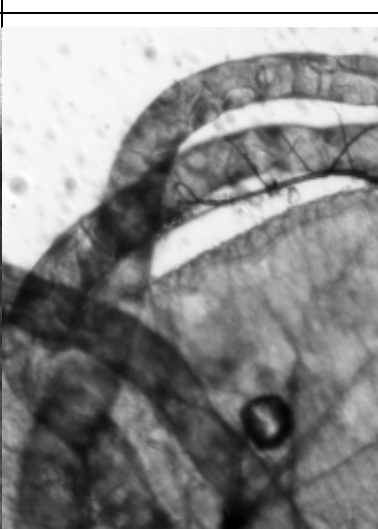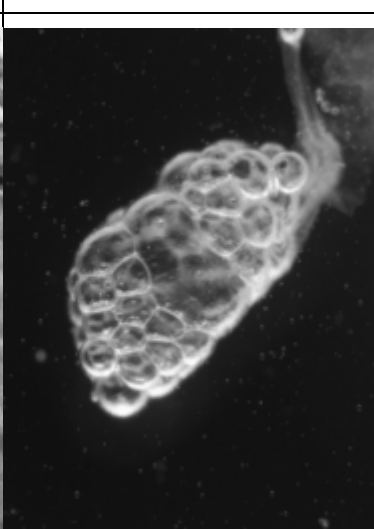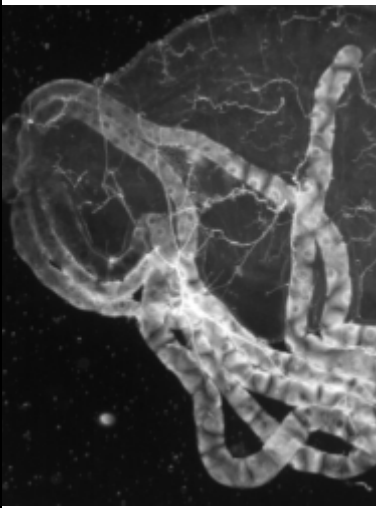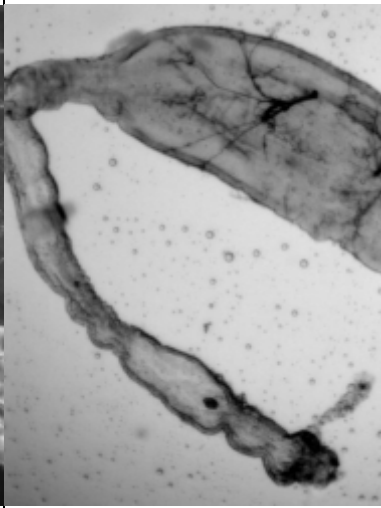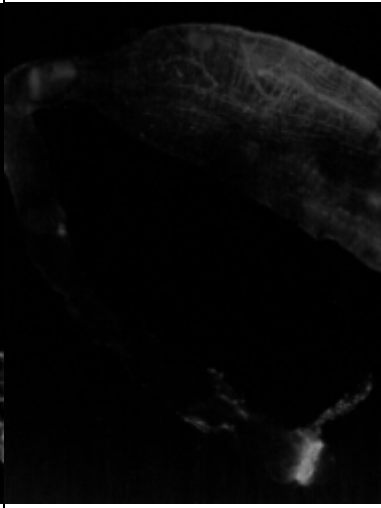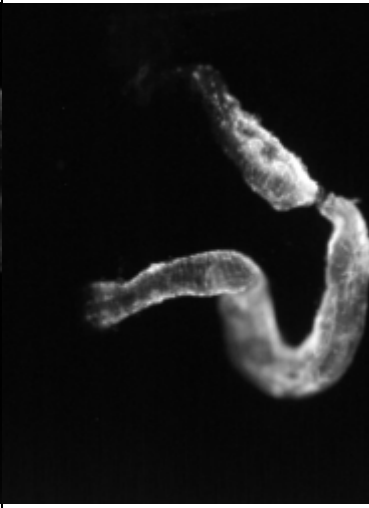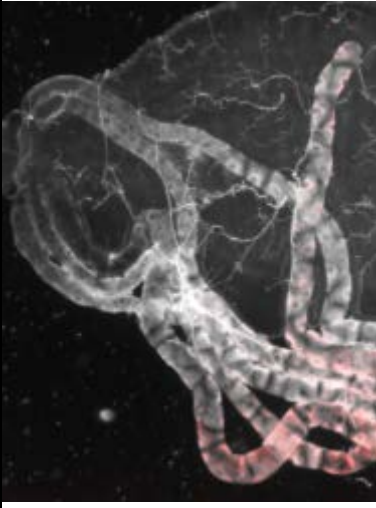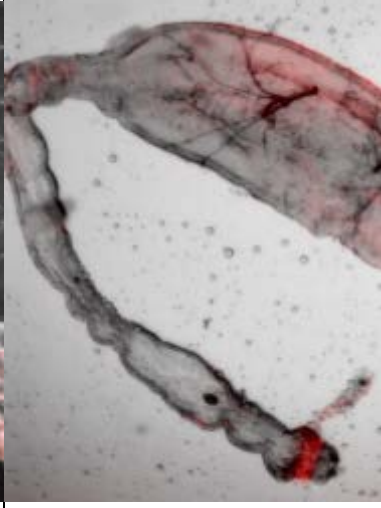
Ovary -
fluorescence
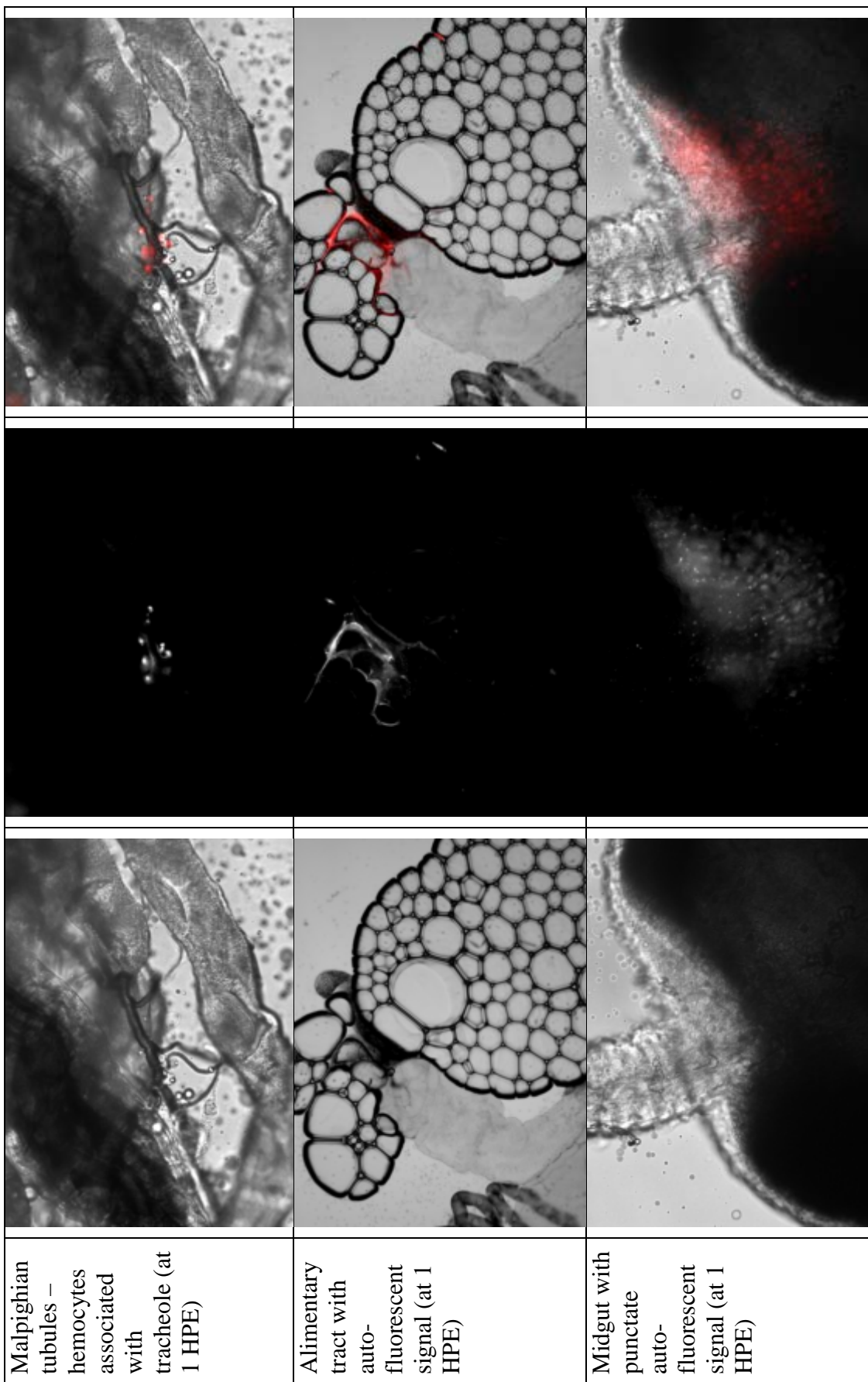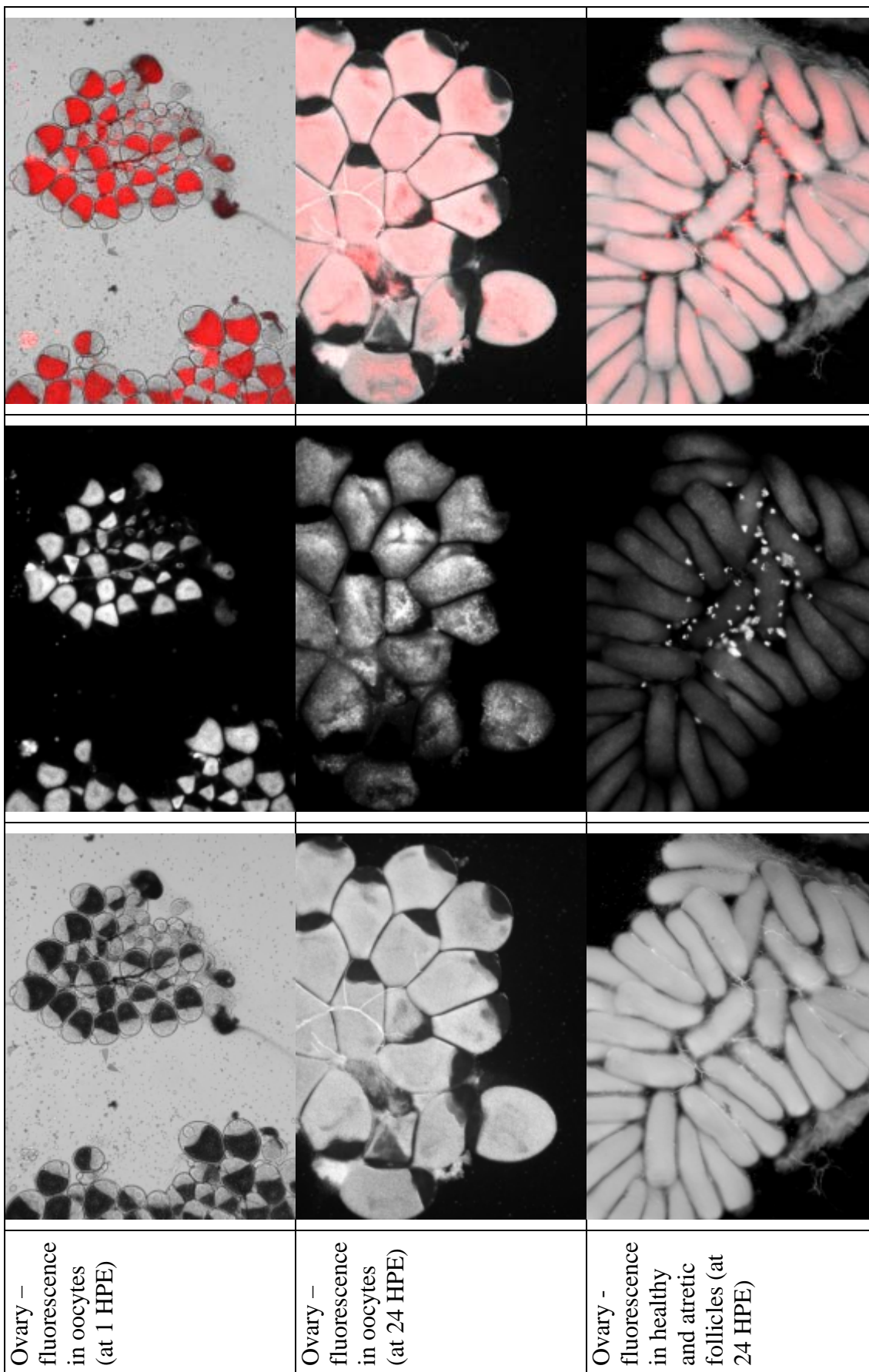in oocytes
and
hemocytes
(at 24 HPE)
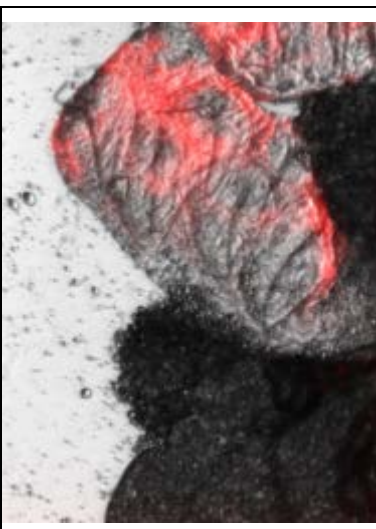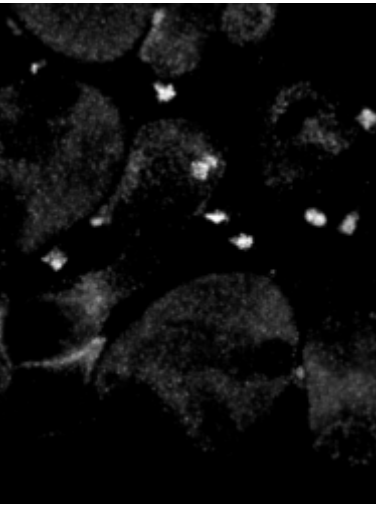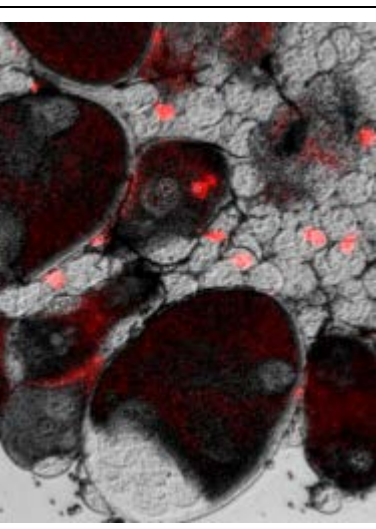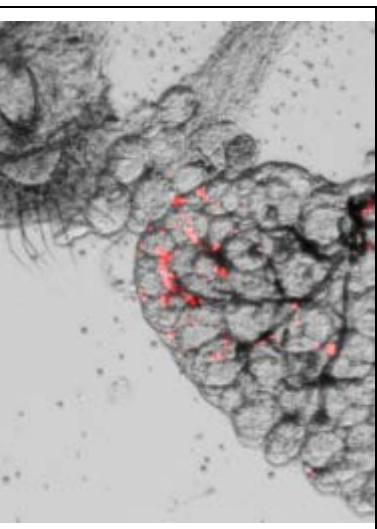
Supplementary Figure 3 – Peritoneal exposure of adult female *Cx. pipiens* with fluorescent-iLacZ

Tissue	Bright Field	RNAi trigger	Merge
Head - signal at injection site (at 24 HPE)			
Thorax – auto-fluorescence in cuticle, hemocytes associated with tracheole (at 24 HPE)			

| Thorax – fat body, hemocytes, and pericardial cell (at 24 HPE) | Abdomen - pericardial cells (at 72 HPE) | Fat body – pericardial cells (at 120 HPE) |
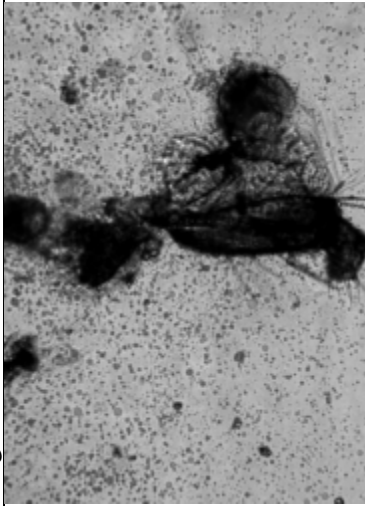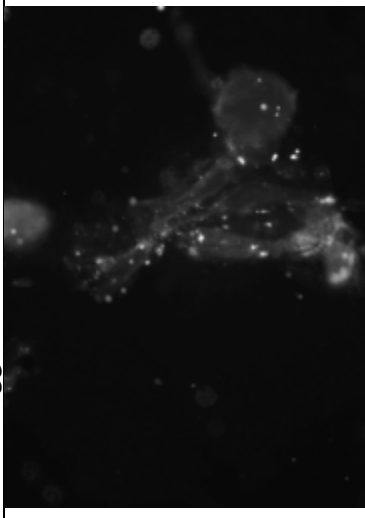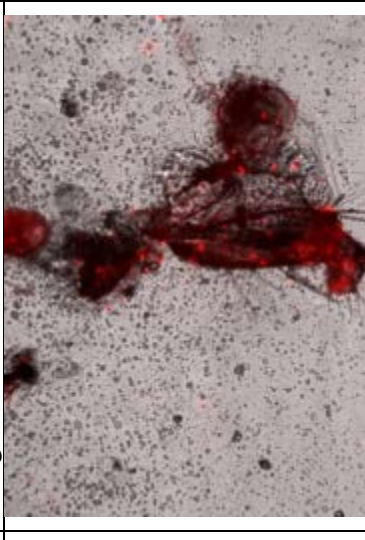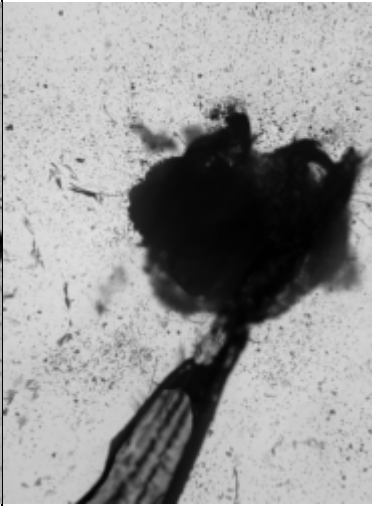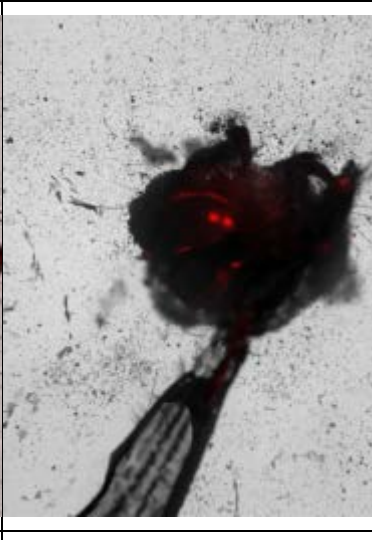
Fat body – hemocytes (at 24 HPE)	Malpighian tubules - hemocytes bound to tracheoles (at 72 HPE)	Diverticula with auto-fluorescent signal (at 24 HPE)
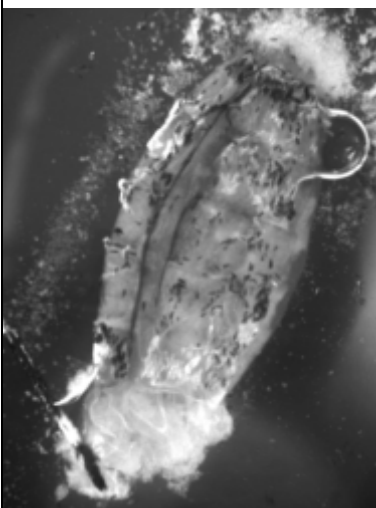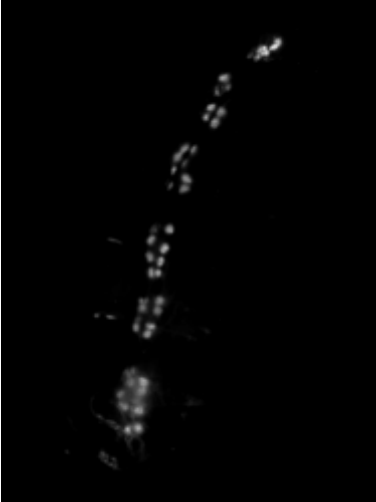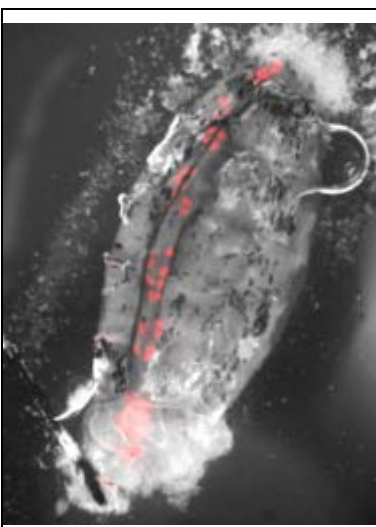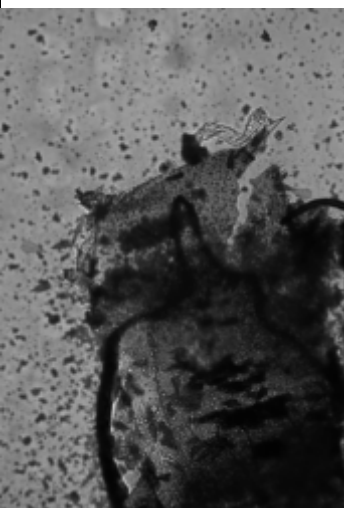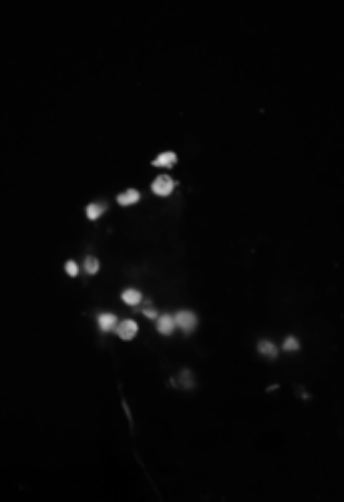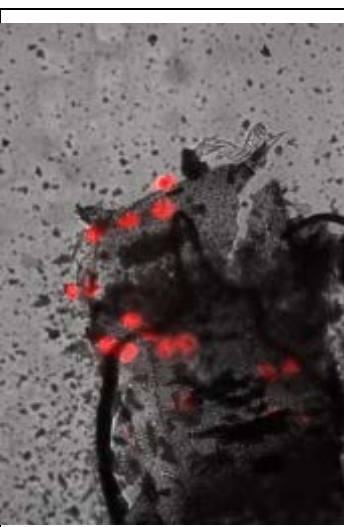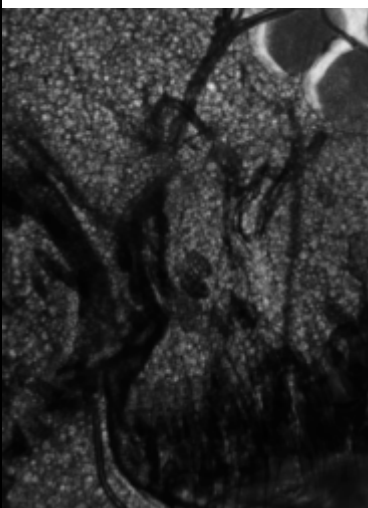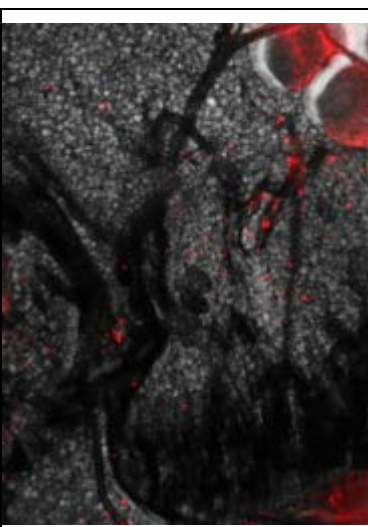
| Alimentary tract with no signal, extracellular signal in Malpighian tubules (at 72 HPE) | Extracellular signal – foregut and midgut lumen (at 24 HPE) | Extracellular signal - hindgut lumen (at 24 HPE) |

| Extracellular signal - rectum lumen and signal in hemocytes (at 72 HPE) | Ovary - fluorescence in hemocytes and oocytes (at 24 HPE) | Ovary - fluorescence in hemocytes (at 72 HPE) |
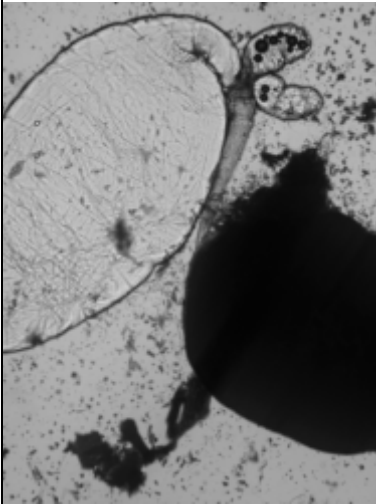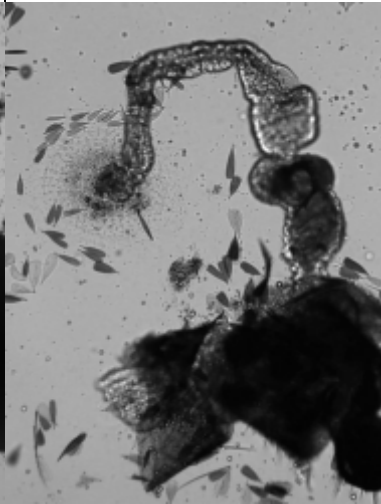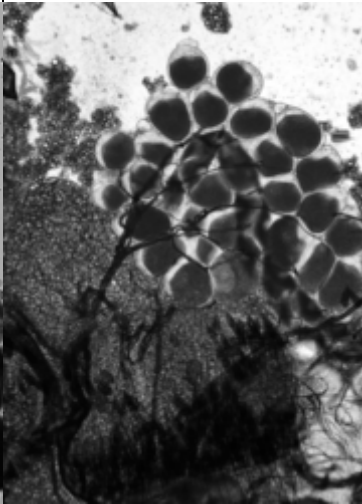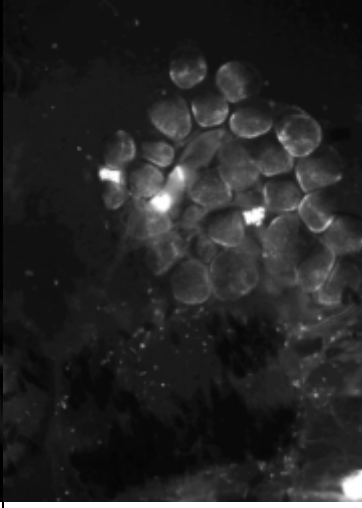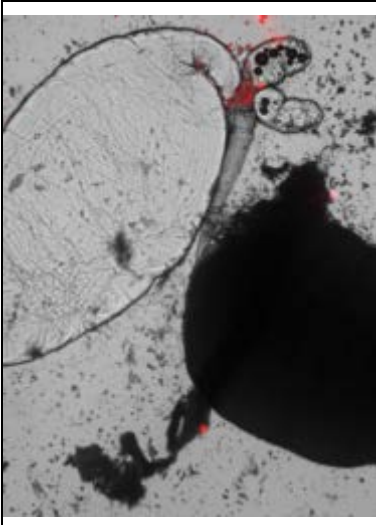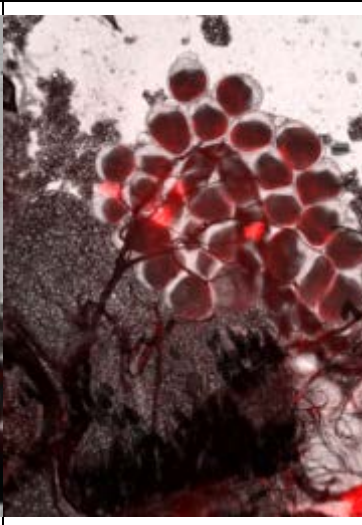
Ovary - fluorescence in hemocytes (at 24 HPE)	Ovary - fluorescence in oocytes (at 24 HPE)
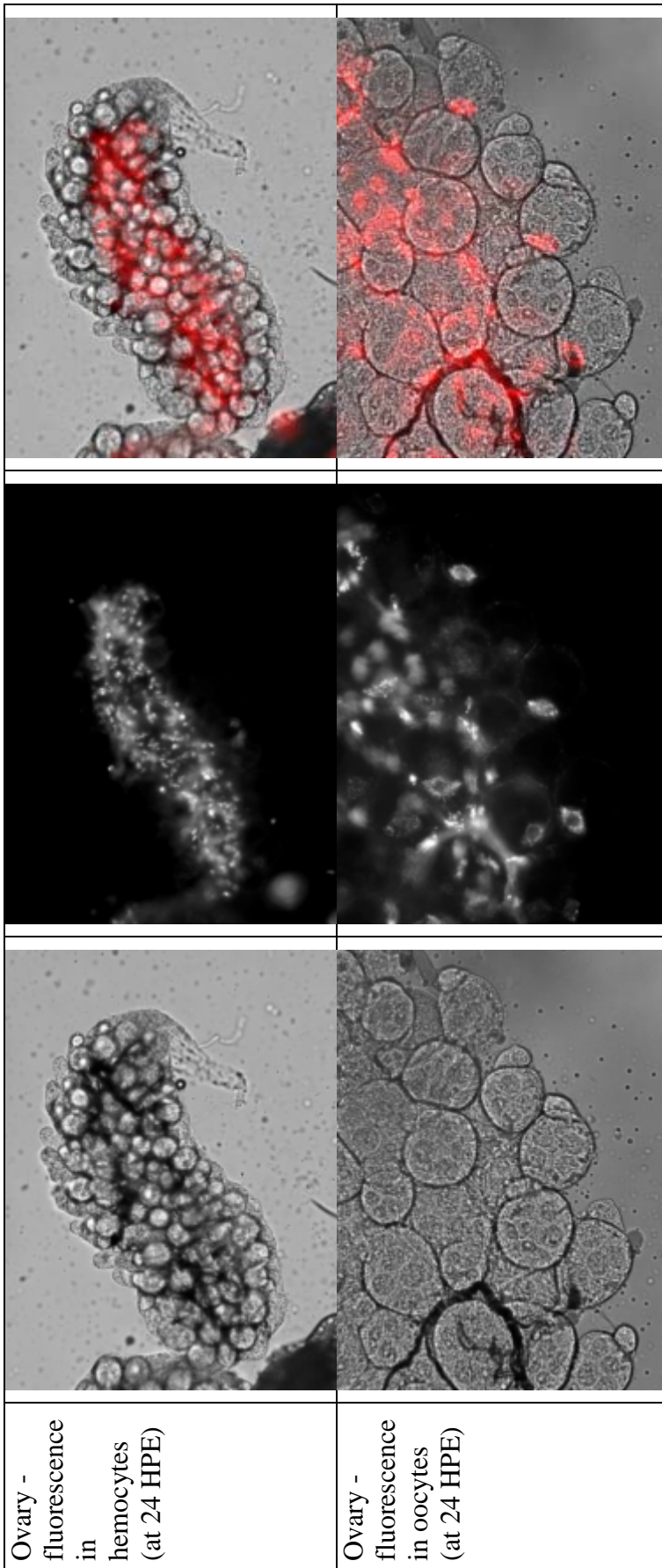
Supplementary Figure 4 – Peritoneal exposure of adult female *Ae. aegypti* with fluorescent-iLacZ 25-48 hours post blood-meal
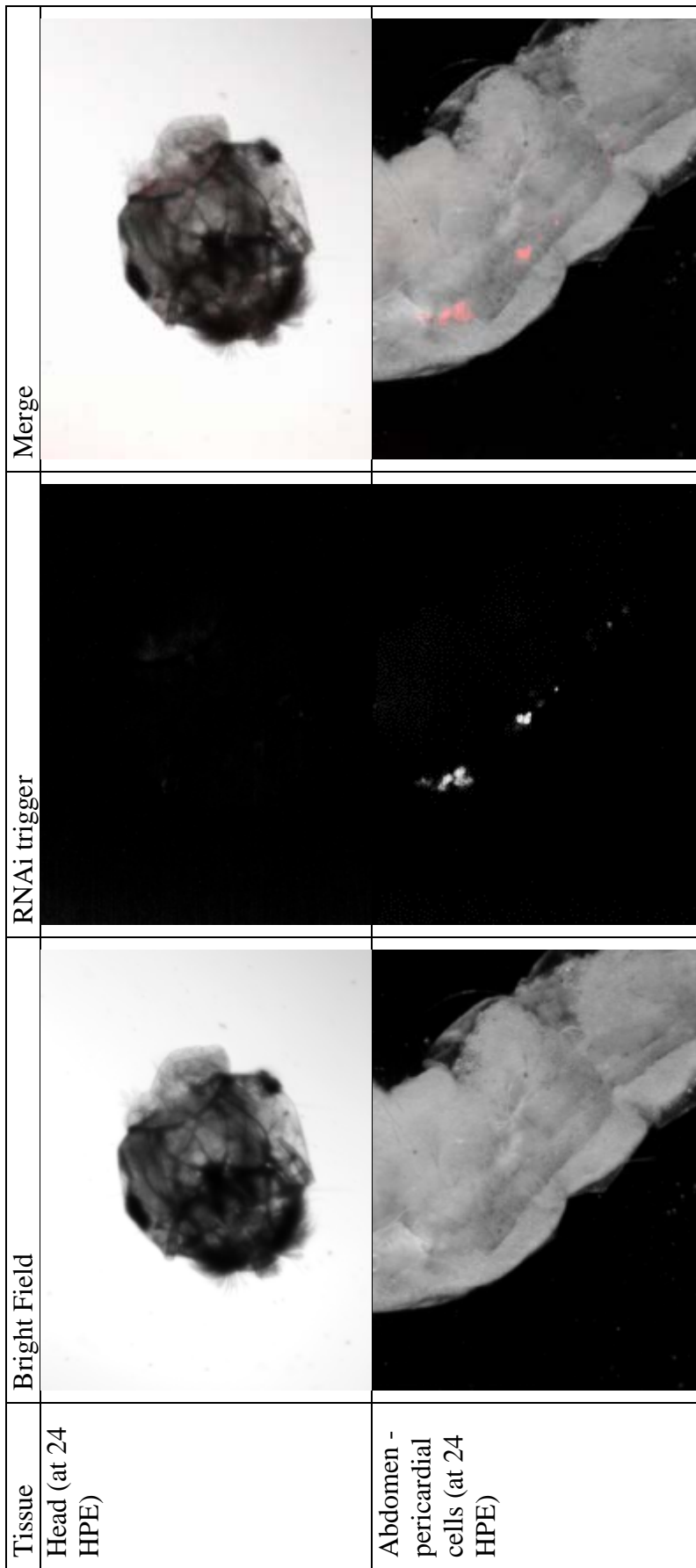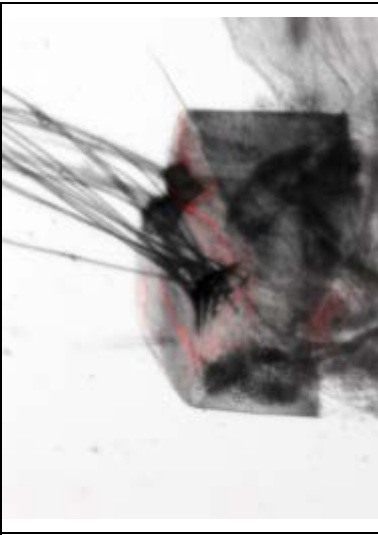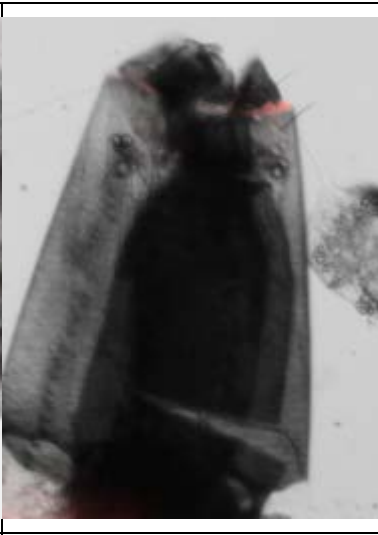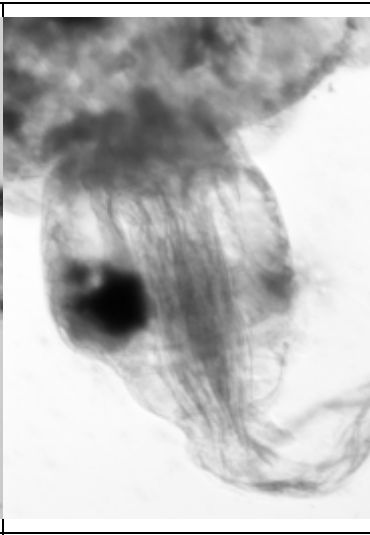

Tissue	Bright Field	RNAi trigger	Merge
Thorax - pericardial cells and auto-fluorescence in cuticle (at 24 HPE)			
Thorax - pericardial cells and auto-fluorescence (at 1 HPE)			
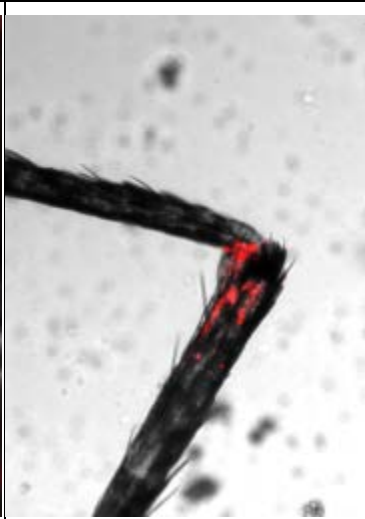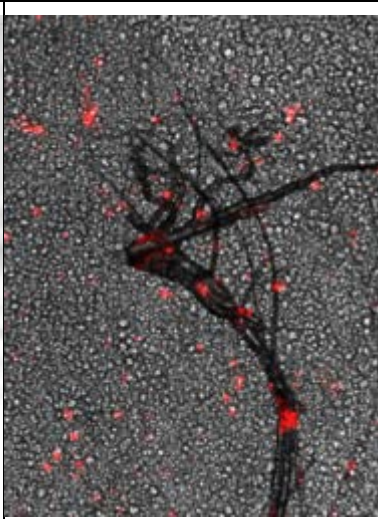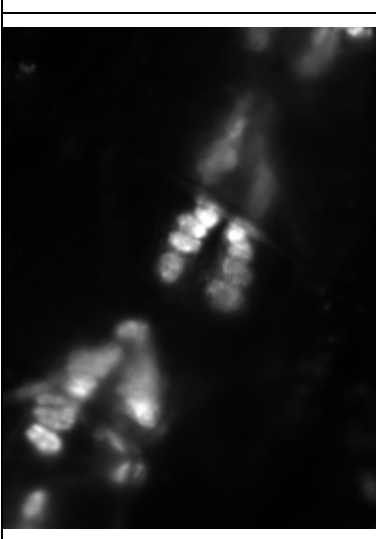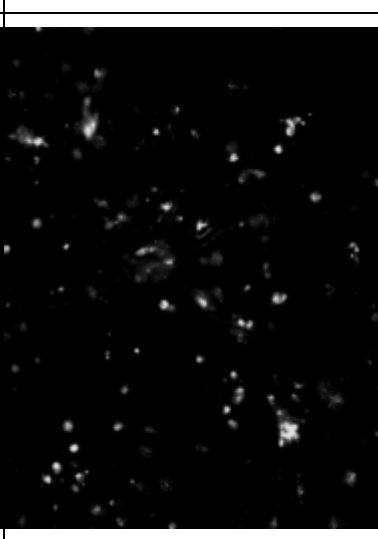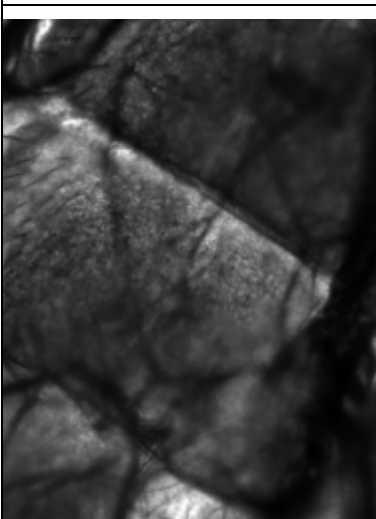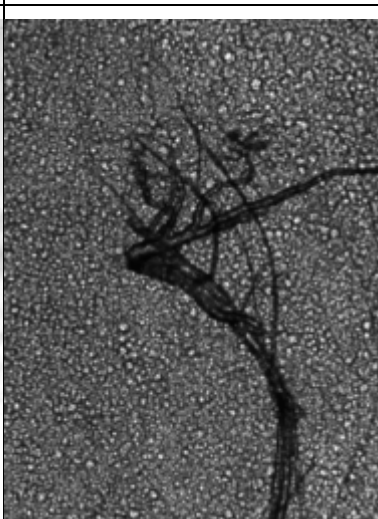
Abdomen - pericardial cells (at 1 HPE)	Abdomen – pericardial cells (at 24 HPE)	Fat body – hemocytes and ovarian follicles (bottom right) (at 1 HPE)
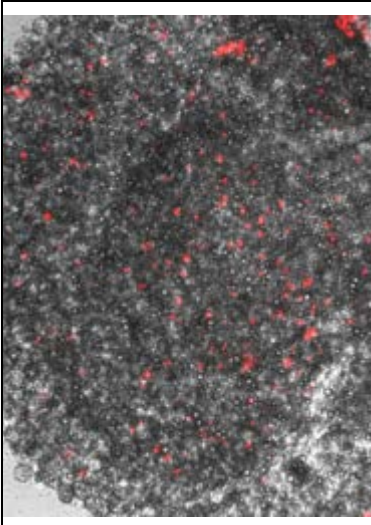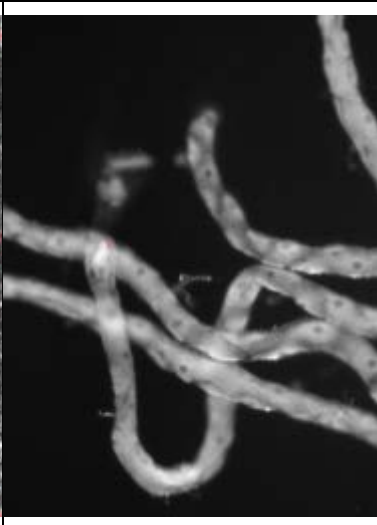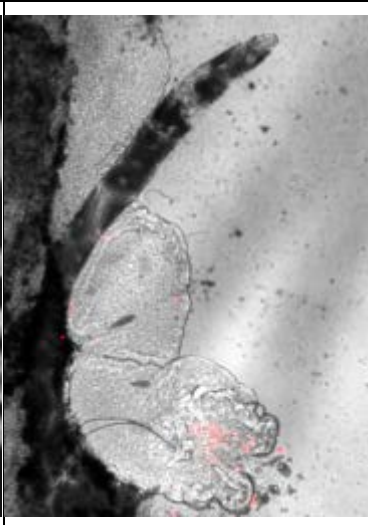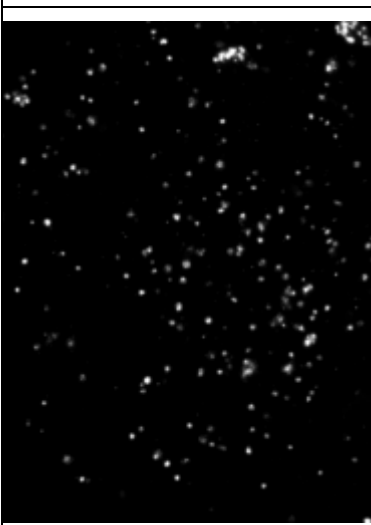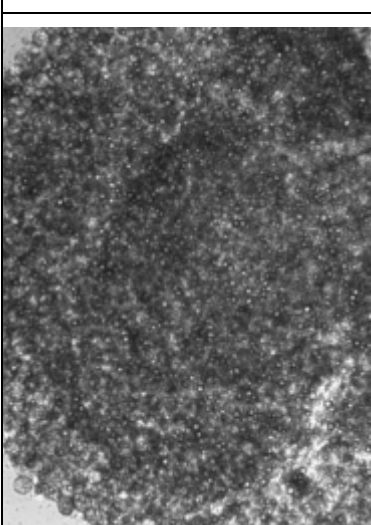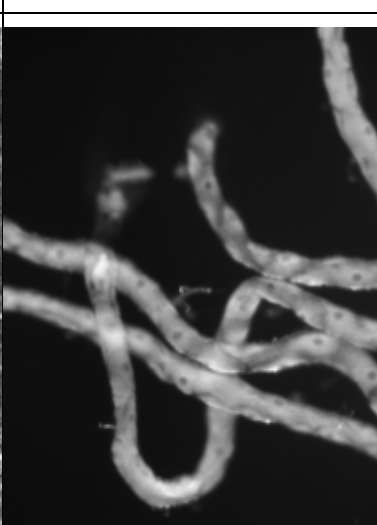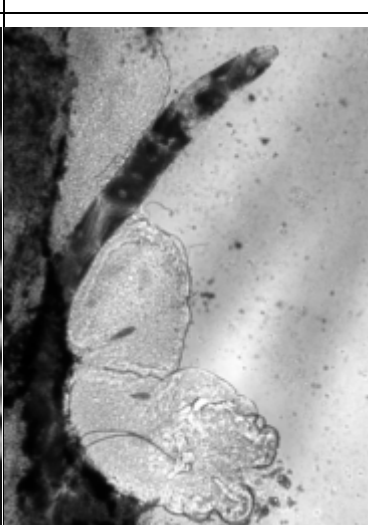
Alimentary tract with no signal and hemocytes (at 1 HPE)	Hindgut and rectum with auto-fluorescent signal (at 1 HPE)	Ovary and fat body–hemocytes and oocytes with bright signal in small atretic follicles (at 1 HPE)

Ovary – fluorescence in small atretic and large healthy follicles (at 24 HPE)	
Ovary - fluorescence in oocytes (at 24 HPE)	
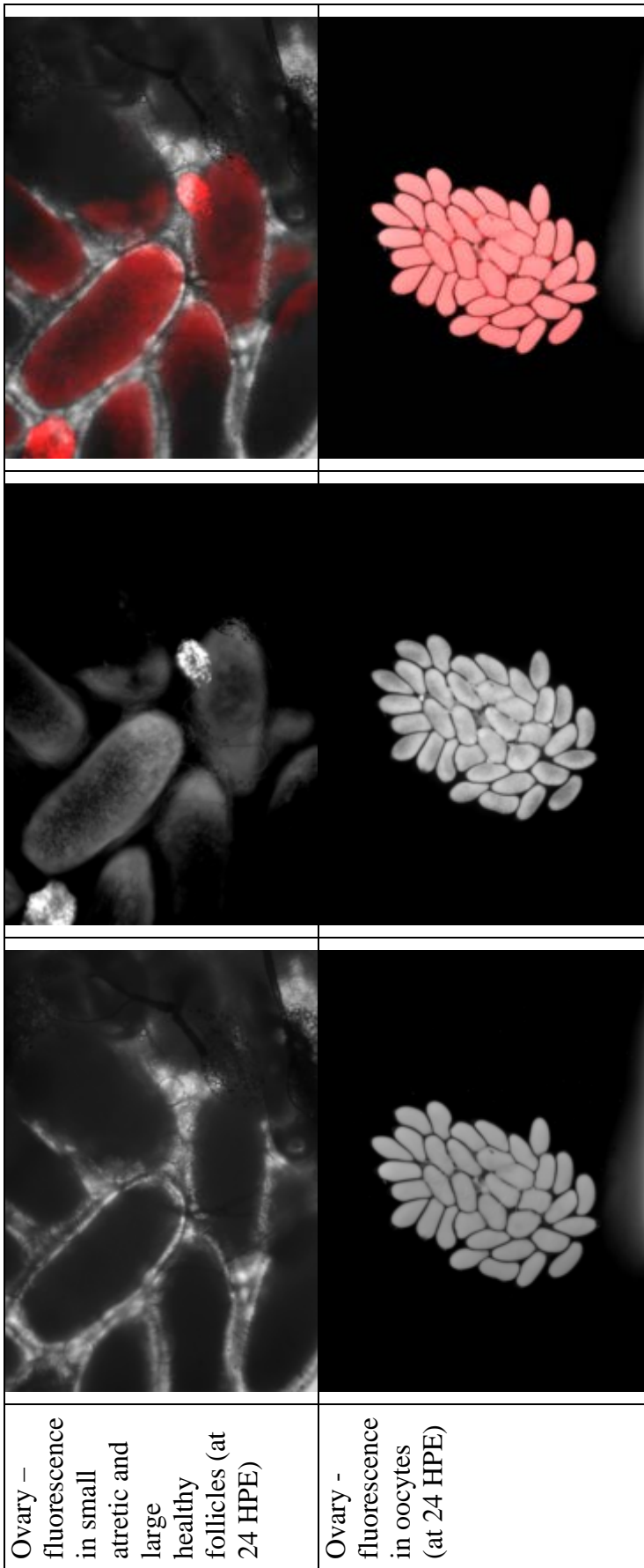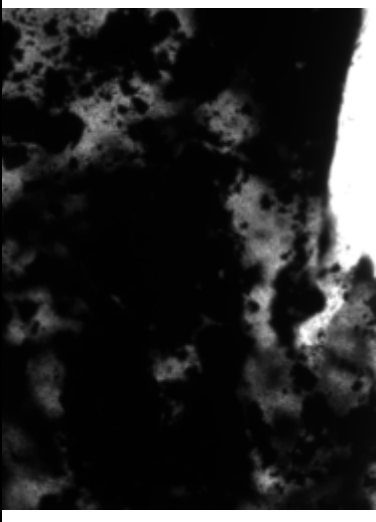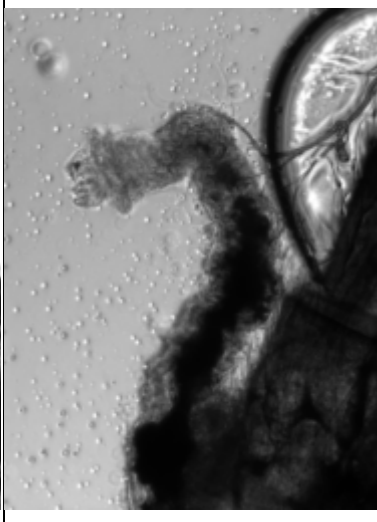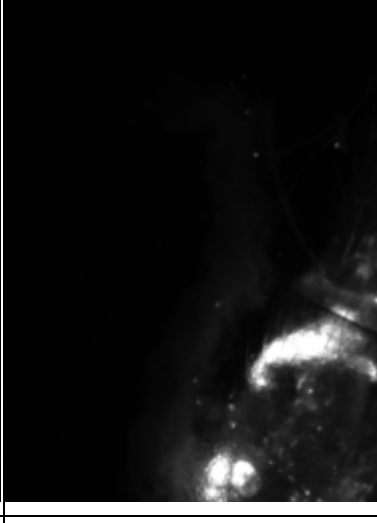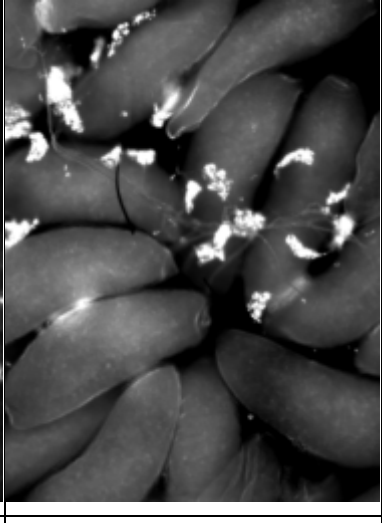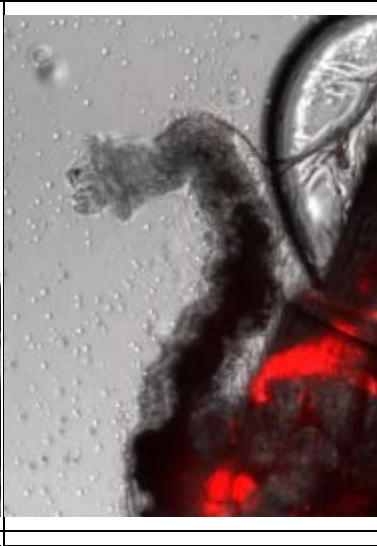
Supplementary Figure 5 – Peritoneal exposure of adult female *An. gambiae* with fluorescent-iLacZ 25-48 hours post blood-meal

Tissue	Bright Field	RNAi trigger	Merge
Head – injection size and hemocytes (at 24 HPE)			
Head – hemocytes in palps (at 24 HPE)			

Abdomen – pericardial cells (at 24 HPE)	Leg – hemocytes (at 1 HPE)	Fat body – hemocytes and (at 1 HPE)

Fat body – hemocytes and (at 1 HPE)	Malpighian tubules – lack of hemocytes (at 1 HPE)	Alimentary tract with no signal and hemocytes (at 1 HPE)

122
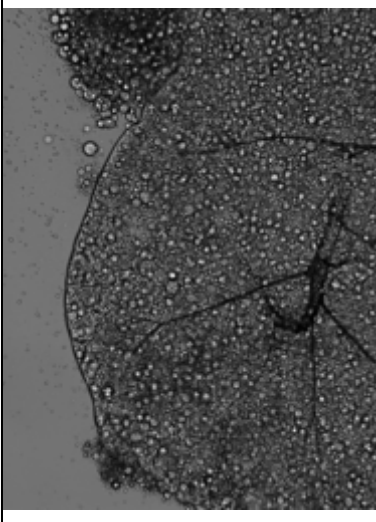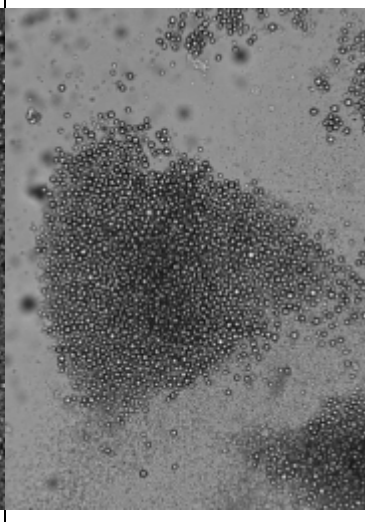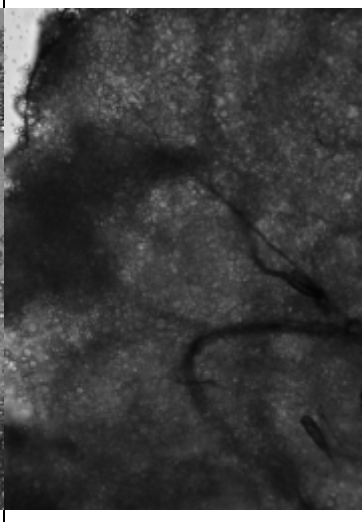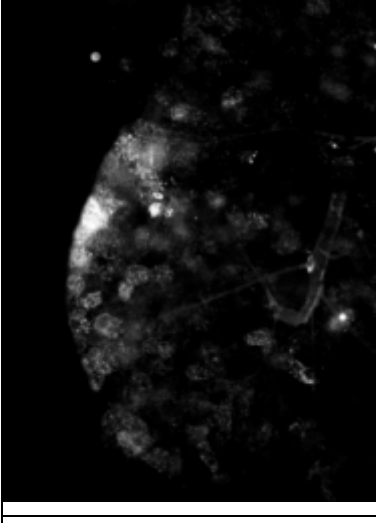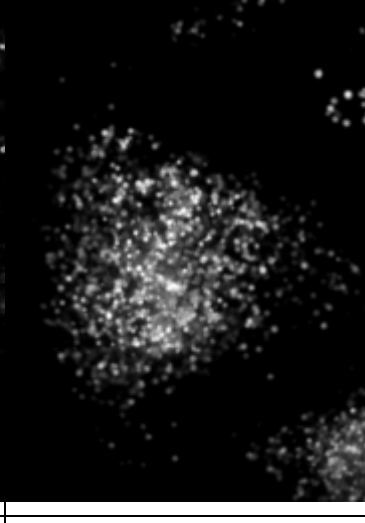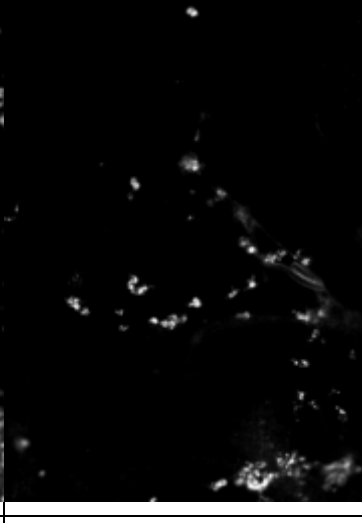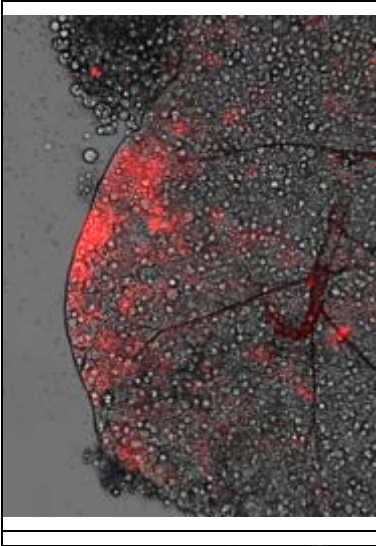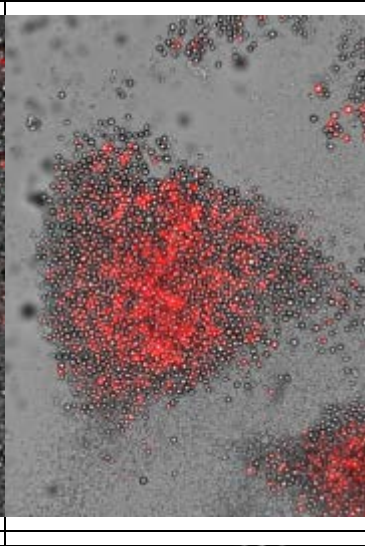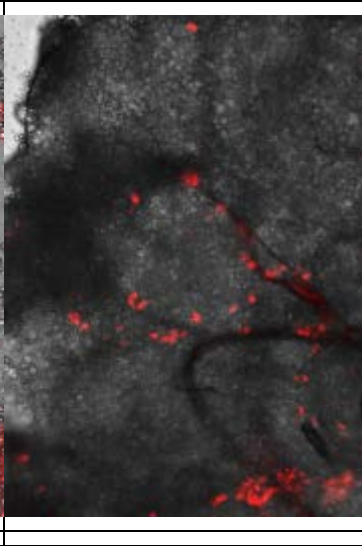
| Midgut with no signal and coagulated blood-meal (at 24 HPE) | Hindgut - no signal and pericardial cells in abdomen (at 24 HPE) | Ovary – fluorescence in atretic and healthy follicles (at 24 HPE) |
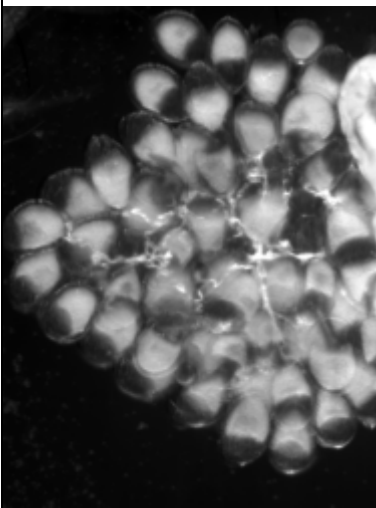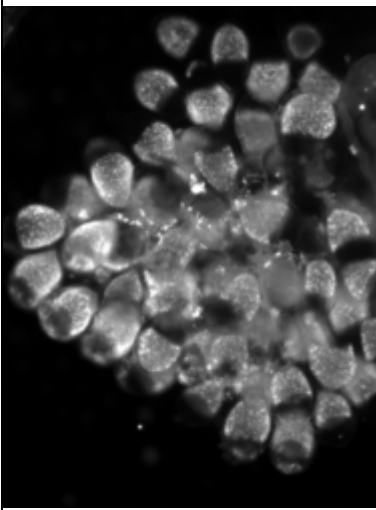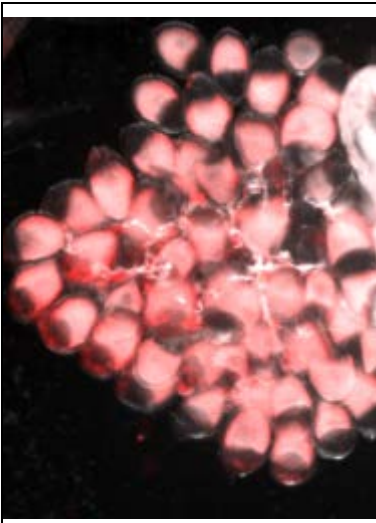
Ovary -
fluorescence
in oocytes
(at 1 HPE)

Supplementary Figure 6 – Peritoneal exposure of adult female *Cx. pipiens* with fluorescent-iLacZ 25-48 hours post blood-meal

Tissue	Bright Field	RNAi trigger	Merge
Head – injection size and hemocytes (at 24 HPE)			
Abdomen – pericardial cells (at 24 HPE)			
Leg – hemocytes (at 1 HPE)			
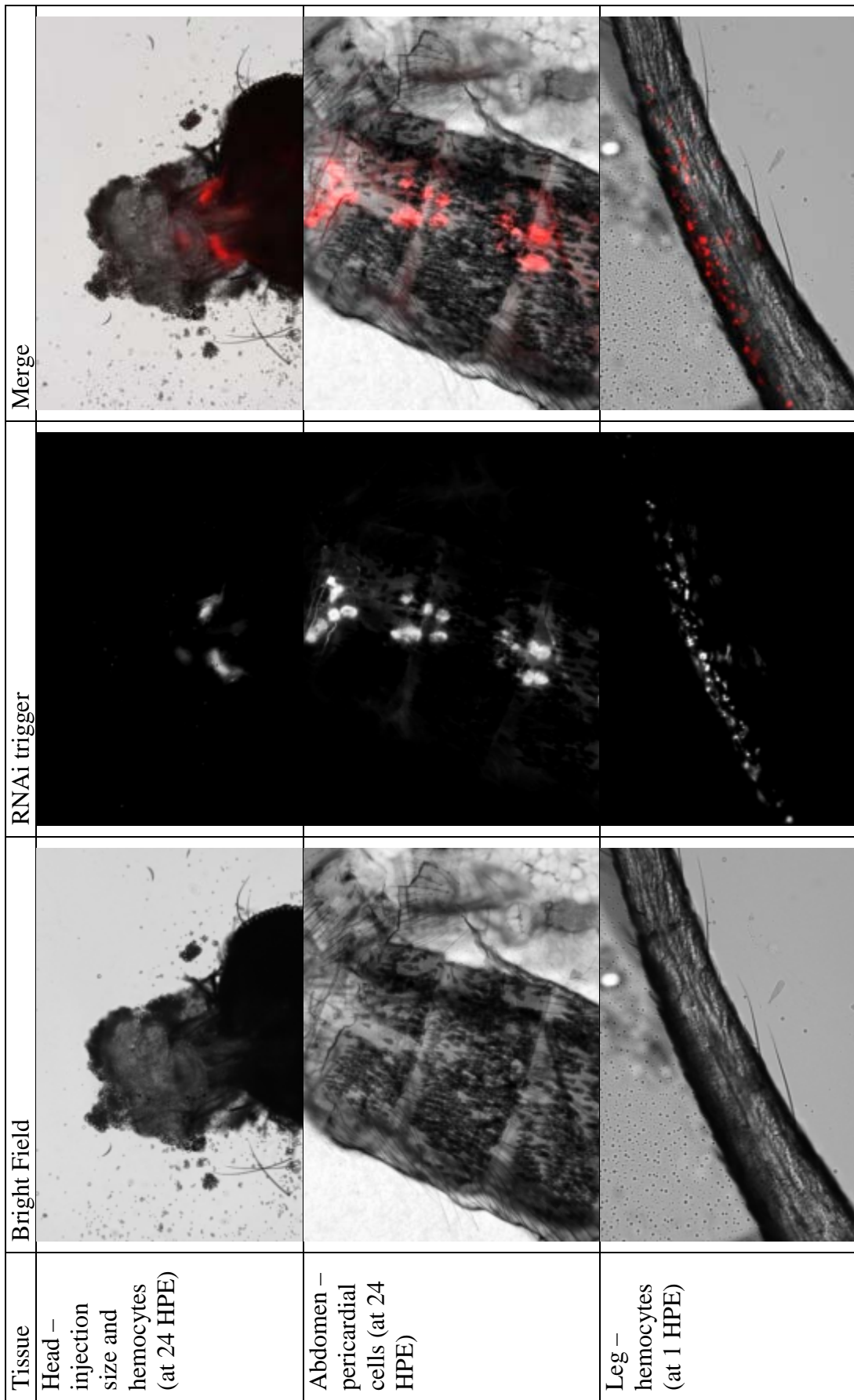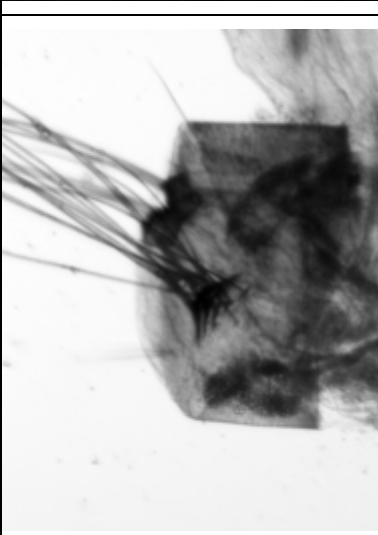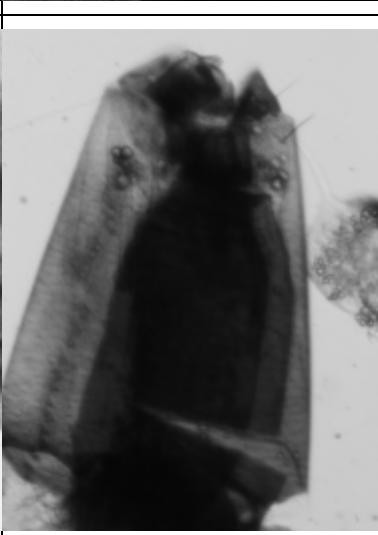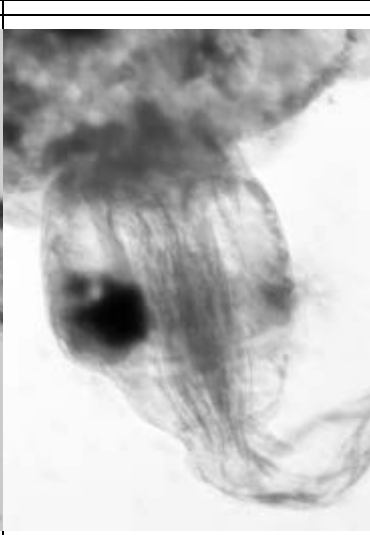
Fat body – fat body and hemocytes (at 24 HPE)	Fat body – fat body (at 24 HPE)	Fat body – hemocytes associated with tracheoles (at 24 HPE)

Malpighian tubules – hemocytes associated with tracheole (at 1 HPE)	Alimentary tract with auto-fluorescent signal (at 1 HPE)	Midgut with punctate auto-fluorescent signal (at 1 HPE)

Ovary – fluorescence in oocytes (at 1 HPE)

Ovary – fluorescence in oocytes (at 24 HPE)

Ovary - fluorescence in healthy and atretic follicles (at 24 HPE)
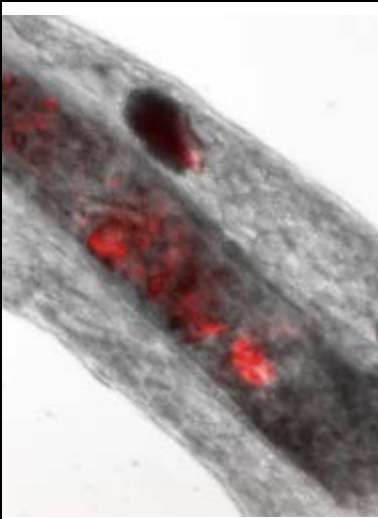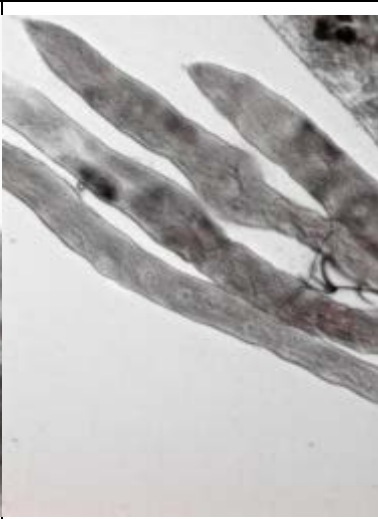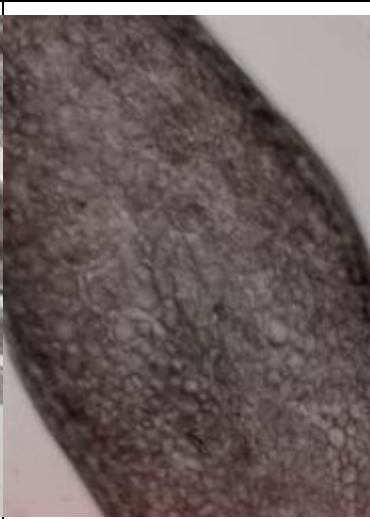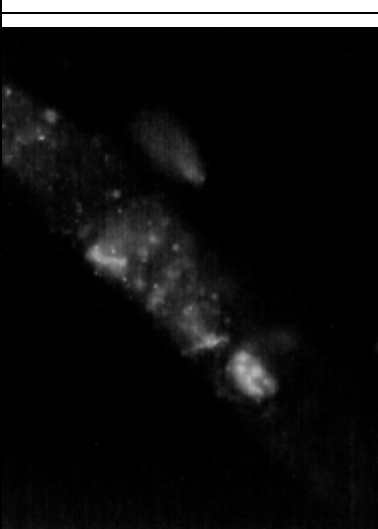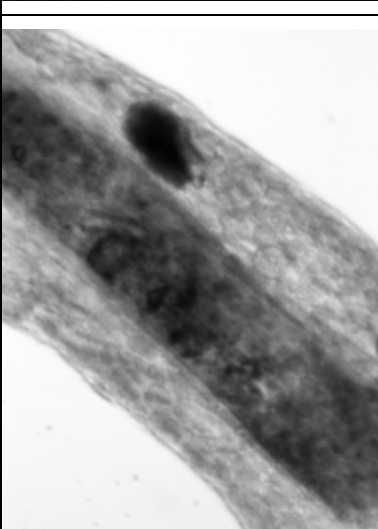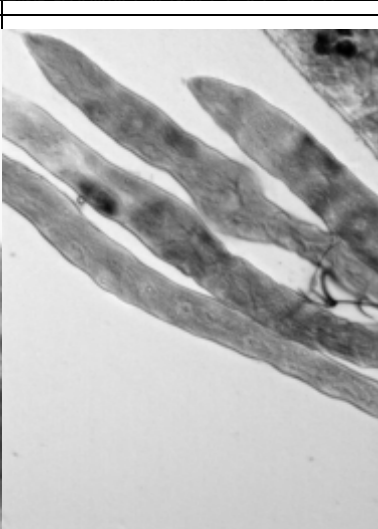
Supplementary Figure 7 – Peritoneal exposure of 4th instar larval *Ae. aegypti* with fluorescent-iLacZ

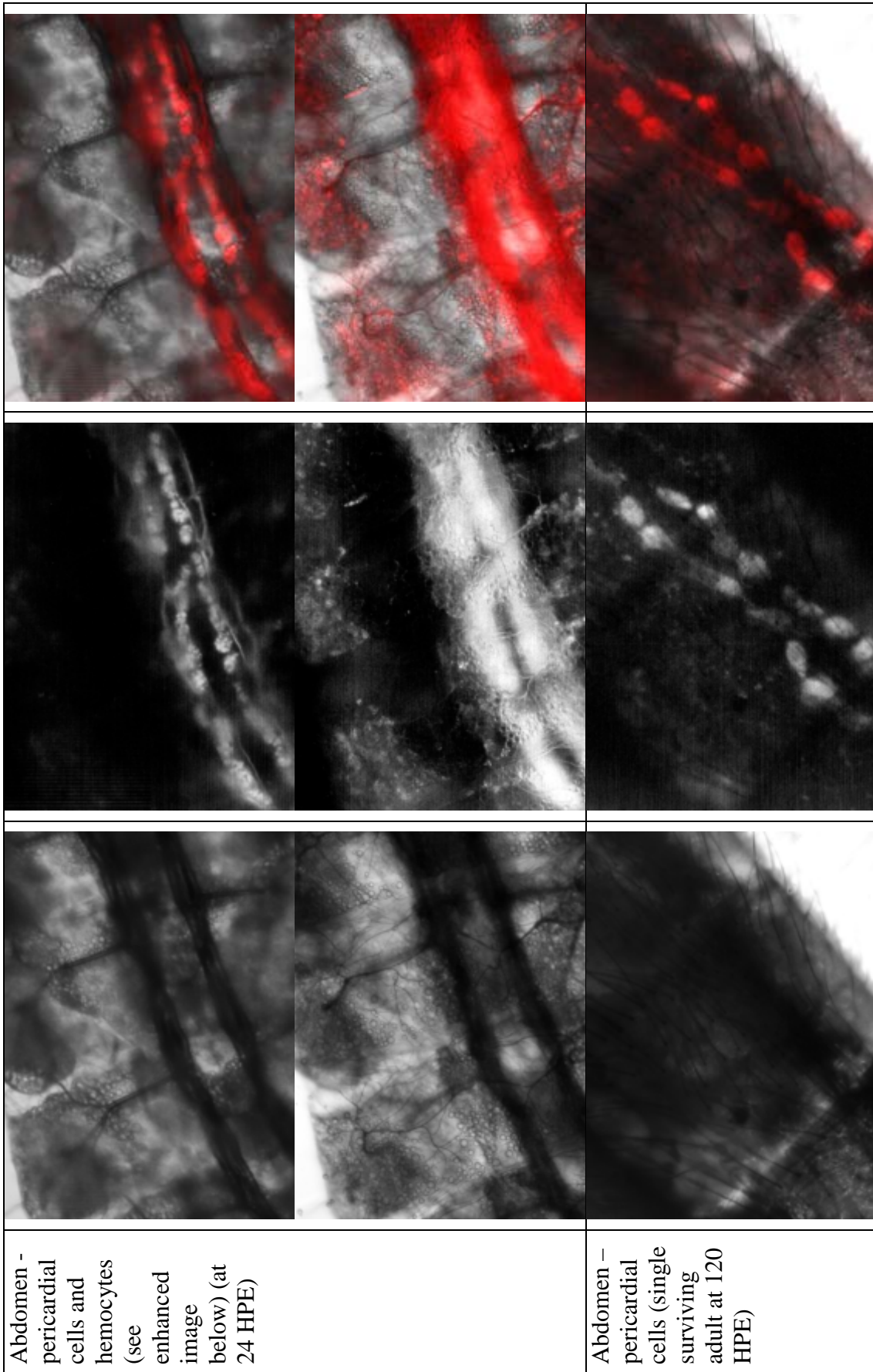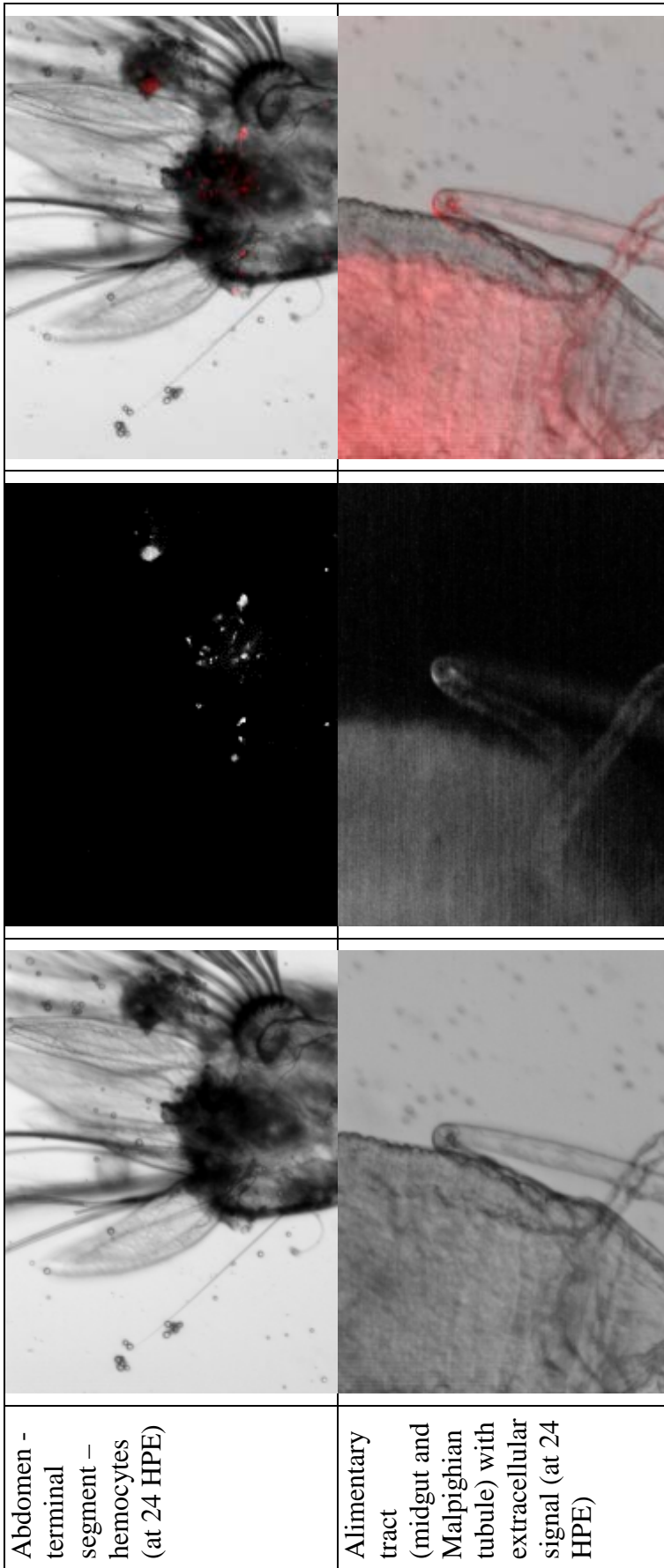| Tissue	Bright Field	RNAi trigger	Merge
Head (at 24 HPE)			
Abdomen - pericardial cells (at 24 HPE)			

Abdomen - terminal segment – auto-fluorescence in cuticle (at 24 HPE)		
Abdomen - Terminal segment - respiratory siphon		
Caecum (at 24 HPE)		

| Alimentary tract (midgut) with extracellular signal (at 24 HPE) | Malpighian tubules (at 24 HPE) | Alimentary tract (anal canal / hindgut) with no signal (at 24 HPE) |

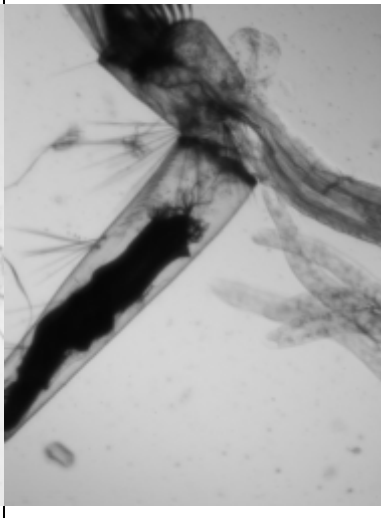**Supplementary Figure 8 – Peritoneal exposure of 4th instar larval *An. gambiae* fluorescent-iLacZ**
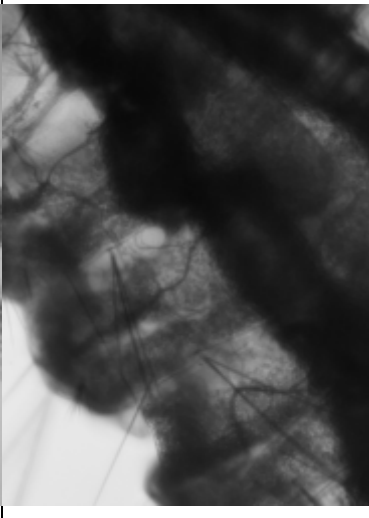
Tissue	Bright Field	RNAi trigger	Merge
Head - hemocytes (at 24 HPE)			

| Abdomen - pericardial cells and hemocytes (see enhanced image below) (at 24 HPE) | | |
| Abdomen – pericardial cells (single surviving adult at 120 HPE) | | |

Abdomen - terminal segment – hemocytes (at 24 HPE)	Alimentary tract (midgut and Malpighian tubule) with extracellular signal (at 24 HPE)

134
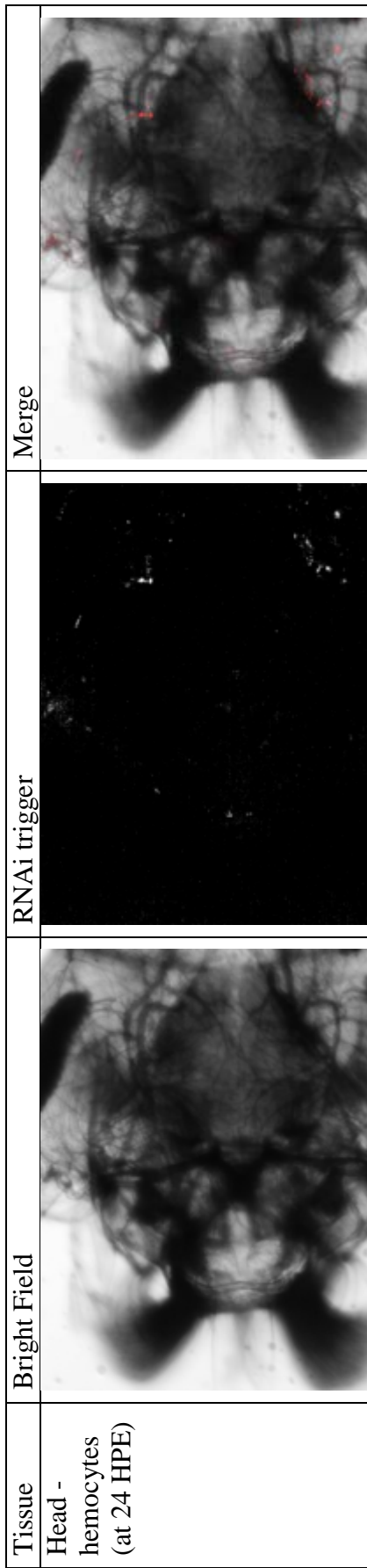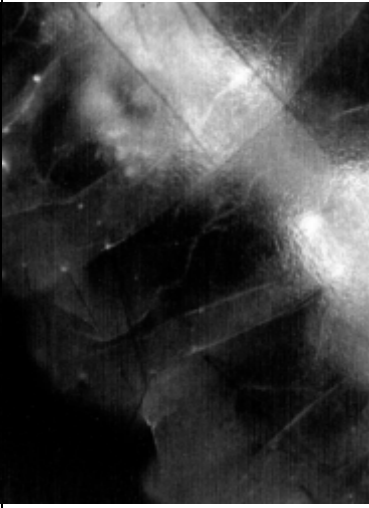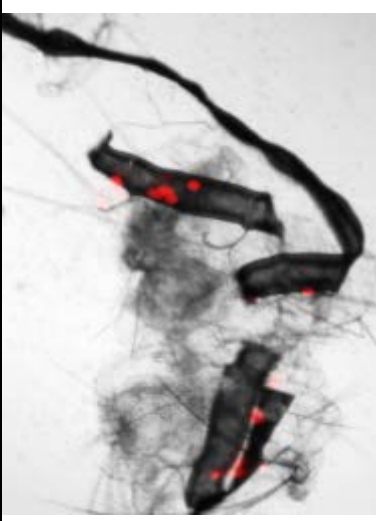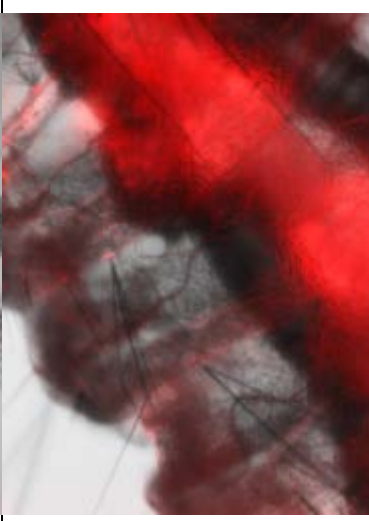
Supplementary Figure 9 – Peritoneal exposure of 4th instar larval *Cx. pipiens* fluorescent-iLacZ

Tissue	Bright Field	RNAi trigger	Merge
Head (at 24 HPE)			
Abdomen - pericardial cells (at 24 HPE)			
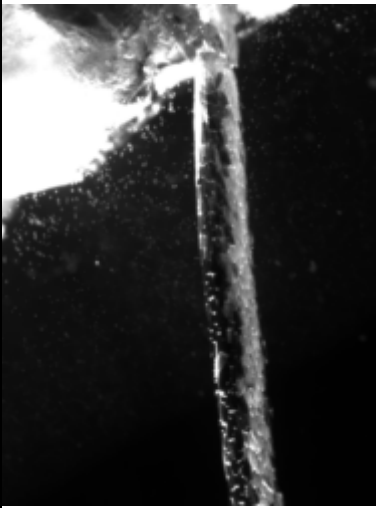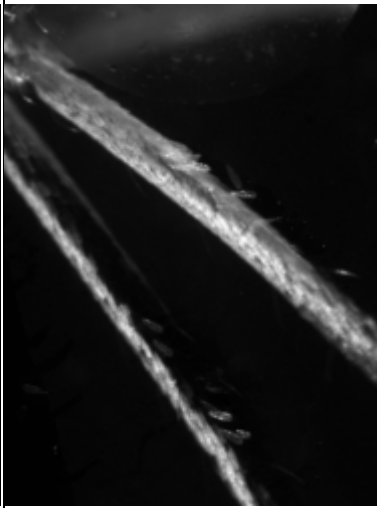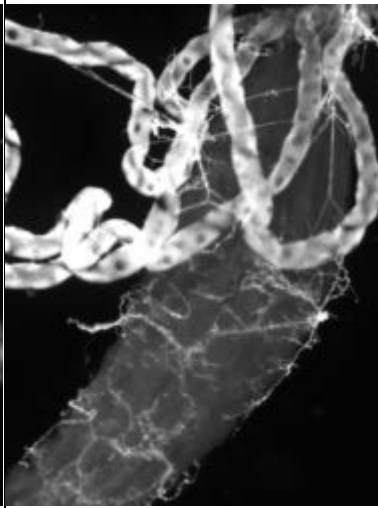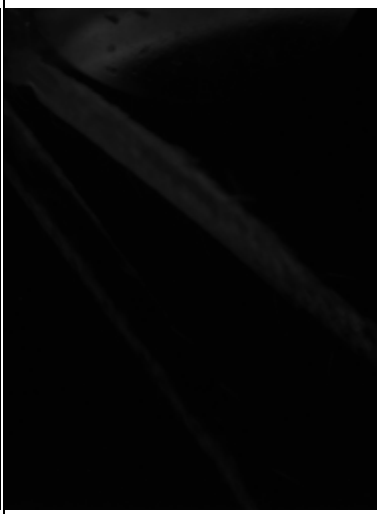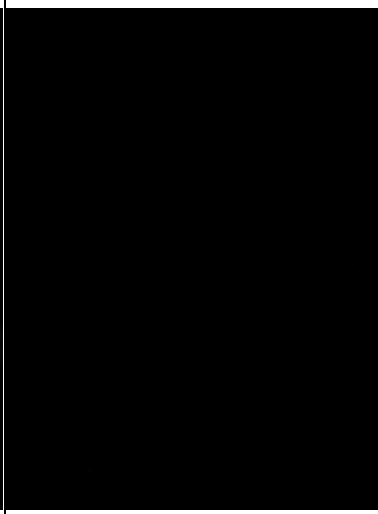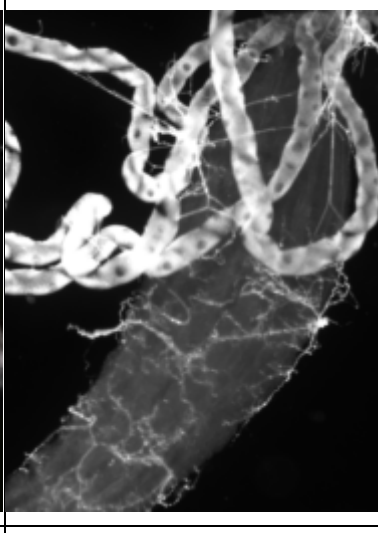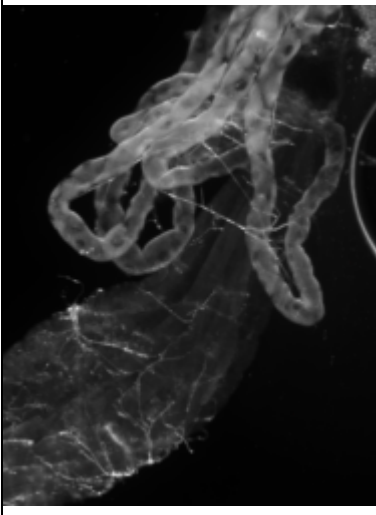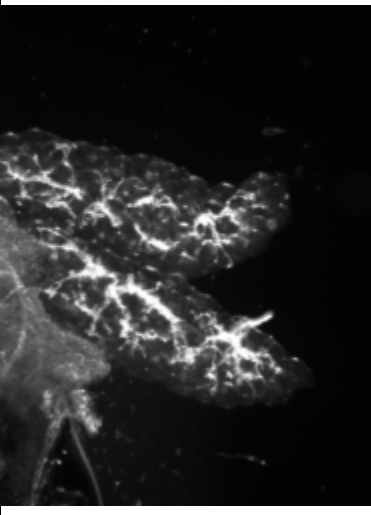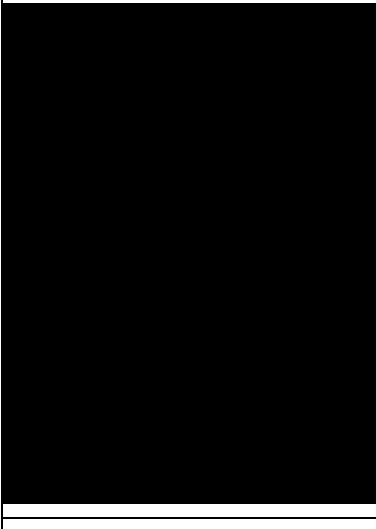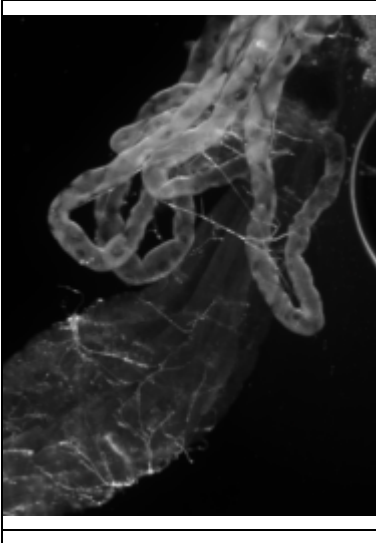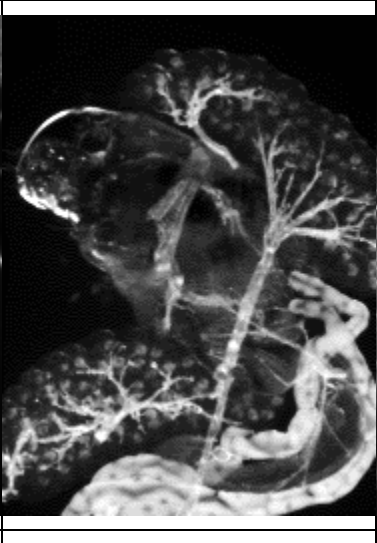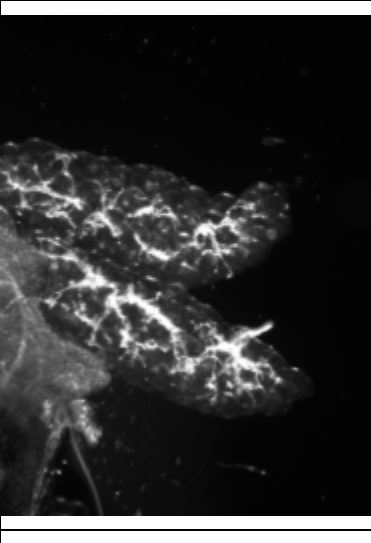
Abdomen – pericardial cells in dissected tissue (at 24 HPE)	Abdomen - Terminal segment - respiratory siphon, Malpighian tubules and anal canal (at 24 HPE)	Abdomen – pericardial cells and hemocytes and auto-fluorescence (at 24 HPE)

| Caecum – auto-fluorescence (at 24 HPE) |
| Alimentary tract (midgut) with extracellular signal (at 24 HPE) |
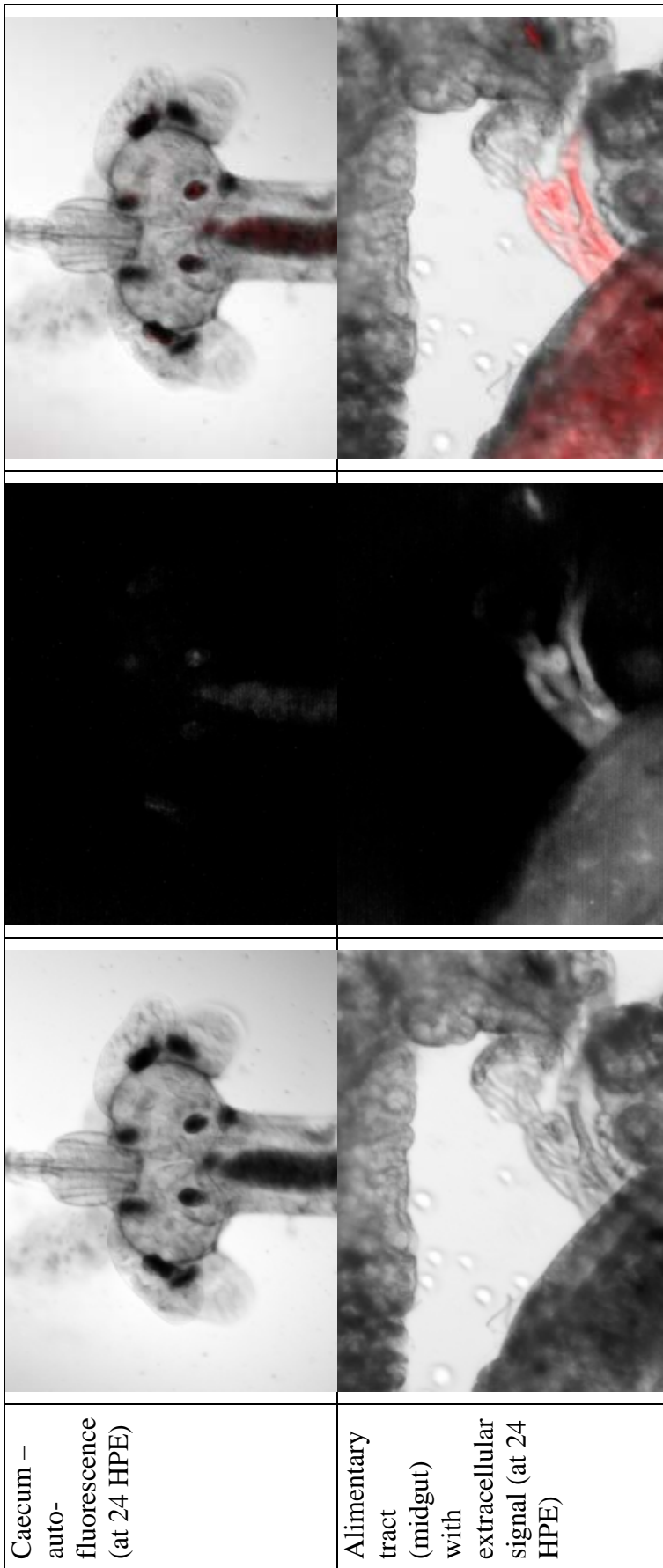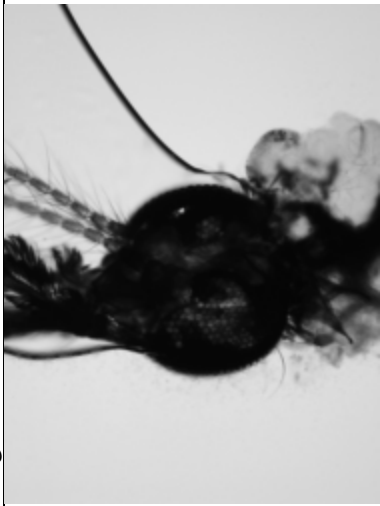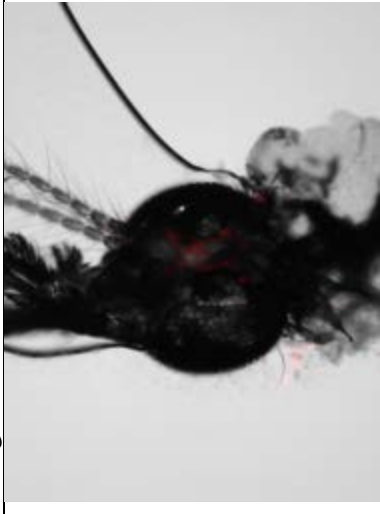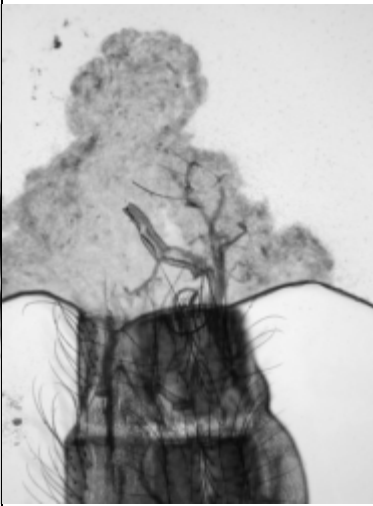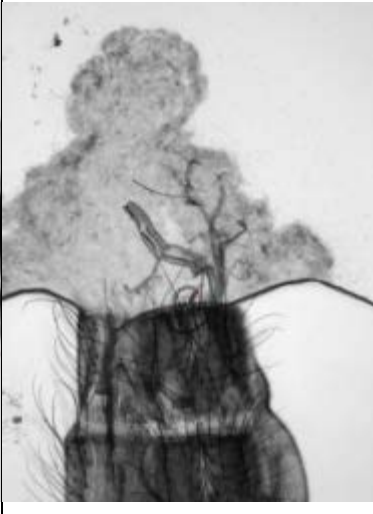
Supplementary Figure 10 – Topical exposure of adult female *Ae. aegypti* with fluorescent-iLacZ

Tissue	Bright Field	RNAi trigger	Merge
Head			
Abdomen – signal on cuticle			
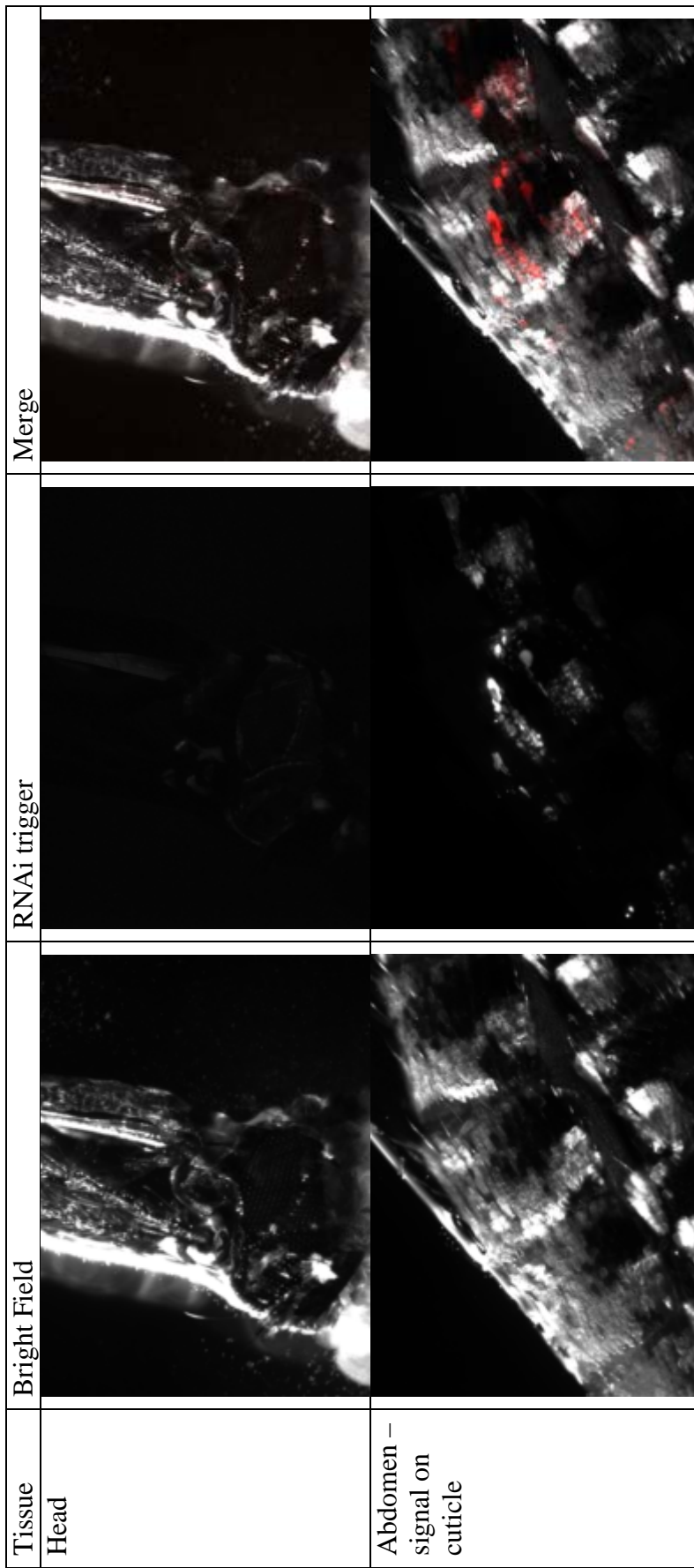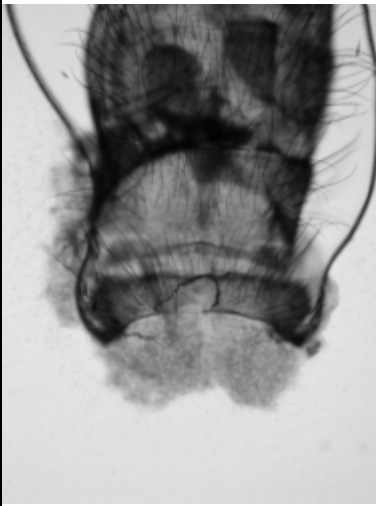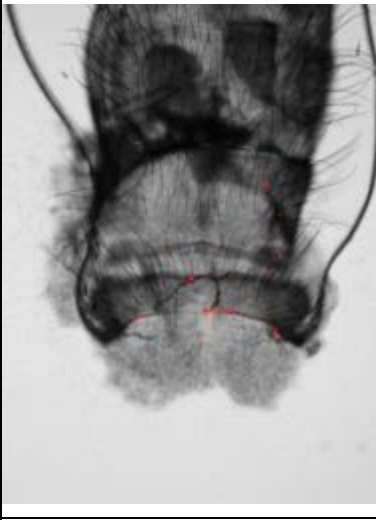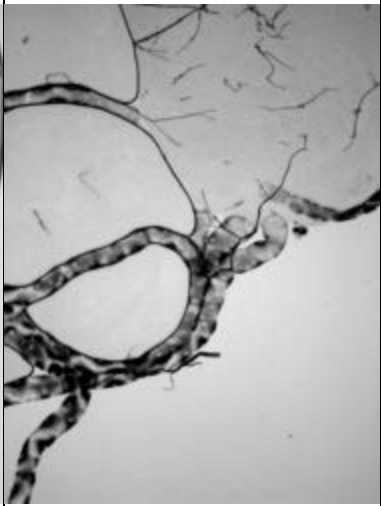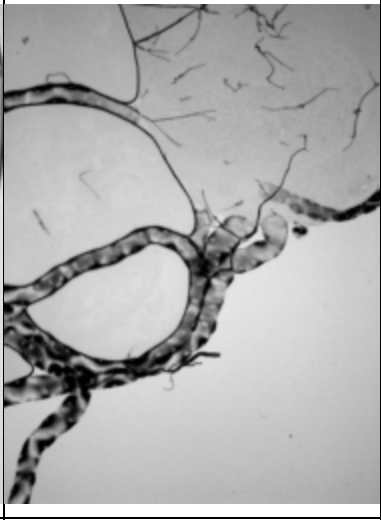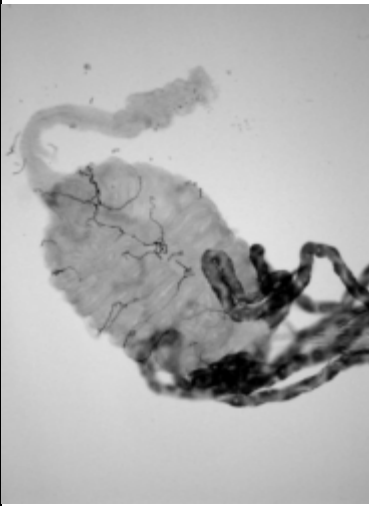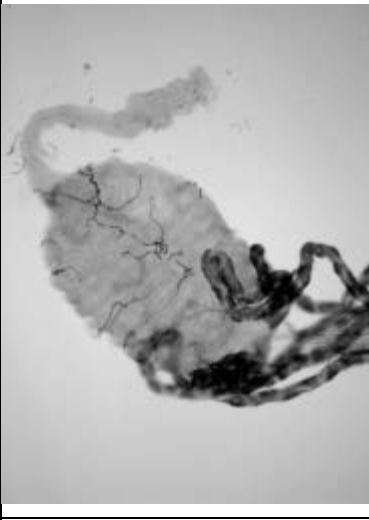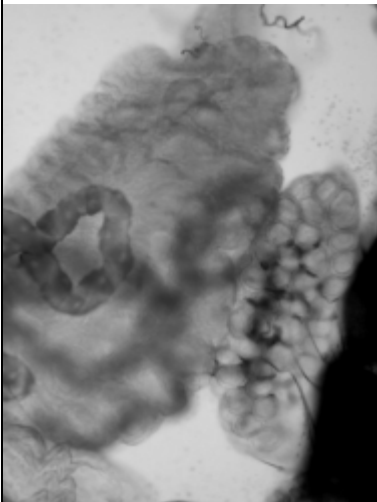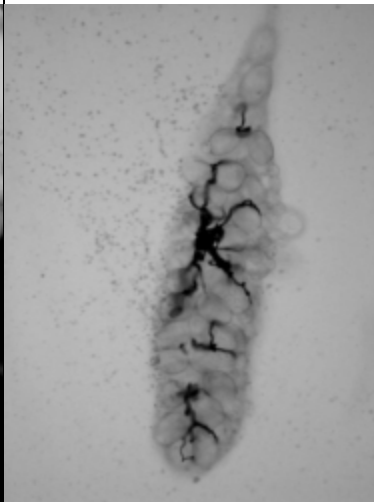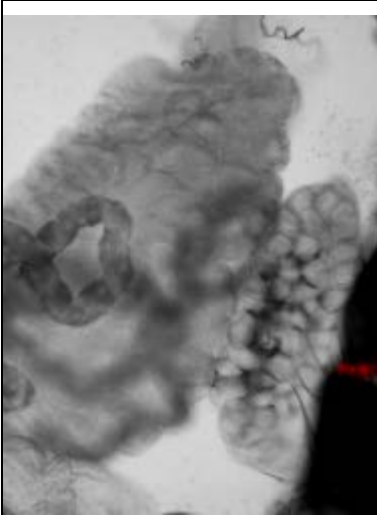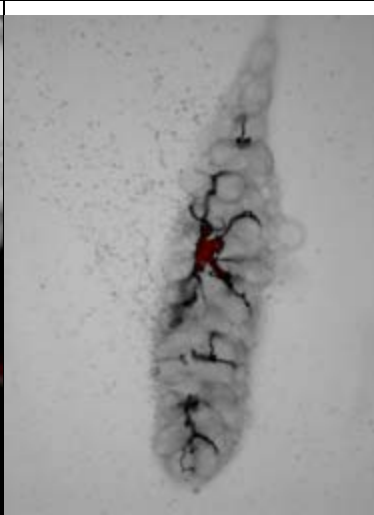
Leg – signal on cuticle	Leg – no signal	Alimentary tract (midgut and Malpighian tubules) with no signal

Alimentary tract (midgut and Malpighian tubules) with no signal	Alimentary tract (hindgut and Malpighian tubules) and ovaries with no signal	Ovary

Supplementary Figure 11 – Topical exposure of adult female *An. gambiae* with fluorescent-iLacZ
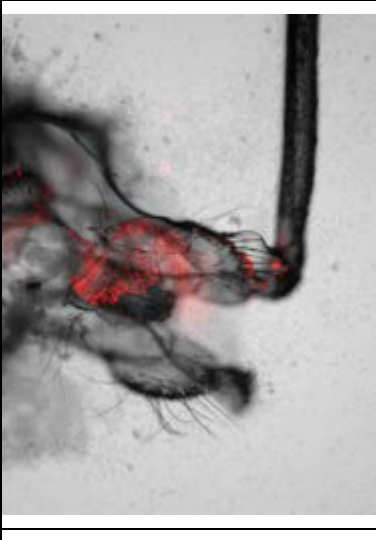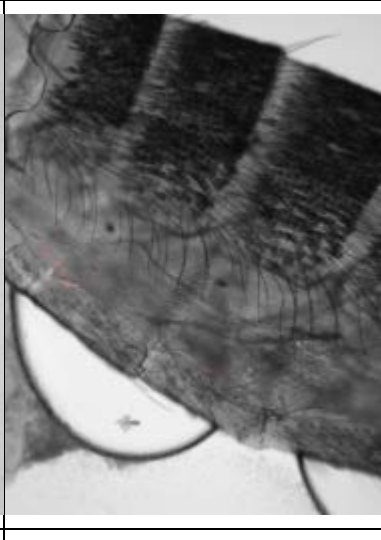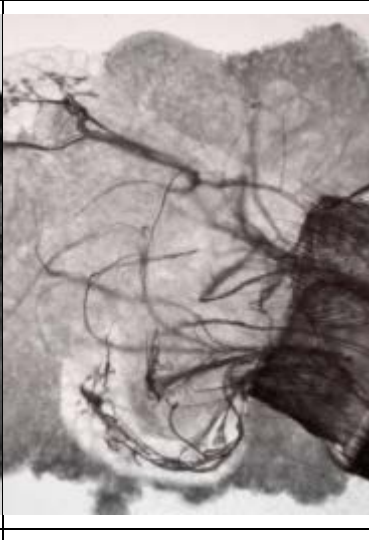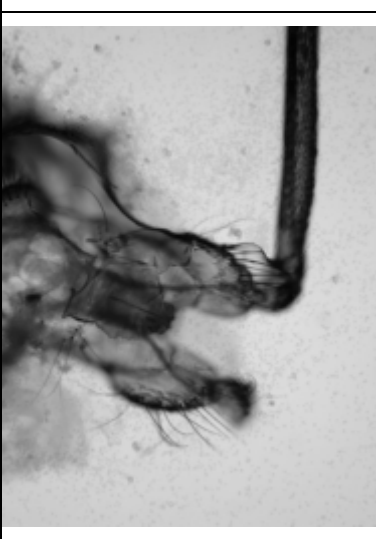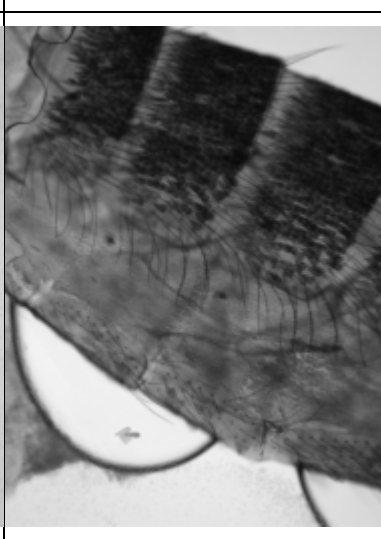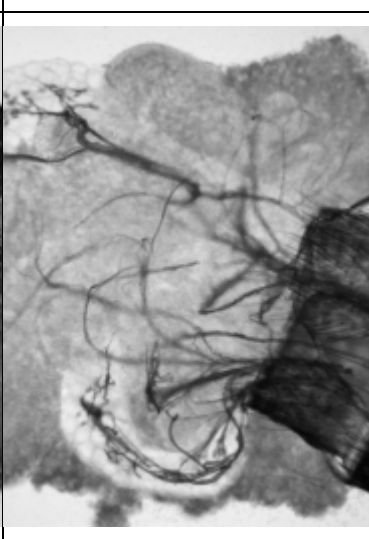
Tissue	Bright Field	RNAi trigger	Merge
Head – auto-fluorescence			
Abdomen – no signal			

Abdomen – signal on cuticle	Alimentary tract (midgut and Malpighian tubules) no signal	Alimentary tract (foregut, midgut and Malpighian tubules) with no signal
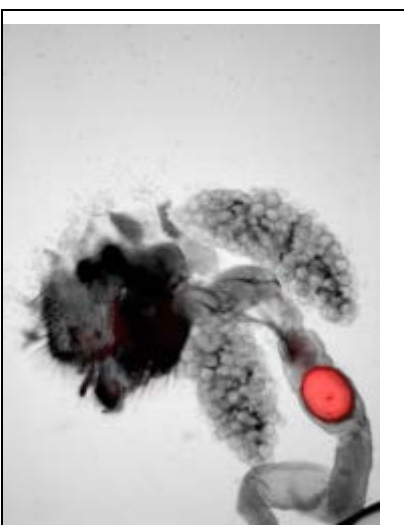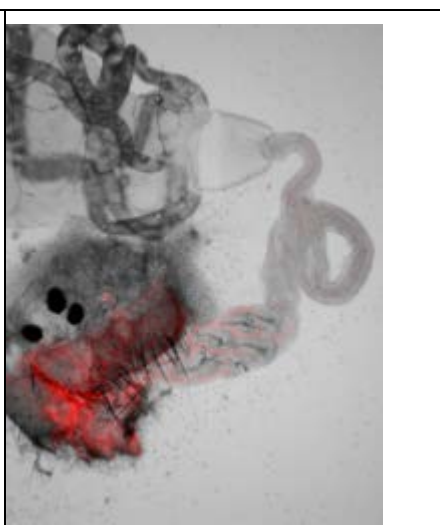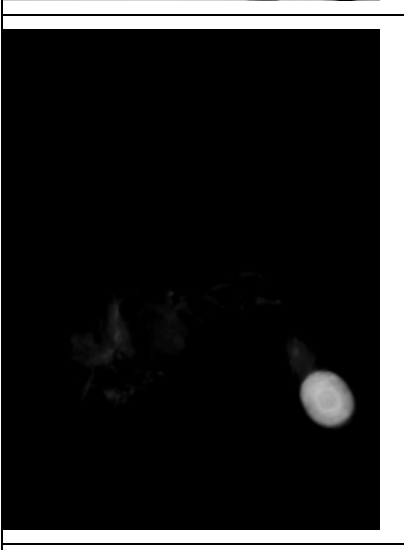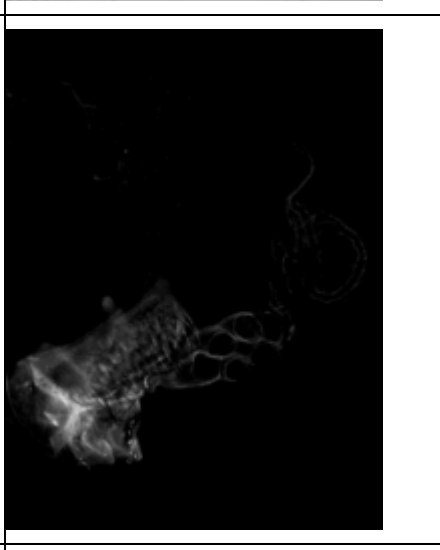
Alimentary tract (midgut and Malpighian tubules) and ovary with no signal	
Ovary – auto-fluorescence in tracheole	

Supplementary Figure 12 – Topical exposure of adult female *Cx. pipiens* with fluorescent-iLacZ

Tissue	Bright Field	RNAi trigger	Merge
Head – signal on cuticle and auto-fluorescence (reflected) in diverticula			
Head – signal on cuticle			
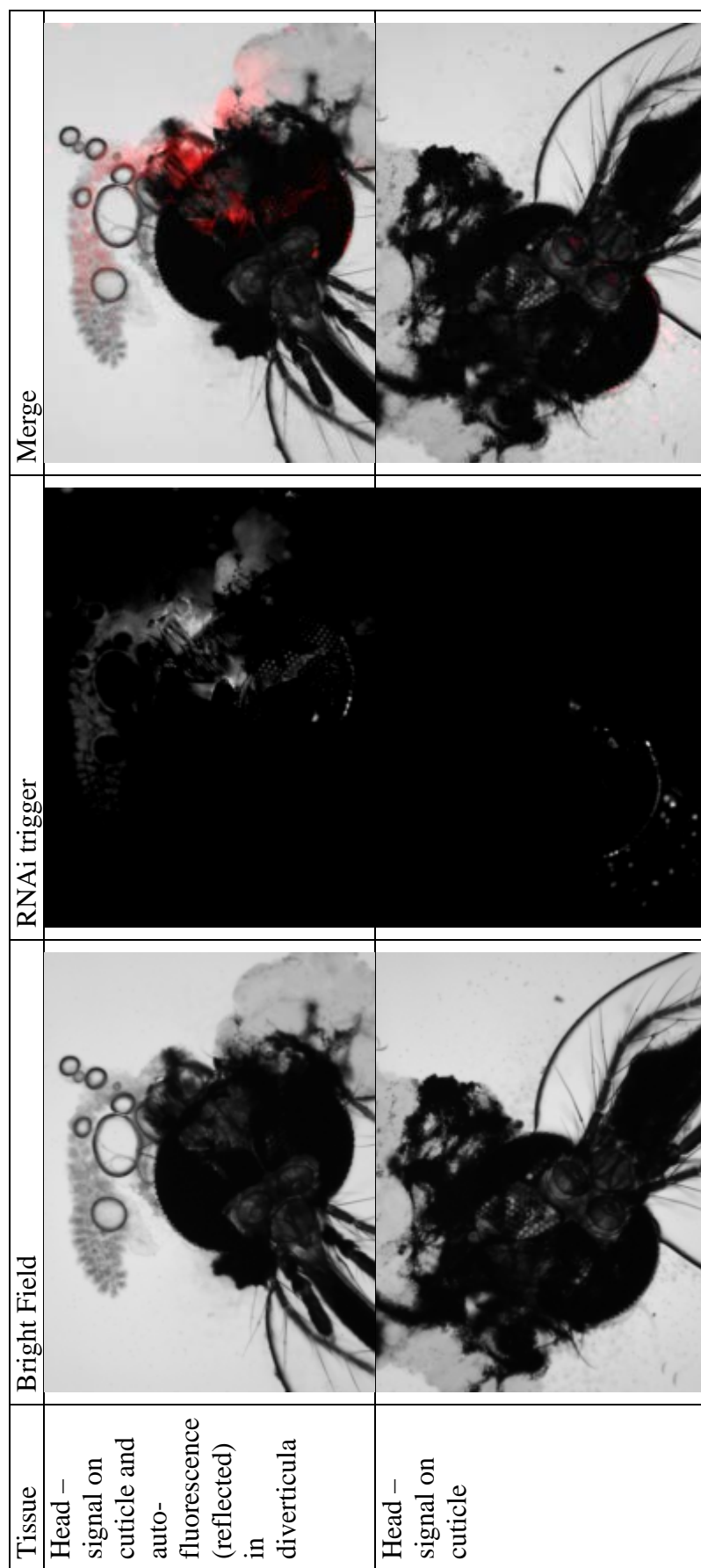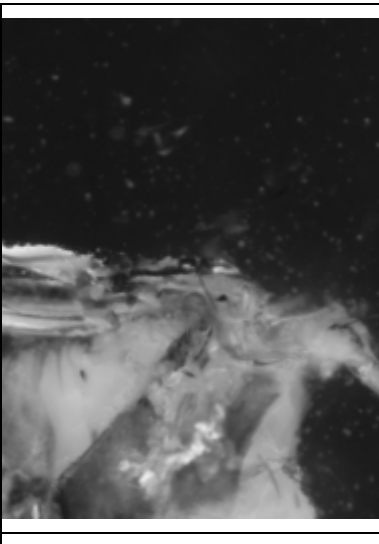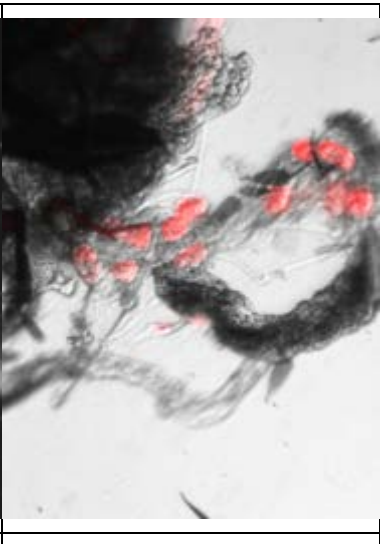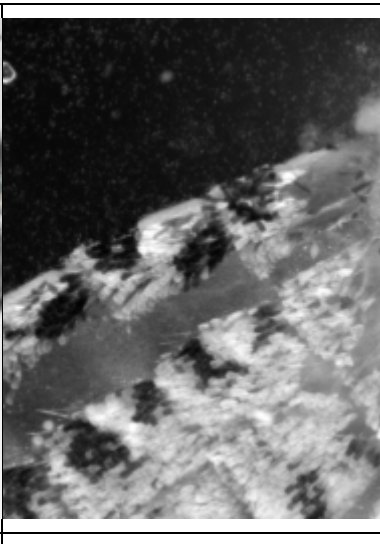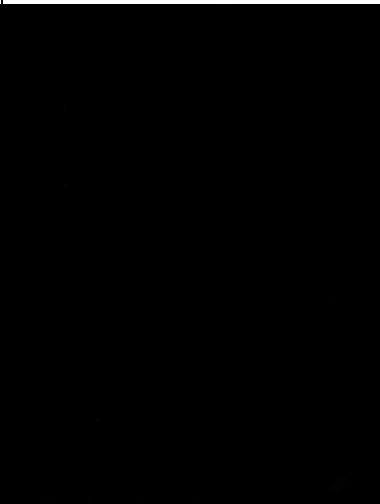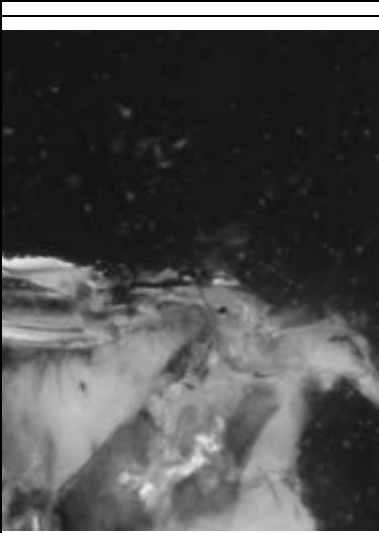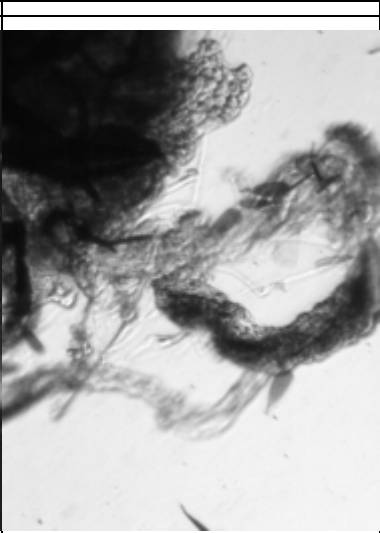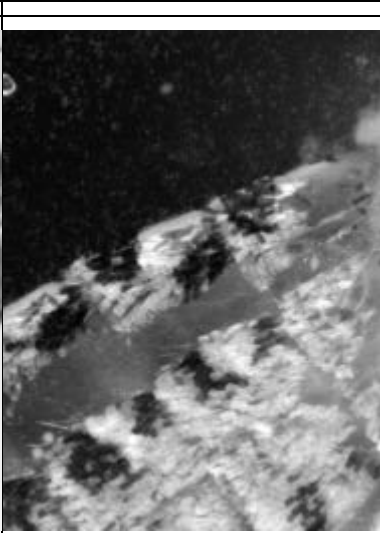
| Thorax – signal on cuticle | Abdomen – signal on cuticle | Abdomen – fat body no signal |

| Leg – signal on cuticle | Alimentary tract – diverticula with auto-fluorescence | Alimentary tract (foregut, midgut and Malpighian tubules) with no signal |
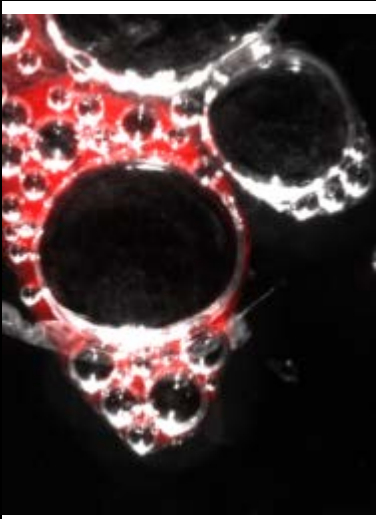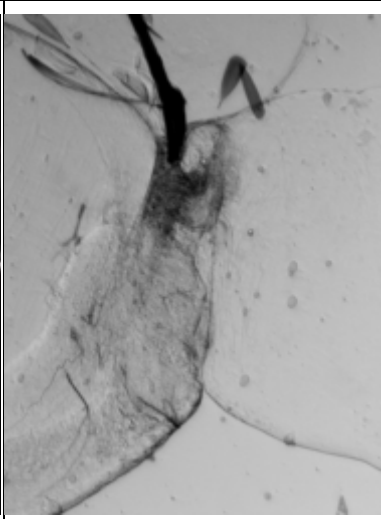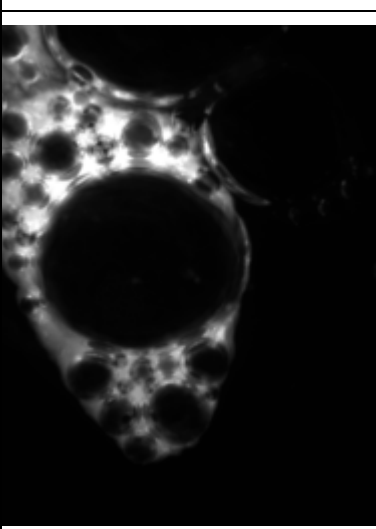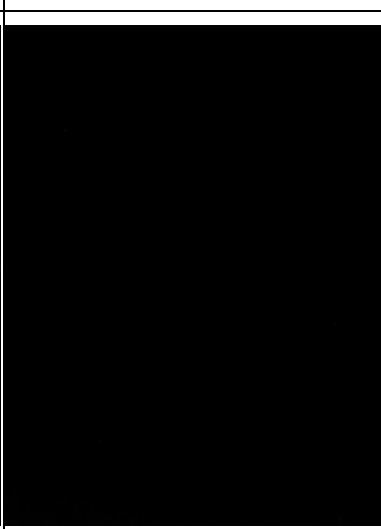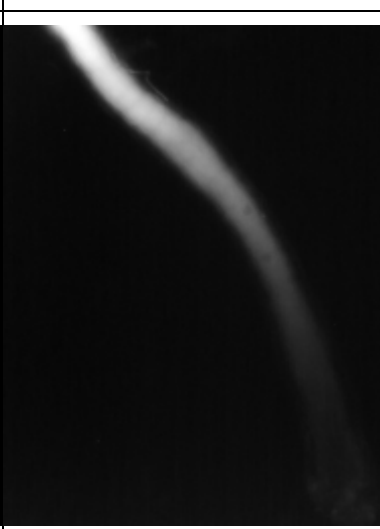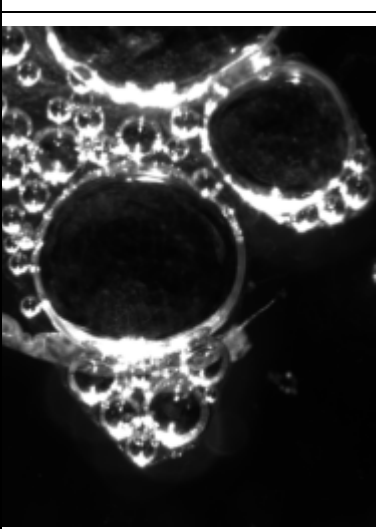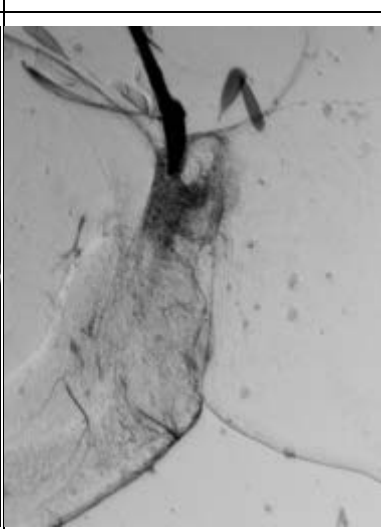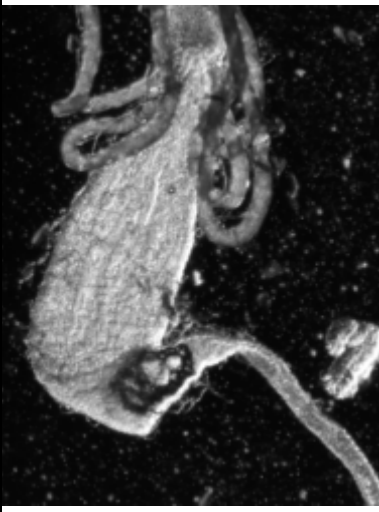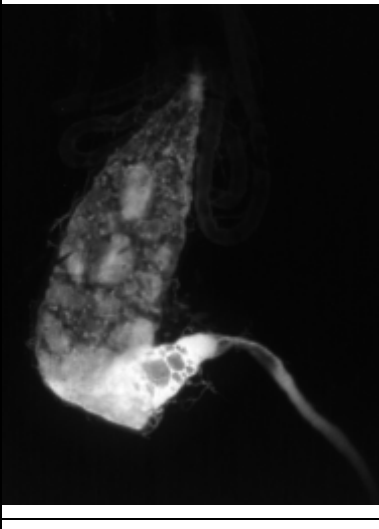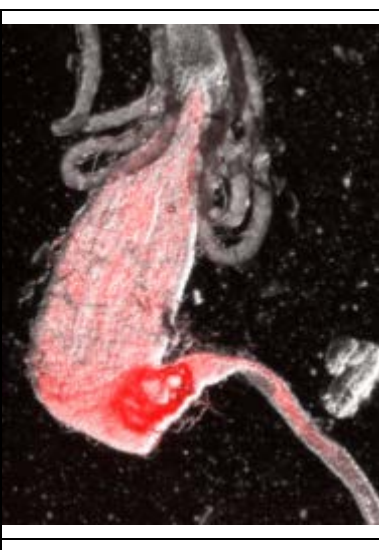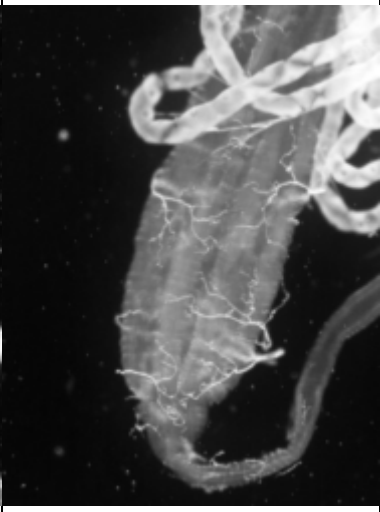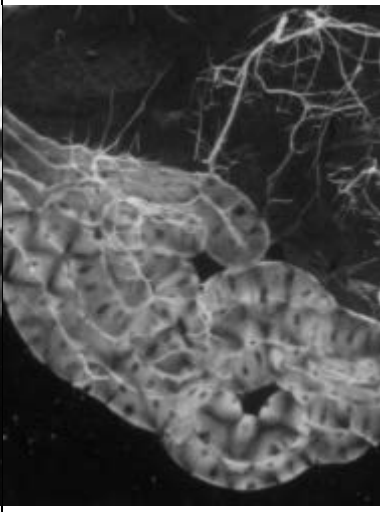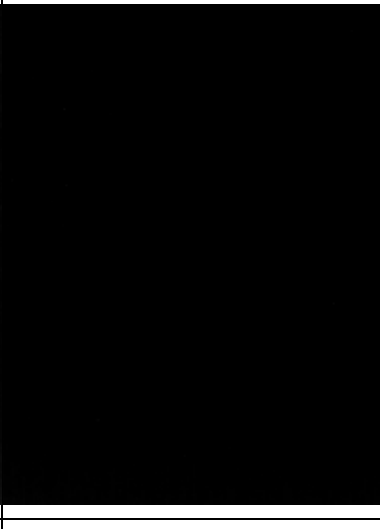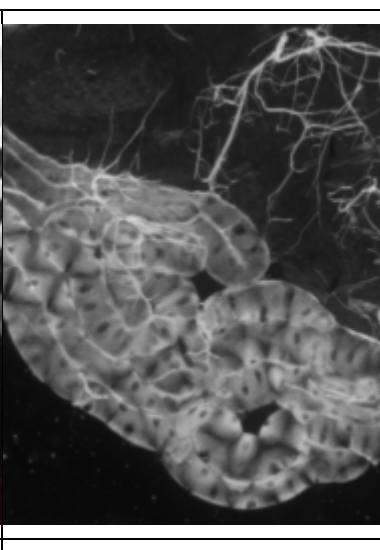
Alimentary tract (hindgut) and ovaries, fluorescent bubble in hindgut lumen probable auto-fluorescence	Abdomen – signal on cuticle and alimentary tract (hindgut, rectum, and Malpighian tubules) with auto-fluorescence (reflected)
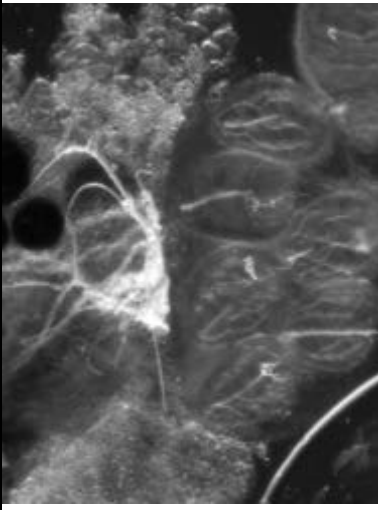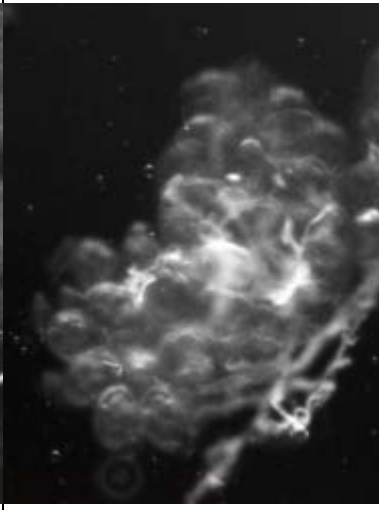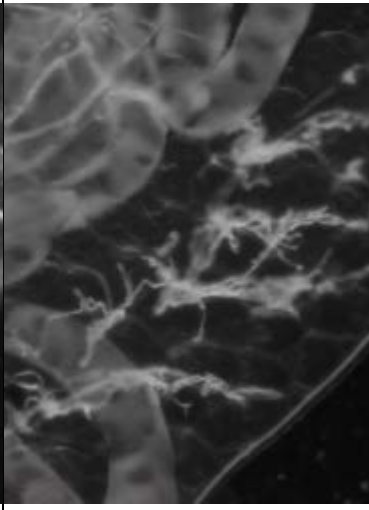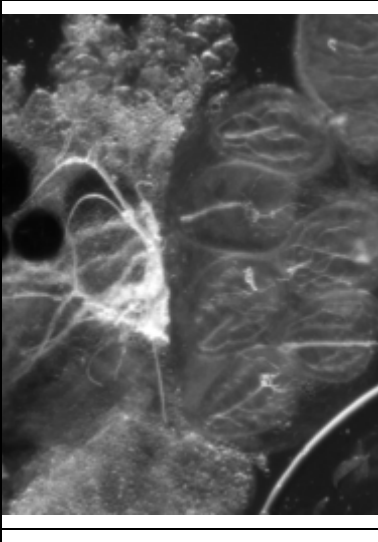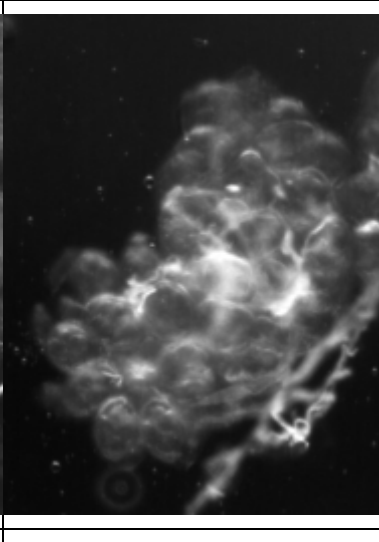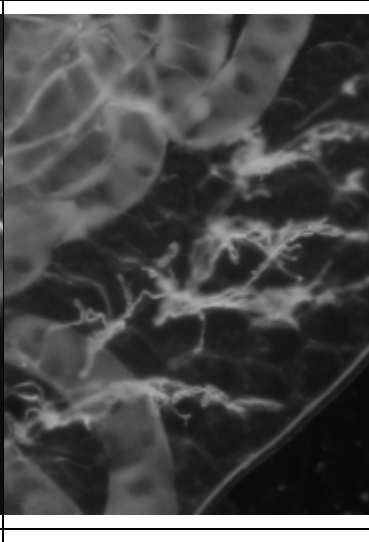
Supplementary Figure 13 – *Per os* **exposure of adult female *Ae. aegypti* with fluorescent-iLacZ**

Tissue	Bright Field	RNAi trigger	Merge
Head - signal at injection site (at 24 HPE)			
Thorax – auto-fluorescence (at 72 HPE)			

148
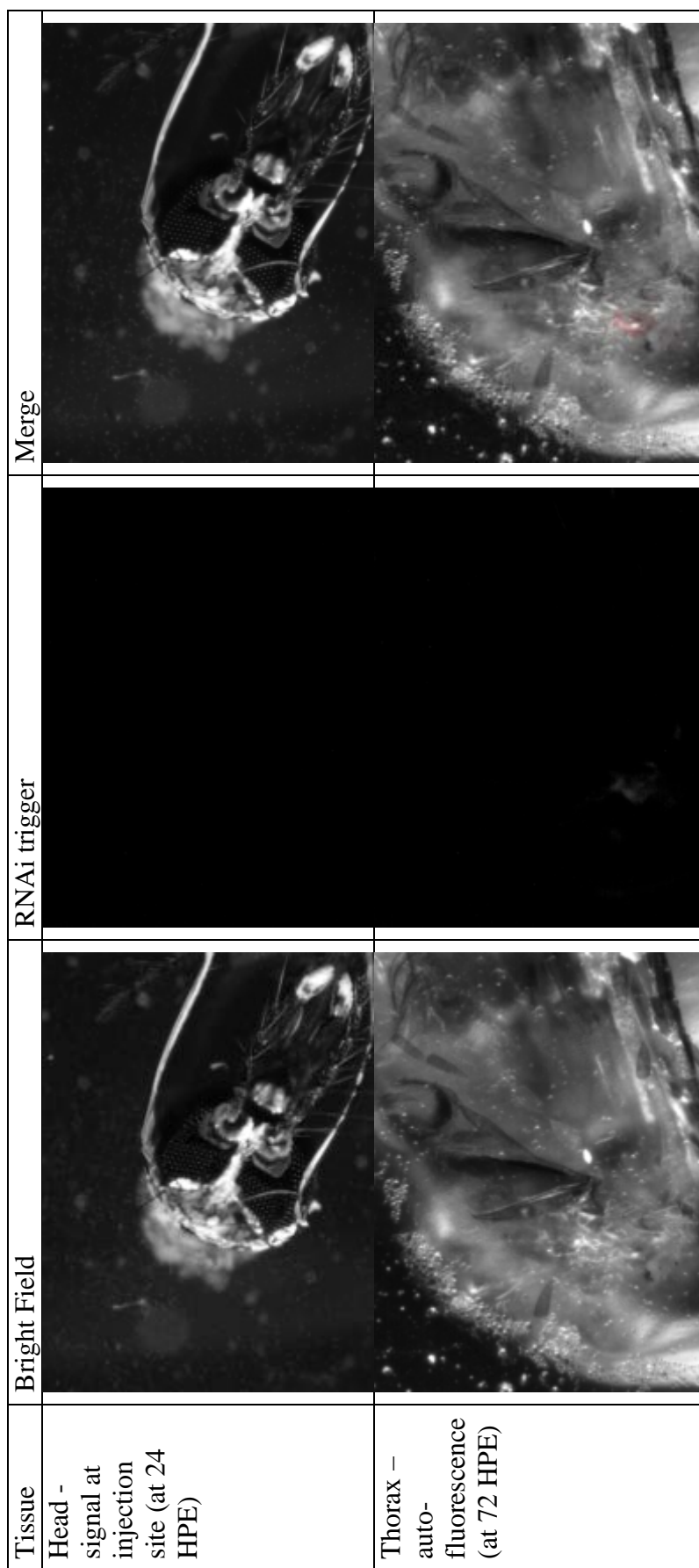
Thorax – no signal (at 72 HPE)

Abdomen - pericardial cells around dorsal vessel (at 72 HPE)

Abdomen – no signal (at 120 HPE)

Diverticula with strong diffuse signal (at 24 HPE)		
Diverticula with no signal (at 120 HPE)		
Alimentary tract – foregut with extracellular signal (at 24 HPE)		

Alimentary tract (foregut, midgut, Malpighian tubules) with extracellular signal (at 24 HPE)	Alimentary tract (foregut, midgut, Malpighian tubules) no signal (at 24 HPE)	Alimentary tract – Malpighian tubules, no signal (72 HPE)

151
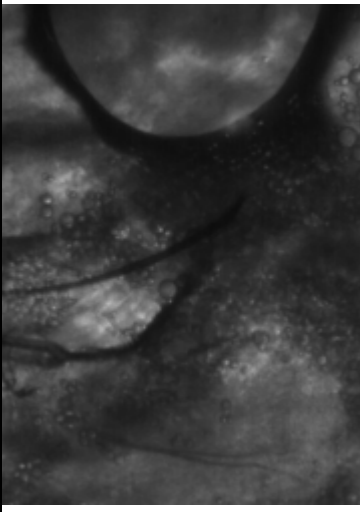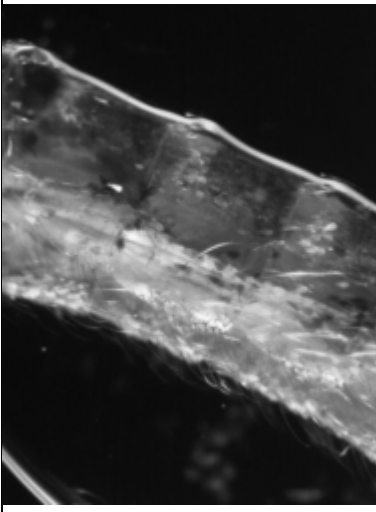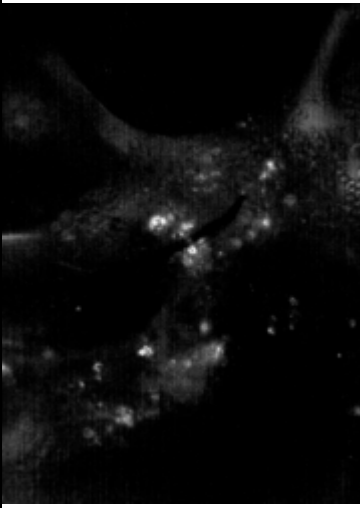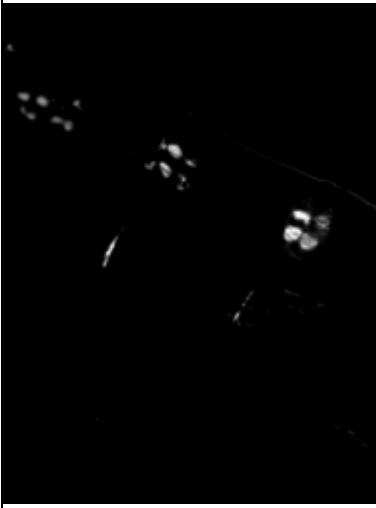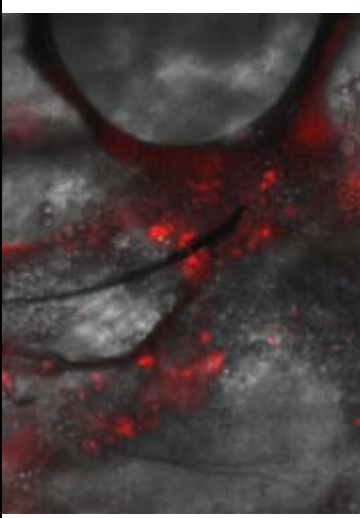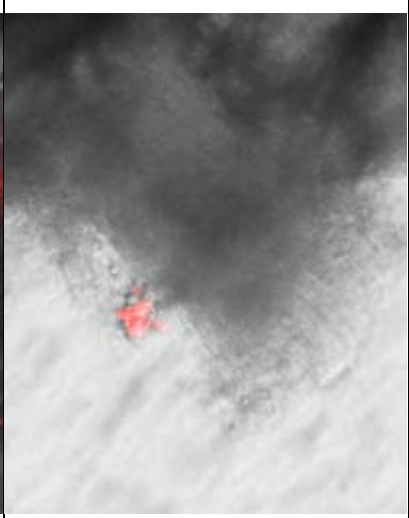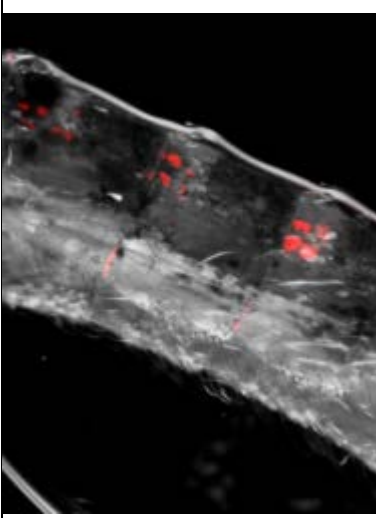
Alimentary tract – rectum, no signal (at 120 HPE)	Ovary – no signal (at 24 HPE)	Ovary and Malpighian tubules – no signal (at 72 HPE)
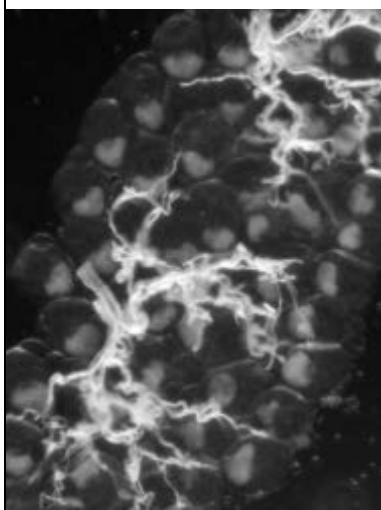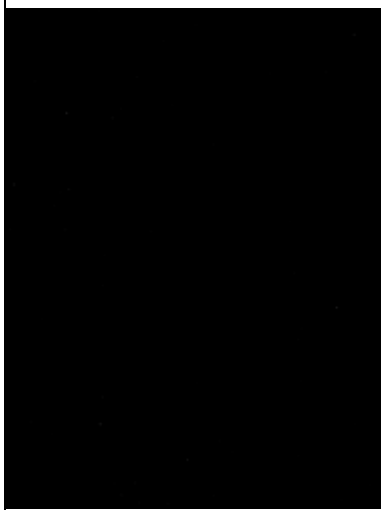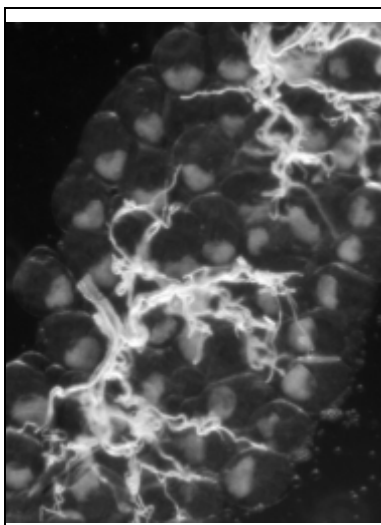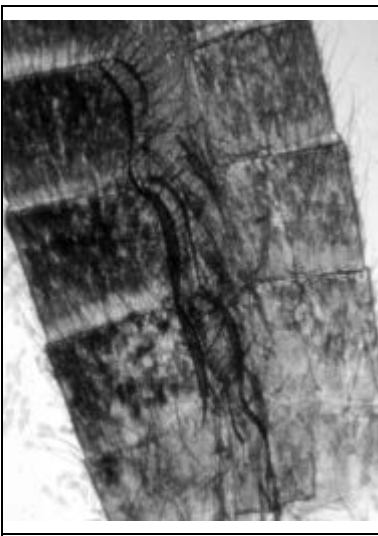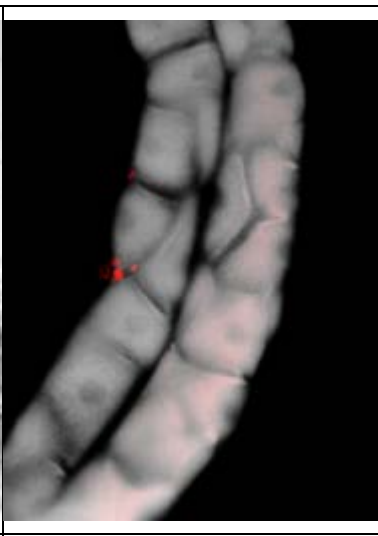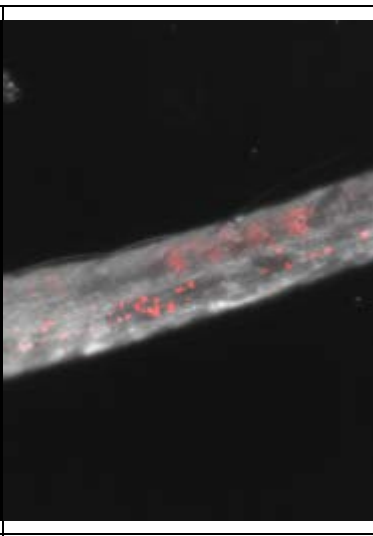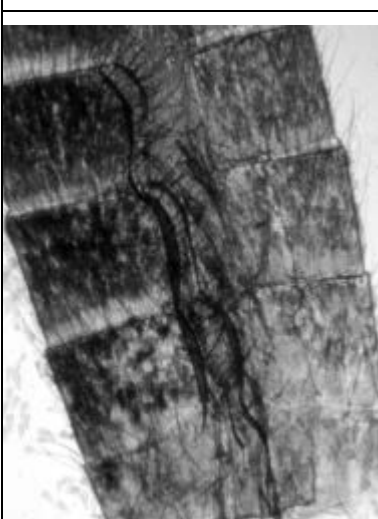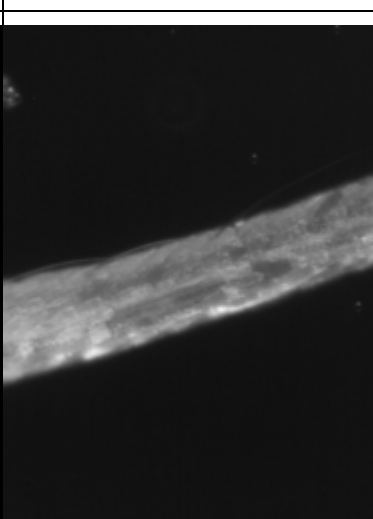
Ovary – no signal (at 120 HPE)
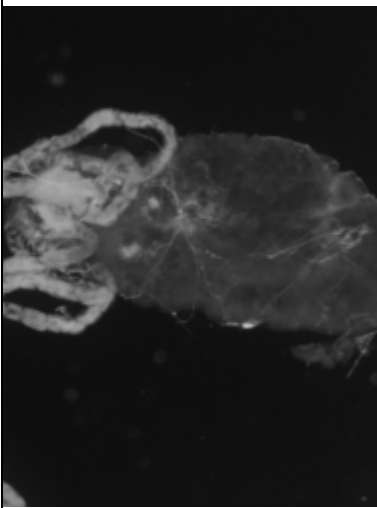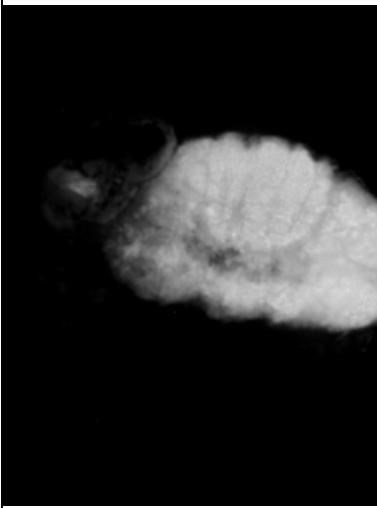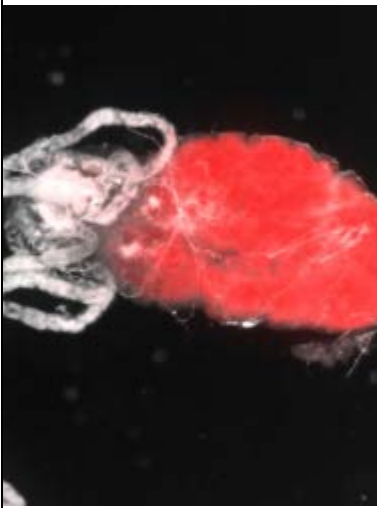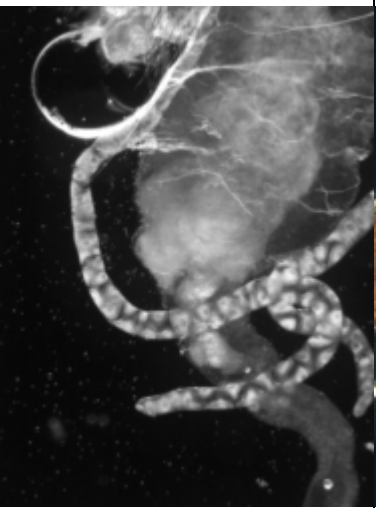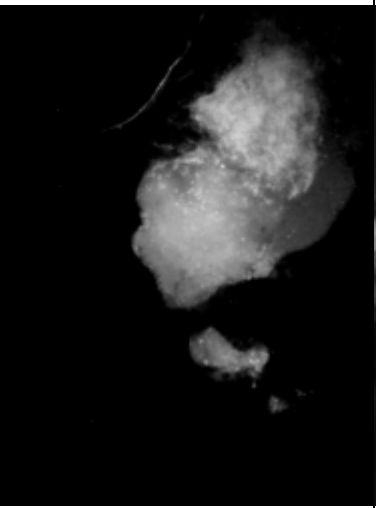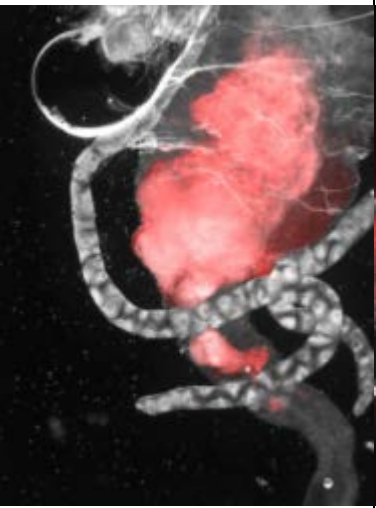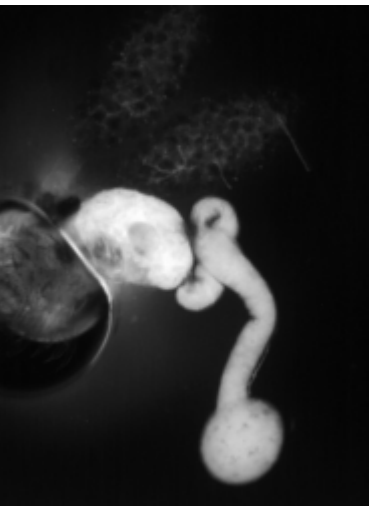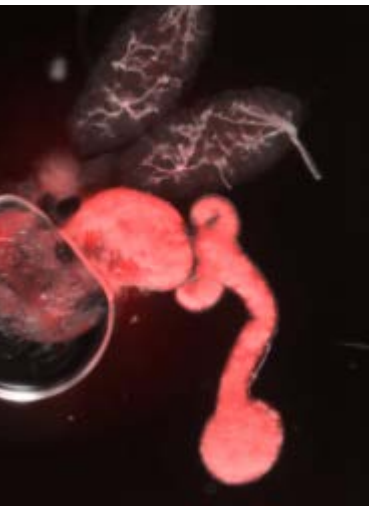
Supplementary Figure 14 – *Per os* **exposure of adult female** *Cx. pipiens* **with fluorescent-iLacZ**

Tissue	Bright Field	RNAi trigger	Merge
Head - signal at injection site (at 24 HPE)			
Head – signal in hemocytes (at 72 HPE)			
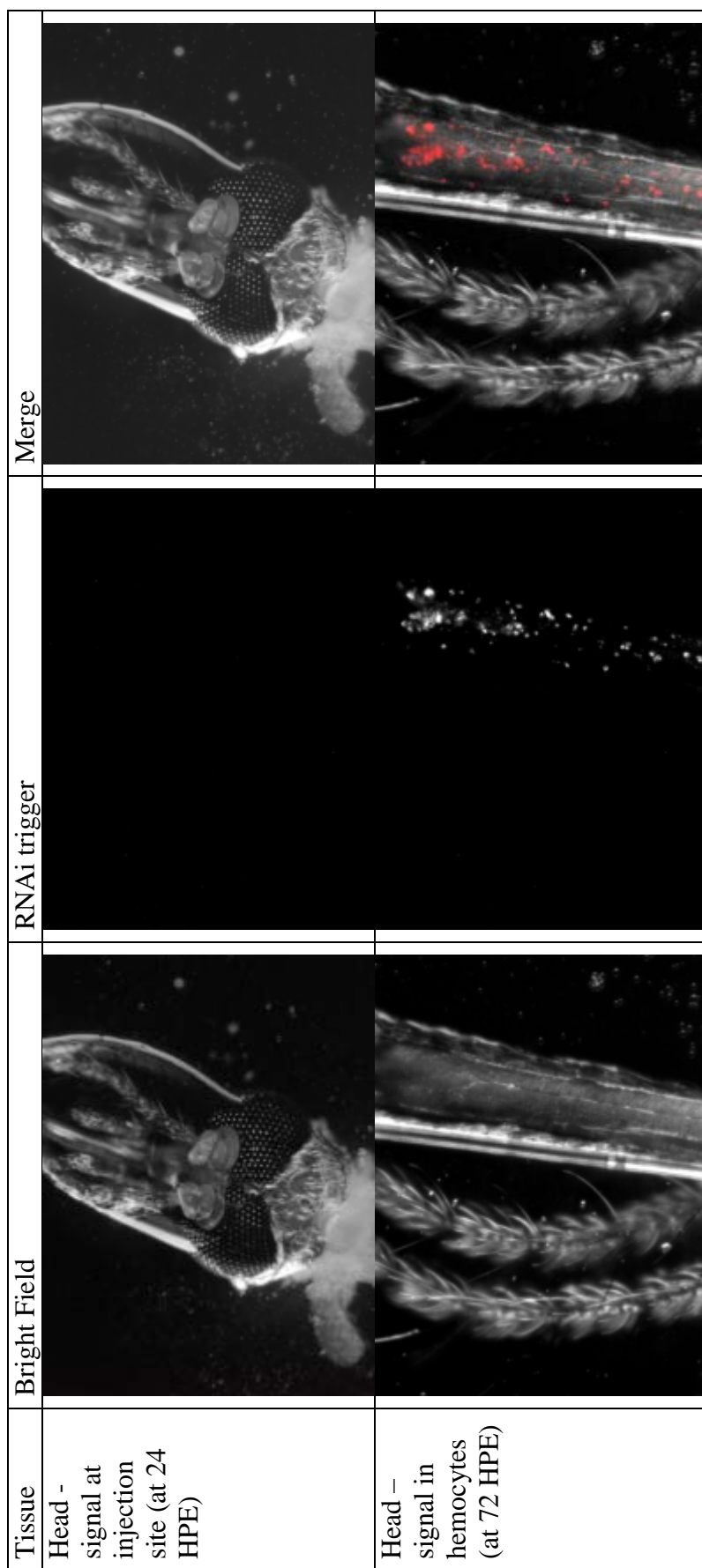
| Thorax – hemocytes (at 72 HPE) | Thorax – hemocytes near muscle tissue (at 72 HPE) | Abdomen - pericardial cells (at 24 HPE) |

Abdomen – no signal (at 120 HPE)	Malpighian tubules - hemocytes bound to tracheoles (at 24 HPE)	Leg - hemocytes (at 72 HPE)

156

| Diverticula with strong signal (at 24 HPE) | Foregut – punctate staining in tissue (at 72 HPE) | Foregut lumen (at 72 HPE) |

Alimentary tract with strong signal in midgut (at 24 HPE)	Alimentary tract with strong signal in midgut and foregut (at 72 HPE)	Hindgut lumen and ovaries (at 24 HPE) * a color version of this image was included to demonstrate visible Cy3

| Ovary – hemocytes (at 72 HPE) | Ovary – no signal (at 72 HPE) |
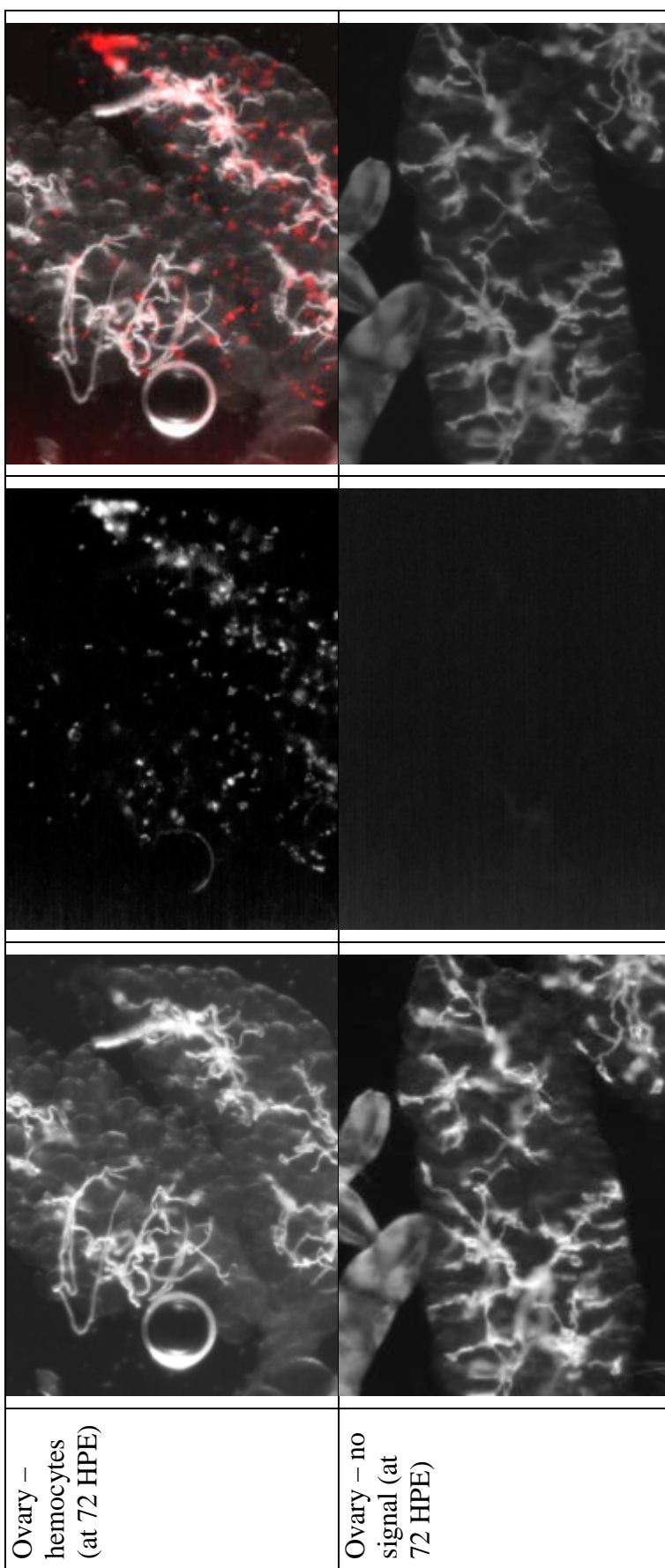
Supplementary Figure 15 – Soaking exposure of 1st instar larval *Ae. aegypti* with fluorescent-iLacZ

Tissue	Bright Field	RNAi trigger	Merge
Head, thorax and abdomen with small punctate signal in intestinal tract (at 2 HPE)			
Head and caecum with signal (at 24 HPE)			

Abdomen with signal in intestinal lumen (at 24 HPE) * Dark spot indicates yeast feed which was not auto-fluorescent	Abdomen with signal in intestinal lumen and excreted from rectum (at 24 HPE)	Head, thorax, and abdomen with signal in intestinal lumen and head (at 72 HPE)

Supplementary Figure 16 – Stability of iLacZ in sucrose meal following exposure to *Ae. aegypti* in insectary conditions.

iLacZ does not degrade following exposure to mosquitoes in sucrose solutions. Sucrose solutions containing 1 mg/ml iLacZ were incubated for 12 hours in insectary conditions in a: closed micro-centrifuge tube (closed), open micro-centrifuge tube lid (open), or an open micro-centrifuge tube lid in a carton of 20 starved adult female *Ae. aegypti* (open + *Ae. aegypti*). Integrity of iLacZ was measured by band intensity following gel electrophoresis compared to frozen iLacZ stock. No significant differences were detected between groups as measured by one way ANOVA.
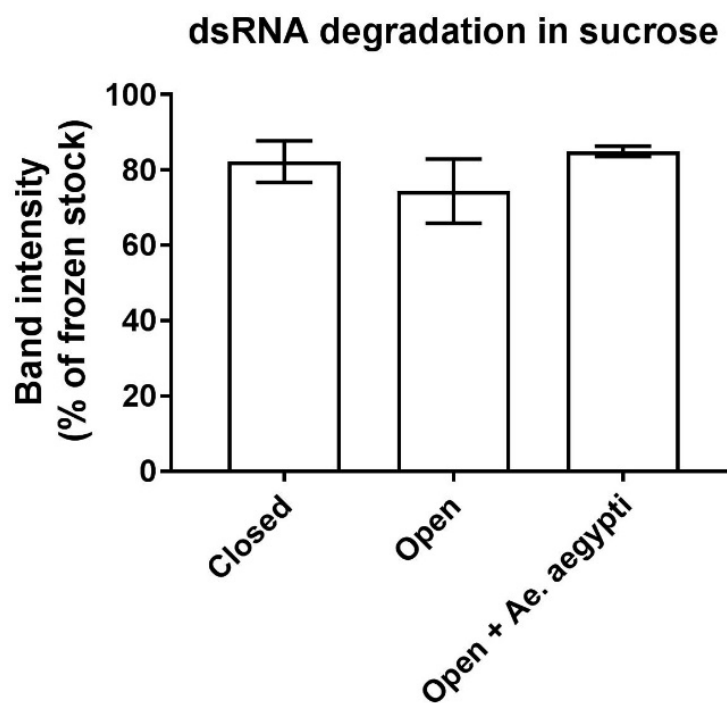
Supplementary Figure 17 – Confocal Z-stack of *Ae. aegypti* ovary 24 hours post peritoneal exposure of fluorescent-iLacZ.

iLacZ uptake assessed by confocal microscopy in non-bloodfed *Ae. aegypti* ovaries. Cross section stack (Z-stack) of *Ae. aegypti* ovaries 24 hours post injection with labelled iLacZ showing DAPI stained nuclei (blue) and Cy5 labelled iLacZ (magenta).
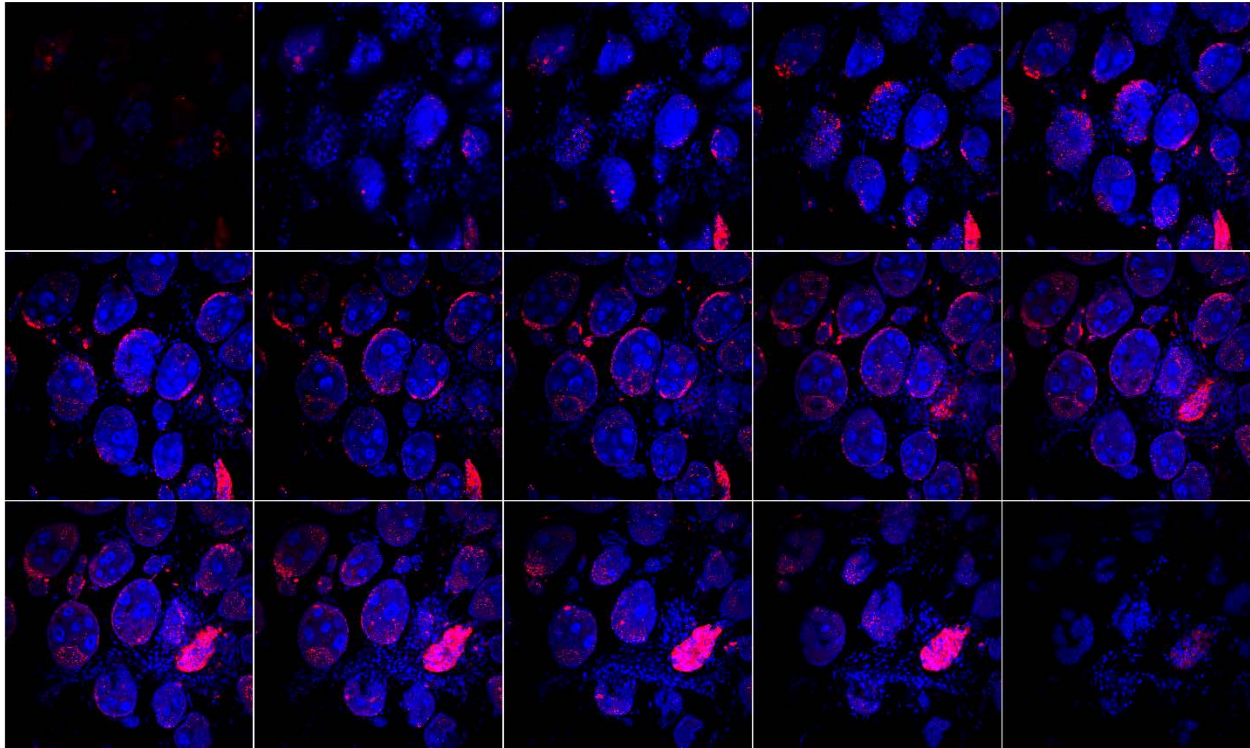
Chapter 4 – RNAi trigger design and knockdown success in mosquito vector species

Abstract

RNAi is a widely used reverse genetics approach, but often yields inconsistent results. In this study, we interrogate the relationship between RNAi trigger design, gene knockdown, and resulting phenotype using the *Inhibitor of Apoptosis 1* (*IAP1*) gene in mosquito vectors and cells. Knockdown of *IAP1* using long double-stranded RNAi triggers (iIAP) activates apoptosis resulting in cell death and subsequent mortality. in *Aedes aegypti, Aedes albopictus, Anopheles gambiae,* but not *Culex pipiens*. To ass that spanned various lengths of the gene produced dramatically different phenotypes both *in vitro* and *in vivo*. Increasing the length of RNAi triggers did not increase potency, but position of triggers correlated to knockdown and cell death. Differences in potency of iIAPs may be linked to sequence composition of the RNAi trigger as well as secondary structure of the target transcript. Furthermore, responsiveness to iIAPs varied by tissue, with ovaries receptive to sub-lethal doses of iIAPs. Overall these findings highlight that biological barriers, species differences, RNAi designs, and tissue differences must be accounted for in order to maximize knockdown of target genes across mosquito species.

Introduction

RNAi emerged as the standard tool for inducible knockdown of target genes in across mosquito systems with hundreds of manuscripts published targeting >600 genes across >66 strains & cell types over the last 20 years [1]. Despite widespread use of RNAi, the ability to induce knockdown of target genes varies significantly from study to study [1]. Inconsistencies in knockdown and phenotypic outcomes have spurred frustration for researchers working on gene function for both basic and applied research ends, in a variety of insect taxa [2-6]. For instance, based on a meta-analysis of RNAi variation in Lepidoptera Terenius et al. concluded that that "questions remain [about] the cause for the high variability at the molecular and cellular level and if techniques can be adapted to increase the efficiency of RNAi" [2]. In some insects, RNases expressed in the hemolymph and midgut limit uptake *in vivo* of archetypical RNAi triggers (short-interfering RNAs and double-stranded RNAs); while in other species RNAi is highly robust [2, 7-9]. Despite a good deal of conjecture regarding the success and failure of RNAi, there has yet to be a comprehensive assessment of RNAi efficacy in relation to experimental design and RNAi trigger design.

One major prerequisite for successful RNAi knockdown is to limit off-target effects that occur frequently in *Drosophila* [10]. To streamline the process of designing double-stranded RNAs (dsRNA) and short-interfering RNA (siRNA) RNAi triggers, tools have been developed to predict RNAi triggers with the highest chance of success [11, 12]. However, there is limited data validating the accuracy of such tools for non-model systems. Furthermore, the same experiment is rarely performed with the same conditions in multiple species. Given the wealth of evidence supporting a robust RNAi response in many mosquito systems, one could assume that RNAi is highly-translatable between systems, but there is limited evidence that RNAi success in one mosquito species will translate to another, or if experiments performed *in vitro* have similar

outcomes *in vivo*. However, variation in RNAi outcomes may also be due to species or system differences which have not been explored in depth.

In addition to the study of RNAi design as a function of increased experimental success, reliable RNAi design is critical to development of RNAi-based insecticides [5]. RNAi offers an alternative, tailorable, non-toxic, and species-specific approach to control of disease vectors, agricultural, and nuisance pest insect species [4, 5, 13]. For instance, in the corn rootworm *Diabrotica virgifera virgifera*, RNAi triggers applied to leaves results in uptake and subsequent death of exposed individuals, protecting the plant [14]. In mosquitoes, RNAi triggers can induce a variety of beneficial phenotypes, such as death, reduced vector competence, and aberrant host-seeking capacity [5].

In this study, we aim to elucidate the extent to which RNAi design alters experimental outcomes within and across mosquito species. We utilize the highly conserved *Inhibitor of Apoptosis 1* (IAP) gene as a model to study the relationship between RNAi design, gene knockdown, and resulting phenotype. Suppression of IAP1 results in activation of apoptosis in mosquito cells resulting in rapid mortality [15]. As such, IAP knockdown can be used as a sensor to determine potency of RNAi triggers and to identify uptake and processing of RNAi triggers at the species and the cell level. Additionally, selection of highly potent IAP RNAi triggers can be utilized to determine the efficacy of RNAi-based insecticides for mosquito control.

Materials and Methods

Mosquito rearing and maintenance

Aedes aegypti (Liverpool), *Aedes albopictus* (Missouri), *Anopheles gambiae* (G3), and *Culex pipiens* (Iowa) larvae were reared in enamel pans and fed daily with a slurry of ground TetraMin™

(Blacksburg, VA). Unless otherwise stated, groups of 50 female pupae were collected ~24 hours prior to emergence and maintained in cartons on a 10% sucrose diet. All life stages were maintained at 27 ^{o}C at 70-80% relative humidity with a 16:8 hour (light:dark) photoperiod.

RNA purification, RNAi trigger synthesis & labelling

Mosquitoes were knocked down at 4 ^{o}C, transferred to TRIzol™ (Invitrogen), homogenized using 1.5 ml pestles and purified according to manufacturer's instructions. RNA was converted to cDNA (ImProm-II™ cDNA synthesis, Promega) then used as template for T7-tagged PCR primers (Supplemental table 1). PCR amplicons were then used to synthesize dsRNA using the MEGAscript™ T7 RNAi (Ambion) followed by phenol:choloroform cleanup. For siRNA generation, ShortCut® RNase III (NEB) was added to dsRNA, and siRNAs were subjected to ethanol precipitation. The Cy3 or Cy5 Label IT® kit (Mirus) was used all fluorescently labelled RNAi triggers. At all stages of preparation, RNA and DNA were re-suspended in nuclease free water and quantified by NanoDrop (Thermo Fisher) and gel electrophoresis.

Quantifying gene knockdown

RNAi-exposed mosquitoes or cell lines were subject to RNA purification (see above). Relative transcript abundance was assessed through RT-qPCR (SYBR® Green Quantitative RT-qPCR Kit, Sigma) or droplet digital PCR (QX200 system with EvaGreen PCR mix, Bio-rad) analysis based on comparison to a reference genes (Supplemental Table 1).

In vivo RNAi trigger exposures

Adult females (3 day post-eclosion maintained on sucrose, or 3-6 day post-eclosion & 24 hours post-feeding on defibrinated sheep blood) were cold-immobilized and held on a petri dish on ice. Individuals were then held by the dorsal side of the thorax and abdomen in a bent needle vacuum saddle. Injections of up to 0.5 µl (800-1600 ng RNAi trigger) were administered directly to the hemolymph via intrathoracic injection through the cervical membrane. For *per os* exposure, groups of 50 mosquitoes were starved for 1 day post-eclosion then exposed to 50 µl (50 µg RNAi trigger) in 10% sucrose in a capillary tube held in place over the carton for 24-72 hours with solutions replenished twice daily. For survival assays, mosquitoes were continually provided with sucrose for duration of the experiment with the solution replenished every 24 hours. For topical exposure, adult females (3 days post-eclosion) were knocked and held on a petri dish on ice. Acetone:RNAi trigger (3 mg/ml) mixtures (3:1) were placed on to the dorsal thorax and abdomen (0.5 µl) and allowed to dry prior to transfer to cartons. Post-treatment, mosquitoes were kept in cartons provided with 10% sucrose and monitored daily for survival until processing.

Cell culture and In vitro RNAi assays

The *Ae. aegypti* Aag2 cell line and *An. gambiae* 4a3b, 4a3a, and Sua 5.0 cell lines were maintained at 28 °C in Schneider's Insect Medium (Sigma) with 10% FBS. *Ae. albopictus* C6/36 cells were maintained in Leibovitz L-15 media (Corning) with 10% FBS. For cell viability and knockdown assays, 96-well plates (~50,000 cells/well for Aag2 and C6/36, 80,000 cells/well for other cell lines) were seeded in 100-200 µl of media for 1-2 hours then exposed to RNAi triggers (if applicable) for 1-2 hours before addition of FBS. For viability, the Non-Radioactive Cell Proliferation Assay (Promega) was followed per the manufacturer's instructions. For knockdown assays, cells were washed three times in sterile PBS at 48 hours post-exposure unless otherwise stated.

Imaging

For *ex vivo* imaging, tissues were washed once in PBS then immediately captured using a Zeiss Axio Scope.A1 with QIClick™ CCD Camera (Q-imaging) and Nikon Elements D software. Image processing and representative panels were prepared using ImageJ (https://imagej.nih.gov/ij/). Fixed tissues were preserved in 4% paraformaldehyde (in PBS) for 20 minutes, washed 3x in PBS, permeablized (0.3% Triton X-100, 1% BSA, 1% Sodium citrate in PBS) for 30 minutes and washed 3x in PBS. Based on the assay, tissues were subjected to staining with Alexa Fluor 488/594 Phalloidin (Life Technologies), propidium iodide in micro-centrifuge tubes containing tissues and ~1ml PBS. Fixed tissues were mounted on slides in ProLong™ Gold Antifade with DAPI (Invitrogen).

Statistical analyses

Graphical representation and statistical analyses of data were performed in Graphpad Prism or R 3.4.3.

Results

Screen for lethal RNAi triggers in An gambiae reveals IAP1 as primary target

As part of a search to develop novel mosquitocidal compounds, a screen for lethal RNAi triggers was performed targeting essential genes in *An. gambiae* cells and adult females (Figure 1, Figure S1). RNAi triggers were designed to target the 5' (RNAi trigger termed "F1R1" in reference to the forward and reverse primers) and/or 3' ("F2R2") region of target genes of interest, and tested for capacity to induce a lethal phenotype *in vitro* in *An. gambiae* 4a3b cells (Figure 1A). RNAi triggers targeting *IAP1* (herein referred to as iIAP) produced the greatest reduction in cell viability (Figure

1A) across a range of doses (Figure 1B). Attempts to induce death *in vitro* and *in vivo* targeting autophagy genes, ABC transporter, vacuolar ATPases, as well as gut specific G12 and tight junction protein genes failed or produced a less dramatic phenotype compared to iIAP (Figure 1, Figure S1). A Caspase 8 RNAi trigger resulted in significant reduction of cell viability within a narrow dose range, but failed to induce mortality *in vivo* and as such was not considered for further study (Figure 1A, Figure S1B). *An. gambiae* IAP triggers were effective across *An. gambiae* cell lines without being toxic to C6/36 *Ae. albopictus* cells (Figure 1C), but required at least 24 hours of incubation to significantly reduce cell viability in *An. gambiae cells* (Figure 1D). Similarly *Ae. aegypti,* or *Cx. pipiens*-specific iIAPs were non-toxic to *An. gambiae* cells (Figure S2). These results show that iIAP are non-toxic and species-specific in mosquito cells.

Next, the effect of iIAPs was tested *in vivo* in *An. gambiae* as well as *Ae. albopictus, Ae. aegypti,* and *Cx. pipiens* via intrathoracic injection in adult females (Figure 2). Survival was reduced after exposure to either F1R1 or F2R2 iIAPs in *Ae. albopictus* and *An. gambiae*. However, in *Ae. aegypti* only F2R2 produced >50% mortality and reduced cell viability in Aag2 cells (Figure 2 B, Figure S3). Neither of the two iIAP designed for the *Cx. pipiens IAP1* produced mortality in *Cx. pipiens.* Considering that the *IAP1* transcript sequence is highly conserved across mosquito species, differences could reflect inter-species differences in RNAi response in outcome or could be due to minor differences in RNAi trigger design.

In a previous study, uptake of RNAi triggers was observed following *per os* exposure in *Ae. aegypti* and *Cx. pipiens* [1]. To determine whether the iIAP exposure outcome for *Cx. pipiens* could differ according to exposure route, *Ae. aegypti, An. gambiae*, and *Cx. pipiens* adult females were exposed to iIAPs *per os*. *Per os* exposure did not result in any significant mortality (Figure

S4). Likewise, topical exposure of iIAPs did not induce any noticeable death in *Ae. aegypti* (Figure S5).

RNAi trigger design alters outcome in Ae. aegypti and An. gambiae

The difference in phenotypic outcome following exposure to homologous iIAP in *Ae. aegypti* but not *An. gambiae* prompted a more thorough analysis of the impact of RNAi trigger design on phenotype. Firstly, Dicer cleavage of F2R2 iIAP was performed to produce short interfering iIAPs (siIAP). Exposure of *Ae. aegypti* or *An. gambiae* to iIAP siRNAs abates death phenotypes (Figure 3, Figure S6). Although no mortality was noted in adult female *Ae. aegypti* exposed to iIAP siRNAs, siIAP uptake was noted in hemocytes and appeared to induce cell death (Figure 3 A & B). To test the impact of siRNA exposure and apparent induction of hemocyte-specific cell death, mosquitoes were exposed to siIAP followed by injection with a non-virulent *Escherichia coli* (Figure 3 C). SiIAP-exposed mosquitoes were significantly more susceptible to infection than control mosquitoes.

To further interrogate the idea that length of the iIAP plays a role in experimental outcome, six additional ~100 base-pair iIAPs spanning the F2R2 iIAP region were tested in for *in vitro* impact in *An. gambiae* 4a3b cells (Figure S6). Of the six designs, only three significantly reduced cell viability and none was as potent as full-length F2R2 iIAP (Figure S6). In this case, reduced trigger length correlates with a reduction in the observed phenotype, but varies depending on location.

Conversely, the impact of longer-length iIAPs were explored in *Ae. aegypti*, for which we generated 17 iIAP triggers spanning the entire *IAP1* transcript, and tested them *in vitro* and *in vivo* (Figure 4A). Trigger length, start position, and stop position did not correlate to knockdown or

phenotype (Figure S7). Exposure to these triggers produced dramatically differed in phenotypic outcomes, but significant reduction in cell viability was observed at each base-pair in at least one iIAP. Indeed, by assessing the average reduction in cell viability per base covered, we observed peaks and troughs of phenotypic outcome along the length of the *IAP1* transcript (Figure 4B). As expected, phenotype of iIAPs was correlated to knockdown of *IAP1*, with higher knockdown correlating to more severe phenotypes (Figure 4 C & 4). However knockdown did not vary drastically between groups, indicating that minor differences in knockdown can have severely different phenotypes. Furthermore, *in vitro* data mirrors *in vivo* data indicating that differences in effect are occurring at the cellular level and manifesting in the whole organism (Figure 4 E & F).

Ovaries are hyper-receptive to iIAPs.

In a previous study, we observed that ovaries in *Ae. aegypti, An. gambiae,* and *Cx. pipiens* accumulate a substantial amount of RNAi trigger after a blood-meal [1]. To identify whether RNAi triggers delivered to the ovaries results in activation of the RNAi pathway, we tested the effect of iIAP F1R1 and F2R2 on oogenesis in *Ae. aegypti*. Injection of iIAPs 24 hours post-bloodmeal (HPBM) resulted in abnormal follicle growth and morphology at 48 HPBM and 72 HPBM (Figure 5 A - D). Additionally, exposure to both low (500 ng) and high (1 µg) doses of iIAP resulted in significant reduction in egg batch size (Figure 5 E - F). Interestingly, although F1R1 and F2R2 triggers differ in overall impact on cell viability *in vitro* and survival *in vivo*, this was not observed in the ovary, wherein exposure to either iIAP resulted in a change in follicle morphology and resulting egg batch size as compared to controls (compare Figure 3, Figure S3 D, and Supplemental table 2).

To determine whether the impact of F1R1 and F2R2 on follicle morphology is a result of activating apoptosis, cell viability was assessed microscopically at 48 and 72 HPBM (Figure 6). Similar to previous findings, the vast majority of developing follicles contained RNAi triggers, but not all follicles appeared abnormal (Figure 6). To determine whether abnormal follicles contained iIAP triggers we imaged follicles following exposure of *Ae. aegypti* to fluorescently labelled triggers. In agreement with previous findings, RNAi triggers were internalized to developing follicle oocytes. RNAi triggers are also known to enter the follicular epithelia [1]. Co-staining nuclei of follicular epithelia revealed small fragmented nuclei of the in follicles containing F1R1 and F2R2 iIAPs, but not in control groups (Figure 6). Loss of follicular epithelia cells also coincided with uptake of propidium iodide and alteration of follicle morphology (Figure 6).

Discussion

Despite continuing frustration with unpredictable success in gene suppression using RNAi in a variety of insect species, there has yet to be a comprehensive assessment of RNAi efficacy in relation to experimental design and RNAi trigger design in mosquitoes and other insects. In a previous study, we showed that species and tissues differ in uptake and degradation of RNAi triggers following exposure [1]. In this study, we specifically addressed issues of RNAi trigger design using the *IAP1* gene from 3 mosquito species. Suppression of IAP1 results in activation of apoptosis in mosquito cells and, thereby, rapid mortality [15]. As such, *IAP1* knockdown was used as a model to study the relationship between RNAi design, gene knockdown, and phenotype. RNAi triggers targeting *IAP1* (iIAPs) were used to determine potency of RNAi triggers and to identify cells which successfully process dsRNA through fluorescent labelling of apoptotic cells. We found that topical and *per os* exposure routes, and use of siRNAs, produced limited knockdown success

across mosquito species,.Intrathoracic exposure to long RNAi triggers induced species-specific, dose-dependent mortality in *Aedes aegypti, Aedes albopictus, Anopheles gambiae,* but not *Culex pipiens*. In *Ae. aegypti*, IAP RNAi trigger placement on the *IAP1* transcript radically altered phenotypic outcome, and was correlated to change in knockdown. Differences in RNAi trigger potency were assessed as a function of trigger design, and revealed that RNAi success is not dependent on nucleotide composition (G:C content), or potential-off target effects. Furthermore, neither length nor position on the target mRNA determined knockdown success; therefore, a combination of dsRNA sequence and target mRNA secondary structure may contribute to knockdown success. Secondary structure of mRNA is known to alter knockdown success using siRNAs and may inhibit knockdown in tissues recalcitrant to RNAi trigger uptake [16]. The results highlight that success in one species does not guarantee success even in closely related gene or species.

Uptake and spread of RNAi triggers in Dipteran species is dictated by length, and dependent on endocytosis [17]. In *Drosophila*, the length of the RNAi trigger is critical for uptake in endocytic cells [17]; but in mosquitoes, high levels of knockdown have been reported, so cellular uptake occurs regardless of RNAi trigger length [1]. In this study, we find siRNA iIAP sequences do not globally induce mortality in the mosquito, nor reduce cell viability *in vitro*, but could induce apoptosis in hemocytes. Longer, ~100 base-pair iIAPs reduced cell viability, but were less effective than a long ~650 base-pair sequence targeting the same region. Overall, increasing RNAi trigger length beyond ~300 base-pairs did not increase knockdown or resulting phenotype *in vitro* and *in vivo* for *Ae. aegypti*.

It should be noted that iIAP sequences were not predicted to induce off-target effects (data not shown here) despite coverage of conserved regions. In *An. gambiae* and *Ae. aegypti* the most drastic phenotypes were noted with triggers covering the zinc finger domain, and as such off target knockdown of a variety of other essential genes containing this domain may be occurring.

In addition to RNAi trigger designs, tissues also influence response to RNAi triggers in bees, beetles, and mosquitoes [3, 18, 19]. In *An. gambiae*, the salivary glands are less permissive to RNAi uptake and knockdown compared to the midgut and ovary [19]. In this study, we report that iIAPs incapable of reducing cell viability and increasing mortality can induce apoptosis in developing ovaries. During oogenesis, ovaries are a sink for RNAi triggers and may concentrate the RNAi trigger dose, but may also be more responsive to RNAi [1]. Follicular epithelia channel RNAi triggers to the oocyte following a bloodmeal [1], but are also responsive to RNAi triggers. Follicular epithelia death was noted following exposure of 500 ng of F1R1 region iIAP in *Ae. aegypti* resulting in abnormal follicle morphology. This dose was insufficient to induce death at the organismal level or reduce cell viability *in vitro*. Removal of the follicular epithelia results in abnormal follicle morphology in gall midge *Heteropeza pygmaea* [20]. As such, these cells may be responsible for change in phenotype and not the oocyte itself.

The sensitivity of developing ovaries to iIAPs also raises questions surrounding the nature of knockdown studies performed in this tissue. When comparing knockdown across different tissues, ovaries are less responsive than some tissues (midgut, Malpighian tubules, whole body tissue) [21, 22], but more responsive than the salivary glands [19]. It may be that RNAi trigger accumulation within the oocyte, which occurs with RNAi triggers before and after a blood meal, or growth of the oocyte during oogenesis, skews knockdown data for this tissue.

We show that although design factors play a key role in outcome for some tissues, all RNAi triggers are likely capable of inducing gene knockdown if delivery occurs to a sufficiently RNAi-responsive cell type. Furthermore, in *Ae.aegypti, An. gambiae,* and *Cx. pipiens*, RNAi triggers are internalized primary by cells capable of pinocytosis, including hemocytes, pericardial cells, ganglia of the ventral nerve cord, as well as oocytes and follicular epithelia in primary follicles [1]. This is congruent with findings in *Drosophila* wherein non-receptor mediated endocytosis of long RNAi triggers was observed [17]. However this method of uptake does not explain why siRNAs only induce apoptosis in phagocytic cells, since pinocytosis should internalize RNAi triggers at the same rate regardless of length. It is likely that siRNAs cannot induce systemic RNAi in mosquito hemocytes, since the sequence is too short to be reverse transcribed and re-expressed via retrotransposons, as is seen for viral RNA [23-25].

Taken together these data show that the impact of different RNAi triggers is conserved between systems of the same species, but sensitivity to different RNAi triggers depends on the cell type and physiological condition.

Literature cited

1. Airs, P.M., *Manipulating cell death and RNA interference processes for mosquito control*, in *Pathobiological Sciences*. 2018, University of Wisconsin Madison.

2. Terenius, O., et al., *RNA interference in Lepidoptera: an overview of successful and unsuccessful studies and implications for experimental design.* J Insect Physiol, 2011. **57**(2): p. 231-45.

3. Cappelle, K., et al., *The involvement of clathrin-mediated endocytosis and two Sid-1-like transmembrane proteins in double-stranded RNA uptake in the Colorado potato beetle midgut.* Insect Molecular Biology, 2016. **25**(3): p. 315-323.

4. Scott, J.G., et al., *Towards the elements of successful insect RNAi.* J Insect Physiol, 2013. **59**(12): p. 1212-21.

5. Airs, P.M. and L.C. Bartholomay, *RNA Interference for Mosquito and Mosquito-Borne Disease Control.* Insects, 2017. **8**(1).

6. Yu, N., et al., *Delivery of dsRNA for RNAi in insects: an overview and future directions.* Insect Science, 2013. **20**(1): p. 4-14.

7. Garbutt, J.S., et al., *Persistence of double-stranded RNA in insect hemolymph as a potential determiner of RNA interference success: Evidence from Manduca sexta and Blattella germanica.* Journal of Insect Physiology, 2013. **59**(2): p. 171-178.

8. Christiaens, O., L. Swevers, and G. Smagghe, *DsRNA degradation in the pea aphid (Acyrthosiphon pisum) associated with lack of response in RNAi feeding and injection assay.* Peptides, 2014. **53**(Supplement C): p. 307-314.

9. Wynant, N., et al., *Identification, functional characterization and phylogenetic analysis of double stranded RNA degrading enzymes present in the gut of the desert locust, Schistocerca gregaria.* Insect Biochem Mol Biol, 2014. **46**: p. 1-8.

10. Seinen, E., et al., *RNAi-induced off-target effects in Drosophila melanogaster: frequencies and solutions.* Brief Funct Genomics, 2011. **10**(4): p. 206-14.

11. Naito, Y., et al., *dsCheck: highly sensitive off-target search software for double-stranded RNA-mediated RNA interference.* Nucleic Acids Research, 2005. **33**(suppl_2): p. W589-W591.

12.   Horn, T. and M. Boutros, *E-RNAi: a web application for the multi-species design of RNAi reagents--2010 update.* Nucleic Acids Res, 2010. **38**(Web Server issue): p. W332-9.

13.   Kolliopoulou, A., et al., *Viral Delivery of dsRNA for Control of Insect Agricultural Pests and Vectors of Human Disease: Prospects and Challenges.* Frontiers in Physiology, 2017. **8**(399).

14.   Baum, J.A., et al., *Control of coleopteran insect pests through RNA interference.* Nature Biotechnology, 2007. **25**: p. 1322.

15.   Liu, Q. and R.J. Clem, *Defining the core apoptosis pathway in the mosquito disease vector Aedes aegypti: the roles of iap1, ark, dronc, and effector caspases.* Apoptosis : an international journal on programmed cell death, 2011. **16**: p. 105-113.

16.   Shao, Y., et al., *Effect of target secondary structure on RNAi efficiency.* RNA, 2007. **13**(10): p. 1631-1640.

17.   Saleh, M.C., et al., *The endocytic pathway mediates cell entry of dsRNA to induce RNAi silencing.* Nat Cell Biol, 2006. **8**(8): p. 793-802.

18.   Jarosch, A. and R.F.A. Moritz, *Systemic RNA-interference in the honeybee Apis mellifera: Tissue dependent uptake of fluorescent siRNA after intra-abdominal application observed by laser-scanning microscopy.* Journal of Insect Physiology, 2011. **57**(7): p. 851-857.

19.   Boisson, B., et al., *Gene silencing in mosquito salivary glands by RNAi.* FEBS Lett, 2006. **580**(8): p. 1988-92.

20.   F., W.D., *Oocyte maturation without follicular epithelium alters egg shape in a dipteran insect.* Journal of Experimental Zoology, 1978. **205**(1): p. 149-155.

21.   Telang, A., et al., *Analysis of ovary-specific genes in relation to egg maturation and female nutritional condition in the mosquitoes Georgecraigius atropalpus and Aedes aegypti (Diptera: Culicidae).* J Insect Physiol, 2013. **59**(3): p. 283-94.

22.   Liu, K., et al., *Aquaporin water channel AgAQP1 in the malaria vector mosquito Anopheles gambiae during blood feeding and humidity adaptation.* Proc Natl Acad Sci U S A, 2011. **108**(15): p. 6062-6.

23.   Poirier, E.Z., et al., *Dicer-2-Dependent Generation of Viral DNA from Defective Genomes of RNA Viruses Modulates Antiviral Immunity in Insects.* Cell Host Microbe, 2018. **23**(3): p. 353-365.e8.

24.   Tassetto, M., M. Kunitomi, and R. Andino, *Circulating Immune Cells Mediate a Systemic RNAi-Based Adaptive Antiviral Response in Drosophila.* Cell, 2017. **169**(2): p. 314-325.e13.

25.   Goic, B., et al., *Virus-derived DNA drives mosquito vector tolerance to arboviral infection.* Nat Commun, 2016. **7**: p. 12410.

Tables & Figures

Supplementary Table 1 – Primers used in study.

Species & Gene	Accession	RNAi trigger	Forward primer	Reverse primer
Ae. aegypti IAP1	AAEL009074-RC	IAP 1	CTTCTTTCACACCGCTCTTA	CTCCCACAGACCGATTTC
	AAEL009074-RC	IAP 2	ATGGCTGGAGTTATGATGGC	AAAGCTGGCATCTATTGGAA
	AAEL009074-RC	IAP 3	CGGTACGGTTTCTACTACGT	TGATAGTTGCTGAACGACTG
	AAEL009074-RC	IAP 4	GTATTAGGATACGAGAAAAC	CTCACAGTTACTATACCACA
	AAEL009074-RC	IAP 5	AGCGAAACGCCTTGAAAGCT	ATGACTGAAGCGAGGATGTTG
	AAEL009074-RC	IAP 6	CTGAAACTAATGAAGGGCGA	ACACTTGGTGACAGATGAAG
	AAEL009074-RC	IAP 7	TGCCGAAGAAGACAATACTG	CGGTCCACCAATAAAACACT
	AAEL009074-RC	IAP 8	TGAGAGTCCTAACCGTTACA	TCATTATAGTGTAGGGAGCA
	AAEL009074-RC	IAP 9 (or F1R1)	GAGTGGAAATCGGTCTGTG	TTCCTTGGGTTTCTGTTTCA
	AAEL009074-RC	IAP 10 (or F2R2)	GAAACTAATGAAGGGCGAAG	ACACTTGGTGACAGATGAAG
	AAEL009074-RC	IAP 11	GAAACTAATGAAGGGCGAAG	TCATTATAGTGTAGGGAGCA
	AAEL009074-RC	IAP 12	TGCCGAAGAAGACAATACTG	TCATTATAGTGTAGGGAGCA
	AAEL009074-RC	IAP 13	GAGTGGAAATCGGTCTGTG	TGATAGTTGCTGAACGACTG
	AAEL009074-RC	IAP 14	AGCGAAACGCCTTGAAAGCT	ACACTTGGTGACAGATGAAG
	AAEL009074-RC	IAP 15	GAGTGGAAATCGGTCTGTG	ACACTTGGTGACAGATGAAG
	AAEL009074-RC	IAP 16	CGGTACGGTTTCTACTACGT	TTCCTTGGGTTTCTGTTTCA
	AAEL009074-RC	IAP 17	CTTCTTTCACACCGCTCTTA	CTCACAGTTACTATACCACA
Ae. albopictus IAP1	AALF001357-RA	IAP F1R1	GAGTAGAGATCGGCCTGT	TTCCTTAGGTTTCTGTTTCA
	AALF001357-RA	IAP F2R2	CAAGGACTGGGAAGCTGAAG	GCACAGCGGACACTTTGTTA
	AALF001357-RA	IAP F2R2m	GAAACTAATGAAGGGCGAAG	ACACTTGTTACAGACGAAG
An. gambiae ABC transporter	AGAP001523-RA	ABC F1R1	GGCGAATGGAATGAATGAGT	GGGATAGTCGGTCGTTGCTA
An. gambiae ATG1	AGAP000098-RA	ATG1 F1R1	GAGTGAGGCCAAAATTACCG	CAAAGTCGCCCACCTTCA

	AGAP000098-RA	ATG1 F2R2	GTTGAAACGACCGGACGAG	GGTACAGCCGTAGTGGTTCG
	AGAP000098-RA	ATG1 F3R3	GGGAAACATAAATTCTTCGAG	GCTCTCCATCTCCTGCAT
An. gambiae ATG5	AGAP010939-RA	ATG5 F1R1	GCTACTTTCCTCTCGTTACTG	ATCAATCGCCTGTTTACC
	AGAP010939-RA	ATG5 F2R2	GCAGAAGAAAGACCACAATC	CGATAGACAGAGATGCAGAA
An. gambiae ATG9	AGAP001762-RA	ATG9 F1R1	GTACGACACGCTGACCAA	GAAACGTCCAGAACAAACC
	AGAP001762-RA	ATG9 F2R2	GTATTATCGGTGGTGGTGAA	TCTCTTCGTTGTGGTTCG
An. gambiae Caspase 8	AGAP009832-RA	C8 F1R1	AGCCTTCAGCGCAATGTT	TCCAATGACGGACTTGATTTC
	AGAP009832-RA	C8 F2R2	CCATGGATCACAGCGACA	ACATTGAACAGCAGCAAACG
An. gambiae G12	AGAP006187-RA	G12 F1R1	CATTCCCAAGCCTACTACAG	CACCACATTCAGCGATTC
	AGAP006187-RA	G12 R2R2	GAATCGCTGAATGTGGTG	ATTTAGTTCCAGCCGAAGA
An. gambiae IAP1	AGAP007294-RA	IAP 0-100	GGACCGGCTGAAGTCGTA	CTCATGCCCGTGTAGAAGAA
	AGAP007294-RA	IAP 100-200	GCGTCAAGTGCTTCAGCT	GTAGTGGCAGTTGCTGTACC
	AGAP007294-RA	IAP 200-300	GTACAGCAACTGCCACTACC	GAAGACATCGCGGAAGAT
	AGAP007294-RA	IAP 300-400	GATGTCTTCCGCCTCGTC	CTGAATCCGCTCGAGGAG
	AGAP007294-RA	IAP 400-500	CTCCTCGAGCGGATTCAG	GACGAAGCAGATCTTGCAGA
	AGAP007294-RA	IAP 500-600	CGTCAACGAGTACAACACC	GAACGGTTGCTGACAGAG
	AGAP007294-RA	IAP F1R1	GCCCATGCACTATCGCTACC	ATTGTGCCGCACGCTGAT
	AGAP007294-RA	IAP F2R2	CTGAAGTCGTACGAGGACTGG	TACAGCCGTAGCACGTTGAT
An. gambiae TJP	AGAP003546-RA	TJP F2R2	TGATGATGACGATGATTACC	CCTACGCCTTATCTTTTGTT
An. gambiae vATPase C	AGAP005845-RA	vATPase C	AACAACAATGACCTGACCTC	TAGTCCTGGTCCTGTGTGAT
	AGAP009486-RA	vATPase H F1R1	CACCGCCAGATATGATTGC	TGCAGGTAGAAGTGCAGATCG
An. gambiae vATPase H	AGAP009486-RA	vATPase H F2R2	ACGACATTGGGGAGTACGTG	GTCTTGCGGGGAGGACTT
	AGAP009486-RA	vATPase H F3R3	GCCAACAAGAAGAAGGAGAG	ACCGACCGACTGGATGTA
Cx. pipiens IAP1	CPIJ002102-RA	IAP F1R1	GAAGGATGAAAACACATCGT	AGTGCTGCCTAATCTGGATA
	CPIJ002102-RA	IAP F2R2	TATCCAGATTAGGCAGCACT	GTACTCTTCGCCCTTCATAA
Plasmid LacZ		LacZ	CGTAATCATGGTCATAGCTGTTTCC	CTTTTGCTGGCCTTTTGCTC

Supplementary Table 2 – *Ae. aegypti* **oviposition output following challenge with 500 ng or 1 µg of IAP F1R1, IAP F2R2, or LacZ RNAi triggers.** Tukey Honest Significant Differences (HSD) tests comparison P values shown below for:

(1) Like for like comparison of 500 ng treatments,

	LacZ_0.5	F1R1_0.5	F2R2_0.5
LacZ_0.5			
F1R1_0.5	0.0035		
F2R2_0.5	0.0019	0.9948	
Untreated	0.9174	0.0097	0.0052

(2) Like for like comparison of 1 µg treatments.

	LacZ_1	F1R1_1	F2R2_1
LacZ_1			
F1R1_1	0.0069		
F2R2_1	0.00007	0.1728	
Untreated	0.6588	0.00025	0.000003

(3) Trans group comparison of 500 ng and 1 µg treatments.

	LacZ_1	F1R1_1	F2R2_1
LacZ_0.5	0.4442	0.00015	0.000001
F1R1_0.5	0.4085	0.92	0.089
F2R2_0.5	0.2743	0.978	0.1485

Figure 1 – Screen for lethal RNAi triggers in *An. gambiae* reveals IAP1 as gene of interest.

(A) *An. gambiae* 4a3b cell viability 72 HPE with RNAi triggers (1 µg), 24 HPE with cyclohexamide (CHX), or background (Media only) as compared to untreated cells. (B) *An. gambiae* 4a3b cell viability 72 HPE with dose curve of IAP F1R1, IAP F2R2, Caspase 8 F2R2, or LacZ control RNAi triggers as compared to untreated cells. (C) Cell viability of *An. gambiae* 4a3a, 4a3b, and Sua 5.0 cells as well as control *Ae. albopictus* C6/36 cells 72 HPE with IAP F1R1 (1 µg) as compared to untreated cells of the same type. (D) *An. gambiae* 4a3b cell viability post-exposure with IAP F2R2 (1 µg) over time. Shaded area indicates incubation period prior to start of cell viability assay (3 hour exposure). All data are the average of 3 or more independent replicates ± SEM. Asterisks indicate statistical significance (One Way ANOVA analyses with Dunnet's test performed on parts A, C, D. Two Way ANOVA with Dunnett's test performed on part B). $*p < 0.05$, $**p < 0.01$, $***p < 0.001$, $****p < 0.0001$.
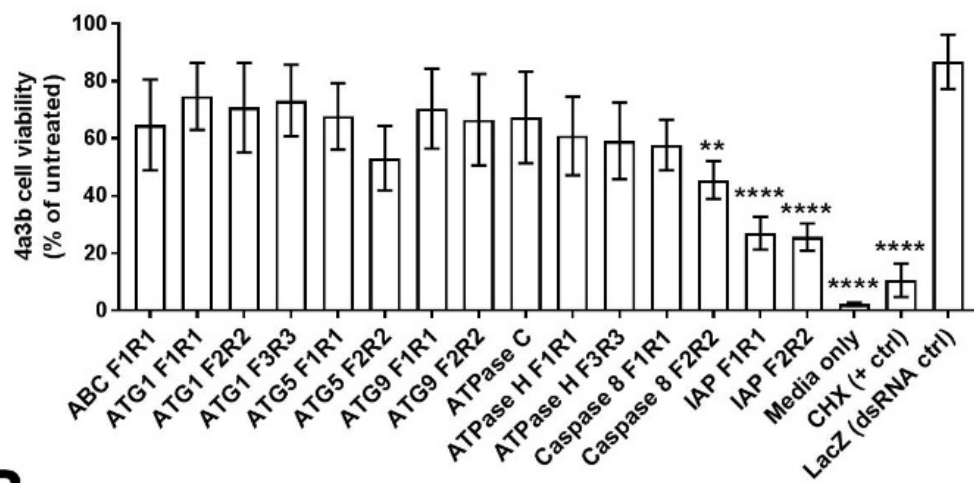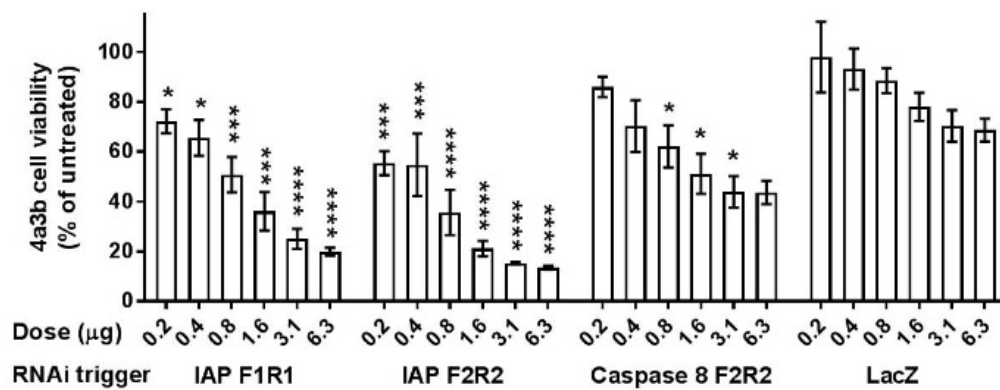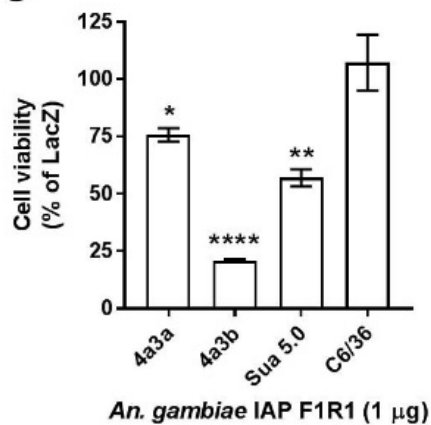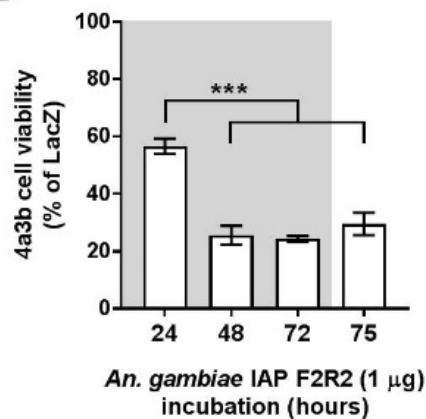
Figure 2 – Mortality induced by *iap1* RNAi knockdown differs by RNAi trigger design and species selection. Kaplan-Meier Survival curves of (A) *Ae. albopictus*, (B) *Ae. aegypti*, (C) *An. gambiae*, and (D) *Cx. pipiens* following peritoneal exposure with 1-2.5 µg of RNAi triggers targeting the 5' (F1R1) or 3' (F2R2) regions of *iap1* as compared to LacZ and untreated controls. All data are the average of 3 or more independent replicates ± SEM. Asterisks indicate statistical significance Kaplan-Meier Survival curve with Log-rank test. *p < 0.05, ****p < 0.0001.

Figure 3 – Short-interfering IAP triggers functional but limited to phagocytic cells. (A) Confocal microscopy of control (left) and siRNA exposed (right) hemocytes with nuclei (blue), actin (green) and siRNA (red). Scale bar = 5 µm. (B) Apoptosis activation in hemocytes determined by TUNEL assay 24 hours post exposure to short-interfering iIAP (siIAP), LacZ (siLacZ) or DNase positive control (+ ctrl). (C) Survival following exposure to short-interfering iIAP (siIAP), LacZ (siLacZ) with and without *E. coli* challenge. All data are the average of 3 or more independent replicates ± SEM. Asterisks indicate statistical significance following One Way ANOVA with Dunnett's test. **p<0.01, ***p < 0.001.

Figure 4 – *Ae. aegypti* **iIAP position impacts experimental outcome** *in vitro* **and** *in vivo***.**

Seventeen iIAP sequences spanning the length of the *IAP1* transcript in *Ae. aegypti,* exposed to Aag2 cells and adult female mosquitoes. (A) Graphical representation of the *IAP1* transcript including untranslated regions (white bar), coding sequence (black bar) and conserved protein domains (gray) including BIR1 (Baculovirus Inverted Repeat 1), BIR2 (Baculovirus Inverted Repeat 2), and Zinc (Zinc finger domain). Location and impact of each iIAP sequence on cell viability illustrated whereby green = no change from controls. For each trigger, numbers represent location along the *IAP1* coding sequence. (B) Impact of iIAP represented as average reduction in cell viability per base of the *IAP1* transcript (see part C). Dashed lines indicate SEM. (C) Average cell viability (± SEM) of Aag2 cells 72 HPE with individual iIAPs compared to controls. (D) Cell viability at 72 HPE vs *IAP1* knockdown at 48 HPE compared to LacZ control. (E) Average survival of adult females (± SEM) 10 days post exposure with individual iIAPs compared to controls. (F) Survival *in vivo* at 10 days post exposure vs cell viability *in vitro* at 72 HPE. All data are the average of 3 independent replicates. Asterisks indicate statistical significance following One Way ANOVA with Dunnett's test whereby *$<p<0.05$, **$p<0.01$, and ****$p <0.0001$.
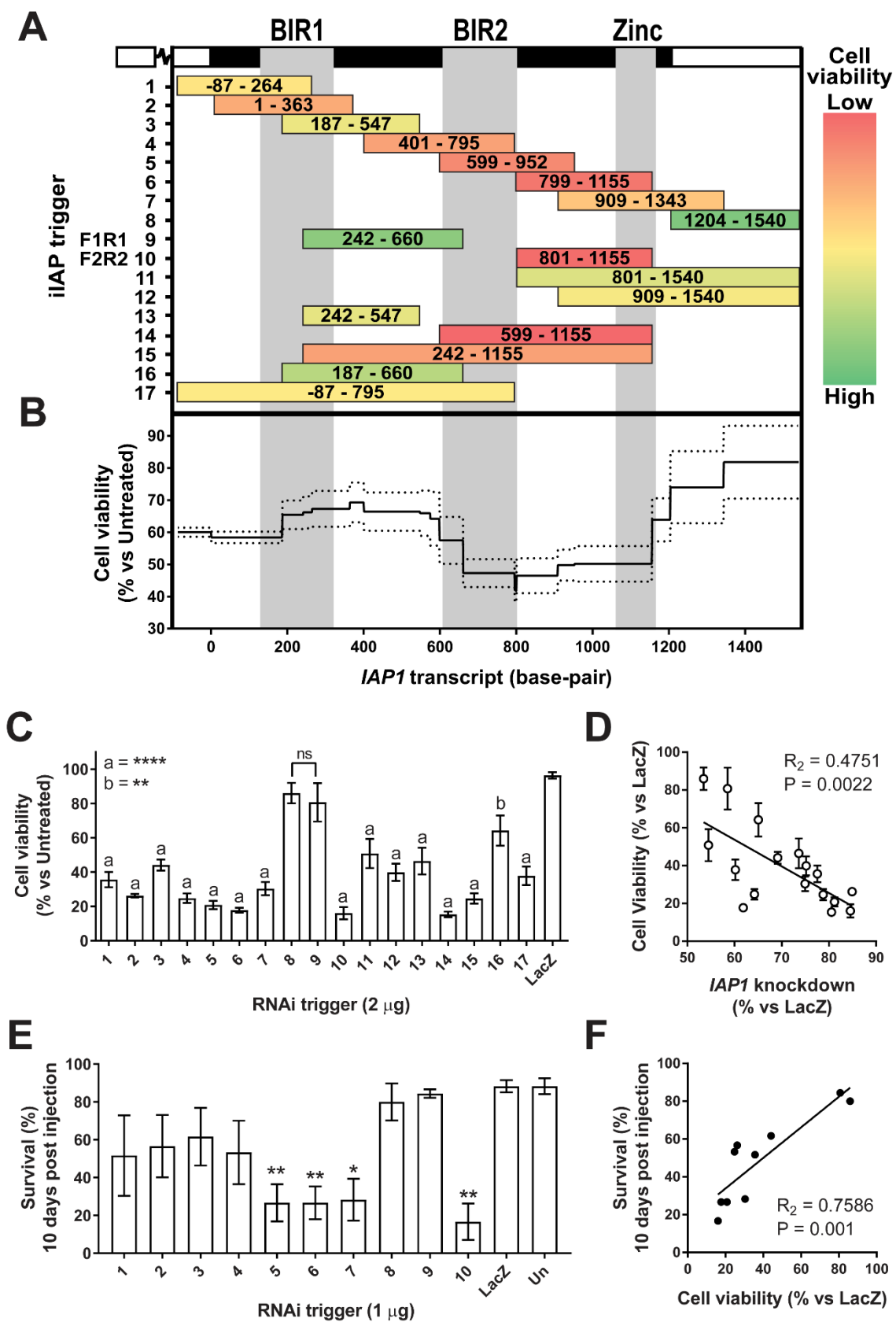
Figure 5 – Ovarian development is hyper-receptive to iIAPs in *Ae. aegypti*. Live individual follicles measured following neutral red staining at 48 HPBM (A,B) and 72 HPBM (C,D). Violin plots of length (A,C) and 2D scatter plots of morphology (B,D) shown. Oviposition output measured as the average number of eggs laid per mosquito at 6 days post blood-meal following treatment with 500 ng (E) or 1 µg (F) of RNAi trigger. All data are the average of 3 independent replicates. Letters indicate statistical significance difference groups following One Way ANOVA with Dunnett's test. Statistical test results for A-D are shown in supplemental table 2.
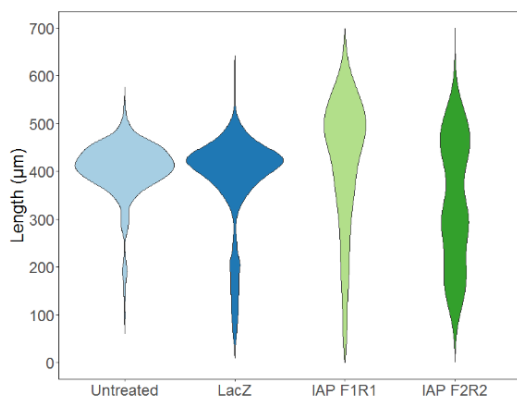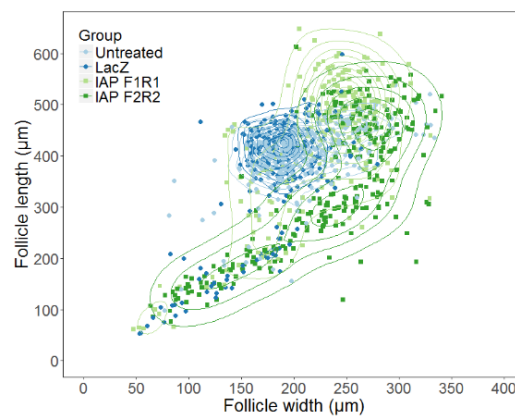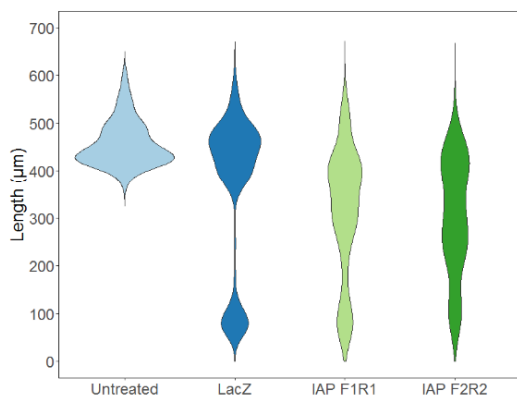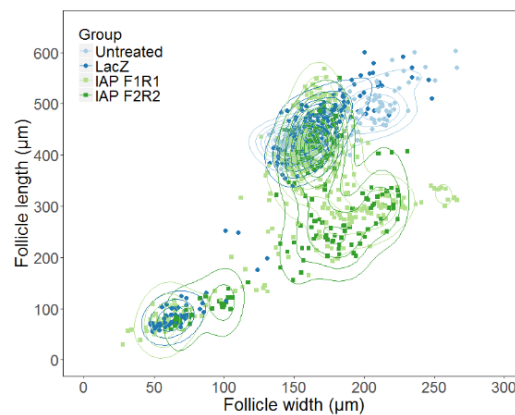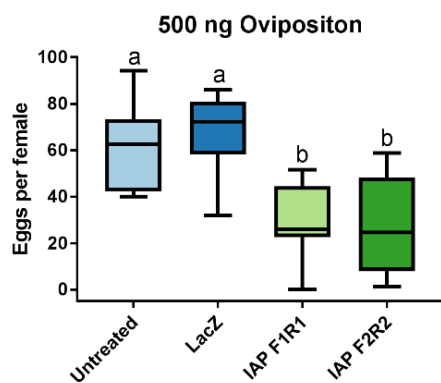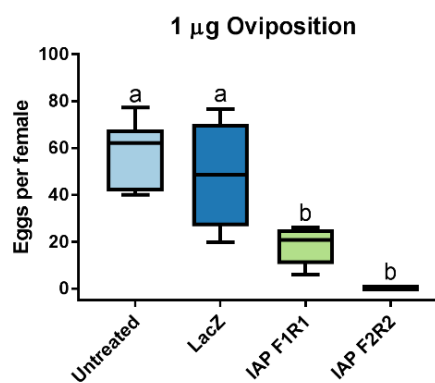
Figure 6 – Primary follicles are susceptible to low and high potency iIAPs during oogenesis.
Image panel of ovaries 48 hours post blood-meal and 24 hours post treatment. (A) nuclei stained with DAPI, (B) fluorescently labelled RNAi triggers, (C) propodium iodide death stain, (D) bright field, and (E) color merge of A (yellow), B (green), and C (red). Groups include (1) iIAP F1R1, (2) iIAP F2R2, (3) LacZ, (4) Untreated. Arrowhead = nurse cell death typical during healthy oogenesis. Scale bar = 250 µm.
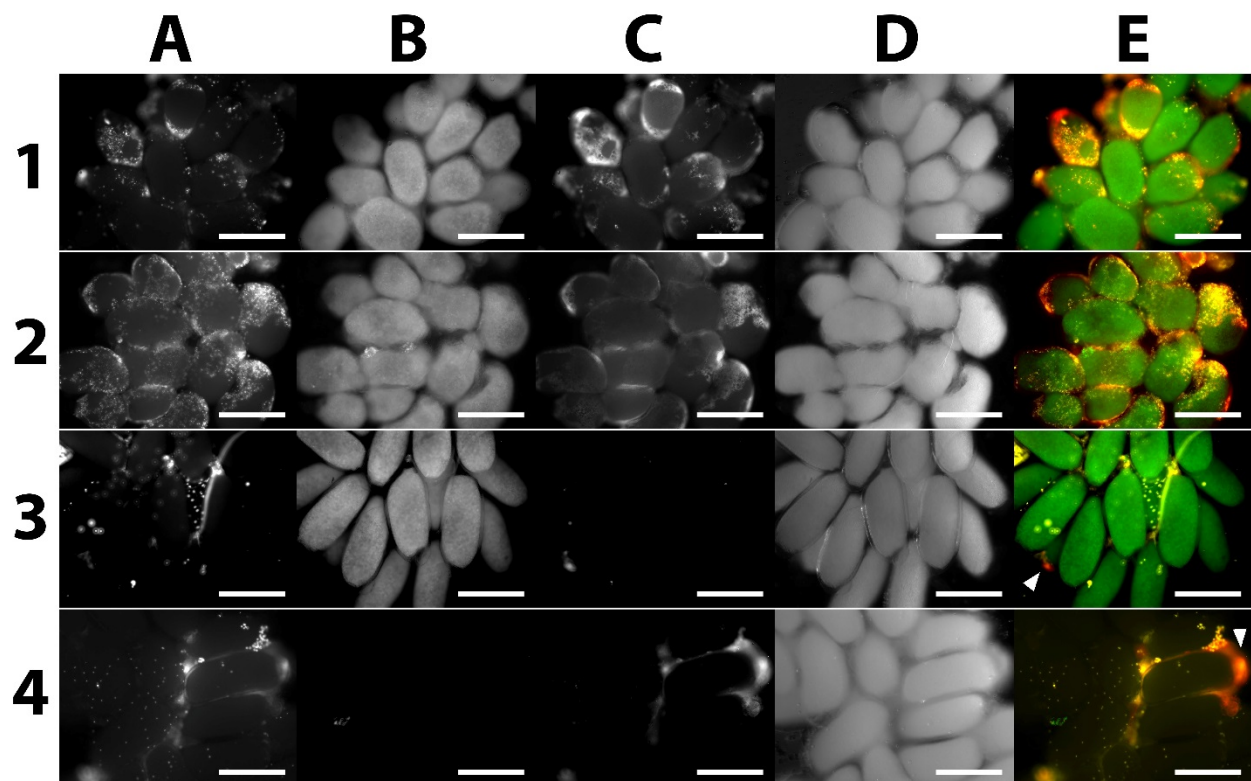
Supplementary Figure 1 – Survival screen for lethal RNAi triggers in adult female *An. gambiae*. Survival curves of 3 day old adult female *An. gambiae* injected with RNAi triggers (1 µg) targeting (A) Autophagy genes (ATGs), (B) Caspase 8, (C) midgut specific G12 gene, (D) midgut specific tight junction protein (TJP), and (E) vacuolar ATPase (vATPase) subunits as compared to LacZ or GFP RNAi trigger controls (1 µg). (F) Semi-Q PCR knockdown of target genes in adult female *An. gambiae* 72 hours post exposure to RNAi triggers (1 µg). Expression of target genes shown relative to housekeeping vATPase C, bars standardized to untreated controls. All data are the average of 3 or more independent experiments ± SEM. Asterisks indicate statistical significance (A-E) Kaplan-Meier Survival curve with Log-rank test, (F) One Way ANOVA with Dunnett's test. ***p < 0.001, ****p < 0.0001.
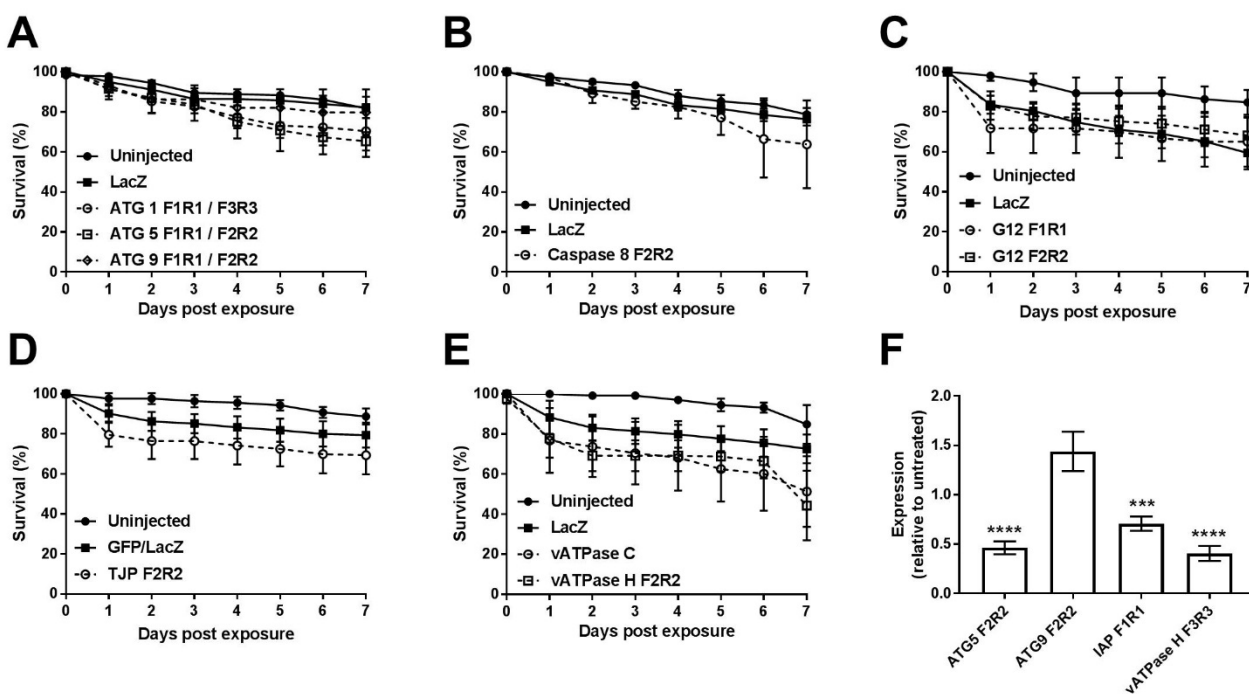
Supplementary Figure 2 – RNAi triggers are species-specific in *An. gambiae* 4a3b cells. Cell viability was monitored following exposure of *An. gambiae* cells to 1, 5, or 10 µg of dsIAP targeting *An. gambiae, Ae. aegypti,* or *Cx. pipiens* IAP1 sequences. Only the *An. gambiae* dsIAP resulted in significant reduction in cell viability compared to LacZ control. Data are the average of 3 or more independent experiments ± SEM. Asterisks indicate statistical significance as determined by One Way ANOVA with Dunnett's test. *$p < 0.05$, **$p < 0.01$.
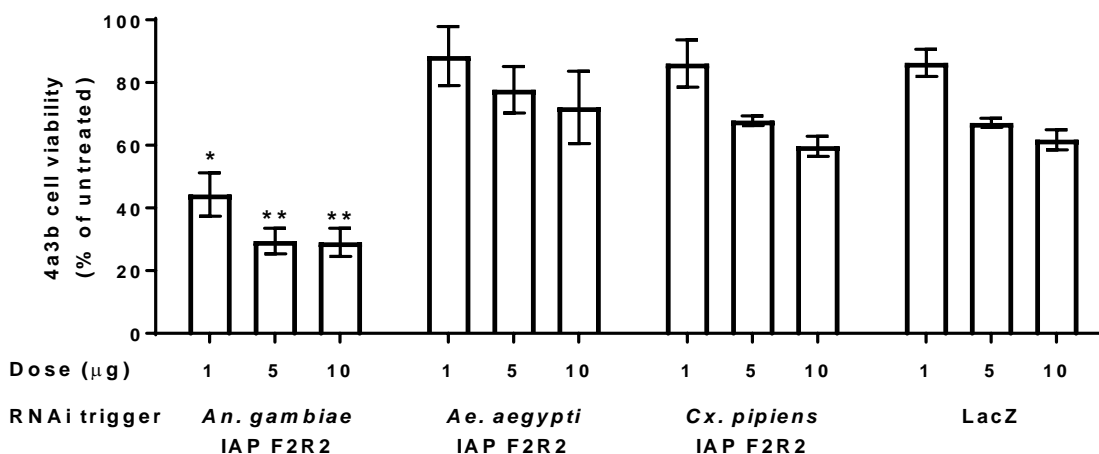
Supplementary Figure 3 – *Ae. aegypti* **IAP F2R2 but not F1R1 iIAP induces cell death** *in vitro***.** (A-C) Survival curves of adult female *Ae. aegypti* following injection with (A) 312 ng, (B) 625 ng, or (C) 1.25 µg of IAP F2R2 or control LacZ. (D) Cell viability following exposure to dose titration of LacZ control RNAi trigger vs IAP F1R1 and IAP F2R2 in *Ae. aegypti* Aag2 cells. (E) Knockdown time-series of *Ae. aegypti IAP1* following exposure to IAP F2R2 in Aag2 cells. All data are the average of 3 or more independent experiments ± SEM. Asterisks indicate statistical significance following (A-C) Kaplan-Meier Survival curve with Log-rank test or (D) One Way ANOVA with Dunnett's test. *p < 0.05, ****p < 0.0001.
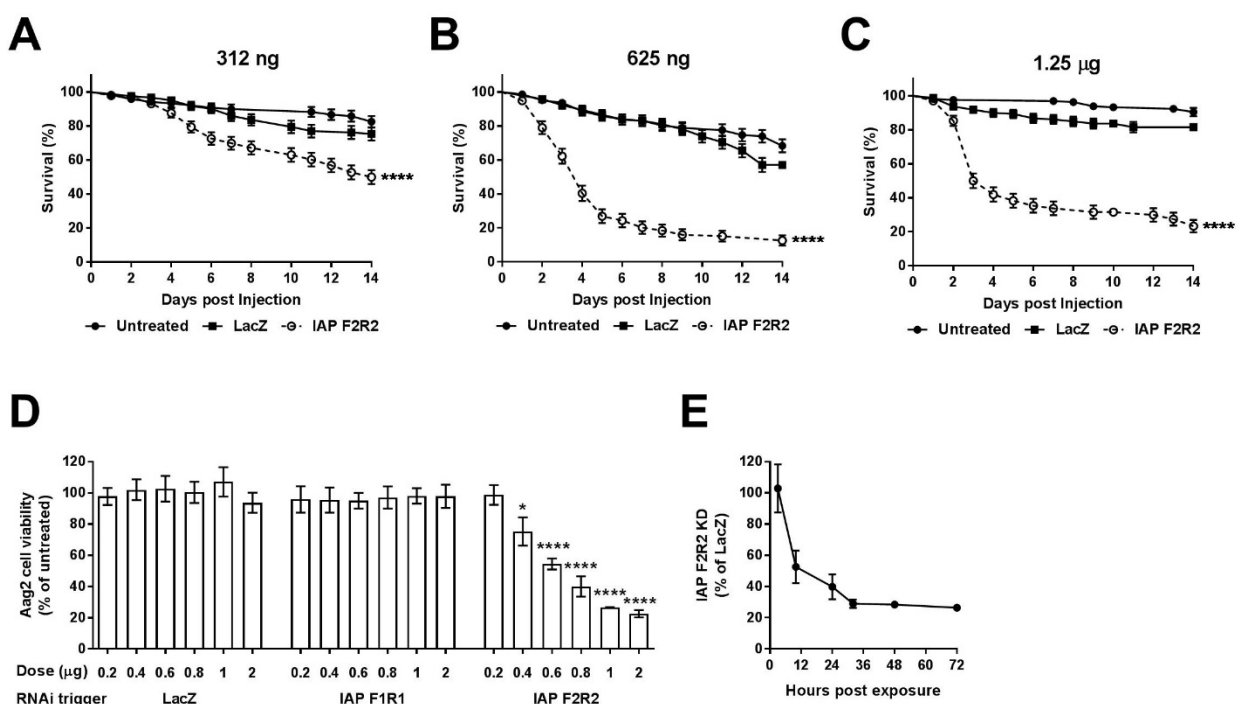
Supplementary Figure 4 – Kaplan-Meier Survival of *Ae. aegypti, An. gambiae,* and *Cx. pipiens* following exposure to 10% sucrose solutions with and without 1 mg/ml iIAP and LacZ RNAi triggers.
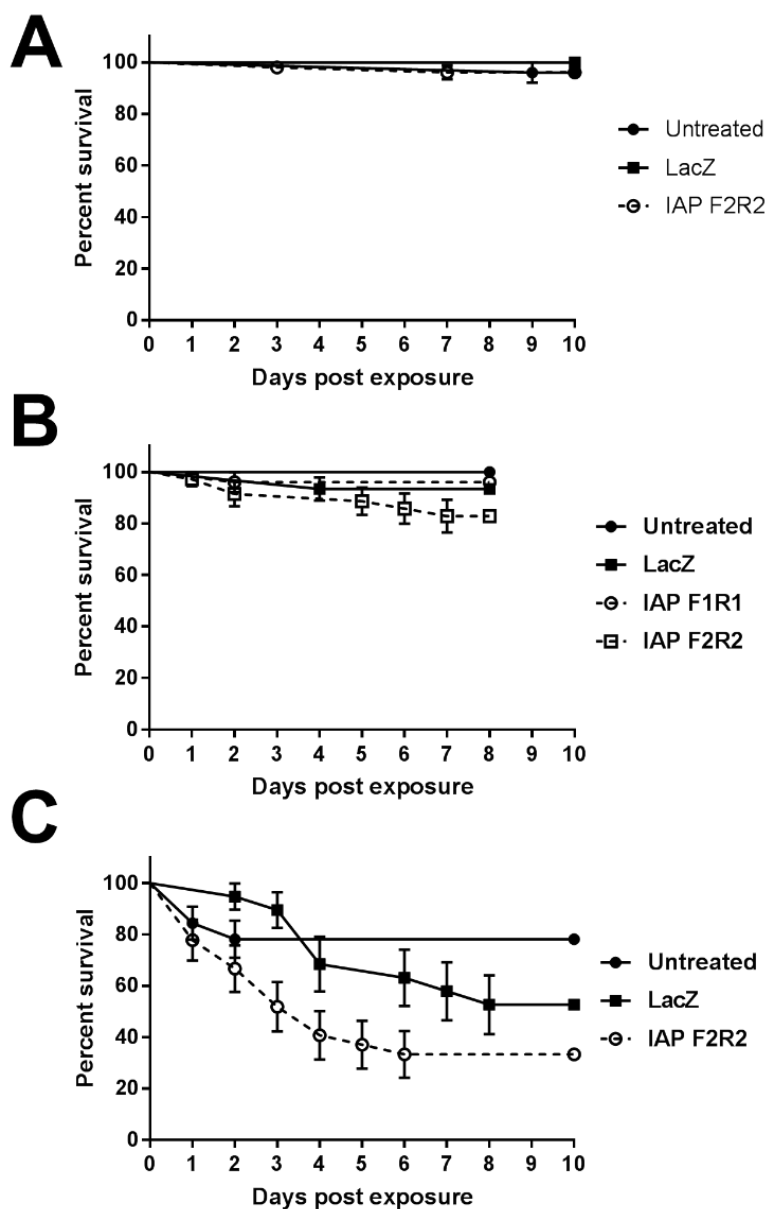
Supplementary Figure 5 – Kaplan-Meier Survival of *Ae. aegypti* following topical exposure to acetone with and without ~1 μg iIAP F2R2 or LacZ.
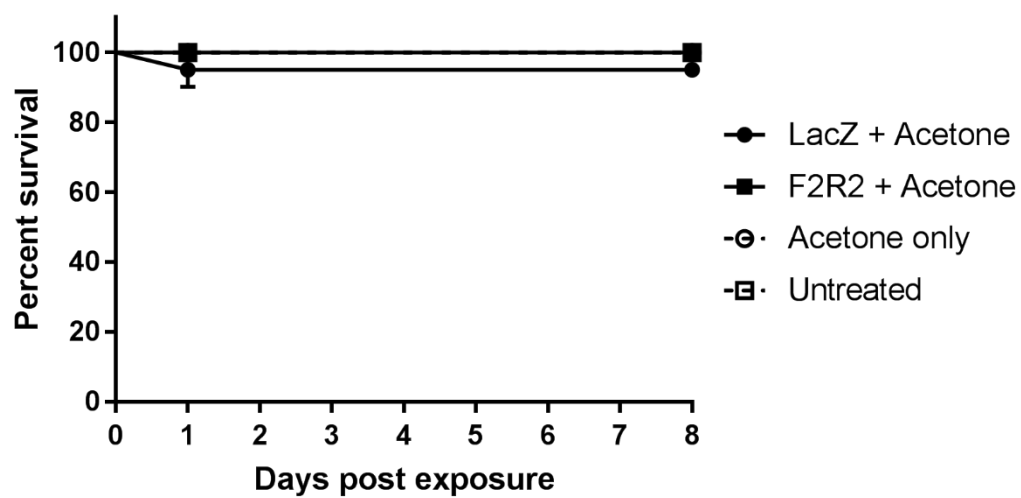
Supplementary figure 6. RNAi design alters outcome in *An. gambiae* 4a3b cells.

Short iIAP triggers targeting the IAP F2R2 region differentially impact cell viability. (A) Gel images of full length IAP F2R2, post-dicer treatment siIAP F2R2, and short IAP sequences spanning the IAP F2R2 region. Red bar indicates predicted size of product matching *An. gambiae iap1* (AGAP007294-RA) in Vectorbase. (B) Graphical representation of iIAP sequence location on F2R2 region of *IAP1* transcript with coding sequence (black bar), sequence annotated as intron (white bar), and conserved protein domains (gray) including BIR2 (Baculovirus Inverted Repeat 2) and Zinc (Zing finger domain). Location and impact of each iIAP sequence on cell viability illustrated whereby red = loss of 4a3b cell viability and green = no change from untreated control. Numbers within each trigger represent specific location along the *IAP1* transcript in relation to the coding sequence. (C) Average cell viability (± SEM) of 4a3b cells 72 HPE with individual iIAP and LacZ sequences in comparison to untreated controls. (D) Average cell viability (± SEM) of 4a3b cells 72 HPE with individual long double-stranded iIAP and LacZ vs short-interfering RNA (siRNA) iIAP and LacZ. All data are the average of 3 independent replicates. Asterisks indicate statistical significance following One Way ANOVA with Dunnett's test whereby *<p<0.05, **p<0.01, and ****p <0.0001.

A

505 bp

dsIAP F2R2

siIAP F2R2

IAP F2R2 fragmented sequence

0-1 1-2 2-3 3-4 4-5 5-6

B

Anopheles gambiae IAP1 F2R2 region

Cell viability

iIAP | BIR2 | "Intron" | Zinc

Low

0-100   588-680
100-200   686-783
200-300   765-884
300-400   876-954
400-500   954-1110
500-600   1107-1209
siIAP F2R2
F2R2   595-1229

High

595   IAP1 transcript   1229

C

4a3b cell viability (% of untreated)

RNAi trigger (1 µg)

0-100, 1-200, 2-300 *, 3-400, 4-500 **, 5-600 ****, F2R2 ****, LacZ

D

4a3b cell viability (% of untreated)

****

RNAi trigger (1µg)

F2R2, LacZ, siIAP F2R2, siLacZ

Supplementary figure 7 – RNAi trigger length and location does not alter efficacy in Aag2 cells. Linear regression analyses comparing (A) RNAi trigger length, (B) RNAi trigger start position, and (C) RNAi trigger stop position versus cell viability (black dot) and target gene knockdown (white dot). No significant correlations ($R^2 > 0.95$) were found.
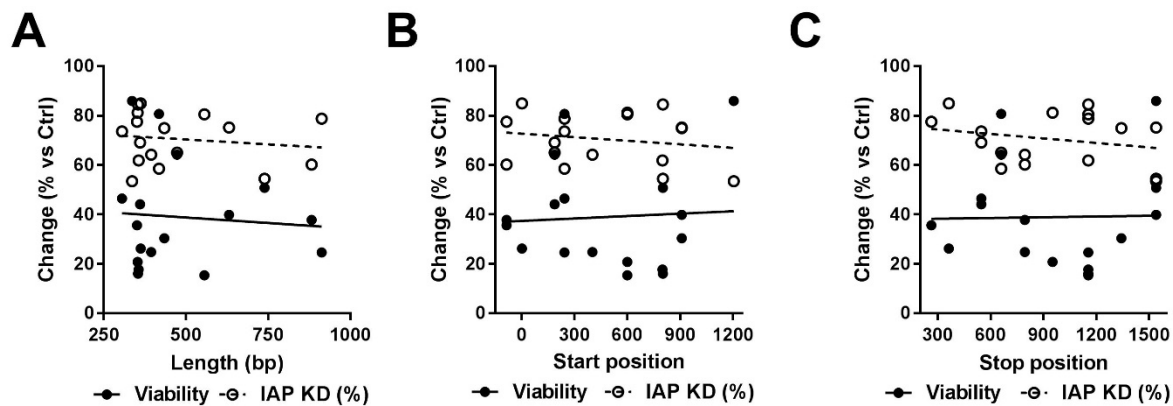
Chapter 5 – A meta-analysis and catalogue of mosquito RNAi studies

Abstract

RNAi has transformed the field of mosquito molecular biology as a reverse genetic tool, a means to study host-pathogen interactions, and a platform to develop novel vector control strategies. However, variation in outcome from study to study may be due to controllable errors such as variance in design of RNAi triggers (double stranded RNAs and short interfering RNAs), or a combination of many other experimental factors. To address variation between RNAi experiments we cataloged all readily searchable instances of RNAi experiments targeting mosquito genes and through a meta-analysis approach, identify common practices that result in the best target gene knockdown. We also use this data to identify common factors underlying high levels of knockdown and find that overall, more highly expressed genes typically result in higher levels of knockdown, probably due to increasing the range by which knockdown can be measured. These data are also made available via an online repository that serves as a fast, searchable database of published RNAi experiments.

Introduction

The use of RNA interference (RNAi) as a tool to suppress mosquito genes has led to a plethora

of studies exploring gene functions within the mosquito as well as mosquito interactions with

other organisms. Exploration of mosquito gene knockdown has been studied from a variety of

perspectives. For one, the RNAi pathway functionality in gene suppression and role in immunity

have been outlined with great detail [1, 2]. For the most part, the core RNAi pathway is

conserved between *Drosophila* and mosquitoes and is considered functional across mosquito

species and strains, as demonstrated through the variety of successful knockdown experiments

throughout the literature [3-5]. However, there has yet to be any consensus on what constitutes

successful knockdown of a target gene, and whether knockdown success is viable across species,

strains, life-stages, and tissues. Furthermore, the limitations surrounding RNAi experimentation

have not been characterized, despite a growing body of available literature. We do know that

RNAi uptake in some tissues is limited, for instance in the salivary glands [6]; but can be

overabundant in other tissues such as the ovaries [7]. Intracellular factors may also lead to

variation in efficacy between species. In *Spodoptera frugiperda*, accumulation of RNAi triggers

within endosomes has also been argued to limit RNAi efficacy [8], however endocytic uptake is

considered essential to RNAi function in *Drosophila* [9]. Loss of RNAi functionality within the

cell is also possible, as demonstrated through dysfunctional Dicer-2 in *Ae. albopictus* C6/36 cells

[10].

The struggle to elicit consistently high levels of gene suppression is not unique to

mosquito biologists; in fact, numerous reports on the potential struggles in implementation of

RNAi in various taxa, with some species that appear to be recalcitrant to the technique [11, 12].

Inconsistent RNAi suppression in Lepidopteran species inspired a mass collaboration to outline

successes and pitfalls from over 150 experiments [13]. The results of this effort included the discovery that some Lepitopteran families (notably Saturniidae) are more receptive to RNAi knockdown than others. Additionally the route of exposure, target tissue, and target gene were found to impact the effective dose and overall knockdown success. These findings have helped to provide a framework for successful RNAi knockdown in Lepitopteran species and at the same time give warnings of the limitations for using RNAi as a technique in particular settings. Similar efforts to address shortcomings of RNAi efficacy in a variety of insects has led to discovery of RNase III type ribonucleases in insect hemolymph and midgut tissues [14-17]. However there is still a lack of information pertaining to successful experiment approaches and whether differences in technique, RNAi design, or biological system alter RNAi success. For mosquitoes, methodological video guides are available for RNAi trigger injections in *Ae. aegypti* (larvae and adults) and *An. gambiae* (adults) [18-20]. While these publications serve as instructional resources when planning and implementing a knockdown experiment, there is no current comprehensive guide which outlines the potential pitfalls for a given RNAi experiment in mosquito species.

In this study we review and analyze meta-data from the available literature and provide a resource for individuals search and re-assess the data. These studies describe the potency of gene suppression when targeting genes with an array of functions in numerous cell types across numerous mosquito species. Variety of outcomes is manifest in RNAi trigger design, method of delivery, and many other methodological differences. The potency of RNAi target gene knockdown ranges from 100% suppression of target gene to 0% knockdown and in rare cases upregulates the target [21, 22]. We hypothesize that these differences in RNAi are not due to random chance but are a function of the RNAi trigger design and methodology along with

intrinsic genetic factors. The sheer number of factors involved prevent traditional statistical analysis and as such we opt for a systematic meta-analytical approach to isolate factors or groups of factors which impede efficacy of RNAi based gene suppression. We also catalog all published information pertaining to the design, production, implementation, and analysis of RNAi knockdown of mosquito genes. This dataset serves as a searchable reference guide of known RNAi designs and documents the level of gene suppression achieved in the context of the experimental design and application reported.

Materials and Methods

Data collection

Data from the available literature in PubMed (http://www.ncbi.nlm.nih.gov/pubmed) was identified using the following search terms: (((((((((RNAi) OR RNA interference) OR dsRNA) OR double stranded RNA) OR siRNA) OR short interfering RNA) OR silencing) OR gene knockdown) AND 'Genus name' AND/OR 'species name'. Species included: *Aedes (Ae. aegypti, Ae. albopictus, Ae. cinereus, Ae. vexans, Ae. triseriatus), Anopheles (An. gambiae, An. albimanus, An. dirus, An. stephensi, An. arabiensis, An. punctipennis), Culex (Cx. pipiens, Cx. quinquefasciatus, Cx. molestus), Ochlerotatus, Culiseta, Haemagogus, Mansonia, Psorophora,* and *Uranotaenia*. Resulting citations were read with all relevant information logged in an excel database either directly from the text or derived from Figures or cited sources. Studies with no apparent experiments suppressing only mosquito genes were excluded. To standardize gene IDs, the text was searched for NCBI or vectorbase accession numbers. If no accession number was given primers or gene sequences were searched using BLAST (http://blast.ncbi.nlm.nih.gov/Blast.cgi) and the best relevant hit was recorded as the target gene.

To calculate RNAi trigger size and position primers were entered to primer BLAST (http://www.ncbi.nlm.nih.gov/tools/primer-blast/) for a given accession number and resulting positions were recorded.

Quantifying gene knockdown

Knockdown (KD) of target genes was recorded as percentage reduction in transcript derived from the text or measured directly from Figures using the imageJ line tool (https://imagej.nih.gov/ij/). In the case of negative fold, the bar length was measured and exact fold reduction was calculated and converted to KD% using: 100-(1 / fold reduction * 100). Error bars were not taken into consideration as these data were published and averages should represent the result of repeated experiments. In the case where evidence was given in the form of an electrophoresis gel or blot, KD was listed as not quantified. Statistical significance of KD was not determined due to the variety of papers and scenarios incorporated into the dataset.

Datasets and scripts

Tables of all data collected, as well as relevant R scripts, and python 3 scripts are available at https://github.com/PaulAirs/RNAidb. To explore the main RNAi dataset visit https://mosquitornai.shinyapps.io/RNAidb2/.

Results

Summary statistics and most common practices in mosquito RNAi

From the available literature we compiled data from 247 publications, including 985 unique RNAi experiments. *Ae. aegypti* and *An. gambiae* are over-represented in mosquito literature and

account for 56% and 29.3% of all studies respectively (Figure 1 A); but in total the data set

contains 14 species including 66 strains and cell lines (Figure S1-S3). On average, 67.33% target

gene knockdown was reported from experiments using quantifiable knockdown methods (Figure

1 B). Although high levels of knockdown were common, low levels of knockdown and a single

report of upregulation were also reported indicating that throughout published literature no lower

boundary exists for knockdown to be considered successful (Figure 1 B). Many valid forms of

assessing knockdown were provided but could not be quantified for this study such as Western

blots, Northern blots, and *in situ* hybridization.

RNAi is robust but varies across species, life-stages, and exposure routes

Initial assessments of the dataset queried individual factors derived from experimental data to

identify which factors, if any, alter RNAi efficacy. We found notable differences between *Ae.*

aegypti and *An. gambiae* (Figure 2 A). These species are more commonly used but are not

statistically more amenable to RNAi. Ranking of species results in highest average knockdown

from *Aedes* species, followed by *Anopheles* species, *Armigeres subalbatus*, and then *Culex*

species (Figure 2 A). All species and the majority of strains have demonstrated above average

knockdown ($> 68\%$) in at least one experiment highlighting that RNAi is robust across insect

taxa.

Likewise, use of different life-stages *in vivo* and cell lines *in vitro* is not limiting to

knockdown success, with the exception of *Cx. quinquefasciatus* embryos that result in reduced

knockdown on average (Figure 2 B). Most groups differ from embryonic exposure, while

knockdown in adults is highly varied but far more commonly used compared to all other groups

(Figure 2 B). Unsurprisingly *in vitro* experiments result in the highest knockdown on average

since these cell types are often hemocyte-like making them more amenable to uptake and can be exposed to RNAi triggers more directly than in *in vivo* systems.

In addition to organismal factors, exposure route also results in drastically different outcomes across mosquito species (Figure 3 A & B). Injections are by far the most common exposure route but this approach also varies (as illustrated in Figure 3 C). Again we find that *in vitro* transfection approaches are most effective, while injections in the embryo stage are least effective (Figure 3 A & B). Intrathoracic injection is by far the most commonly used approach among adults and is also utilized for delivery in larvae and pupae, though *per os* approaches are most common for larvae overall. Interestingly, intrathoracic injections result in higher knockdown on average compared to direct hemolymph injection (Figure 3 A & B). How differences in injection placement impact knockdown efficacy are unknown, but again high levels of knockdown are possible for all exposure routes tested and therefore these approaches are not limiting to knockdown success.

Dose, tissue, and time point impact knockdown of the same gene in the same species.
Of the various experimental factors tested, no single factor appears to limit knockdown success when assessing the data as a whole. Dose was not correlated to knockdown, with higher doses equally ineffective at inducing high knockdown as low doses (Figure S4 A). Similarly: infection status (Figure S5), mosquito age at exposure (for adults, Figure S6 A), and time of knockdown measurement following exposure (Figure S6B) are not correlated to knockdown success across all experiments. However, knockdown measured over time does vary in studies where multiple time-points are taken, increasing from 24-96 hours post exposure and falling after 246 hours post

exposure (Figure 4) [7]. Increasing dose also increases knockdown for the same experiment (Figure S4 B).

Gene expression but not gene target or trigger design increases knockdown success

To identify aspects of the target gene which may hinder knockdown success, we measured both gene length and standard expression as compared to knockdown (Figure 5). Surprisingly we found that higher gene expression is correlated with higher knockdown using adult *Ae. aegypti* RNAseq data matched to knockdown data. Since gene length was not associated with knockdown, we assessed whether RNAi trigger length in base-pairs (Figure S7 A) as well as coverage of the target gene coding sequences (Figure S7 B) had any effect, but this does not appear to be the case. RNAi triggers designed were ~400 base-pairs on average, with only 5% of studies using siRNAs, and only one example of an RNAi trigger between 25-100 base-pairs in length. While no differences occur in knockdown efficacy, best-practices typically utilize long dsRNAs.

Discussion

Determination of RNAi limitations in mosquito species is essential to improve RNAi methodology as well as address roadblocks to developing field applicable RNAi triggers for pest and vector control [5, 12]. In this study we catalogue RNAi experiment data from 247 publications and 985 unique RNAi experiments testing knockdown in 14 mosquito species. This dataset also acts as a rapidly searchable database of all aspects surrounding RNAi experiments, which can serve to reduce experimental variability and increase knockdown success for knockdown of new and previously studied genes. Principally we find that RNAi is robust across

species and experimental techniques. However 46% of experiments fail to induce >50% target gene knockdown.

To identify potential causes in low knockdown we assessed a variety of factors and found that increased target gene expression is correlated to increased knockdown. Higher base levels of expression are known to result in more drastic phenotypes when suppressed in *Agrilus planipennis* [23]. We also found instances where knockdown produces less than desired outcomes, notably in experiments in *Cx. quinquefasciatus* embryos and from direct hemolymph injections in adults. It may be that expression of nucleases in the hemolymph reduce knockdown for hemolymph injections as opposed to intrathoracic injections, which are far more commonly used. Nuclease expression in the hemolymph and gut tissues is known to limit RNAi success in diverse insect taxa [14, 15, 17]. However the spread of RNAi triggers following injection into the thorax is not well characterized. Following hemolymph injections via the cervical membrane, RNAi triggers accumulate in hemocytes, pericardial cells of the dorsal vessel, and ovaries [7]. Thoracic injection may reduce immediate spread of RNAi triggers and prevent accumulation in these cells.

For all factors assessed, high levels of knockdown have been achieved, however timing of knockdown assessment is critical, with gene silencing most effective between 72-120 hours post exposure, but can persist further. Considering that RNAi triggers are mostly cleared from tissues within the first 72 hours post exposure [7], it is probably that persistent knockdown is a result of systemic RNAi in mosquito species. Systemic RNAi can occur in Dipteran species following reverse transcription of dsRNA which is re-expressed via retrotransposons [24, 25]. Systemic RNAi may be bolstered by presence of viruses, however infection in *Ae. aegypti* adults marginally decreases knockdown efficacy compared to uninfected individual (see Figure S5, p =

0.07). This was not the case for *An. gambiae*. Injections of RNAi triggers as well as exposure to pathogens are known to increase expression of RNAi pathway genes in insects [1, 23]. Therefore, exposure to RNAi triggers alone may result in systemic gene knock down and genetic integration of the RNAi trigger, although this has yet to be deciphered.

When assessing genetic differences, longer RNAi triggers occur with far more frequency compared to siRNAs and smaller (<100 base-pair) sequences, but use of longer products does not increase success when applied. Long double stranded RNAs are preferable due to cost-efficiency for production, but extremely long sequences >600 base-pairs may be unnecessary and will introduce likelihood for mismatching errors during production. More importantly than cost, siRNAs also fail to enter cells and elicit high levels of knockdown *in lieu* of transfection reagents, unless exposed to embryos or neonate larvae.

Overall, these data reiterate the strength of RNAi in mosquitoes and provide a platform to search published RNAi studies as a guide for future research.

Literature cited

1.   Blair, C.D., *Mosquito RNAi is the major innate immune pathway controlling arbovirus infection and transmission.* Future microbiology, 2011. **6**(3): p. 265-277.

2.   Sanchez-Vargas, I., et al., *RNA interference, arthropod-borne viruses, and mosquitoes.* Virus Research, 2004. **102**(1): p. 65-74.

3.   Hoa, N.T., et al., *Characterization of RNA interference in an Anopheles gambiae cell line.* Insect Biochem Mol Biol, 2003. **33**(9): p. 949-57.

4.   Hussain, M., K. Etebari, and S. Asgari, *Chapter Seven - Functions of Small RNAs in Mosquitoes*, in *Advances in Insect Physiology*, A.S. Raikhel, Editor. 2016, Academic Press. p. 189-222.

5.   Airs, P.M. and L.C. Bartholomay, *RNA Interference for Mosquito and Mosquito-Borne Disease Control.* Insects, 2017. **8**(1): p. 4.

6.   Boisson, B., et al., *Gene silencing in mosquito salivary glands by RNAi.* FEBS Lett, 2006. **580**(8): p. 1988-92.

7.   Airs, P.M., *Manipulating cell death and RNA interference processes for mosquito control*, in *Pathobiological Sciences*. 2018, University of Wisconsin Madison.

8.   Yoon, J.-S., D. Gurusamy, and S.R. Palli, *Accumulation of dsRNA in endosomes contributes to inefficient RNA interference in the fall armyworm, Spodoptera frugiperda.* Insect Biochemistry and Molecular Biology, 2017. **90**: p. 53-60.

9.   Saleh, M.C., et al., *The endocytic pathway mediates cell entry of dsRNA to induce RNAi silencing.* Nat Cell Biol, 2006. **8**(8): p. 793-802.

10.   Brackney, D.E., et al., *C6/36 Aedes albopictus Cells Have a Dysfunctional Antiviral RNA Interference Response.* PLoS Neglected Tropical Diseases, 2010. **4**(10): p. e856.

11.   Katoch, R., et al., *RNAi for insect control: current perspective and future challenges.* Appl Biochem Biotechnol, 2013. **171**(4): p. 847-73.

12.   Scott, J.G., et al., *Towards the elements of successful insect RNAi.* J Insect Physiol, 2013. **59**(12): p. 1212-21.

13.   Terenius, O., et al., *RNA interference in Lepidoptera: an overview of successful and unsuccessful studies and implications for experimental design.* J Insect Physiol, 2011. **57**(2): p. 231-45.

14.   Song, H., et al., *A double-stranded RNA degrading enzyme reduces the efficiency of oral RNA interference in migratory locust.* Insect Biochemistry and Molecular Biology, 2017. **86**: p. 68-80.

15.   Wynant, N., et al., *Identification, functional characterization and phylogenetic analysis of double stranded RNA degrading enzymes present in the gut of the desert locust, Schistocerca gregaria.* Insect Biochem Mol Biol, 2014. **46**: p. 1-8.

16.   Luo, Y., et al., *Towards an understanding of the molecular basis of effective RNAi against a global insect pest, the whitefly Bemisia tabaci.* Insect Biochemistry and Molecular Biology, 2017. **88**: p. 21-29.

17.   Wang, K., et al., *Variation in RNAi efficacy among insect species is attributable to dsRNA degradation in vivo.* Insect Biochemistry and Molecular Biology, 2016. **77**: p. 1-9.

18.   Garver, L. and G. Dimopoulos, *Protocol for RNAi assays in adult mosquitoes (A. gambiae).* Journal of visualized experiments : JoVE, 2007: p. 230.

19.   Drake, L.L., et al., *RNAi-mediated Gene Knockdown and In Vivo Diuresis Assay in Adult Female Aedes aegypti Mosquitoes.* Journal of Visualized Experiments, 2012: p. 1-7.

20.   Zhang, X., et al., *Chitosan/Interfering RNA nanoparticle mediated gene silencing in disease vector mosquito larvae.* Journal of visualized experiments : JoVE, 2015.

21.   Sun, G., et al., *Synergistic action of E74B and ecdysteroid receptor in activating a 20-hydroxyecdysone effector gene.* Proceedings of the National Academy of Sciences of the United States of America, 2005. **102**: p. 15506-15511.

22.   Sim, S., et al., *Transcriptomic profiling of diverse Aedes aegypti strains reveals increased basal-level immune activation in dengue virus-refractory populations and*

identifies novel virus-vector molecular interactions. PLoS neglected tropical diseases, 2013. **7**: p. e2295.

23. Rodrigues, T.B., et al., *Identification of highly effective target genes for RNAi-mediated control of emerald ash borer, Agrilus planipennis.* Scientific Reports, 2018. **8**(1): p. 5020.

24. Tassetto, M., M. Kunitomi, and R. Andino, *Circulating Immune Cells Mediate a Systemic RNAi-Based Adaptive Antiviral Response in Drosophila.* Cell, 2017. **169**(2): p. 314-325.e13.

25. Goic, B., et al., *Virus-derived DNA drives mosquito vector tolerance to arboviral infection.* Nat Commun, 2016. **7**: p. 12410.

Tables & Figures

Supplementary Table 1 – Tukey HSD values for life-stage comparisons of knockdown averages.

Compared groups	difference	lower	upper	p adj
Embryo-Adult	-14.990963	-27.2753	-2.70665	0.0079105
In vitro-Adult	**13.00103**	**2.031789**	**23.97027**	**0.0108979**
Larvae-Adult	4.401521	-5.99295	14.79599	0.7751234
Pupae-Adult	11.644464	-3.01762	26.30655	0.1915107
In vitro-Embryo	**27.991993**	**11.93753**	**44.04645**	**0.0000224**
Larvae-Embryo	**19.392484**	**3.725116**	**35.05985**	**0.0067229**
Pupae-Embryo	**26.635427**	**7.86316**	**45.40769**	**0.0010799**
Larvae-In vitro	-8.599509	-23.2585	6.059497	0.4949076
Pupae-In vitro	-1.356566	-19.2959	16.58272	0.9995923
Pupae-Larvae	7.242943	-10.3508	24.83666	0.7927461

Figure 1 – Summary statistics from RNAi dataset. (A) Cumulative number of publications per year, per species. (B) Knockdown of target gene as compared to controls following exposure to RNAi triggers
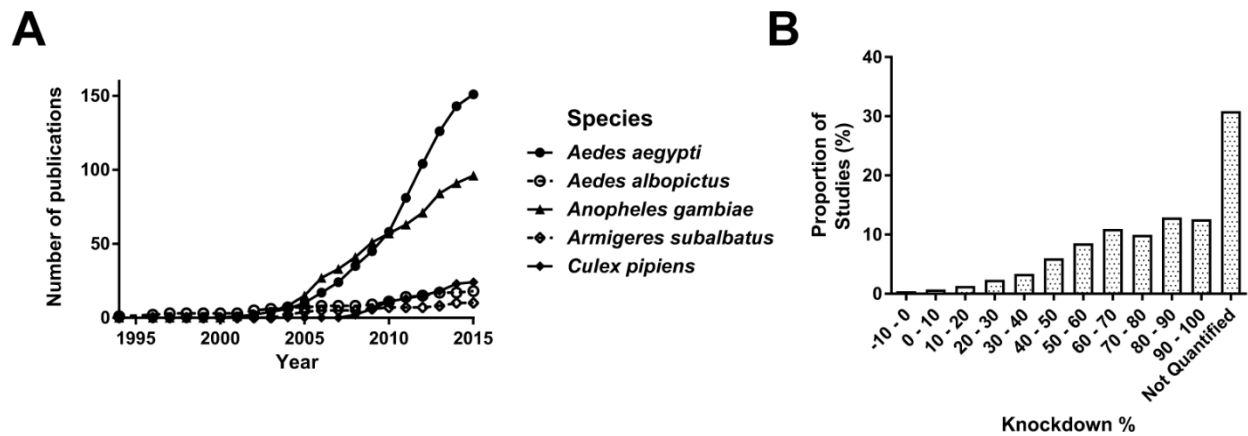
Figure 2 – Species and life-stage differences in RNAi efficacy. Combined box and dot plots showing (A) knockdown results per species. One-Way Tukey HSD test were found between *Ae. aegypti* and *An. gambiae* but not for other combinations, likely due to limited *n*. (B) knockdown results per species and system (life-stages *in vivo* and *in vitro*). Significant differences calculated by Tukey HSD test shown in Supplemental Table 1.
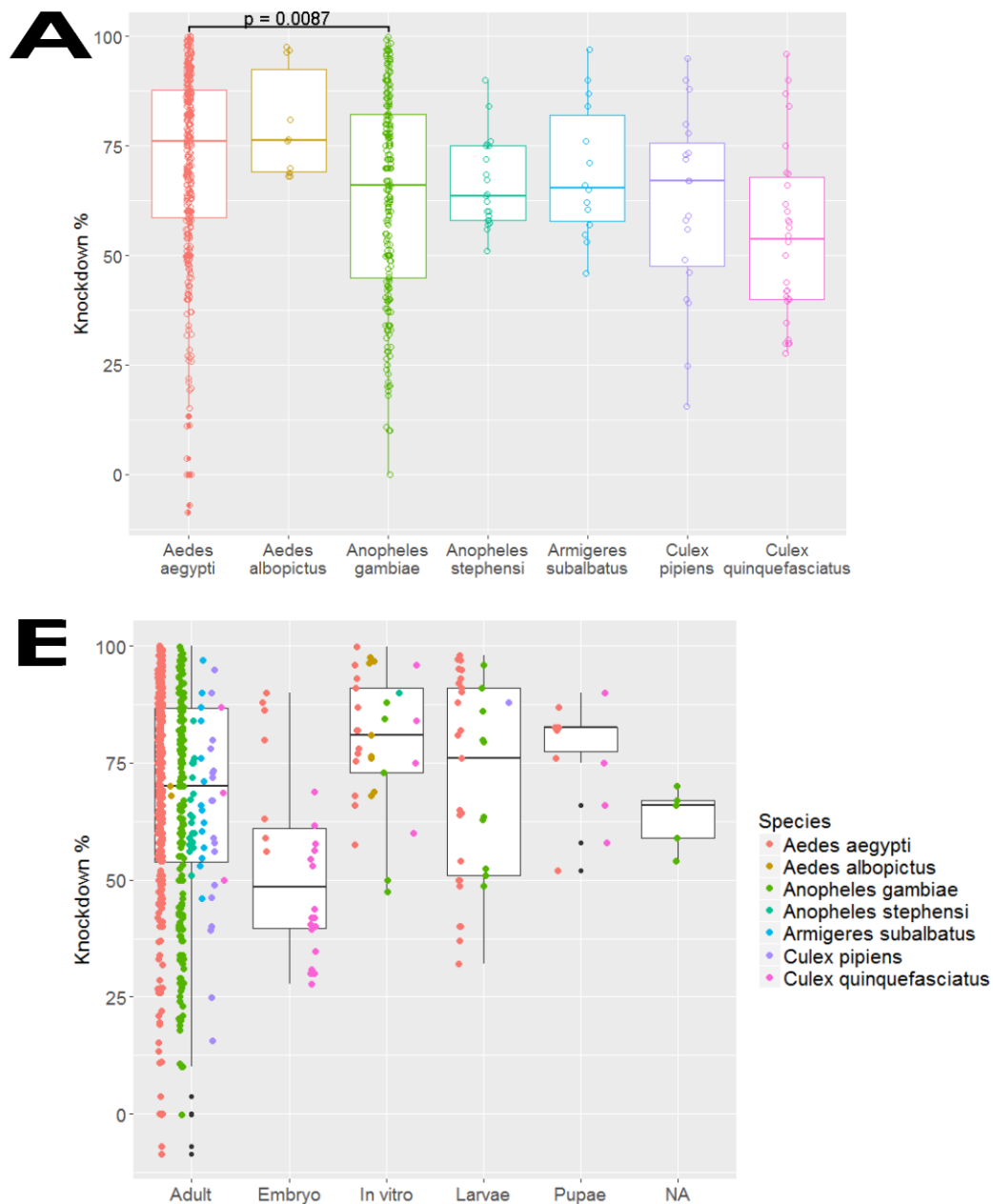
Figure 3 – Exposure route related to knockdown success in some systems. (A) Dot and box plot showing knockdown of target genes in select species (color), life-stages (shape) for different exposure routes. (B) Tukey HSD test for multiple comparisons of part A. (C) Illustrations of injection methods described in the literature.

ANOVA Tukey HSD comparisons	Adjusted p
Injection Intrathoracic-Injection Embryonic	0.0014851
Injection Unspecified-Injection Embryonic	0.0022113
Transfection-Injection Embryonic	0.0000107
Injection Intrathoracic-Injection Hemolymph	0.0075368
Transfection-Injection Hemolymph	0.0000588

Injection specifications:
I   Haemolymph
II   Mesothoracic spiracle
III   Intratoracic
IV   Intersegmental
V   Abdominal
VI   Not specified

Figure 4 – Knockdown peaks days post injection. Multiple linear regression from experiments wherein knockdown is measured over 3 or more time points. Blue line indicates average with SEM shaded in gray. Colors indicate time points from 12 individual experiments performed.
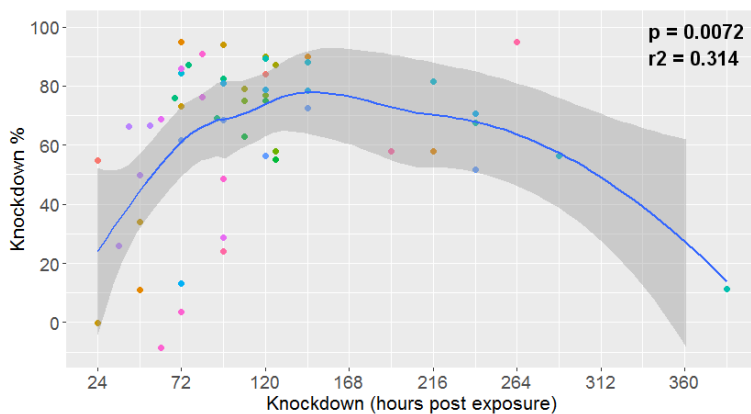
Figure 5 – Gene expression but not length correlated to knockdown success. (A) Gene lengths vs knockdown across all data. Blue bar indicates linear regression trend line with gray shaded error. (B) Relative expression of genes in adult female *Ae. aegypti* with reported knockdown in adult female *Ae. aegypti*.
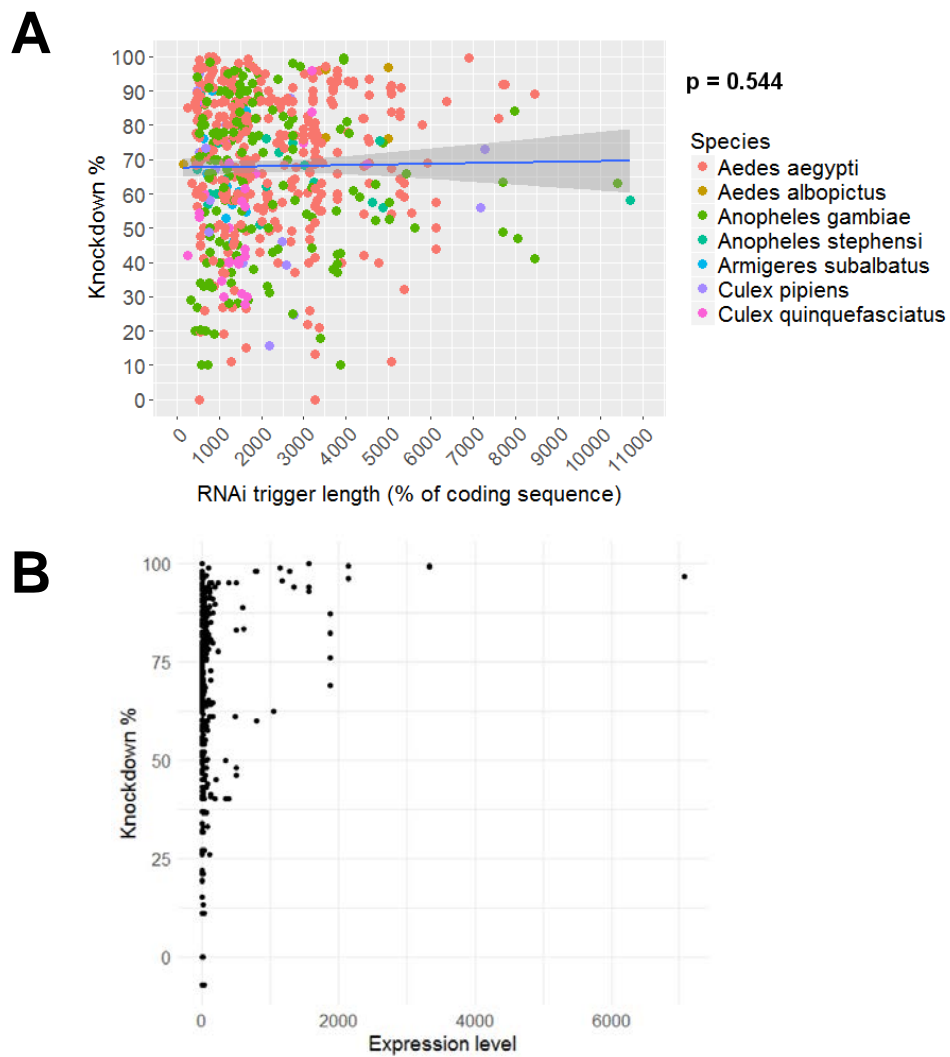
Supplementary Figure 1 – RNAi experiments displayed as number of experiments per life stage per strains in *Aedes* species.
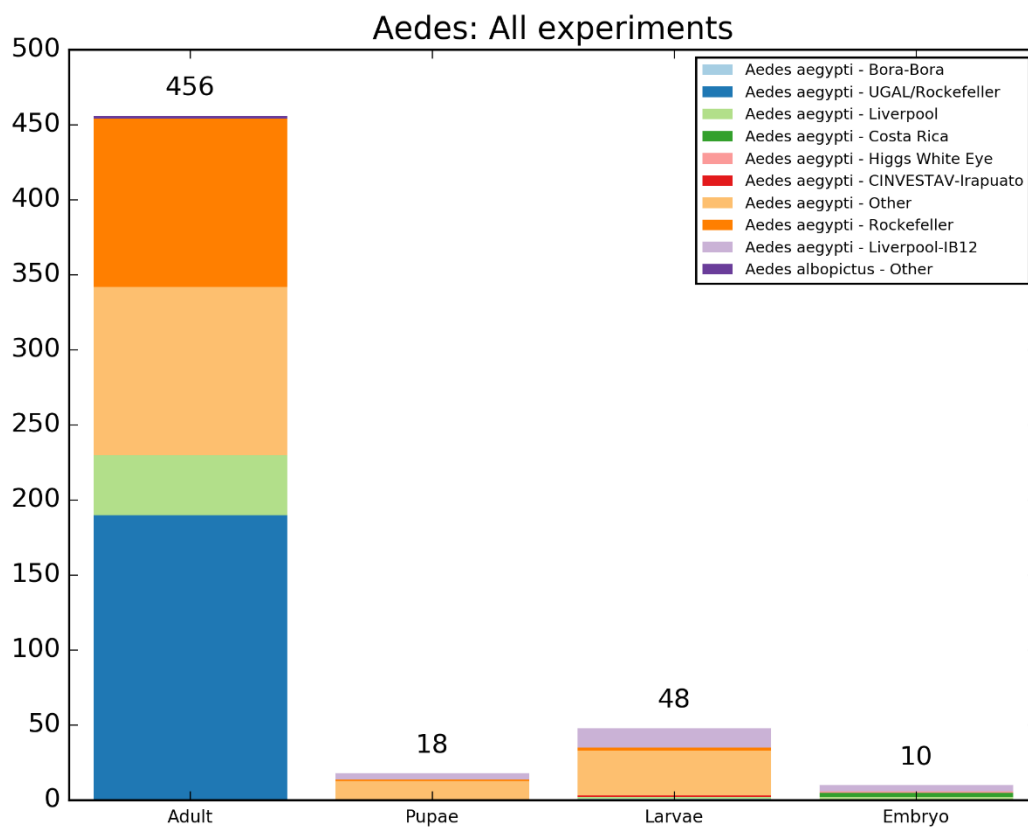
Supplementary Figure 2 – RNAi experiments displayed as number of experiments per life stage per strains in *Anopheles* species.
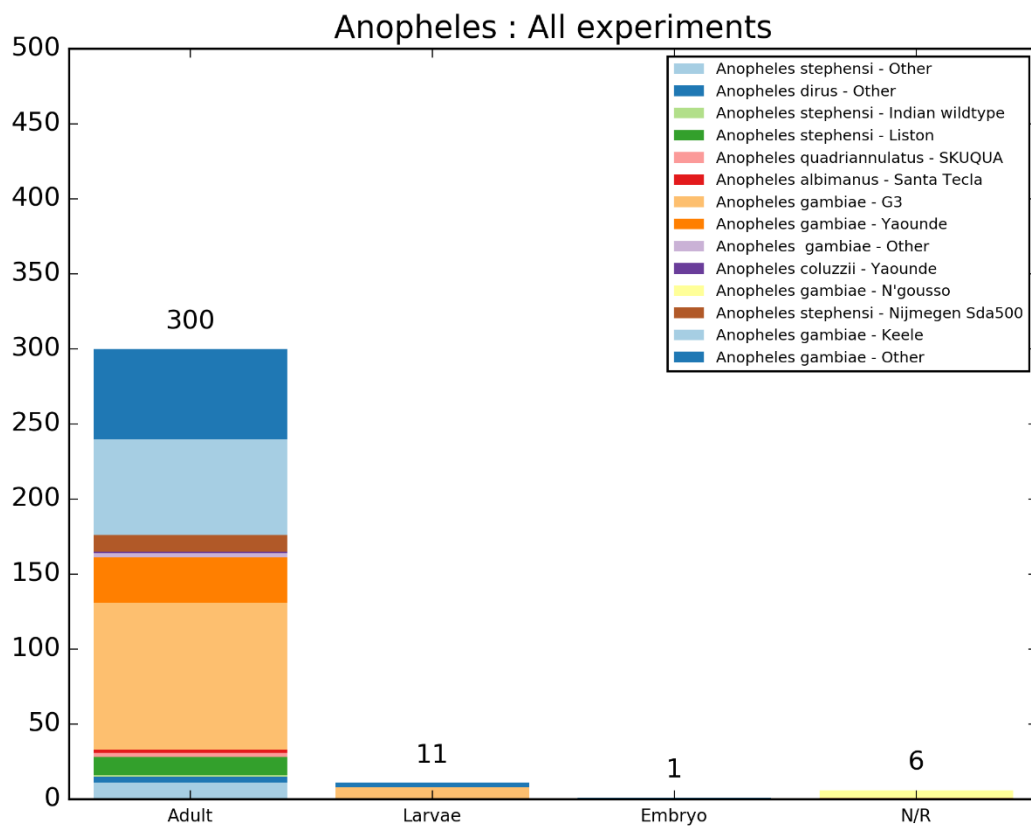
Supplementary Figure 3 – RNAi experiments displayed as number of experiments per life stage per strains in *Culex* species.
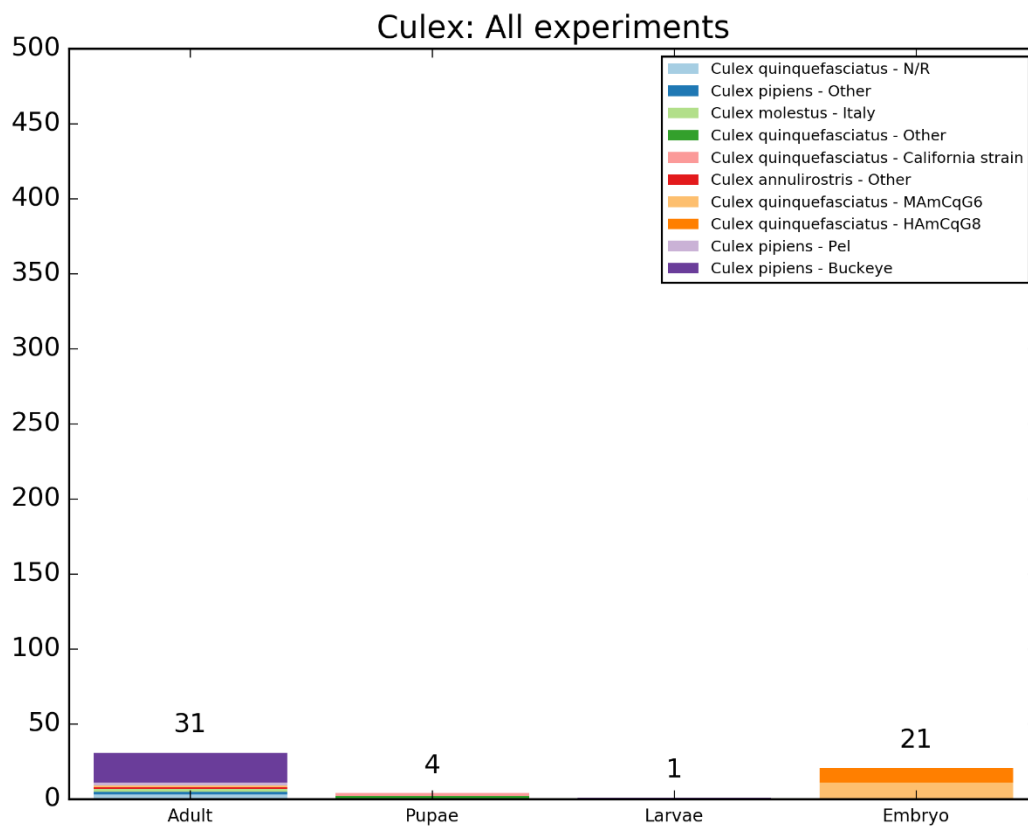
Supplementary Figure 4 – RNAi trigger dose is not correlated to knockdown across all experiments as measured by linear regression. Blue bar indicates linear regression trend line with gray shaded error.
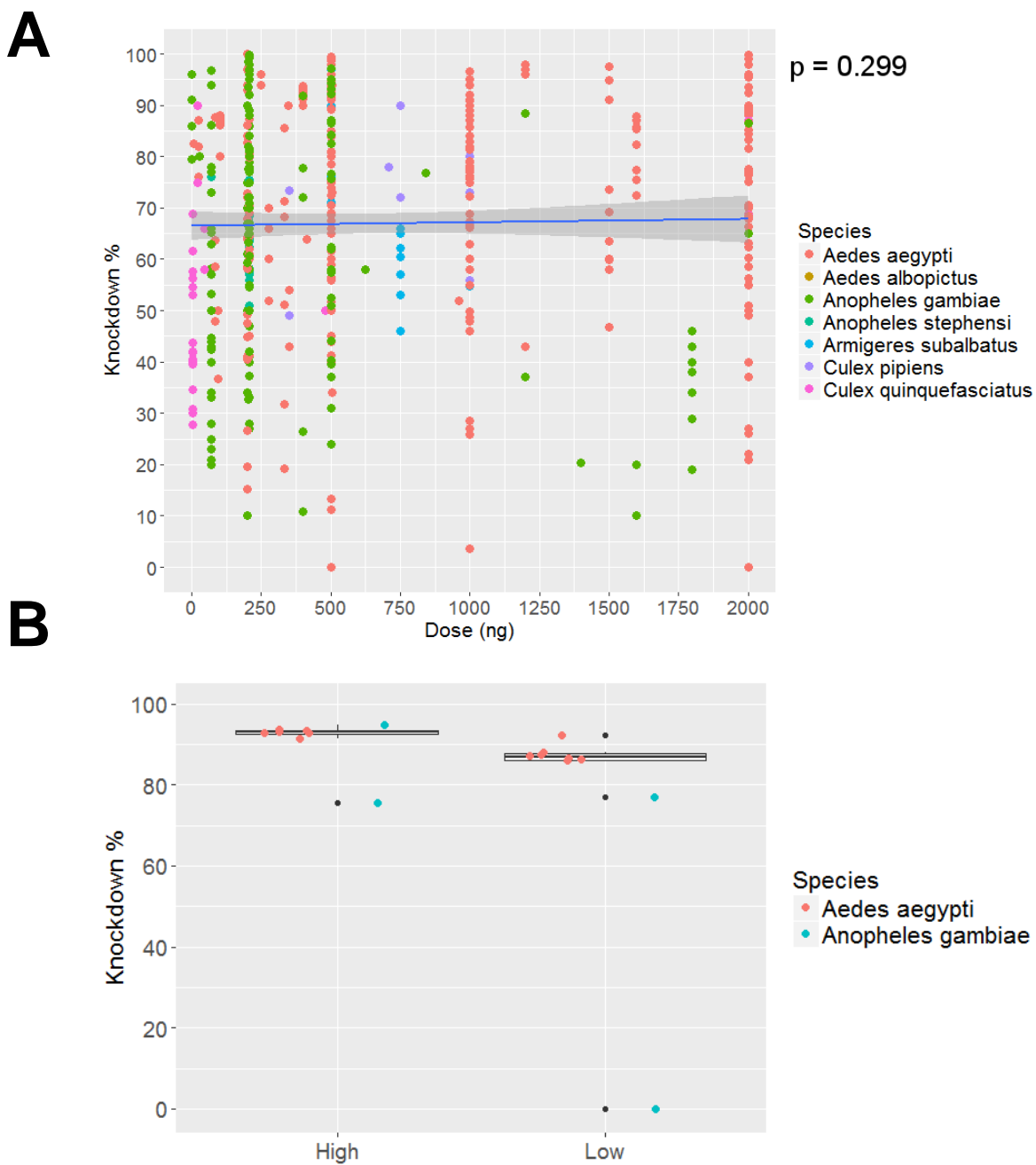
Supplementary Figure 5 – Infection status does not correlate to RNAi knockdown across species. Infected (TRUE) and uninfected (FALSE) individuals during RNAi experiments as measured by two tailed Welches T-Test.
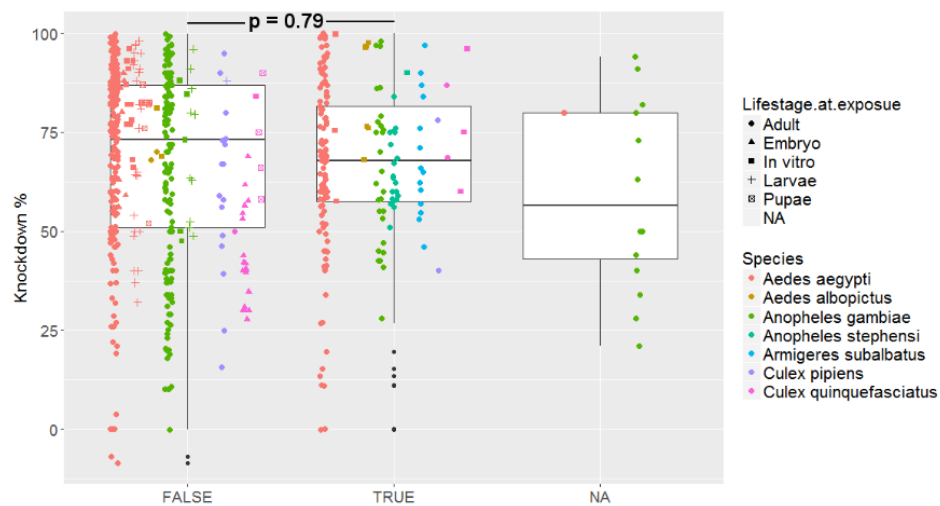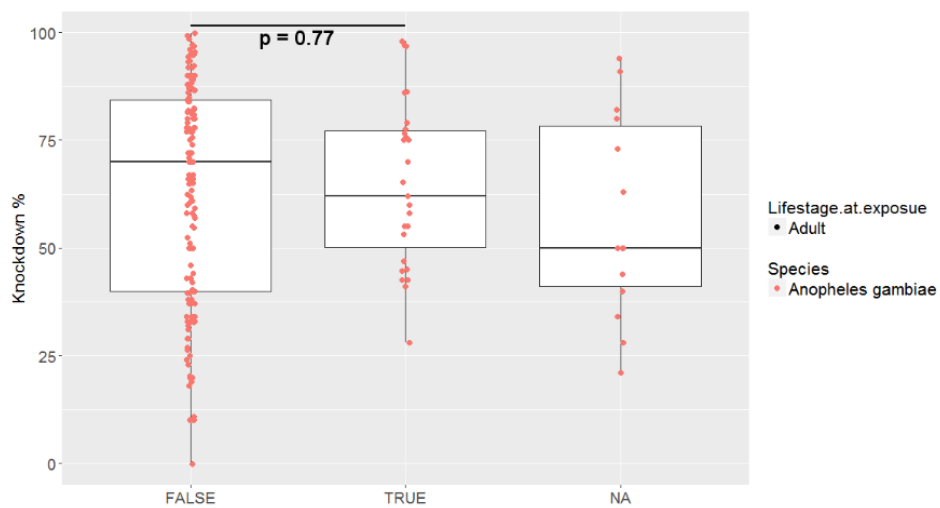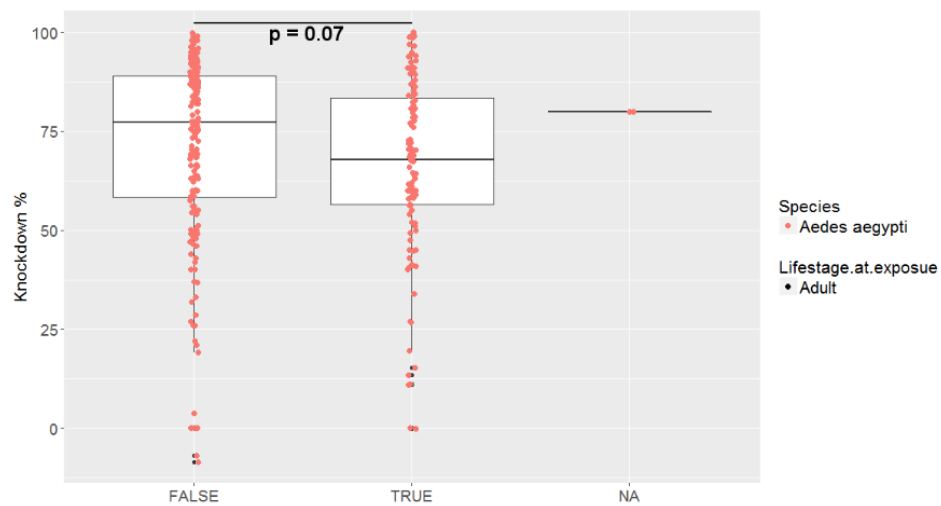
Supplementary Figure 6 – Timing is not related to knockdown across all experiments. (A) Age of adult female mosquitoes at the time of exposure correlated to knockdown and (B) time of knockdown measurement post exposure correlated to knockdown in all experiments. Blue bar indicates linear regression trend line with gray shaded error.
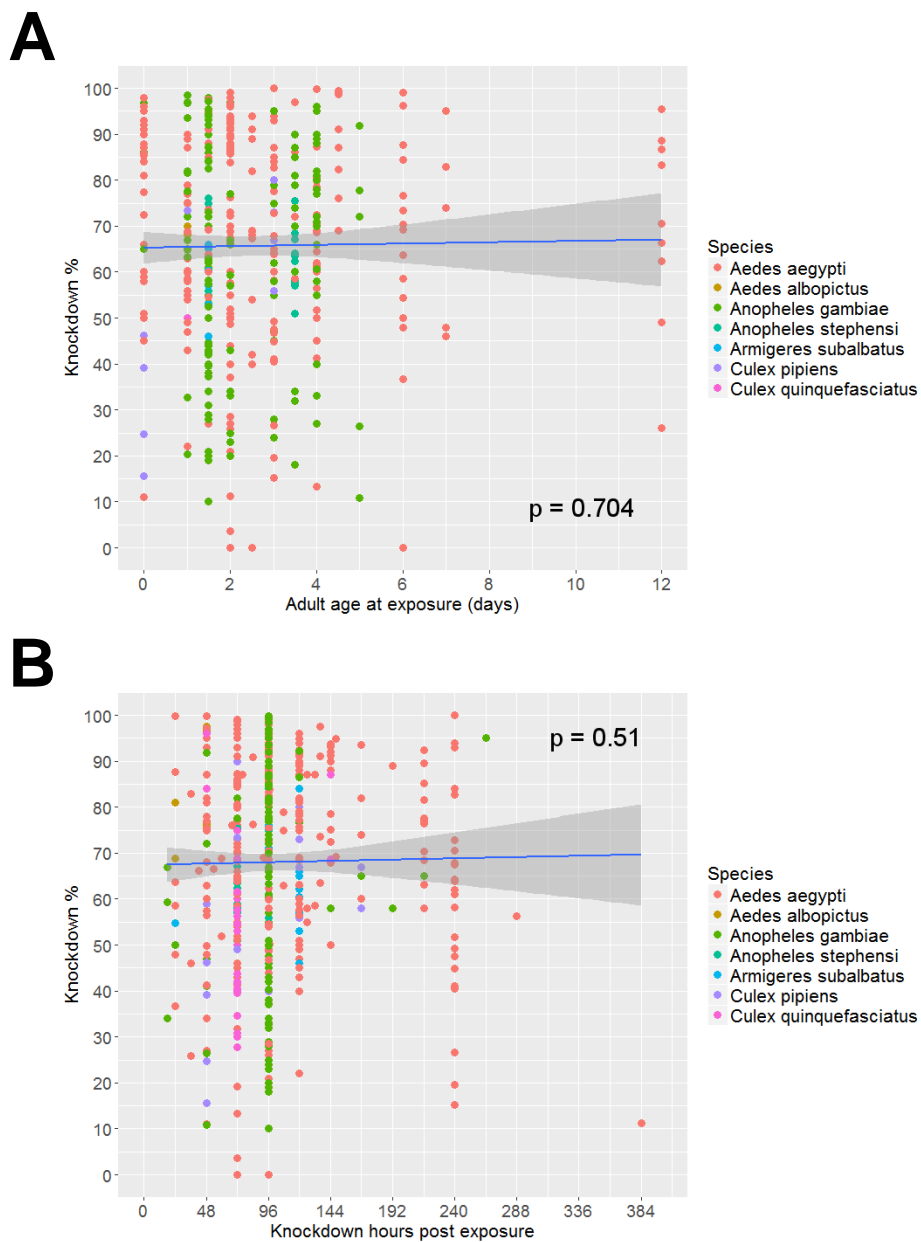
Supplementary Figure 7 – RNAi trigger length does not correlate to increased knockdown.

(A) Length of trigger in base-pairs, or (B) length of trigger as a proportion of the target gene coding sequence covered. Blue bar indicates linear regression trend line with gray shaded error.
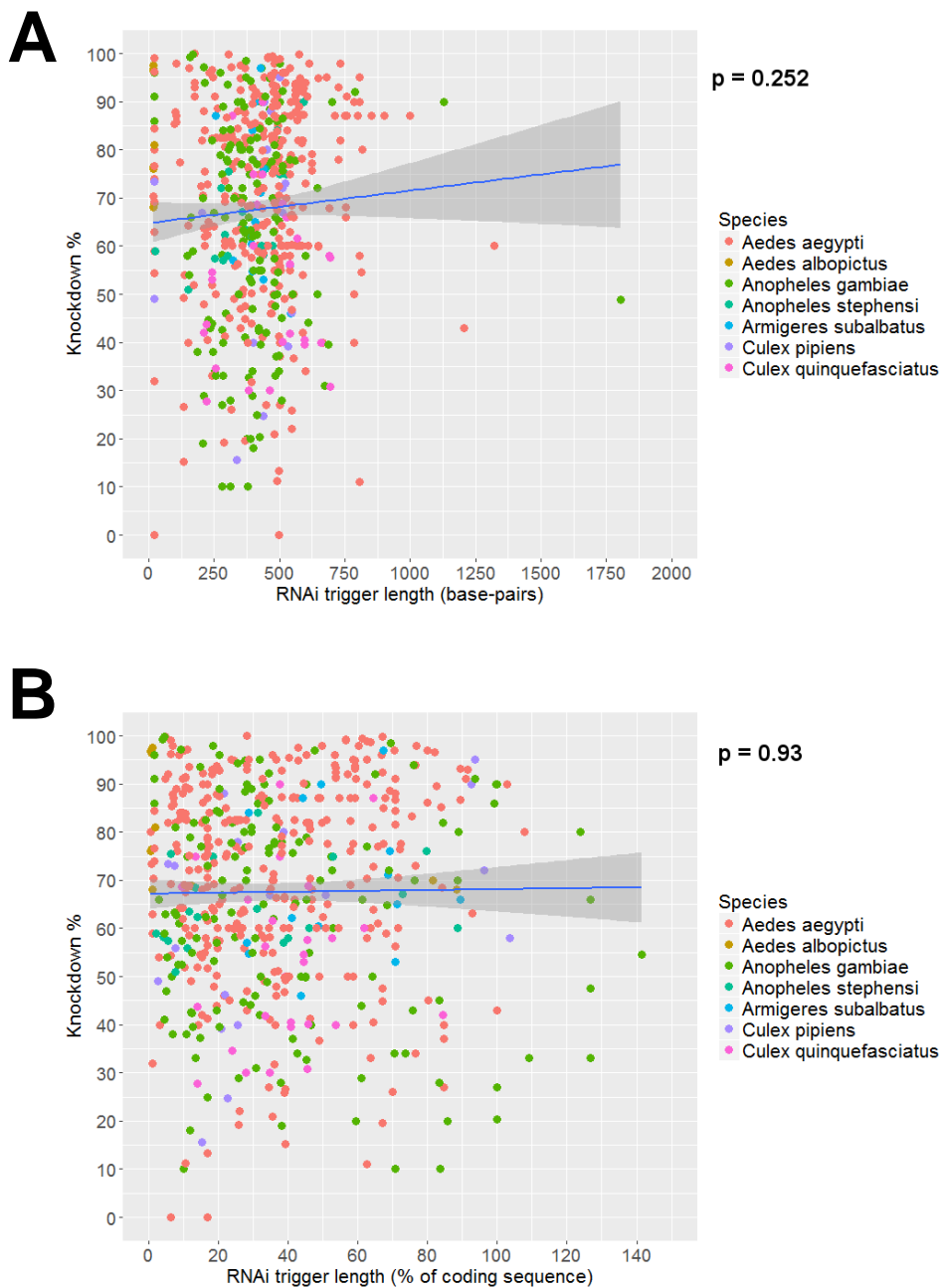
Chapter 6 – Impact of sugar composition on meal distribution, longevity, and insecticide toxicity in *Aedes aegypti*

Abstract

Attractive Toxic Sugar Baits (ATSBs) are an inexpensive and field applicable approach to deliver a variety of insecticides to sugar-seeking mosquitoes. We reasoned that carbohydrate chemistry could alter the performance and efficacy of ATSBs, so tracked the uptake, distribution, and impact on survival for female *Aedes aegypti* provided with twelve different aqueous sugar meals. We observed that sucrose is always diverted to the ventral diverticulum, but maltose, mannose, and raffinose sugars disperse to both the diverticulum and midgut. Sugar meals composed of arabinose, lactose, or cellobiose are significantly more toxic to *Ae. aegypti* than sucrose, with or without the addition of boric acid insecticide. The addition of arabinose to simple ATSBs (comprised of sucrose and boric acid insecticide) increased mortality even in the presence of non-toxic sugar sources. In choice assays, mosquitoes were equally likely to feed on ATSBs with arabinose despite the toxicity associated with arabinose ingestion. Furthermore, we assessed the biodistribution of double-stranded RNA (dsRNA) and the potency of boric acid and as a function of sugar composition. Despite altering uptake destination, *per os* delivery of dsRNA in different sugar meals results in formation of large precipitates that pass through the alimentary tract with no detectable uptake into midgut epithelia or other tissues. We conclude that sourcing sugar meals with sugars that have inherent toxic properties may improve ATSB efficacy in the field.

Introduction

Mosquito vector and nuisance species are increasingly thwarting control efforts as a result of metabolic and genotypic insecticide resistance (Liu, 2015; Russell et al., 2011). Populations of the Yellow fever mosquito, *Aedes aegypti*, are resistant to pyrethroids, organophosphates, and organochlorines across many continents (Vontas et al., 2012). New strategies, including novel delivery modalities and new chemistries with different modes of action are desperately needed to re-build an arsenal of approaches to combat mosquito-borne disease (Zaim and Guillet, 2002). Current control options target for adult mosquitoes target those that are on the wing (e.g., ultra-low volume contact spray), resting (e.g., insecticide residual spraying) or host-seeking (insecticide impregnated fabrics in homes) (Raghavendra et al., 2011; Rose, 2001). Attractive Toxic Sugar Baits (ATSBs) are an emerging insecticide delivery modality that involves provision of an insecticide-spiked simple sugar solution that acts as an attractant for nectar-seeking mosquitoes. ATBSs offer a cost-effective field-applicable intervention approach that targets a different and essential physiological demand (Fiorenzano et al., 2017; Foster, 1995). In current formulations, sugars act as attractants and phago-stimulants; but their role in meal destination and impact on ATSB efficacy is often overlooked.

Plants provide shade, ovipositional sites, and offer essential nourishment for flight and reproduction in mosquitoes (Clements, 1992; Foster, 1995). Understanding the role of plants in mosquito survival is therefore key to any control effort. Major vector species, including *Ae. aegypti, Ae. albopictus,* and *Anopheles gambiae,* have species-specific preferences for particular flowers, fruits, and seed pods (Ignell et al., 2010; Manda et al., 2007a; Manda et al., 2007b; Muller et al., 2011). Floral nectaries provide essential sugars to meet the energetic demands of mosquito activity and are frequently visited by both male and female mosquitoes, the latter of which feed on

nectar when available, both before and after blood-feeding (Foster, 1995; Martinez-Ibarra et al., 1997). Nutrition provided by preferred plants also significantly increases longevity, egg batch size, and vector competence (Gu et al., 2011; Manda et al., 2007a; Manda et al., 2007b; Muller et al., 2017). Sucrose is a major component of many floral nectars, is readily resourced, and inexpensive. As such, sucrose is a standard delivery substrate for oral insecticides in ATSBs in laboratory settings and in the field (Fiorenzano et al., 2017). In actual floral nectaries with high sucrose content, mosquitoes also encounter mono- and oligosaccharides including mannose, galactose, raffinose, maltose, and melibiose; many of which have been isolated from mosquito midguts (Manda et al., 2007a; Manda et al., 2007b; Percival, 1961; Wykes, 1952). In addition to floral nectaries, honeydew, extra-floral nectaries, tree sap, and foliage contain a broader diversity of sugars on which mosquitoes can feed but which are rarely studied (Foster, 1995; Ignell et al., 2010; Muller and Schlein, 2005; Muller et al., 2011). The impact of different sugars and sugar compositions on attractiveness and efficacy of ATSBs has yet to be elucidated.

Beyond impacting fitness, sugars have species-specific effects in terms of ingestion prevalence, volume, and distribution in the alimentary canal (Friend et al., 1988; Friend et al., 1989; Galun and Fraenkel, 1957). Chemoreceptors on the labrum, labella, tarsi, and cibarium likely dictate the biochemical decision-making process that result in the distinct distribution of sugar and blood meals (Friend and Smith, 1977). In *Culiseta inornata*, the destination of sugars is dependent on the chemical structure of the sugar meal; sugars containing B-glucosidyl linkages, such as cellobiose and raffinose, are diverted to the midgut (Schmidt and Friend, 1991). In *Ae. aegypti,* sucrose meals are directed exclusively to the diverticula and blood meals are directed exclusively to the midgut (Trembley, 1952). In *Anopheles quadrimaculatus* and *Culex pipiens,* blood is sometimes found in the ventral diverticulum as well as the midgut (Day, 1954; Trembley, 1952).

When combined, blood and sugar meals appear in both the midgut and the diverticula in *Ae. aegypti*, depending on concentration (Day, 1954). *Ae. aegypti* also show a strong preference for disaccharides over monosaccharides, and particularly prefer sucrose over other sugars (Ignell et al., 2010). Therefore, we reasoned that sugar distribution fate could alter attraction to, uptake, and potency of ATSBs. Active ingredients used in ATSBs range from broad-spectrum insecticides (boric acid, pyrethroids, spinosad) to species-specific RNAi triggers (Fiorenzano et al., 2017). Additionally the attractant sugar used in ATSBs ranges from simple sucrose solutions to fruit juices. Combinations of sugars are known to impact longevity in *Ae. aegypti* but have yet to be studied in the context of ATSB potency (Galun and Fraenkel, 1957). In this study we examine the uptake, distribution, and effect on longevity of 12 different sugars post-ingestion in *Ae. aegypti*. We aslo assess the impact of sugar meal composition on delivery of ATSB chemical (boric acid) and molecular (double-stranded RNA) insecticides.

Materials and methods

Mosquito rearing and sugar exposure

Aedes aegypti Liverpool strain mosquitoes were maintained at 28 °C in 70% relative humidity with a 16:8 hour (light:dark) photoperiod. Larvae were fed daily with a slurry of ground TetraMin™ (Blacksburg, VA) in ddH$_2$O. Unless otherwise stated, 50 female pupae were collected in cartons and maintained on a 10% sucrose diet for the first 24 hours post-eclosion, then starved for 48-72 hours prior to sugar exposure. Sugars tested include: monosaccharides (Arabinose (L-(+)-Arabinose, Sigma, A3256-25G), Fructose (D(-)Fructose, Sigma, F3510), Galactose (D(+)Galactose, Sigma, G6404-10G), Glucose (β-D-Glucose, MP Biomedicals, 100953), Mannose (D(+)-Mannose, Sigma, M-8296)), disaccharides (Cellobiose (D(+)-Cellobiose, 98%; Acros Organics, 528-50-7), Lactose (Lactose, Acumedia, 7231A), Maltose (Maltose, Sigma, M-

5885), Melibiose (α-D-Melibiose, Chem-Impex International), Sucrose (Sucrose, Roundy's), Trehalose (D-(+)-Trehalose Dihydrate, Fisher BioReagents, BP2687100)), and a trisaccharide (Raffinose (D(+)-Raffinose, Sigma, R-0514)). All sugars were prepared at a concentration of 0.5 M, with the exception of Cellobiose (0.25 M), in autoclaved ddH$_2$O and heated to 55 $^{\circ}$C in a water bath to dissolve precipitate if necessary.

Blood-feeding

Starved mosquitoes (n = 50) were exposed to defibrinated sheep blood (HemoStat Laboratories, CA) through a Parafilm M® (Bemis company®, WI) membrane, using a blown glass membrane feeder. Following blood-feeding, mosquitoes were cold-immobilized so that unfed or partially fed individuals could be removed.

Sugar distribution, uptake prevalence, and engorgement

Starved mosquitoes (n = 50) were exposed to cotton wicks in a 1.5 mL tube with a sugar solution containing 0.5% red food dye (Red food color, McCormick®, MD) for 30 minutes. Specimens were cold-immobilized at 4 $^{\circ}$C, counted, and inspected for presence of dye in the abdomen while on ice using a Zeiss Stemi 508 dissection microscope. For each replicate of the experiment, alimentary tracts of fifteen visibly fed or engorged mosquitoes were dissected in PBS and observations were recorded for the destination and volume of the dyed sugar solution present in the diverticulum, midgut, or both. The amount of sugar and dye in the respective area of the alimentary canal was marked as absent (not visible), present (visible but not filling the tissue), or engorged (filling the entire volume of the tissue to the point of distention). Three to five replicates with 50 mosquitoes per group were performed.

Insecticide toxicity assays

Starved mosquitoes (n = 50) were fed *ad libitum* on sugar soaked cotton pads either with or without 0.25% boric acid; these cotton pads were replaced every 24-48 hours for ten days. Dead mosquitoes were removed by aspiration and counted daily. Three to six replicates were performed for each combination of sugar with boric acid.

Choice assay

Starved mosquitoes (n = 30-50) were provided two cotton pads soaked in 10 mL of sugar / 0.25% boric acid solution containing 65 μL of red or blue food dye (McCormick®, MD) for one hour. Food dye color was alternated between groups for each replicate. One pad of each group contained sucrose only to serve as a preference control. Individuals were cold anesthetized at 4 °C and held on ice to inspect the whole body for the presence of dye(s) in the abdomen. Three replicates were performed.

Tracking dsRNA distribution per os

A 377 bp fragment of LacZ (pGEM T-easy, Promega) was amplified using GoTaq Flexi DNA polymerase (Promega) with Forward (TAATACGACTCACTATAGGG-CTTTTGCTGGCCTTTTGCTC) and Reverse (TAATACGACTCACTATAGGG-CGTAATCATGGTCATAGCTGTTTCC) primers (presented with the T7 sequence underlined). PCR products were purified by Wizard® SV PCR Clean-Up kit (Promega) tested by gel and NanoDrop (Thermo Scientific) then subject to dsRNA synthesis using the MEGAscript™ T7 RNAi kit (Ambion). dsRNA was purified by phenol:chloforom cleanup, and isopropanol

precipitation followed by fluorescent tagging using the Cy3 Label IT® kit (Mirus). dsRNA was then tested by gel and NanoDrop (Thermo Scientific). Five to 7 borosilicate glass capillary tubes (Kwik-Fill™, World Precision Instruments) were filled with ~10 µl of dsRNA (1 mg/ml) in 0.5 M sugar solutions and immediately provided to groups of 20 starved mosquitoes for 24 hours (see Fig. S1). Individuals were then cold-anesthetized at 4 °C and dissected (n = 5) in PBS as described above, fixed in 4% paraformaldehyde at 4 °C and imaged by Zeiss Axio Scope.A1 and Nikon Elements D software. Three replicates of the feeding assay were performed.

Results & Discussion

The primary sugars used for ATSB formulations are sucrose or a fruit juice blend along with boric acid or similar broad spectrum insecticide (Fiorenzano et al., 2017; Muller et al., 2010a; Muller et al., 2010b; Qualls et al., 2015). The effectiveness of boric acid as an oral insecticide has been recorded, but the physiological effects of the sugars aloneoften is not documented. There is a growing body of evidence showing the impact of plant sugar availability and fitness. For instance, Mangoes (*Mangifera indica*) are known to reduce longevity, egg production, and *Plasmodium falciparum* infection intensity compared to glucose (Hien et al., 2016). Mangoes and other fruits contain cellulose, arabinose, and galactose in abundance mostly in pectin polysaccharides, which can be released by fungal enzymatic degradation when rotting (Ahmed and Labavitch, 1980; Núñez Sellés et al., 2002; Olle et al., 2000; Prasanna et al., 2004). In the present study, we assess the role of 12 sugars in feeding physiology, longevity, and capacity to deliver oral insecticides.

Sugar meal composition alters uptake and distribution in Ae. aegypti

Sugar uptake was assessed in *Ae. aegypti* females, measured as the proportion of individuals with visibly distended abdomens following a 30 minute exposure to 12 different sugar meals (Table 1).

Raffinose, a trisacscharide was the sugar on which the highest proportion (85.1%) of mosquitoes fed to engorgement, followed by the disaccharides maltose (80.4%), trehalose (75.9%), and sucrose (75.5%).

Sugar distribution was measured as a percent of engorged tissues from fed individuals (Table 1, Fig. S2). As expected, all of the sugars tested were primarily directed to the sugar storage organ, the ventral diverticulum. Sugars were also directed to the midgut to varying extents for all sugars, except arabinose and fructose which were never observed in the midgut. Interestingly, raffinose sugar meals were observed exclusively in the midgut of 70.9% of individuals (Table 1). To determine whether temperature alters uptake prevalence or distribution, sucrose meal distribution was tracked at 21 ºC and 37 ºC; no significant differences in proportion fed or tissue distribution were observed (Fig. S3). These data corroborate previous findings for *Ae. aegypti* preference of di- saccharides over mono- saccharides but this is true only for certain sugars (Ignell et al., 2010).

Arabinose, lactose, and cellobiose decrease adult female Ae. aegypti longevity

Survival of *Ae. aegypti* exposed to 12 different sugars was assessed over a ten-day period. Arabinose, cellobiose, and lactose significantly reduced survival compared to sucrose and water controls but not compared to the starved group, which died at a faster or similar rate (Fig. 1). Fructose, galactose, glucose, maltose, mannose, melibiose, raffinose, sucrose, and trehalose treatment groups increased survival compared to water, but differed in end point survival (Fig. S4). Galactose and melibiose treatment groups displayed 42.5% and 40.7% mortality respectively, significantly lower than the sucrose control (13.4%) (Fig. S4). Following exposure to lactose,

many individuals exhibited considerable abdominal distension and died, a phenotype rarely seen in dead individuals in other groups (Fig. 1B).

Although arabinose and lactose appear to induce mortality, it is unclear whether death is a function of starvation, acute toxicity, or both. To elucidate whether sugar meal composition impacts mosquito longevity in a nutrient rich background, survival assays were performed with *Ae. aegypti* provided with arabinose, lactose, galactose, or sucrose meals immediately following a blood meal (Fig. 1C). Mosquitoes provided with galactose and sucrose survived as expected, but arabinose and lactose-exposed groups died at a similar rate to mosquitoes exposed to arabinose and lactose in the absence of a blood meal (compare Fig. 1A & 1C). This confirms previous findings regarding the propensity of *Ae. aegypti* to sugar feed both before and after blood-feeding (Martinez-Ibarra et al., 1997).

To investigate whether the impact of arabinose or lactose on longevity was a function of acute toxicity, survival was monitored following exposure to sugars mixed with sucrose at 0.5 M and at 0.25 M concentrations (Fig. 1D). The presence of sucrose reduced, but did not eliminate, mortality as compared to arabinose or lactose meals alone in a dose-dependent manner (compare Fig. 1A & 1D). Lower concentrations of arabinose and lactose were associated with a decrease in mortality (Fig. 1D). This result indicates that both arabinose and lactose induce mortality, regardless of the availability of sucrose.

Sugar meal composition alters boric acid potency in Ae. aegypti

Reduced longevity of *Ae. aegypti* following uptake of arabinose, lactose, or cellobiose prompted the question of whether sugar meal composition can be altered to enhance the potency of ATSB solutions. To test this, *Ae. aegypti* survival was monitored following exposure to sugar solutions

spiked with 0.25% boric acid (Fig. 2, Fig. S5). Results were similar to survival with sugars alone, in that exposure to toxic sugars (arabinose, cellobiose, lactose) resulted in an increased rate of death compared to non-lethal sugars (galactose, maltose, melibiose, raffinose, sucrose). If greater uptake or delivery of boric acid to the midgut was limiting to boric acid toxicity, raffinose and maltose would be expected to induce death at a greater rate compared to other groups, which was not the case (compare Fig. S2 and Fig. S5). Therefore, the uptake and destination of an ATSB does not drastically alter potency of the ATSB active ingredient, but the presence of inherently toxic sugars does.

Arabinose & sucrose mixtures enhance ATSB potency without decreasing attractiveness.

Initial survival assays indicated lactose and arabinose as potential ATSB active ingredients. Lactose was both unattractive (see Table 1) and ineffective when mixed with sucrose (see Fig. 1D), while arabinose was the readily fed upon and induced the most rapid mortality alone (Fig. 1A), in combination with sucrose (Fig. 1D), and in combination with boric acid (Fig. 2 & Fig. S3). As such, arabinose was selected for further study.

The utility of supplementing ATSBs with toxic sugars will be limited if the ATSB is inherently repellent or less attractive than nearby sugar sources. To test the attractiveness of arabinose compared to sucrose, we designed a choice assay comparing uptake and survival following exposure to sugar meals with and without boric acid and in the presence of non-toxic sucrose controls (Fig. 3A). Uptake prevalence was measured by presence of dye when exposed to a non-toxic sucrose control versus solutions of sucrose arabinose, and/or 0.25% boric acid (Fig. 3B, Fig. S6). There was no significant preference for or against 0.25% boric acid, but 100% of fed individuals chose sugar over arabinose (Fig. 3B). The addition of sucrose to arabinose solutions

abated any preference for the sucrose only control, indicating that arabinose is not repellent, but may not be as attractive as sucrose (Fig. 3B). In *Drosophila melanogaster,* arabinose elicits a weak sweet gustatory sensor response while lactose elicits no response (Dahanukar et al., 2007). These findings suggest that arabinose likely does not strongly trigger a gustatory response in *Ae. aegypti,* despite being toxic. Individuals rarely fed on both sugars, or failed to feed during the choice assay, but this did not differ between groups (Fig. S6).

Following the choice assay, groups were continuously exposed to treatment groups and non-toxic sucrose controls and monitored for survival (Fig. 3C). Providing a non-toxic sucrose meal increased longevity of *Ae. aegypti* exposed to boric acid or arabinose (compare Fig. 3C with Fig. 2 and Fig. 1A & D). However, exposure to arabinose/boric acid resulted in 41% mortality 10 days post-exposure, indicating that some feeding on non-preferred sugars still occurs even in the presence of more attractive sucrose meals. The addition of arabinose to sucrose as well as sucrose/boric acid solutions resulted in the highest mortality (Fig. 3C). These results reveal that optimizing sugar compositions can enhance attractiveness, uptake, sugar meal destination, and lethality of an ATSB and perhaps other *per os* insecticide formulations.

Sugar destination does not facilitate uptake of dsRNA

RNAi triggers offer a highly tailored, species- and even tissue-specific alternative to boric acid and other broad spectrum insecticides currently used as ATSB active ingredients (Airs and Bartholomay, 2017). RNAi triggers have been effectively delivered *per os* in a variety of insect taxa and incorporation of RNAi trigger insecticides in ATSBs is of great interest as a means of improving ATSB species-specificity (Fiorenzano et al., 2017; Whyard et al., 2009). To determine whether sugar meals can facilitate uptake and spread of RNAi triggers, fluorescently labelled

dsRNA was provided to *Ae. aegypti* adult females in sugar solutions with a propensity to locate to the ventral diverticulum (sucrose) or to the midgut (maltose, mannose, and raffinose). Strong signal was found throughout the alimentary canal. But in each case, fluorescence was limited to the lumen barrier and did not cross into gut cells (Fig. 4). No dsRNA was detected in any tissue outside of the alimentary lumen with the exception of dsRNA detection in the proboscis in raffinose fed individuals (Fig. S7). Condensation of dsRNAs into small and large clumps was observed in the ventral diverticulum of individuals provided sucrose and maltose groups (Fig. S7D). Following condensation in the ventral diverticulum, dsRNA signal accumulated in the midgut and hindgut, but was not seen in the Malpighian tubules (Fig. S7E). Clumping of dsRNA possibly contributes to the lack of uptake and dissemination to other tissues when delivered *per os*.

We observed that dsRNA delivered to the ventral diverticulum exhibits clumping as the contents of the diverticulum dehydrate, possibly causing the dsRNA to increase in concentration to the point of precipitation (Fig. S7).

Conclusions

Collecting and testing sugar contents of known anti-mosquito plants may act as a key resource for integrated pest management strategies in the eradication of mosquito-borne disease. This study highlights the impact of sugar meal composition on mosquito attraction, longevity, and ATSB efficacy. Further understanding of toxic elements of attractive plants may also be invaluable in generating naturally sourced ATSBs and improving ATSB formulations.

Acknowledgements

Literature cited

Ahmed, A.E., Labavitch, J.M., 1980. Cell Wall Metabolism in Ripening Fruit. Plant Physiology 65, 1009.

Airs, P.M., Bartholomay, L.C., 2017. RNA Interference for Mosquito and Mosquito-Borne Disease Control. Insects 8.

Clements, A.N., 1992. The biology of mosquitoes, First edition. ed. Chapman & Hall, London ; New York.

Dahanukar, A., Lei, Y.T., Kwon, J.Y., Carlson, J.R., 2007. Two Gr genes underlie sugar reception in Drosophila. Neuron 56, 503-516.

Day, M.F., 1954. The mechanism of food distribution to midgut or diverticula in the mosquito. Aust J Biol Sci 7, 515-524.

Fiorenzano, J.M., Koehler, P.G., Xue, R.D., 2017. Attractive Toxic Sugar Bait (ATSB) For Control of Mosquitoes and Its Impact on Non-Target Organisms: A Review. Int J Environ Res Public Health 14, 398.

Foster, W.A., 1995. Mosquito sugar feeding and reproductive energetics. Annu Rev Entomol 40, 443-474.

Friend, W.G., Schmidt, J.M., Smith, J.J.B., Tanner, R.J., 1988. The Effect of Sugars on Ingestion and Diet Destination in Culiseta-Inornata. Journal of Insect Physiology 34, 955-961.

Friend, W.G., Smith, J.J., 1977. Factors affecting feeding by bloodsucking insects. Annu Rev Entomol 22, 309-331.

Friend, W.G., Smith, J.J.B., Schmidt, J.M., Tanner, R.J., 1989. Ingestion and Diet Destination in Culiseta-Inornata - Responses to Water, Sucrose and Cellobiose. Physiological Entomology 14, 137-146.

Galun, R., Fraenkel, G., 1957. Physiological effects of carbohydrates in the nutrition of a mosquito, Aedes aegypti and two flies, Sarcophaga bullata and Musca domestica. J Cell Comp Physiol 50, 1-23.

Gu, W., Muller, G., Schlein, Y., Novak, R.J., Beier, J.C., 2011. Natural plant sugar sources of Anopheles mosquitoes strongly impact malaria transmission potential. PLoS One 6, e15996.

Hien, D.F., Dabire, K.R., Roche, B., Diabate, A., Yerbanga, R.S., Cohuet, A., Yameogo, B.K., Gouagna, L.C., Hopkins, R.J., Ouedraogo, G.A., Simard, F., Ouedraogo, J.B., Ignell, R., Lefevre, T., 2016. Plant-Mediated Effects on Mosquito Capacity to Transmit Human Malaria. PLoS Pathog 12, e1005773.

Ignell, R., Okawa, S., Englund, J.E., Hill, S.R., 2010. Assessment of diet choice by the yellow fever mosquito Aedes aegypti. Physiological Entomology 35, 274-286.

Liu, N., 2015. Insecticide resistance in mosquitoes: impact, mechanisms, and research directions. Annu Rev Entomol 60, 537-559.

Manda, H., Gouagna, L.C., Foster, W.A., Jackson, R.R., Beier, J.C., Githure, J.I., Hassanali, A., 2007a. Effect of discriminative plant-sugar feeding on the survival and fecundity of Anopheles gambiae. Malar J 6, 113.

Manda, H., Gouagna, L.C., Nyandat, E., Kabiru, E.W., Jackson, R.R., Foster, W.A., Githure, J.I., Beier, J.C., Hassanali, A., 2007b. Discriminative feeding behaviour of Anopheles gambiae s.s. on endemic plants in western Kenya. Med Vet Entomol 21, 103-111.

Martinez-Ibarra, J.A., Rodriguez, M.H., Arredondo-Jimenez, J.I., Yuval, B., 1997. Influence of plant abundance on nectar feeding by Aedes aegypti (Diptera: Culicidae) in southern Mexico. J Med Entomol 34, 589-593.

Muller, G., Schlein, Y., 2005. Plant tissues: the frugal diet of mosquitoes in adverse conditions. Med Vet Entomol 19, 413-422.

Muller, G.C., Beier, J.C., Traore, S.F., Toure, M.B., Traore, M.M., Bah, S., Doumbia, S., Schlein, Y., 2010a. Successful field trial of attractive toxic sugar bait (ATSB) plant-spraying methods against malaria vectors in the Anopheles gambiae complex in Mali, West Africa. Malar J 9, 210.

Muller, G.C., Junnila, A., Schlein, Y., 2010b. Effective control of adult Culex pipiens by spraying an attractive toxic sugar bait solution in the vegetation near larval habitats. J Med Entomol 47, 63-66.

Muller, G.C., Junnila, A., Traore, M.M., Traore, S.F., Doumbia, S., Sissoko, F., Dembele, S.M., Schlein, Y., Arheart, K.L., Revay, E.E., Kravchenko, V.D., Witt, A., Beier, J.C., 2017. The

invasive shrub Prosopis juliflora enhances the malaria parasite transmission capacity of Anopheles mosquitoes: a habitat manipulation experiment. Malar J 16, 237.

Muller, G.C., Xue, R.D., Schlein, Y., 2011. Differential attraction of Aedes albopictus in the field to flowers, fruits and honeydew. Acta Trop 118, 45-49.

Núñez Sellés, A.J., Vélez Castro, H.T., Agüero-Agüero, J., González-González, J., Naddeo, F., De Simone, F., Rastrelli, L., 2002. Isolation and Quantitative Analysis of Phenolic Antioxidants, Free Sugars, and Polyols from Mango (Mangifera indicaL.) Stem Bark Aqueous Decoction Used in Cuba as a Nutritional Supplement. Journal of Agricultural and Food Chemistry 50, 762-766.

Olle, D., Baron, A., Lozano, Y.F., Brillouet, J.M., 2000. Enzymatic degradation of cell wall polysaccharides from mango (Mangifera indica L.) puree. J Agric Food Chem 48, 2713-2716.

Percival, M.S., 1961. Types of Nectar in Angiosperms. The New Phytologist 60, 235-281.

Prasanna, V., Prabha, T.N., Tharanathan, R.N., 2004. Pectic polysaccharides of mango (Mangifera indica L): structural studies. Journal of the Science of Food and Agriculture 84, 1731-1735.

Qualls, W.A., Muller, G.C., Traore, S.F., Traore, M.M., Arheart, K.L., Doumbia, S., Schlein, Y., Kravchenko, V.D., Xue, R.D., Beier, J.C., 2015. Indoor use of attractive toxic sugar bait (ATSB) to effectively control malaria vectors in Mali, West Africa. Malar J 14, 301.

Raghavendra, K., Barik, T.K., Reddy, B.P., Sharma, P., Dash, A.P., 2011. Malaria vector control: from past to future. Parasitol Res 108, 757-779.

Rose, R.I., 2001. Pesticides and public health: integrated methods of mosquito management. Emerg Infect Dis 7, 17-23.

Russell, T.L., Govella, N.J., Azizi, S., Drakeley, C.J., Kachur, S.P., Killeen, G.F., 2011. Increased proportions of outdoor feeding among residual malaria vector populations following increased use of insecticide-treated nets in rural Tanzania. Malar J 10, 80.

Schmidt, J.M., Friend, W.G., 1991. Ingestion and Diet Destination in the Mosquito Culiseta-Inornata - Effects of Carbohydrate Configuration. Journal of Insect Physiology 37, 817-828.

Trembley, H.L., 1952. The distribution of certain liquids in the esophageal diverticula and stomach of mosquitoes. Am J Trop Med Hyg 1, 693-710.

Vontas, J., Kioulos, E., Pavlidi, N., Morou, E., della Torre, A., Ranson, H., 2012. Insecticide resistance in the major dengue vectors Aedes albopictus and Aedes aegypti. Pesticide Biochemistry and Physiology 104, 126-131.

Whyard, S., Singh, A.D., Wong, S., 2009. Ingested double-stranded RNAs can act as species-specific insecticides. Insect Biochem Mol Biol 39, 824-832.

Wykes, G.R., 1952. An Investigation of the Sugars Present in the Nectar of Flowers of Various Species. New Phytologist 51, 210-215.

Zaim, M., Guillet, P., 2002. Alternative insecticides: an urgent need. Trends Parasitol 18, 161-163.

Tables & Figures

Table 1 – Sugar meal composition alters uptake and destination in *Ae. aegypti*. Starved adult females exposed to sugar solutions for 30 minutes then inspected for proportion fed (n = 50). Engorged individuals dissected to determine location of sugar meal in the ventral diverticulum, midgut, or both (n = 15). All data are the average of 3 or more independent experiments (± SD).

Carbohydrate class	Name	Uptake prevalence (% ± SD)	Engorged tissues (% ± SD)				
			Ventral diverticulum only†	Midgut only†	Ventral diverticulum & Midgut	Ventral diverticulum allᐃ	Midgut allᐃ
Monosaccharide	Arabinose	40.5 (33.6)	100 (0.0)	0 (0)	0 (0)	100 (0.0)	0 (0)
	Fructose	55.6 (27.0)	100 (0.0)	0 (0)	0 (0)	100 (0.0)	0 (0)
	Galactose	41.9 (30.6)	83.7 (15.2)	2.5 (5)	13.8 (12.9)	97.5 (5)	16.3 (15.2)
	Mannose	17.2 (21.6)	44.4 (50.9)	16.7 (28.9)	38.9 (34.7)	83.3 (28.9)	55.6 (60)
	β-glucose	54.8 (7.5)	95.5 (3.8)	0 (0)	4.4 (3.8)	100 (0.0)	4.4 (3.8)
Disaccharide	Cellobiose	25.7 (29.8)	58 (41.1)	2 (3.4)	39.8 (38.3)	98 (3.4)	41.7 (41.1)
	Lactose	4.7 (2.1)	66.6 (57.8)	0 (0)	33.3 (57.8)	100 (0.0)	33.3 (57.8)
	Maltose	80.4 (14.1)	46.1 (18.6)	2.2 (3.8)	51.6 (21.2)	97.8 (38.5)	53.9 (18.6)
	Melibiose	28.5 (36.2)	71.3 (30.9)	2.2 (3.8)	26.3 (35.4)	97.8 (38.5)	28.6 (39.2)
	Sucrose	75.5 (11.4)	97.8 (3.8)	0 (0)	2.2 (3.8)	100 (0.0)	2.2 (3.8)
	Trehalose	75.9 (14.3)	84.4 (10.2)	0 (0)	15.6 (10.1)	100 (0.0)	15.6 (10.1)
Trisaccharide	Raffinose	85.1 (17.8)	29.1 (5.1)	0 (0)	70.9 (5.1)	100 (0.0)	70.9 (5.1)

† - Individuals with only one engorged tissue (ventral diverticulum or midgut) following a sugar meal.
ᐃ – All individuals with engorged tissue following a sugar meal.

Supplementary Table 1 – Statistical analysis of survival of adult female *Ae. aegypti* provided with the sugars listed below. P values are shown for each test performed as graphically represented in the text and supplementary text.

Fig. 1A & Supplementary Fig. 4			
Test:	Log-rank (Mantel-Cox) test		
Groups	Sucrose	Water	Starved
Arabinose	<0.0001	<0.0001	0.0646
Cellobiose	<0.0001	0.0009	<0.0001
Fructose	0.0001	<0.0001	<0.0001
Galactose	<0.0001	<0.0001	<0.0001
Glucose	0.0057	<0.0001	<0.0001
Lactose	<0.0001	<0.0001	0.0173
Maltose	0.0148	<0.0001	<0.0001
Mannose	0.6321	<0.0001	<0.0001
Melibiose	<0.0001	<0.0001	<0.0001
Raffinose	0.0311	<0.0001	<0.0001
Sucrose	N/A	<0.0001	<0.0001
Trehalose	<0.0001	<0.0001	<0.0001
Water		N/A	<0.0001
Starved			N/A
Fig. 1C			
Test:	Log-rank (Mantel-Cox) test		
Groups	Sucrose		
Arabinose	<0.0001		
Galactose	0.4032		
Lactose	<0.0001		
Sucrose	N/A		
Fig. 1D			
Test:	Log-rank (Mantel-Cox) test		
Groups	Sucrose		
Arabinose 0.5 M	<0.0001		
Arabinose 0.25 M	<0.0001		
Lactose 0.5 M	<0.0001		
Lactose 0.25 M	0.0417		
Sucrose	N/A		
Fig. 2 & Supplementary Fig. 5			
Test:	Log-rank (Mantel-Cox) test		
Groups	Sucrose	Sucrose + boric acid	Starved
Arabinose	<0.0001	<0.0001	0.1227

Cellobiose	<0.0001	<0.0001	0.7167
Galactose	<0.0001	<0.0001	<0.0001
Lactose	<0.0001	<0.0001	0.0142
Maltose	<0.0001	0.4105	<0.0001
Melibiose	<0.0001	<0.0001	<0.0001
Raffinose	<0.0001	<0.0001	<0.0001
Sucrose	N/A	<0.0001	<0.0001
Sucrose + boric acid		N/A	<0.0001
Starved			N/A

Fig. 3B	
Test:	One-way ANOVA with Dunnet's test
Groups	Sucrose
Sucrose, Arabinose & Boric Acid	0.9946
Sucrose & Arabinose	0.936
Arabinose & Boric Acid	<0.0001
Arabinose	<0.0001
Sucrose & Boric Acid	>0.9999

Fig. 3C	
Test:	Log-rank (Mantel-Cox) test
Groups	Sucrose
Sucrose, Arabinose & Boric Acid	<0.0001
Sucrose & Arabinose	<0.0001
Arabinose & Boric Acid	<0.0001
Arabinose	0.7178
Sucrose & Boric Acid	<0.0001

Figure 1 – Sugar meal composition alters longevity in adult female *Ae. aegypti*. (A, C, D) Longevity of adult females measured for ten days with continuous exposure to sugar meals, water, or starved (n = 50). (A) Kaplan-Meier survival curve for sugar meals that decrease *Ae. aegypti* longevity compared to water. Additional data for other sugars tested shown are in Supplementary Figure 4. (B) Representative dead individuals following exposure to (left) sucrose, and (right) lactose sugar meals. Scale bar = 500 µm. (C) Kaplan-Meier survival curve of *Ae. aegypti* provided with select sugar meals following a blood meal. (D) Kaplan-Meier survival curve of *Ae. aegypti* provided with sugar meal mixtures including arabinose & sucrose, lactose & sucrose, or sucrose alone whereby both sugars are at a concentration of 0.5 M or 0.25 M. Statistical analyses of these data are provided in Supplementary Table 1. Data are the result of 3 or more replicates with a total of at least 150 individuals per group.
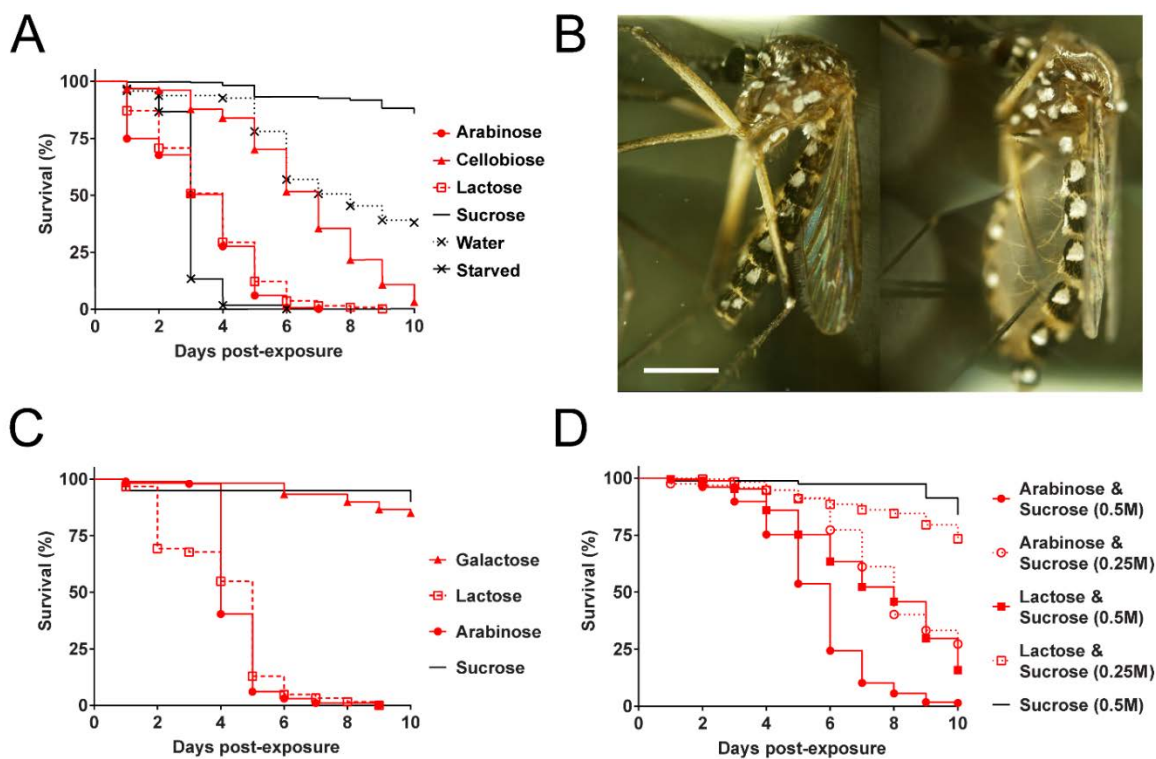
Figure 2 – Sugar meal composition can alters boric acid potency in *Ae. aegypti*. Kaplan-Meier survival curve of *Ae. aegypti* adult females continuously exposed to a sugar meal containing 0.25% boric acid compared to sucrose only and starved controls (n = 50). Additional data for other sugars tested shown are in Supplementary Figure 5. Statistical analyses of these data are provided in Supplementary Table 1. Data are the result of 3 replicates with a total of at least 150 individuals per group.
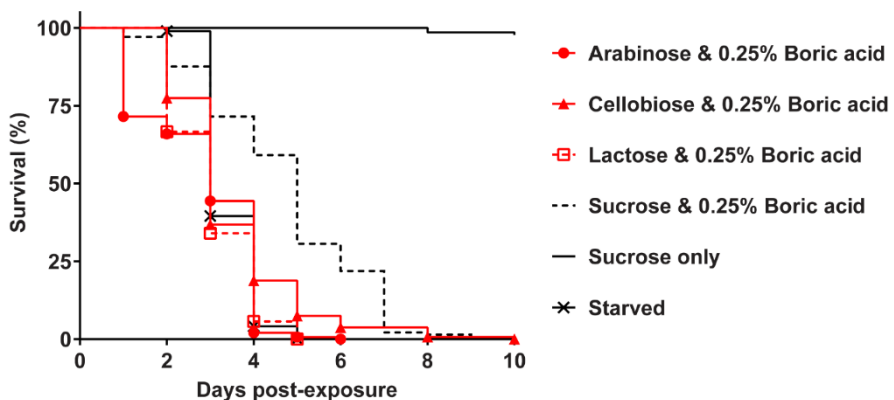
Figure 3 – Arabinose enhances ATSB potency without decreasing attractiveness. (A) Experimental setup showing choice of non-toxic sucrose vs treatment group. (B) Feeding preference (average ± SEM) calculated as proportion of individuals engorged on treatment solution as compared to sucrose solution (n = 30-50). Asterisks indicate statistical significance (One-Way ANOVA with Dunnett's test compared to sucrose control group) where ****p < 0.0001. (C) Kaplan-Meier survival curve of *Ae. aegypti* adult females following exposure to choice assay (n = 30-50). Statistical analyses of these data are provided in Supplementary Table 1. Data are the result of 3-4 replicates with a total of at least 150 individuals per group.
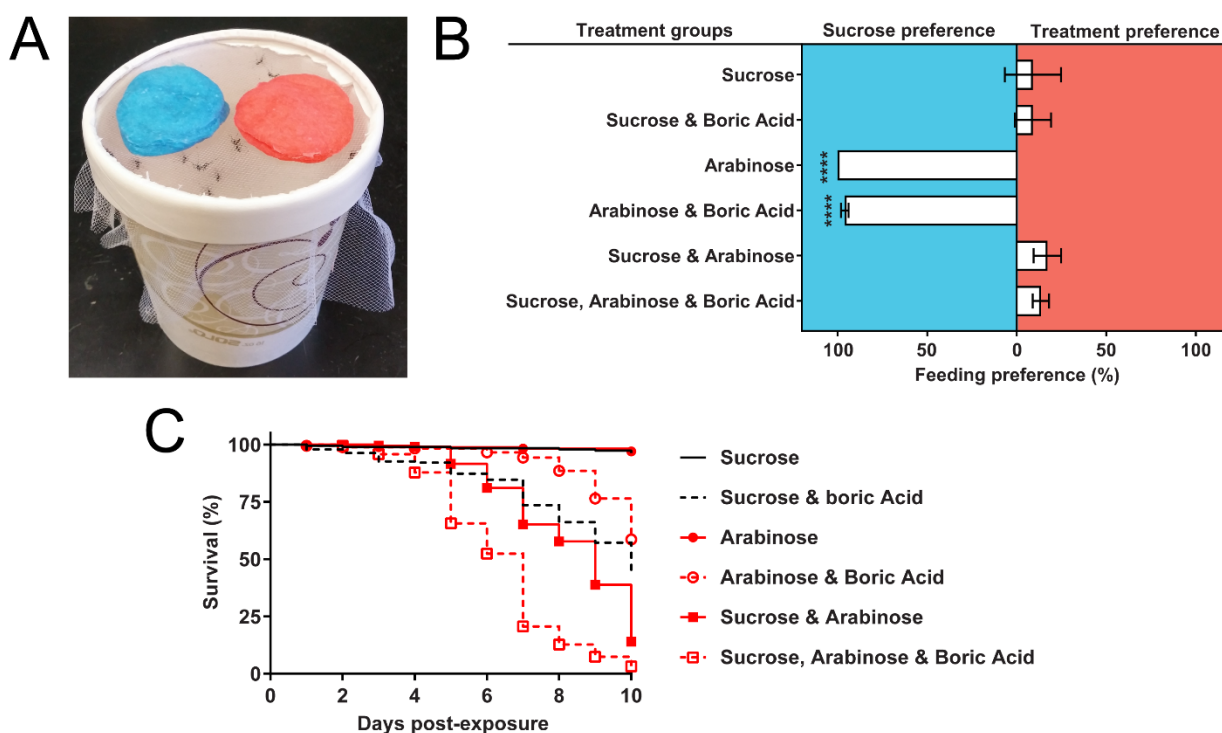
Figure 4 – Ingested dsRNA does not disseminate beyond the foregut lumen in *Ae. aegypti*.
Representative images of *Ae. aegypti* foregut tissue following exposure to labelled dsRNA in maltose (a, b, c), raffinose (d, e, f), or sucrose (g, h, i) sugar meals. Fluorescent dsRNA (a, d, g), bright field (b, e, h) and merged (c, f, i) channels shown. Scale bar = 500 µM. Data are the result of 3 replicates with a total of 60 individuals exposed per group and images captured from 15 individuals per group.
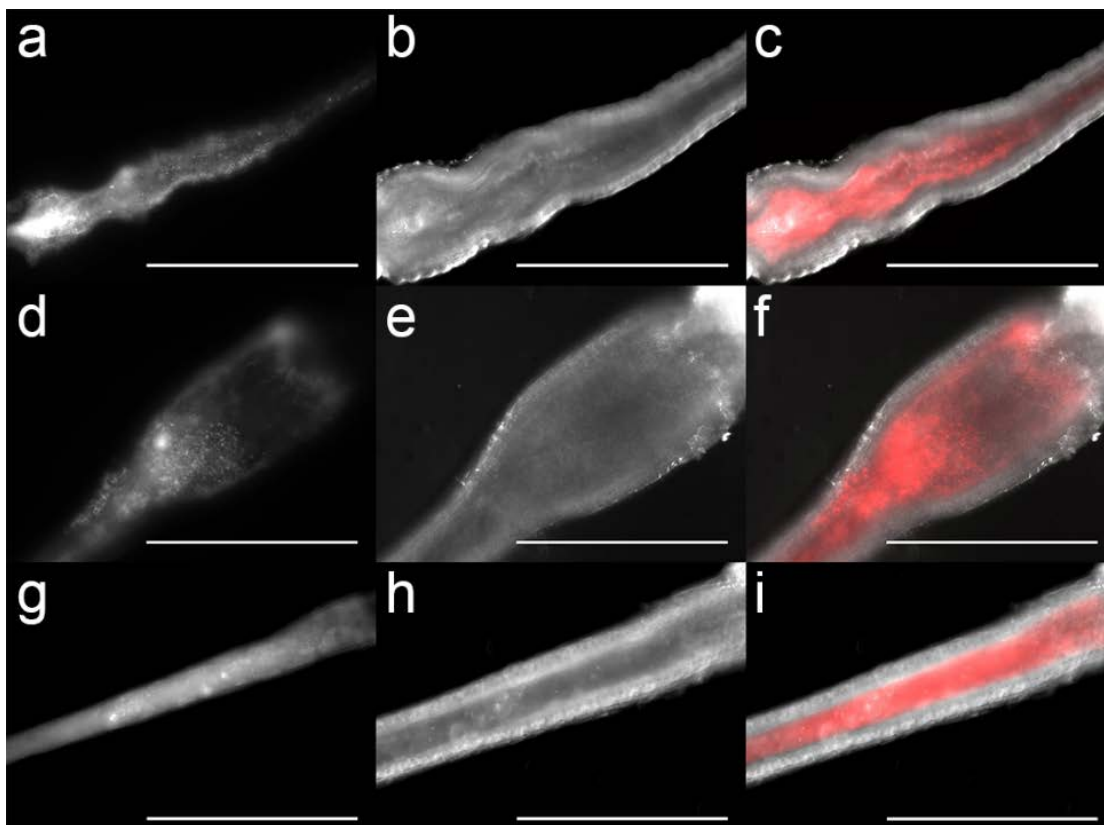
Supplementary Figure 1 – Capillary feeding method. Newly emerged mosquitoes exposed to capillaries containing sugar solution and food dye. Capillaries refilled twice daily to ensure solution was continuously available. Here solution is added by capillary action (vertical – 90º angle), tubes are then aligned and taped to Styrofoam, which is placed onto a carton (with mesh) containing mosquitoes. Capillaries are inserted <1 cm into each carton to ensure mosquitoes can land on the mesh and reach the capillary.

Supplementary Figure 2 – Sugar meal composition dictates gastrointestinal tract destination in adult female *Ae. aegypti*. The location of sugar meals immediately following uptake was measured as the proportion of engorged tissues in visibly fed individuals (n = 15). Data are the average of 3 or more biological replicates for a total of at least 45 individuals per group.
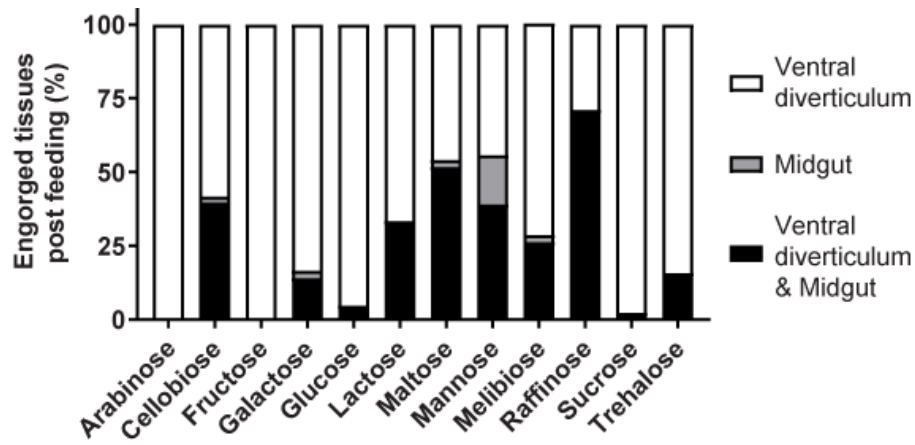
Supplementary Figure 3 – Temperature does not alter sucrose ingestion or destination in the gastrointestinal tract. Starved adult female *Ae. aegypti* were exposed to sugar solutions for 30 minutes then inspected for (A) evidence of feeding to engorgement (n = 50), (B) location of sugar meal in the ventral diverticulum (white bar) or no tissues (black bar) (n = 15). All data are the average ± SEM of 3 or more biological replicates compared by two-tailed paired t-tests, no significant differences were found.
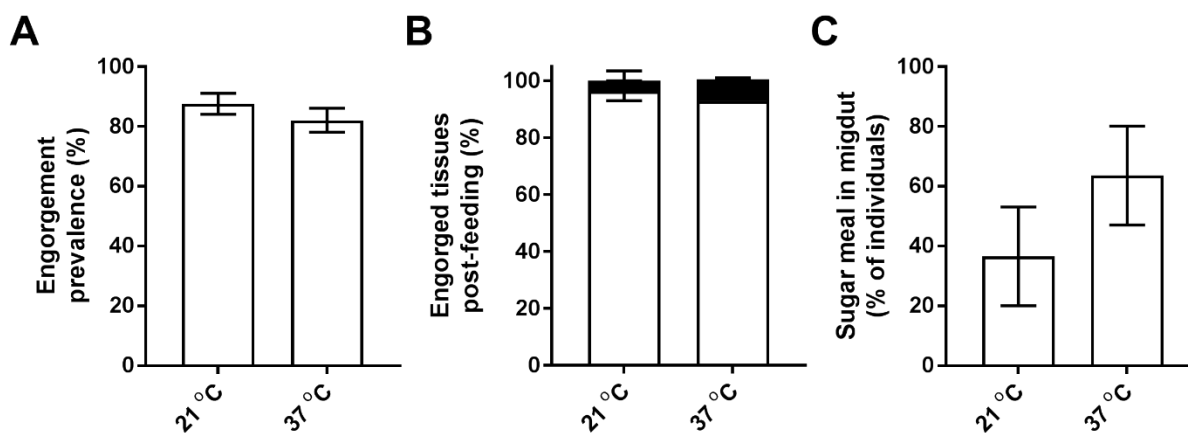
Supplementary Figure 4 – *Ae. aegypti* longevity following continuous exposure to different sugar meals. Kaplan-Meier survival curves are shown for exposure to (A) arabinose, (B) cellobiose, (C) fructose, (D) galactose, (E) glucose, (F) lactose, (G) maltose, (H) mannose, (I) melibiose, (J) raffinose, and (K) trehalose treatments in comparison to sucrose, water, and starved controls (n = 50). Survival data for mosquitoes exposed to other sugars tested are shown in Figure 1. Statistical analyses of these data are provided in Supplementary Table 1. Data are the result of 3 or more replicates for a total of at least 150 mosquitoes per group.
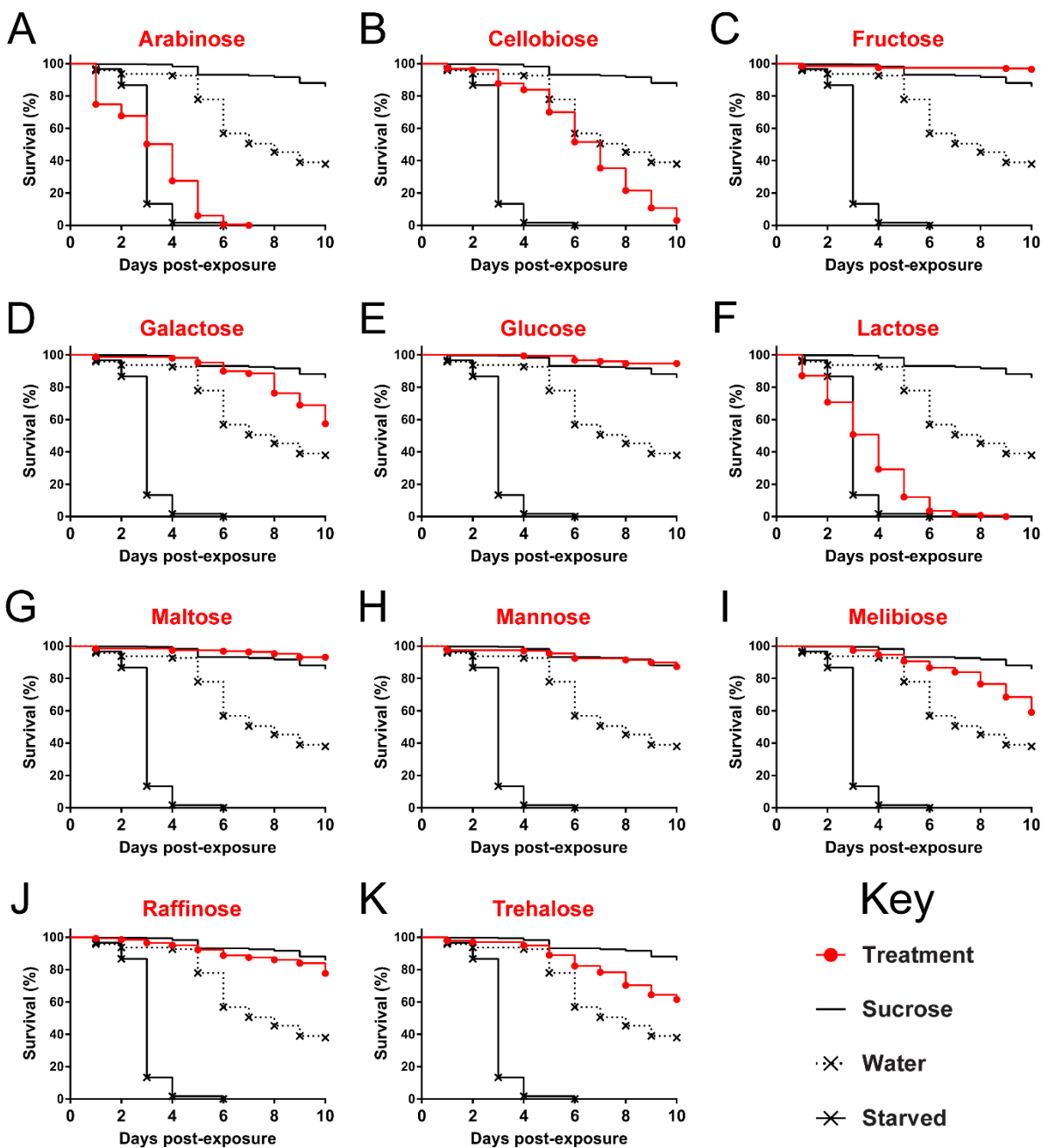
Supplementary Figure 5 – *Ae. aegypti* **longevity following continuous exposure to different sugar meals with 0.25% boric acid.** Kaplan-Meier survival curves following exposure to (A) arabinose, (B) cellobiose, (C) galactose, (D) lactose, (E) maltose, (F) melibiose, and (G) raffinose treatments all mixed with 0.25% boric acid (n = 50). Controls include sucrose & 0.25% boric acid, sucrose only, and starved individuals (n = 50). Statistical analyses of these data are provided in Supplementary table 1. Additional data for other sugars tested are shown in Figure 2. Data are the result of 3 replicates for a total of at least 150 mosquitoes per group. Statistical significance shown in Supplementary Table 1.
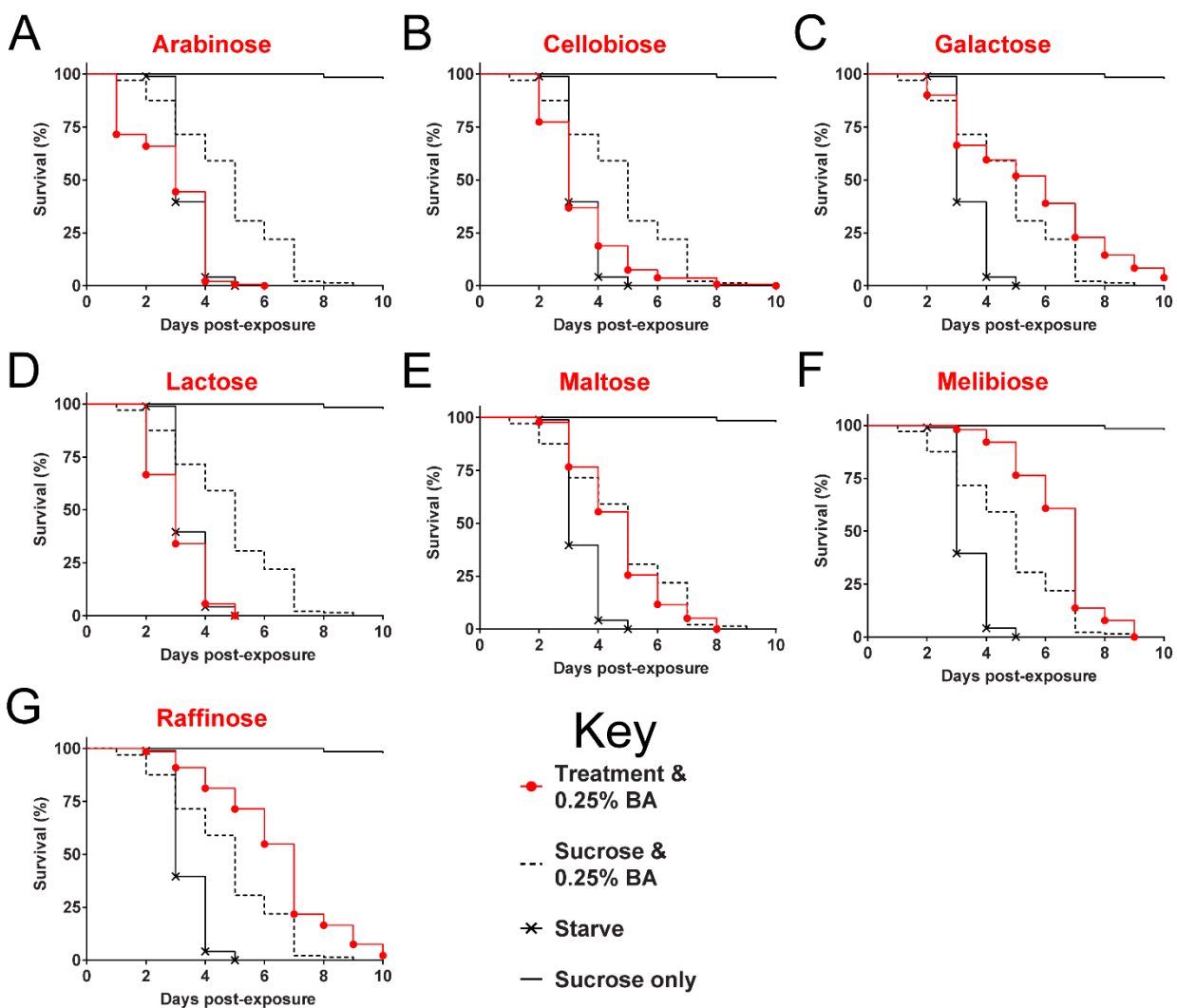
Supplementary Figure 6 – Choice assay for adult female *Ae. aegypti* provided with sugars colored with blue or red food coloring, with and without boric acid. Uptake of sucrose solution, treatment solution, both, or neither (unfed) 1 hour post exposure was visually inspected in whole body mosquitoes according to color of the gastrointestinal tract within the abdomen (n = 30-50). Data are the result of 3-4 replicates for a total of at least 150 mosquitoes per group.
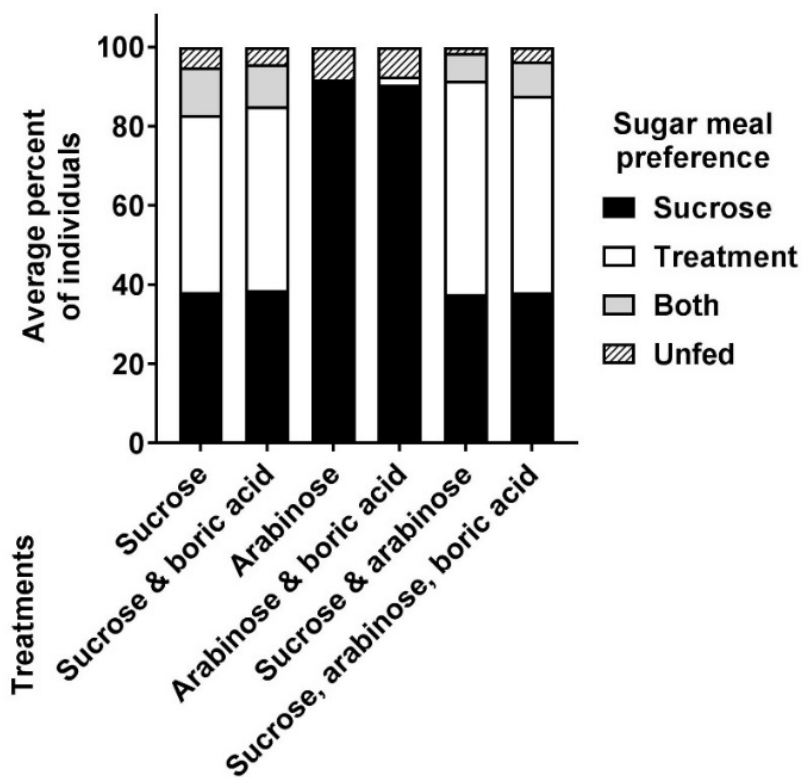
Chapter 7 – Summary

"…they had done their work without thought of use and that throughout the whole history of science most of the really great discoveries which had ultimately proved to be beneficial to mankind had been made by men and women who were driven not by the desire to be useful but merely the desire to satisfy their curiosity." - Abraham Flexner (excerpt from "The usefulness of useless knowledge", Harpers, Vol 179, October 1939).

To study mosquitoes is to attempt to satisfy both curiosity and produce results which directly benefit humanity. In recent times mosquito biologists have had reasons to celebrate with progress made towards eradicating malaria, river blindness, and a growing appreciation for neglected tropical diseases. Gargantuan efforts to control malaria have reduced malaria mortality by 60% worldwide (2000-2015) [1]. Awareness of the burden of malaria alone has elicited the Bill and Melinda Gates foundation, the Carter Foundation, among many other philanthropic organizations to enable ambitious and creative scientific research projects. Through the Gates foundation and the FNIH I found myself in a space free to ask basic questions and make observations in an unhindered environment. This work began with the goal of eradicating malaria through RNA interference (RNAi). However, with minimal understanding of the limitations of RNAi in mosquitoes, experiments vary wildly in knockdown success of target genes and this in turn limits inferences and confidence in the technique. Through reviews and meta-analyses of published literature, creation of RNAi design tools, and basic molecular studies in mosquito systems, this dissertation work addresses the limitations and strengths of RNAi as a basic molecular biology tool as well as an applied vector control approach.

In recent years, the rise and rapid spread of emerging vector borne diseases (VBDs) such as Zika and Chikungunya viruses have demonstrated the threat such diseases pose on global health [2]. It is likely that many other VBDs are in the process of spreading; we know that *Leishmania* parasites are rampant in war torn areas of the Middle East and are spreading with forced migration out of Syria [3]. Similarly, *Trypanosoma cruzii* have been found in over 50% of triatomine bugs tested in the Southern USA with likely autochthonous cases reported in these areas [4, 5]. Coupling the emergence and spread of VBDs with spread of multiple insecticide resistance traits [6-8] in areas heavily reliant on chemical insecticides can lead to devastation unless novel, multi-disciplinary efforts are made to control vectors [9]. One area of particular interest for development is utilization of genetic tools, including RNAi, to suppress genes required for transmission of VBDs or survival of the vector itself [10].

A large part of this dissertation has focused inducing cell death via suppression of the Inihibtor of Apoptosis 1 (IAP1) gene. This interest began with characterization of cell death events in *Aedes triseriatus* and led to exploration of the role of cell death genes on cell and organismal survival. These results spurred an effort to investigate whether RNAi can be harnessed to produce species-specific RNAi insecticides. Studies investigating RNAi experimental design and predictability have uncovered hurdles required to pass before RNAi can be utilized as an alternative to current insecticides. At the same time, studies suppressing IAP1 highlight the potential for RNAi to induce species specific mortality. Reviewing approaches to take RNAi over these hurdles discuss incorporation of other novel intervention strategies including the use of entomopathogens as synergistic delivery vehicles, or environmentally stable but non-toxic nanoparticle carriers [10-13].

Beyond death, there is great potential to explore the role of RNAi in long term immunity in mosquito species. We are only beginning to understand the impact of RNAi trigger exposure on individual mosquitoes and their offspring. Part of this work identifies cells such as the follicular epithelia of the ovaries which have increased sensitivity to RNAi, but the role in these cells and others on systemic RNAi and immunity are unknown. We know that RNAi can provide protection against viruses over long periods in shrimp, and is essential to preventing viral superinfection in Diptera [14, 15]. The future for RNAi in mosquitoes may therefore be one of inducing death, or providing vaccination of vectors against VBDs which continue to threaten global health.

Literature cited

1.   Cibulskis, R.E., et al., *Malaria: Global progress 2000 – 2015 and future challenges.* Infectious Diseases of Poverty, 2016. **5**: p. 61.

2.   Weaver, S.C., et al., *Zika, Chikungunya, and Other Emerging Vector-Borne Viral Diseases.* Annual Review of Medicine, 2018. **69**(1): p. 395-408.

3.   Al-Salem, W.S., et al., *Cutaneous Leishmaniasis and Conflict in Syria.* Emerg Infect Dis, 2016. **22**(5): p. 931-3.

4.   Curtis-Robles, R., et al., *Analysis of over 1500 triatomine vectors from across the US, predominantly Texas, for Trypanosoma cruzi infection and discrete typing units.* Infection, Genetics and Evolution, 2018. **58**: p. 171-180.

5.   Gunter, S.M., et al., *Likely Autochthonous Transmission of Trypanosoma cruzi to Humans, South Central Texas, USA.* Emerging Infectious Diseases, 2017. **23**(3): p. 500-503.

6.   Russell, T.L., et al., *Increased proportions of outdoor feeding among residual malaria vector populations following increased use of insecticide-treated nets in rural Tanzania.* Malaria Journal, 2011. **10**(1): p. 80.

7.   Liu, N., *Insecticide resistance in mosquitoes: impact, mechanisms, and research directions.* Annu Rev Entomol, 2015. **60**: p. 537-59.

8.   Vontas, J., et al., *Insecticide resistance in the major dengue vectors Aedes albopictus and Aedes aegypti.* Pesticide Biochemistry and Physiology, 2012. **104**(2): p. 126-131.

9.   Zaim, M. and P. Guillet, *Alternative insecticides: an urgent need.* Trends Parasitol, 2002. **18**(4): p. 161-3.

10.   Airs, P.M. and L.C. Bartholomay, *RNA Interference for Mosquito and Mosquito-Borne Disease Control.* Insects, 2017. **8**(1): p. 4.

11.   Ji, S.J., et al., *Recombinant scorpion insectotoxin AaIT kills specifically insect cells but not human cells.* Cell Res, 2002. **12**(2): p. 143-50.

12.   Silva L. E. I., et al., *A new method of deploying entomopathogenic fungi to control adult Aedes aegypti mosquitoes.* Journal of Applied Entomology, 2018. **142**(1-2): p. 59-66.

13.   Phanse, Y., et al., *Biodistribution and Toxicity Studies of PRINT Hydrogel Nanoparticles in Mosquito Larvae and Cells.* PLoS Neglected Tropical Diseases, 2015. **9**(5): p. e0003735.

14.   Loy, J.D., et al., *dsRNA provides sequence-dependent protection against infectious myonecrosis virus in Litopenaeus vannamei.* J Gen Virol, 2012. **93**(Pt 4): p. 880-8.

15.   Goic, B., et al., *Virus-derived DNA drives mosquito vector tolerance to arboviral infection.* Nat Commun, 2016. **7**: p. 12410.